AD NUMBER

AD830296

NEW LIMITATION CHANGE

TO

Approved for public release, distribution unlimited

FROM

Distribution authorized to U.S. Gov't. agencies and their contractors; Operational and Administrative Use; Jul 1964. Other requests shall be referred to Army Materiel Command, Alexandria, VA 22304.

AUTHORITY

USAMC ltr, 2 Jul 1973

ENGINEERING DESIGN HANDBOOK

AMMUNITION SERIES

SECTION 4, DESIGN FOR PROJECTION

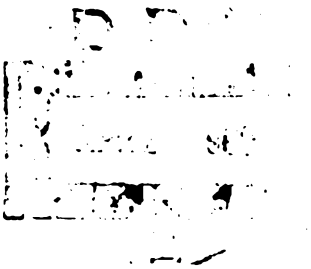

HEADQUARTERS, U. S. ARMY MATERIEL COMMAND

JULY 1964

198

PREFACE

This handbook is the fourth of six handbooks on artillery ammunition and forms a part of the Engineering Design Handbook Series of the Army Materiel Command. Information concerning the other handbooks on artillery ammunition, together with the Table of Contents, Glossary and Index, will be found in AMCP 706-244, Section 1, Artillery Ammunition--General.

The material for this series was prepared by the Technical Writing Service of the McGraw-Hill Book Co., based on technical information and data furnished principally by Picatinny Arsenal. Final preparation for publication was accomplished by the Engineering Handbook Office of Duke University, Prime Contractor to the Army Research Office-Durham for the Engineering Design Handbook Series.

Agencies of the Department of Defense, having need for Handbooks, may submit requisitions or official requests directly to Publications and Reproduction Agency, Letterkenny Army Depot, Chambersburg, Pennsylvania 17201. Contractors should submit such requisitions or requests to their contracting officers.

Comments and suggestions on this handbook are welcome and should be addressed to Army Research Office-Durham, Box CM, Duke Station, Durham, North Carolina 27706.

#830296

HEADQUARTERS
UNITED STATES ARMY MATERIEL COMMAND
WASHINGTON, D. C. 20315

31 July 1964

AMCP 706-247, Section 4, Design for Projection, forming part of the Ammunition Series of the Army Materiel Command Engineering Design Handbook Series, is published for the information and guidance of all concerned.

(AMCRD)

FOR THE COMMANDER:

OFFICIAL:

SELWYN D. SMITH, JR.
Major General, USA
Chief of Staff

R. O. DAVIDSON
Colonel, GS
Chief, Administrative Office

DISTRIBUTION: Special

TABLE OF CONTENTS

Section 4 - Design for Projection

TABLE OF CONTENTS

Section 4 - Design for Projection (continued)

SECTION 4

DESIGN FOR PROJECTION

PROPELLANTS AND INTERIOR BALLISTICS

PROPELLANTS, GENERAL

4-1. Introduction. The purpose of propellant design is to select the correct formulation and granulation to satisfy a given set of conditions. The limitations imposed by these conditions constitute the design problems. To achieve the desired results from a given propellant, it is necessary to consider such factors as cartridge case volume, rate of bore erosion, reduction of flash and smoke, ballistic uniformity, and high-velocity requirements balanced against pressure limitations. It may not be possible to satisfy all of these considerations; therefore, a certain amount of compromise is necessary.

From practical considerations, propellants should be made from relatively cheap, nonstrategic materials which are available in large quantity. The rate of burning of the propellant should be controlled so that the rate of gas evolution does not develop pressure peaks within the gun tube in excess of the gun stress limits. The burnt propellant should leave little or no residue, since unburned material corrodes bores, creates smoke, and reduces gun efficiency. It is also desirable that the explosion gases be as cool as possible at the muzzle to reduce flash and so prevent exposure of the gun position by night. By the same token, it is desirable that the explosion be smokeless to prevent obscuration of the target or revealing the gun position by day. Cooler-burning propellants decrease the tendency to erode bores. While nitrocellulose has a certain amount of inherent instability, it has retained its position as a general ingredient of propellants because it can be made satisfactorily stable by the addition of stabilizing materials and because of the lack of a large supply of more stable materials possessing its advantageous characteristics.

The black powder* originally used as a military propellant has been completely displaced by propellant compositions at one time referred to as "smokeless powders," which invariably contain nitrocellulose. Smokeless powder is a misnomer, because these propellants are not used in the form of powder, and do liberate varying amounts of smoke.

On a composition basis, propellants are divided into the following three groups.

a. Single-Base Propellants. Nitrocellulose is the principal active ingredient of single-base propellant (see table 4-23). It may contain a stabilizer (usually possessing plasticizing properties) or any other material in a low state of oxidation, in addition to nitro compounds, and inhibiting or accelerating materials such as metals or metallic salts. M1 propellant is an example of a single-base propellant.

b. Double-Base Propellants. "Double-base" generally defines propellant compositions containing nitrocellulose and nitroglycerin. A better definition describes a double-base propellant as one containing nitrocellulose and a liquid organic nitrate which gelatinizes the nitrocellulose. It may also contain additives similar to the single-base compositions. Nitroglycerin propellants have not been used extensively in

*Black powder is the generic name originally applied to a mixture of charcoal, sulfur, and potassium nitrate and now also applied to compositions containing bituminous coal and sodium nitrate in place of the charcoal and potassium nitrate. The [illegible] ratio of the components of the potassium nitrate-charcoal-sulfur has remained essentially the same for over 400 years, since any modification of the ratio has been found to produce adverse results. Although black powder is no longer used as a propellant, it is still used as an igniting material for propellants, time fuzes, base-ejecting shells, and the like. Black powder is coated with graphite to increase its loading density and to reduce the build-up of static charge.

the United States as standard propellants because their high explosion temperature makes them quite corrosive, reducing the service life of the gun; furthermore, they may possibly be in short supply in an emergency. M2 propellant is an example of double-base propellant.

c. Triple-Base Propellants. These propellants have three basic active ingredients: nitrocellulose, nitroglycerin, and nitroguanidine, in addition to such other additives as may be necessary. M15 propellant is an example of a triple-base propellant.

Table 4-23 is a breakdown of compositions of standard propellants. In these compositions, the dinitrotoluene and nitroglycerin act as gelatinizing and moistureproofing agents which contribute to the ballistic potential; diphenylamine and ethyl centralite are used as stabilizers; dibutylphthalate and triacetin are nonexplosive gelatinizing agents which also contribute to flashlessness; nitroguanidine is dispersed throughout the nitrocellulose-nitroglycerin colloid as a finely divided crystalline powder which contributes to ballistic potential and flashlessness; potassium sulfate and cryolite are used as chemical flash reducers; while tin is used as a decoppering agent.

4-2. Forms of Nitrocellulose. Some types of nitrocellulose are distinguished by name, including the following (see table 4-2).

a. Pyroxylin, or collodion, is soluble in a mixture of ether and ethanol and contains from about 8 to about 12 percent of nitrogen. Pyroxylin is distinguished from other types of nitrocellulose by its partial solubility in ethanol. The pyroxylin used for military purposes contains 12.20 ± 0.10 percent of nitrogen, while that used in the manufacture of blasting explosives has a nitrogen content of 11.5 to 12.0 percent.

b. Pyrocellulose has a nitrogen content of 12.60 ± 0.10 percent, and is completely soluble in a mixture of 2 parts of ether and 1 part of ethanol. Pyrocellulose for military use is manufactured from cotton linters or wood cellulose obtained commercially from wood pulp.

c. Guncotton contains 13 percent or more of nitrogen, that used for military purposes containing a minimum of 13.35 percent. Only 6 to 11 percent of this type of nitrocellulose is soluble in ether-ethanol mixture, but it is completely soluble in acetone, as are practically all types of nitrocellulose.

d. Blended Nitrocelluloses are mixtures of pyrocellulose and guncotton. These are designed to have desirable solubility and viscosity characteristics as well as a specified nitrogen content.

PROPELLANT COMPOSITION

4-3. Criteria for Selection of Propellant Materials. In the manufacture of propellants it may be desirable to incorporate with the nitrocellulose other materials in order to modify the properties of the nitrocellulose. These materials may be either incorporated or coated on the surface, and are used to (1) increase stability, (2) decrease hygroscopicity, (3) change heat of explosion, (4) control burning, (5) reduce muzzle flash, (6) reduce smoke, (7) increase electrical conductivity, and (8) reduce bore residue. Table 4-1 lists some of the materials used to achieve these ends, with specific applications.

a. Stability. Since propellants must be stored for long periods and then must function reliably when used, they must not decompose in storage. Of primary concern is the fact that nitrocellulose by itself is not stable. In common with other nitrate esters, nitrocellulose breaks down autocatalytically to yield acid decomposition products which accelerate the decomposition rate once decomposition has started. Stabilizers are added to the propellant colloid to reduce the decomposition rate.[1]

Stabilizers react with the acid decomposition products, as they are formed, to neutralize them and thus prevent acceleration of the decomposition. When deterioration has progressed to a point where the neutralizing action of the stabilizer is no longer significant, the decomposition rate accelerates. The appearance of an acid odor and subsequently visible red fumes indicate that the propellant has become unsafe for further storage or use. (See paragraphs 4-65 through 4-75.)

b. Hygroscopicity. Hygroscopic propellants are undesirable both because absorption of moisture reduces the ballistic power, and renders the propellant unstable chemically and physically, and because variations in moisture content alter the ballistic characteristics unpredictably. Propellants are made as nonhygroscopic as possible by including moisture-resisting materials in the colloid or by coating the surface of the propellant grain with moisture-resisting materials.

c. Heat of Explosion. The heat of explosion is controlled to reduce muzzle flash and bore erosion, since high heats of explosion produce muzzle flash and high rates of bore erosion, especially at high rates of fire. For discussion of flash from guns see references 2, 3, 4, 5, 6, 7, and 8. The heat of explosion is governed by the material included in the propellant composition. A high oxygen content produces a high heat of explosion; therefore, it is advisable to formulate propellant compositions with low oxygen balance to lower the heat of explosion.

d. Control of Burning. The rate of burning is controlled to govern the pressure within the gun tube and to reduce flash. In addition to being controlled by proper grain geometry (paragraphs 4-10 through 4-20), the rate of burning may be further modified by coating the propellant grain with a deterrent material that diffuses into the grain and makes the outside surface burn slower than the main body of the propellant. The depth to which the deterrent diffuses into the surface is controlled by the temperature and duration of the coating process.

e. Flash and Smoke. The importance of the elimination (or at least reduction) of muzzle flash and smoke lies in the elimination of a source of detection of the gun battery and in the prevention of target obscuration. The goal in design for flash reduction is a propellant that will be consumed close to the breech, thereby allowing the combustion products to cool before they exit from the muzzle. This goal is opposed to the high muzzle pressure necessary to produce high projectile velocities.

Muzzle flash may be resolved into two components. The first flash is due to the burning of incandescent propellant gases, occurring at the muzzle, immediately after the emergence of the projectile. The second flash, due to the combustion of H_2 and CO in the propellant gases with atmospheric oxygen, occurs a fraction of a second later some distance in front of the muzzle. Its illumination intensity is far greater than the first flash.[2] Alkali metal salts have been found effective in reducing secondary flash, as they prevent the chain reactions which occur in oxidation of hydrogen to water; they also form nuclei in the emergent gases on which the explosion-produced water vapor may condense, thereby creating smoke.[3]

An alternative method of reducing flash is to incorporate large amounts of nitrogen into the propellant composition thereby diluting the amounts of inflammable H_2 and CO in the muzzle gases. Oxygen balance is important in the reduction of flash and smoke because an adequate supply of oxygen reduces smoke by converting all of the carbon in an explosive to gaseous form.

f. Electrical Conductivity. Graphite is coated on the grains to increase their surface electrical conductivity in order to reduce the danger arising from an accumulation of a static charge during propellant handling. The graphite also serves to lubricate the grains and so increases packing density.

g. Residues. Propellant formulations are compounded so that unoxidized carbon remains low, since unburned carbon produces bore residue and smoke. Lead carbonate and tin are materials that may be added to reduce coppering.

Table 4-1 lists some of the more commonly used materials that are added to propellants and indicates their functions. It should be noted that some items are multipurpose.

Table 4-1

Substitutes and additives

Material \ Function	Reduce hygroscopicity	Stabilizer	Plasticizer	Deterrant	Reduce flame temperature	Reduce flash	Reduce bore erosion	Increase electrical conductivity	Control burning rate	Source of oxygen
Nitroglycerin (NG)	X		X							X
Nitroguanidine						X	X			
Dinitrotoluene (DNT)	X		X	X			X		X	
Methyl centralite (Sym-dimethyldiphenylurea)			X	X		X	X		X	
Ethyl centralite (Sym-diethyldiphenylurea)	X	X	X	X	X	X	X		X	
Diethyleneglycoldinitrate (DEGN)			X*			X	X			
Diphenylamine (DPA)		X†								
Dibutylphthalate (DBT)	X		X	X	X	X	X		X	
Diethylphthalate (DET)						X	X		X	
Trinitronaphthalene		X			X					
Mineral jelly		X	X		X		X			
Barium nitrate						X				
Potassium nitrate						X				
Potassium perchlorate						X			X	
Potassium sulfate						X				
Tin (powdered)										
Graphite								X		
Carbon black										
Cryolite						X				

* Thermally more stable than NG.
† Stabilizer for single-base propellants only.

REFERENCES AND BIBLIOGRAPHY

1. Davis, T. L., "Chemistry of Powder and Explosives," John Wiley and Sons, New York, 1943, p. 266 ff.

2. "Internal Ballistics," The Philosophical Library, New York, 1951, pp. 3, 4, 80, 81.

3. Chemical Suppression of Gun Muzzle Flash, Franklin Institute Report, 15 January 1954, ASTIA No. AD-31197 (CONFIDENTIAL).

4. Laidler, K. J., "Chemical Kinetics," McGraw-Hill Book Co., New York, 1950, pp. 318-323.

5. Cocke et al, Study of Physical Mechanism of Muzzle Flash, CARDE Report No. 210/45.

6. Report on Muzzle Flash, BRL Report No. 426, 19 November 1943 (CONFIDENTIAL).

7. Muzzle Flash and Its Suppression, BRL Report No. 618, 10 February 1947.

8. Midwest Research Institute, Contractor's Reports on W-323-072-ORD-2163-27-4.

4-4. Description of Propellant Manufacture. The basic propellant material is nitrocellulose, which is made by nitrating cellulose derived from cotton linters or wood pulp. The manufacture of nitrocellulose propellants consists of two distinct processes: (1) manufacture of the nitrocellulose, and (2) manufacture of the propellant from the nitrocellulose. Nitrocellulose is a nitrate formed by esterification of cellulose. The wood pulp is purified at a pulp mill by either the sulfite or sulfate process to yield a high alpha cellulose content, and sent to the nitrating plant in continuous rolls. Linters cellulose is bleached and sent to the nitrating plant in bales. At the nitrating plant the wood cellulose is shredded, and the linters are picked to expose the fibers, and then dried. Nitration is accomplished by the du Pont mechanical dipper process. The proper degree of nitration results by adjustment of the nitric acid-sulfuric acid-water ratio. When nitration is complete, the contents of the nitrating vessel are centrifuged, and the acid fortified for reuse. The nitrocellulose is submitted to a lengthy series of acid and neutral atmospheric pressure boils to remove occluded acids. This comprises the stabilization process. This process also accomplishes a certain amount of viscosity reduction. At the conclusion of stabilization the nitrocellulose must meet the stability, physical, and chemical requirements of Specification JAN-N-244.

Table 4-2

Military grades of nitrocellulose (Per Specification JAN-N-244)

Grade	Class	Nitrogen, percent
Grade A	Pyrocellulose	
Type I		12.60 ± 0.10
Type II		12.60 ± 0.15
Grade B	Guncotton	13.35 minimum
Grade C	Blended (guncotton)	
Type I		13.15 ± 0.05
Type II		13.25 ± 0.05
Grade D	Pyroxylin (collodion)	12.20 ± 0.10

The grade of nitrocellulose in widest military use contains 13.15 percent nitrogen. This grade is blended from pyrocellulose (12.60 percent nitrogen) and high grade guncotton (13.35 percent nitrogen). See paragraph 4-5. The pyrocellulose is soluble in the ether-ethanol solvent while the guncotton is soluble only to a limited degree, so that the pyrocellulose acts as a binder.

Nitrocellulose is softened or gelatinized by various volatile and nonvolatile solvents, including ether-alcohol mixtures, acetone, nitroglycerine and other nitrate esters, and dibutylphthalate and other phthalates. In the gelatinized state, it may be formed by extrusion or rolling.

4-5. Colloiding. The product obtained by dissolving nitrocellulose in a mixture of ether and ethyl alcohol is called the colloid. Since water-wet nitrocellulose will not dissolve in the ether alcohol solvent, it is centrifuged to approximately 30-percent moisture content and then dehydrated by forcing alcohol through the nitrocellulose under pressure. The alcohol-saturated blocks of nitrocellulose, as they are received from the dehydrating press, are put into a dough mixer, to which, after the blocks are broken up, the additional solvent is added. This step in the process is continued until a satisfactory colloid is obtained.* Diphenylamine or other stabilizer (dissolved in the solvent) is also added at this stage. From the mixer, the crumbly mass is blocked under pressure, and is worked until it is freed from lumps.

In their colloided form, the constituents of the propellant are packed together so densely that the hot gases do not travel through the mass as they would if the propellant grain were porous, but instead, the gases travel across the grain surface. Burning is stabilized by the transfer of energy from the burning zone into the body of the grain. The burning surface recedes into the solid at a relatively low velocity. The linear rate is independent of the grain shape. The result is that the propellant burns in layers at a rate that can be controlled by varying the pressure. The mass rate is a function of shape in addition to other things. Proper rate of conversion of propellant to gas

*The determination of "satisfactory" colloid is still an art.

is brought about by dimensioning of the grain to give the proper surface area. The proper grain shape is produced in the final manufacturing operation by forcing the colloid through dies. (See paragraphs 4-7 through 4-9.) As the propellant comes from the graining dies, it contains almost 50 percent solvent, whose recovery is an important consideration. The "green" grains shrink as they are dried and this shrinkage must be allowed for in the design of the graining dies. Purposeful solvent recovery is carried on until the concentration is reduced to about 12 to 15 percent, after which it is no longer economically feasible. The remaining solvent, down to 0.2 to 3 percent, depending on grain size, is removed either by air drying or water drying.[1,2] Double-base propellants are not subjected to solvent recovery or water drying.

The process just described is the conventional method of manufacturing artillery propellants, which may vary in web from 0.014 to 0.100 inch. When dimensions get larger than this, solvent recovery is such a difficult problem that solventless methods are used. These methods will not be covered here, since they find very little application in artillery propellant manufacture.

For an alternative method of propellant manufacture that has been successfully applied to small arms propellant manufacture, see reference 3. This is the Ball Powder Process used by the Olin Mathieson Chemical Corporation. Although apparently competitive with the conventional solvent-extrusion process for small arms propellants, it does not seem suited for production of larger granulations.

4-6. Relative Costs of Propellant Manufacture. It is not economically feasible for commercial manufacturers of explosives to maintain plants for production of military explosives in peacetime. For this reason, the Ordnance Department has established contractor-operated systems at Ordnance plants to handle wartime military requirements and standby or reduced production in peacetime. Table 4-3, prepared by the Ordnance Ammunition Command, gives some indication of the relative costs of buying propellant materials commercially (where available) and manufacturing in government plants.

Table 4-3

Ammunition component cost for the quarter ended 31 December 1954, propellants, explosives, and chemicals

Nomenclature	Purch. or Gov't. Plt.	Mfg. Cost or Purch. Price	Indirect Cost-3%	Total Cost	Unit
Barium Nitrate, Class D, Granulation 140	Purchased	$0.168	$0.005	$0.173	Lb
Dinitrotoluene	Gov't. Plt.	0.119	0.004	0.123	Lb
Diphenylamine	Gov't. Plt.	0.387	0.011	0.398	Lb
Diphenylamine-Grained for Powder	Gov't. Plt.	0.366	0.011	0.377	Lb
Ethyl Centralite (Carbamite) Class III	Purchased	0.928	0.028	0.956	Lb
Mortar, 4.2", M8 (Increment Charge M6 and Increment Charge M8)	Gov't. Plt.	1.49	0.045	1.535	Lb
Mortar, 60-mm and 81-mm, Increment Packaging (Increment M1A1, M2A1, and M3A1)	Gov't. Plt.	3.18	0.10	3.28	Lb
Nitroglycerin	Gov't. Plt.	0.204	0.006	0.210	Lb
Nitroguanidine Class A or B	Purchased	0.26	0.008	0.268	Lb
Powder, Black, Grade A4	Purchased	0.33	0.01	0.34	Lb

Table 4-3

Ammunition component cost for the quarter ended 31 December 1954, propellants, explosives, and chemicals (cont)

Nomenclature	Purch. or Gov't. Plt.	Mfg. Cost or Purch. Price	Indirect Cost-3%	Total Cost	Unit
Powder, Black, Meal Grade	Purchased	0.32	0.01	0.33	Lb
Powder, Black, Grade FFFG	Purchased	0.316	0.009	0.325	Lb
Powder, Black, Grade A1	Purchased	0.311	0.009	0.320	Lb
Powder, Black, Sodium Nitrate, Class A	Purchased	0.11	0.003	0.113	Lb
Propellant, M2	Purchased	0.67	0.02	0.69	Lb
Powder, Black, Potassium Nitrate, Cannon Grade	Purchased	0.33	0.01	0.34	Lb
Propellant, M6	Purchased	0.574	0.017	0.591	Lb
Powder, M9, for Ignition Cartridge M4 and M5 (60-mm Mortar)	Purchased	1.03	0.03	1.06	Lb
Powder, M9, for Ignition Cartridge M3 and M6 (81-mm Mortar)	Purchased	0.82	0.025	0.845	Lb
Propellant, IMR 4895	Purchased	0.70	0.021	0.721	Lb
Propellant, IMR 4996	Purchased	0.70	0.021	0.721	Lb
Propellant, IMR 7005	Purchased	0.75	0.023	0.773	Lb
Propellant, M12, IMR 7013	Purchased	0.70	0.021	0.721	Lb
Propellant, Western Ball, Type II, WC 820	Purchased	0.799	0.024	0.823	Lb
RDX	Gov't. Plt.	0.382	0.01	0.392	Lb
Solvent, Double Base Multiperforated Propellant (M2)	Gov't. Plt.	0.783	0.023	0.806	Lb
Solvent, Single Base Multiperforated Cannon Powder (Propellant M1, M6, and M10)	Gov't. Plt.	0.42	0.012	0.432	Lb
Solvent, Single Base Single Perforated Propellant	Gov't. Plt.	0.474	0.014	0.488	Lb
Solvent, Triple Base Single Perforated Propellant	Gov't. Plt.	0.597	0.018	0.615	Lb
Trinitrotoluene	Gov't. Plt.	0.145	0.004	0.149	Lb

REFERENCES AND BIBLIOGRAPHY

1. Tschappat, W. H., "Textbook of Ordnance and Gunnery," John Wiley and Sons, New York, 1917, ch. I.
2. Hayes, T. J., "Elements of Ordnance," John Wiley and Sons, New York, 1938, ch. I.
3. Chemical Engineering, McGraw-Hill Book Co., New York, December 1946, pp. 92-96, 136-139.

DETERMINATION OF GRAIN DESIGN FOR A SPECIFIC WEAPON

4-7. Fitting the Web to the Gun. The potential thermal energy of a propellant when fired in a gun is partially converted into the kinetic energy of the projectile. The proportion of the total available energy that can be communicated to the projectile is limited by the length of travel of the projectile in the gun tube, maximum pressure, expansion ratio, friction and heat-conduction energy losses, and so on. The required maximum pressure is controlled by the ballistician through the proper choice of propellant granulation web. The web and propellant weight combination which produces maximum velocity at a specified pressure is the optimum charge.

Propellant grains are commonly designated as either degressive or progressive. A degressive grain burns with a continually decreasing surface until the grain is completely consumed, while a progressive grain burns with a continually increasing surface. The burning rates are functions of the grain geometry (form). (See paragraphs 4-10 through 4-20.) Because of nonsimultaneity of ignition, end-burning, nonuniformity of web, and nonhomogeneities of various types, all propellants are somewhat degressive. In general, it is not practical to manufacture grains that are wholly degressive, or wholly progressive.

A propellant designed to fit a given set of ballistic conditions must have its burning rate closely controlled, which is accomplished within close limits by proper design of the web dimensions. Burning may also be controlled by diffusing a material, which decreases the rate of burning of the propellant, into the surface of the propellant grain. In this discussion, it is assumed that the selected composition is compatible with the several general requirements, such as hygroscopicity, stability, and so on (see paragraph 4-3) which are prerequisites for any propellant composition. Based on this assumption, the proper design and subsequent acceptance of a particular composition for a given weapon is made as follows.

At least three small lots of propellant are made for the particular weapon to which the improved composition is to be fitted or for which a propelling charge is required.* With a knowledge of the weapon characteristics and of the functioning of other propellant compositions in the weapon, an attempt is made to manufacture these three propellants over a fairly wide web range; one lot will have a web that burns slightly too slowly, one will burn at nearly the correct rate, and one will burn a little too fast for the weapon.†

Each of the three lots of propellant is test-fired in the weapon for which it is being designed, in order to establish the charge-velocity and charge-pressure relationships. This is done by slowly building up the amount of charge used until a quantity of charge is reached that will produce the service velocity of the weapon, or to a point where the firings must be discontinued either because the pressure limit has been exceeded or because the chamber capacity has been reached. Since further calculations are based on the results of these test firings, they should be conducted with care.

The following is an application of the principle described above: Figure 4-1 represents the charge-velocity and charge-pressure curves for three experimental lots of propellant plotted on the same ordinate. Examining these curves, it can be determined that Lot 1 does not meet the ballistic requirements of the weapon because the rated maximum pressure (48,000 psi)‡ will be exceeded before the desired muzzle velocity of 3,500 ft per sec is attained; the medium web propellant (Lot 2) also fails to meet requirements for the same reason;

---

*From preliminary interior ballistic calculations there probably is available an estimate of the web required. However, it is usually considered advisable to test-fire webs slightly larger and slightly smaller (±10 percent) than the estimated web, in addition to the one indicated, because of the lack of specific data providing an accurate value of the burning rate.

†The relative quickness of a propellant is defined as the ratio of dP/dt of a test propellant to dP/dt of a standard propellant of the same composition taken at the same initial temperature and loading density of a closed chamber (bomb). (See paragraphs 4-10 through 4-20.)

‡The rated maximum pressure for any type of gun is that value of the maximum pressure which is specified in the propellant specification as the upper limit of average pressure which may be developed by an acceptable propellant in the form of propelling charges which will impart the specified muzzle velocity to the specified projectile.

the slowest propellant (Lot 3) can meet the requirements. The completion of propellant selection depends on the interpretation of these curves.

Figures 4-2 and 4-3 are constructed from data taken from the curves of figure 4-1. Figures 4-2 and 4-3 are called "design curves." Figure 4-2 represents the relationship between web size and velocity at 95 percent of the rated maximum pressure. Figure 4-3 is a web-charge curve, at service velocity (3,500 ft per sec), plotted from values taken from the charge-velocity curves. The values used for plotting curve 2 are obtained by tracing, on the charge-pressure curve of figure 4-1, the abscissa which represents 95 percent of the rated maximum pressure (46,000 psi). Wherever this trace intersects a pressure curve, the ordinate of the intersection is traced to the right to where it intersects the corresponding charge-velocity curve. From this latter intersection, the corresponding velocity is obtained. This value is plotted against the web of the propellant in figure 4-2. Having obtained the web-velocity curve (figure 4-2), the ordinate representing the service velocity (3,500 ft per sec) can be traced to the point of intersection with the curve, and the corresponding abscissa determined. This value represents the web that will give a service velocity at 95 percent of the rated maximum pressure. In this example, the most desirable web to meet the ballistic requirements is found to be 0.099 inch. Projecting this web value vertically to figure 4-3, it is found that approximately 409 ounces of propellant will be required.

While the determination of the optimum web was successful in this particular example, it may not be so successful under all conditions. For instance, it may be that the normal ballistic requirements of a certain weapon are too severe for a given propellant composition.

4-8. Determination of Web Range. Once the optimum web for a given composition has been determined, it may not be feasible to manufacture a grain with exactly the prescribed dimensions. To meet this difficulty, a web

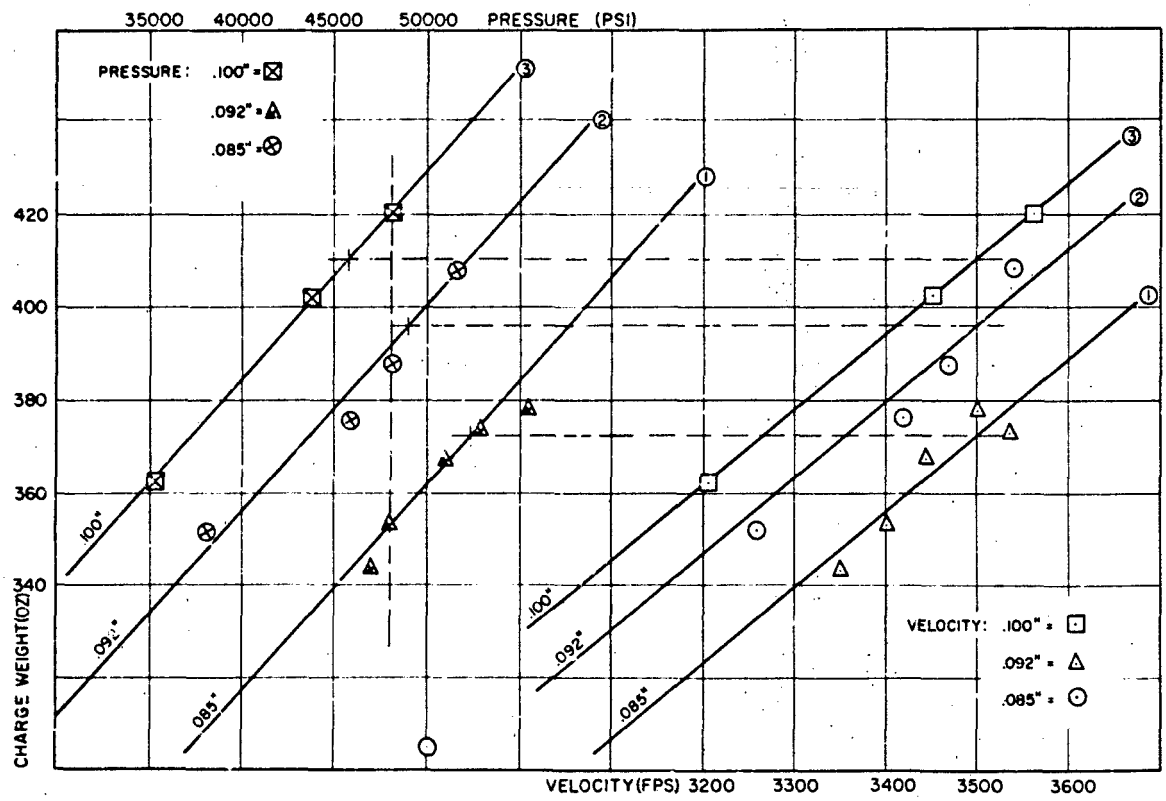

Figure 4-1. Pressure velocity curve

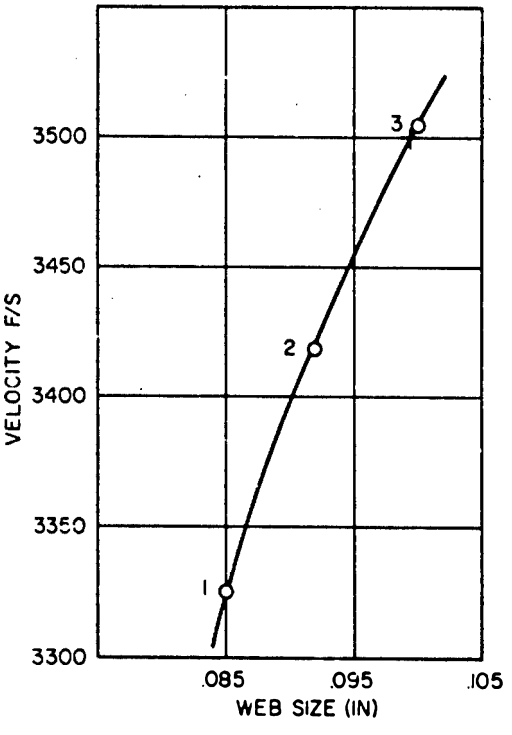

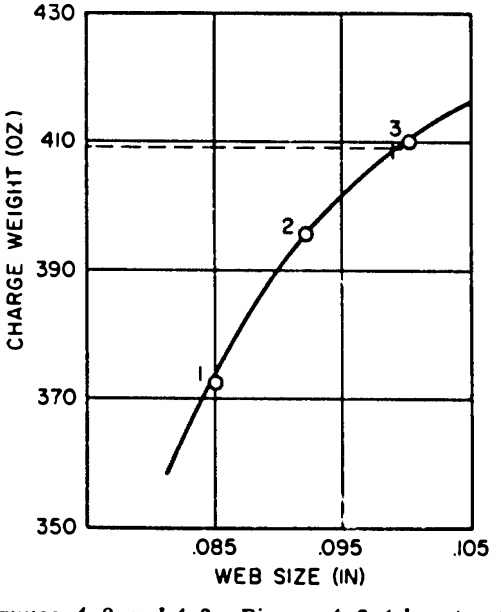

Figures 4-2 and 4-3. Figure 4-2 (above) represents the relationship between web size and velocity at 95 percent of the rated maximum pressure, and figure 4-3 (below) is a web-charge curve

range of thickness must be established. The lower limit of web thickness is set by pressure limitations, while the upper limit depends on such things as flashlessness and chamber capacity. To establish the web range, it is necessary to fire several propellant lots with web thicknesses approaching the maximum and minimum web limits in the particular gun for which the grain is intended. To indicate any tendency to produce erratic pressures, the charge weights of these firings should be somewhat in excess of those required to give service velocity. The web range established should be as wide as possible for manufacturing feasibility when the gun-ammunition combination is desired to deliver a velocity close to the maximum attainable. Under this condition, the web range that will satisfy the requirements is very narrow and requires tight control of manufacturing processes.

Since the optimum web was determined by assuming 95 percent of the rated maximum pressure, it is therefore the thinnest web that can be used. Any material reduction of the web will tend to develop a service pressure in excess of the allowable maximum. However, thin webs (which tend to produce high pressures) are somewhat desirable since they require less charge to meet a given set of ballistic conditions.

Large webs tend to leave unburnt propellant at the muzzle and to increase the muzzle pressure. Both factors increase the tendency to flash. If the web is too thick, the chamber capacity may be exceeded before the velocity level is attained. In certain large-chamber, high-velocity guns the velocity at a constant pressure may begin to decrease as the web exceeds a certain value (this is not a common occurrence with normal guns).

REFERENCES AND BIBLIOGRAPHY

1. Alexander, Jerome, "Colloid Chemistry," D. Van Nostrand, New York, 1919, vol. 4, pp. 117-120.

2. McFarland, "Textbook of Ordnance and Gunnery," John Wiley and Sons, New York, 1929.

3. Marshall, "Explosives," Blakiston, New York, 1919, vol. 1, pp. 312-313.

4. Picatinny Arsenal Technical Report No. 165.

5. Proof Officer's Manual, Aberdeen Proving Grounds, February 1929, pp. 158-162.

LIST OF SYMBOLS*

- D = maximum outer grain diameter
- D_g = die diameter, or external diameter of green grain
- D_D = dry grain diameter
- d = inner diameter of grain perforation
- d_g = pin diameter, or green perforation diameter
- d_D = dry perforation diameter
- L = grain length (usually 2 to 3 times the maximum diameter)
- W = web, or minimum distance between two directly opposing surfaces
- W_i = inner web, or minimum distance between two directly opposite interior surfaces of the grain
- W_{ig} = green inner web
- W_{iD} = dry inner web
- W_o = outer web, or minimum distance between an interior surface and a directly opposing exterior surface
- W_{og} = green outer web
- W_{oD} = dry outer web
- W_a = average of the inner and outer webs
- W_{aD} = average dry web
- P = pin circle diameter
- S_{wo} = percent shrinkage of outer web
- S_{wi} = percent shrinkage of inner web
- S_d = percent shrinkage of perforation

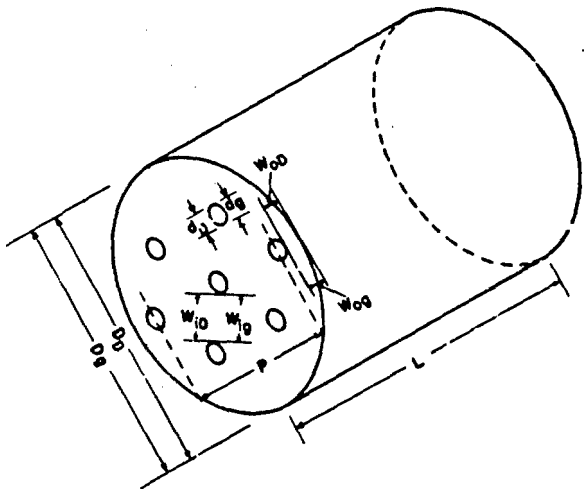

Figure 4-4. Multiperforated grain

4-9. In paragraphs 4-7 and 4-8, the procedure for establishing web size was described. In this section, the procedure for designing the proper-sized die to manufacture a grain of desired web size will be described.

Propellants are shaped into their final form in a plastic condition. This plasticity is the result of the use of volatile solvents to disperse the nitrocellulose among the other ingredients of the colloid. Subsequent evaporation of the solvents during the drying process causes a shrinkage of the grain that must be allowed for in the grain design. As stated in the preceding paragraphs, a major factor in the control of burning rate is the control of the web dimensions. Once the dry grain dimensions and percentage shrinkage for a given composition have been established, the propellant can be made with reasonable assurance that its dry dimensions will be close to expectation. The following formulas are used.

$$S_{wo} = \frac{W_{og} - W_{oD}}{W_{og}} \times 100 \quad (1)$$

$$S_{wi} = \frac{W_{ig} - W_{iD}}{W_{ig}} \times 100 \quad (2)$$

$$S_d = \frac{d_g - d_D}{d_g} \times 100 \quad (3)$$

$$D_D = 3d_D + 4W_{aD} \text{ (for multiperforated grain)} \quad (4)$$

$$d_g \text{ (pin size)} = \frac{d_D}{100 - S_d} \times 100 \quad (5)$$

$$W_{aD} = \frac{W_{id} + W_{od}}{2} \quad (6)$$

$$\frac{W_{oD}}{W_{id}} = 1.00 \text{ to } 1.15 \text{ (for multiperforated grains)} \quad (7)$$

$$D_g \text{ (bore)} = 3d_g + 2W_{og} + 2W_{ig} \quad (8)$$

$$P \text{ (pin diameter circle)} = 2d_g + 2W_{ig} \quad (9)$$

*See figure 4-4 for application of symbols.

$$W_{og} = \frac{W_{oD}}{100 - S_{wo}} \times 100 \qquad (10)$$

$$W_{ig} = \frac{W_{iD}}{100 - S_{wi}} \times 100 \qquad (11)$$

For example, to design the die and pin plate necessary for the manufacture of a propellant with an average web of 0.0220 inch and a perforation diameter of 0.0127 inch, assume the shrinkages for this composition for this web are S_d = 21.0 percent, S_{wo} = 35.0 percent, S_{wi} = 25.0 percent, and the ratio $\frac{W_{oD}}{W_{iD}}$ = 1.04. The solution is as follows.

$$d_g \text{ (pin size)} = \frac{0.0127}{100 - 21} \times 100 = \underline{0.0161} \qquad (5)$$

$$W_{oD} = 0.0229 \text{ in. and } W_{iD} = 0.0211 \text{ in.}$$

$$W_{aD} = \frac{W_{iD} + W_{oD}}{2} = 0.022 \text{ in.} \qquad (6)$$

$$W_{og} = \frac{W_{oD}}{100 - S_{wo}} \times 100 \qquad (10)$$

$$= \frac{0.0229}{100 - 35} \times 100 = 0.0352 \text{ in.}$$

$$W_{ig} = \frac{W_{iD}}{100 - S_{wi}} \times 100 \qquad (11)$$

$$= \frac{0.0211}{100 - 25} \times 100 = 0.0281 \text{ in.}$$

$$D_g \text{ (bore)} = 3d_g + 2W_{og} + 2W_{ig} \qquad (8)$$

$$D_g = 3(0.0161) + 2(0.0352) + 2(0.0281) = \underline{0.175}$$

$$P \text{ (pin circle diameter)} = 2d_g + 2W_{ig}$$

$$P = 2(0.0161) + 2(0.0281) = \underline{0.0883}$$

This completes all the data required for multiperforated propellant except the length, which is usually about 2.1 times the dry diameter (D). The dimensions of the die, pin plate, and length of cut are:

d_g = (pin diameter) = 0.0161 in.
D_g = (bore diameter) = 0.175 in.
P = (pin circle diameter) = 0.0883 in.
L = (grain length) = 0.110 in.

This example is typical for web calculations. The shrinkage values actually vary widely for different propellant compositions. Representative shrinkage data for some common propellants are given in table 4-4.

Table 4-4

Representative shrinkage data (percentages)

Composition	Type	Web (dry)	L	S_d	S_{Wi}	S_{Wo}	W_a
M1	MP	.03	7	25	40	27	33
	SP	.02	3	40	...	...	20
M2	MP	.035	3	14	20	20	20
	SP	.03	4	33.5	...	...	7
		.09	1.3	14	...	...	25.5
M6	MP	.103	3.5	27	32	24.5	28.5
M10	MP	.04	6	38	40	29	34
	SP	.024	9.5	40.5	...	...	34.5
		.018	5.2	49	...	...	30.5
M15	MP	.055	2	13	7.5	7.5	7.5
M17	MP	.098	1	10	13	1	7.5

CONTROL OF BURNING SURFACE

4-10. Notation. Each of the authors of the various ballistics systems which we are about to consider has used his own set of symbols to define the parameters involved. Because this condition exists in the literature, it has been difficult to standardize on any one set of symbols. However, where possible, an attempt has been made to use consistent notation here. In the instances where different notation has been used by different authors to define the same quantity, the symbols have been changed to read alike. Where apparently similar, but not identical, quantities have been encountered, it has been impossible to identify such parameters by uniform notation, and, in such cases, the symbols from the original treatises have been retained. Tables of the original notation found in the references are given in table 4-7.

4-11. Burning of Propellants. The burning of propellants is a surface phenomenon. A propellant grain burns in parallel layers, in directions perpendicular to its ignited surfaces, at a rate dependent on the initial temperature and pressure. Under constant pressure, a propellant burns with uniform velocity. An increase in initial temperature or pressure causes an increase in the characteristic burning rate of a composition, so that a rapid acceleration of burning rate results from burning a propellant under confinement. Under variable pressures, as in a gun, a grain will burn at a variable rate.

4-12. Linear Burning Rate. The linear burning rate is the distance (in inches) normal to any surface that the propellant burns in unit time (say, one second). Theoretically, this property is a function of the chemical composition of the propellant and is not a function of propellant geometry. At present, there are two methods used to determine burning rates, the strand burner and the closed bomb.

a. Strand Burner. This method is applicable only if the propellant is in the shape of a strand, or a strip, such as in rocket propellants (in which it has its most pertinent application). This device measures the time required for a propellant strand to burn a predetermined distance (five inches between fixed electric probes). With this method, it is possible to measure burning rates at any temperature. However, burning rates are usually measured at -40°C, +21°C, and +71°C, at pressures varying from atmospheric up to 50,000 psi at any specified pressure intervals.

b. Closed Bomb.[2] This method is used for most gun propellants, which are not usually manufactured in the form of strands. The closed bomb is a thick-walled, steel-alloy cylinder with removable threaded plugs in front and rear which permit access to its interior. The front plug contains the ignition mechanism, and the rear plug contains a piezoelectric gage. The bomb is cooled by a water jacket.

The closed bomb test is used to obtain data, under varying conditions of temperature and pressure, for use in determining the interior ballistic properties of propellants, such as the linear burning rate, relative quickness, and relative force. This test allows a prediction to be made of the behavior of any given propellant in any gun, serves as a manufacturing control test, and may serve as a substitute for proving ground tests. Usually, the output of the gage is recorded as time-rate of pressure rise as a function of the pressure.

When the closed bomb test is used, a comparison is made between closed bomb results of a propellant under test and of previous lots of propellants of the same composition of known ballistic value. Mathematical treatment of closed bomb results, dP/dt as a function of p, together with propellant granulation form functions (paragraph 4-20), yields the linear burning rate dX/dt. The actual method of obtaining the data may vary at different establishments, but at Picatinny Arsenal an oscillographic method is used, which measures the pressure developed in the bomb by means of a quartz piezoelectric gage. The circuitry used enables the charge generated by the gage to cause the horizontal deflection (V_X) of an oscilloscope trace to be proportional to the pressure (P) in the bomb, while vertical deflection (V_Y) is proportional to the rate of change of pressure (dP/dt) at the same instant. The maximum pressure developed in the bomb is measured as the maximum horizontal deflection of the trace.

In this method, the data are obtained as oscillograms superposed on rows of calibration dots. (See figure 4-5, which illustrates a typical

trace.) The dots are set 0.25 volt apart (corresponding to approximately 5,000-lb pressure increments) and distances between dots are measured by use of a transparent interpolator, shown in figure 4-6. The complete description of the apparatus and test procedure may be found in reference 1. Interpretation of the data obtained from the oscillograms enables a determination of the ballistic properties of the propellant under test.

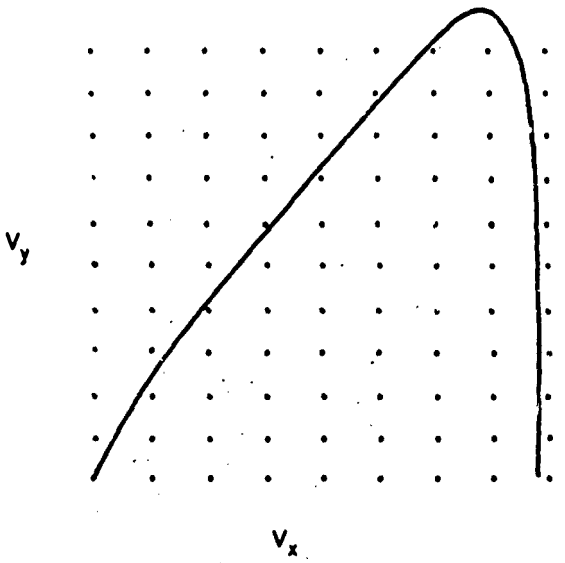

Figure 4-5. Pressure (P) versus rate of change of pressure (dP/dt)

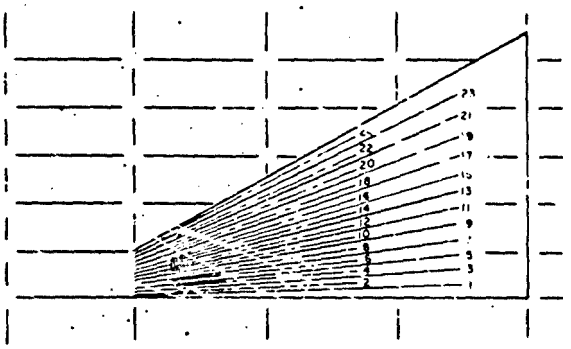

Figure 4-6. Transparent interpolator

This description is confined to methods of calculation and interpretation of the data obtained. The values of V_x and V_y may be converted respectively to values of pressure and rate of change of pressure by equations (12) and (13), which are derived in appendix I of reference 3.*

$$P = K(C_x V_x) \tag{12}$$

$$dP/dt = \frac{K}{RV_y}\left[\frac{1}{1 - \Delta m\left(\frac{C_y}{C_x}\right)}\right] \tag{13}$$

where

- P = pressure developed by the burning propellant
- dP/dt = time-rate of change of pressure of the burning propellant
- K = gage constant of the piezoelectric gage
- V_x = voltage across the capacitance C_x
- V_y = voltage across resistance R
- C_x = capacitance of the pressure-measuring circuit
- C_y = capacitance of the rate-of-change measuring circuit
- R = resistance in the rate-of-change measuring circuit
- Δm = slope = $\Delta V_y/\Delta V_x$ at any point on the curve.

The expression

$$\left[\frac{1}{1 - \Delta m\left(\frac{C_y}{C_x}\right)}\right]$$

is a correction factor due to the capacitor C_y in the rate-measuring circuit. A nomograph has been devised which enables this correction factor to be read directly from the dP/dt curve with a minimum of mathematical computation.

---

*For the sake of consistency within this section, the symbols of the original reference have been substituted as follows:

	Original reference[3]	This handbook
a	= covolume of propellant	= η
a_i	= covolume of igniter	= η_i
B	= shortened notation for equation (15)	= C
C	= shortened notation for equation (16)	= H
h	= propellant web	= W
m_o	= weight of unburned propellant	= C
m_i	= weight of igniter	= C_i
w	= grain width	= D
Z	= fraction of web burned	= N/C
slope	= $\Delta V_x/\Delta V_y$	= Δm

To calculate a linear burning rate from the oscillographic data obtained, a method used at Picatinny, considered to be the best-balanced between accuracy and speed, uses equation (14).

$$\frac{dX}{dt} = \frac{dZ/dt}{S_x/V_o} \tag{14}$$

$$= \frac{\left[\left(\frac{1}{1 + \frac{G}{P - P_i}}\right) - \left(\frac{1}{1 + \frac{G}{P - P_i}}\right)^2\right]\left[\frac{dP}{dt}\left(\frac{H}{P - P_i}\right)\right]}{S_x/V_o}$$

where

P and dP/dt are obtained as described above

P_i is the pressure due to the burning of igniter alone, which is obtained empirically. About 300 psi are developed by two grams of black powder in a 174-cc bomb. For rough approximation, P_i in equation (14) may be taken equal to zero.

G is calculated from equation (15).

$$G = \frac{(P_{max} - P_i)\left[1 - (\eta + \frac{C}{C_i}\eta_i)D_o\right]}{(\eta - b)D_o} \tag{15}$$

in which

- C = weight of propellant
- C_i = weight of igniter
- η = propellant covolume by the method of reference 4. For sample calculation, see reference 3, Appendix II-F, p. 19 ff.
- η_i = igniter covolume, assumed to be 0.87 cm^3/gm. (See reference 5.)
- D_o = loading density of propellant, alone, C/V_B
- b = specific volume of propellant; the reciprocal density before combustion. (For sample computation, see reference 3, Appendix II-G, p. 20.)

H is calculated from equation (16).

$$H = \frac{1 - \left(b + \frac{C_i}{C}\eta_i\right)D_o}{(\eta - b)D_o} \tag{16}$$

$Z = \frac{N}{C}$ = fraction of powder burned

$$= F\left[\frac{1}{\left[(1 + \frac{G}{P - P_i})\right]}\right]$$

dZ/dt = rate of burning of fraction of powder burned at time t = (17)

$$\left[\left(\frac{1}{1 + \frac{G}{P - P_i}}\right) - \left(\frac{1}{1 + \frac{G}{P - P_i}}\right)^2\right]\left[\frac{dP}{dt}\left(\frac{H}{P - P_i}\right)\right]$$

S_x/V_o = ratio of surface area to original volume when grain has burned a distance x, normal to grain surface.

Form functions of Z and S_x/V_o in terms of X may be calculated for each grain geometry. The form functions for the most common geometries are included in paragraph 4-20, where they are correlated with their equivalent expressions in the Hirschfelder interior ballistic system.

A consideration of dP/dt versus P, plus the appropriate form function, equation (14), yields the linear burning rate, dX/dt with respect to P, for a particular grain geometry.

$$\frac{dX}{dt} = \frac{dZ/dt}{S_x/V_o} = \text{linear burning rate} \tag{14}$$

After the linear burning rates have been calculated from equation (14), the procedure is to plot these values against pressure on appropriate graph paper (figure 4-7) to determine a burning equation. The burning of most propellants seems to follow one of three general laws:

$$dx/dt = a + BP \tag{18}$$

$$dx/dt = BP^n \tag{19}$$

$$dx/dt = a + BP^n \tag{20}$$

where a, B, and n are constants. (See paragraph 4-15.)

4-13. Relative Quickness. Relative quickness is defined as the ratio of the average rate of pressure rise of a propellant lot under test to the average rate of pressure rise of a standard

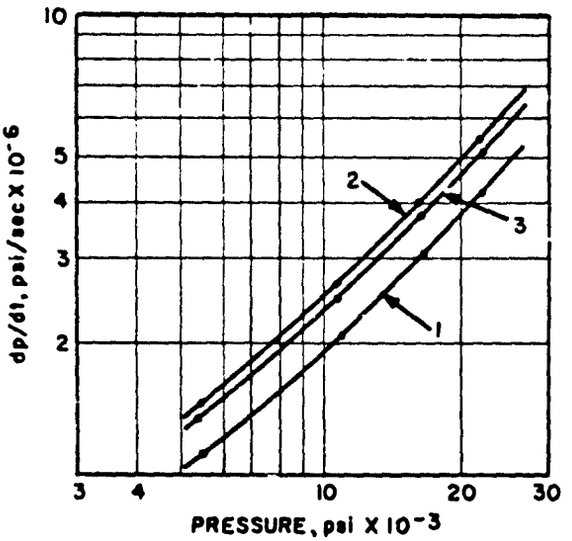

Figure 4-7. Linear burning rate versus pressure

propellant of the same formulation at the same specified pressures when each is fired in the same bomb under the same loading density and test conditions. When the test sample and standard propellant are similar in quickness, the relative quickness can be taken as the ratio of the V_y values without making any corrections for the circuit capacitance. When the quickness of the test propellant and standard differ widely, equations (12) and (13) must be used to obtain the correction for V_y before comparison can be made. The values of dP/dt are plotted as functions of P (calculated from the 0.25-volt intervals of V_x). The values of dP/dt at 5, 10, 15, 20, and 25 thousand psi are taken from the graph (figure 4-7) and the relative quickness is calculated as in the example below. (See table 4-5.)

4-14. Relative Force. In interior ballistics use, the term "force" is related to the energy released by a given propellant; that is, Force = $(PV)_T = nRT_v$, where (in closed bomb work) P is the maximum pressure developed and V is the volume of the bomb. Since the bomb volume is constant, relative force is defined as the ratio of the observed maximum pressure developed by a lot of propellant under test, to the maximum pressure developed by a standard propellant, when each is fired in the same bomb under the same test conditions. Since pressure is measured as $P = KC_xV_x$ [equation (1)], if C_x is constant the relative force reduces to the ratio of the maximum x-voltages

Table 4-5

Relative quickness and relative force

P	dP/dt x 10^{-6}			Rel. quickness, ratio test/std. (%)		Rel. force, ratio test/std. (%)	
	Prop. #1 (std.).	#2	#3	#2	#3	#2	#3
*5,000	1.03	1.32	1.27	123	123		
6,000	1.18	1.55	1.46	132	124		
10,000	1.82	2.44	2.27	134	125		
15,000	2.73	3.50	3.35	128	123	$\frac{1.77}{1.81}$ =	$\frac{1.76}{1.81}$ =
20,000	3.67	4.70	4.55	128	124		
25,000	4.66	6.09	5.82	131	126	98.0	97.2
Avg Max				130	124		
	V_x 1.81	1.77	1.76				

*Value of dP/dt used, extrapolated.

recorded on the oscillograms. Values of maximum V_x are obtained by measuring a vertical tangent to the trace at the point of maximum pressure, using the 0.25-volt interpolator. A sample calculation of relative force is included above.

For a complete description of closed bomb technique as used at Picatinny Arsenal, see reference 3. Another application of closed bomb information as used by the Navy is described in reference 7.

4-15. The Proportional Law of Burning Rate.[8] The minimum distance between any two adjacent surfaces of a propellant grain is called the web. The rate at which the web decreases is a function of the gas pressure produced in a gun due to the burning of propellant grains. It is assumed that burning proceeds only on the inner and outer grain surfaces, that is, burning of the ends of the grains is neglected. The type of burning most usually encountered follows equation (19), $dx/dt = BP^n$ (in. per sec). For M10 propellant this equation would be

$$\frac{dx}{dt} = 4.53 \times 10^{-3} P^{0.7} \qquad (21)$$

For ease of computation, it is desirable to express burning rate as proportional to pressure

$$\frac{dx}{dt} = r_1 = BP \qquad (22)$$

or, to make equation (19) more useful in the Hirschfelder system, an attempt is made to make n equal to unity, in which we consider what should be the value of the coefficient B to make n = 1, while the value of r_1 remains constant. The value of B used in equation (22) is an effective value. This effective value is obtained from a plot of the curve of equation (21). (See figure 4-8.) A curve of this nature allows a person desiring to use a proportional law to obtain a value of B that best represents the actual burning law over a desired pressure range.

The abscissa is first divided into arbitrary intervals. Then, for each of these intervals, the portion of the curve (from the start of the interval to the maximum point of the curve included in the interval) is replaced by a line of least-square fit. The least squares are obtained

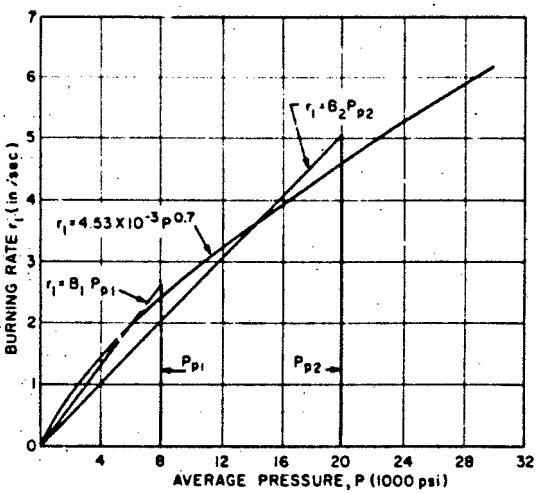

Figure 4-8. Proportional law to determine value of B for n = 1

at three-, six-, and nine-tenths of the maximum value of an interval. The maximum value for the intervals is called the peak pressure (P_p), distinguishing it from all other values, which are average pressure values. The slope of each of the straight lines thus obtained is B. It can be seen from figure 4-8 that, as the peak pressure increases, the slope decreases; thus, the maximum value of B occurs at the minimum peak pressure. Values of B are plotted against peak pressures in figure 4-9.

4-16. Effect of Grain Shape on Burning Rate. Although the linear burning rate of a propellant is characteristic of the formulation and the pressure, the granulation affects the overall rate at which the propellant is transformed to gas, since the surface exposed is determined by the granulation. The best form of propellant grain from a ballistic viewpoint is one which, with the smallest weight of charge, will impart a prescribed velocity to a projectile without developing a pressure in excess of the permitted maximum. In this connection, uniformity of ballistic effect must also be considered. Figure 4-10 illustrates the relation between grain shape and ballistic effect. It should be noted that, for equal weights of identical propellant composition, the position of the pressure peak in the gun is very weakly dependent on the grain shape, while projectile velocity depends only on charge weight. The criterion for the selection of a particular granulation is the maximum pressure.

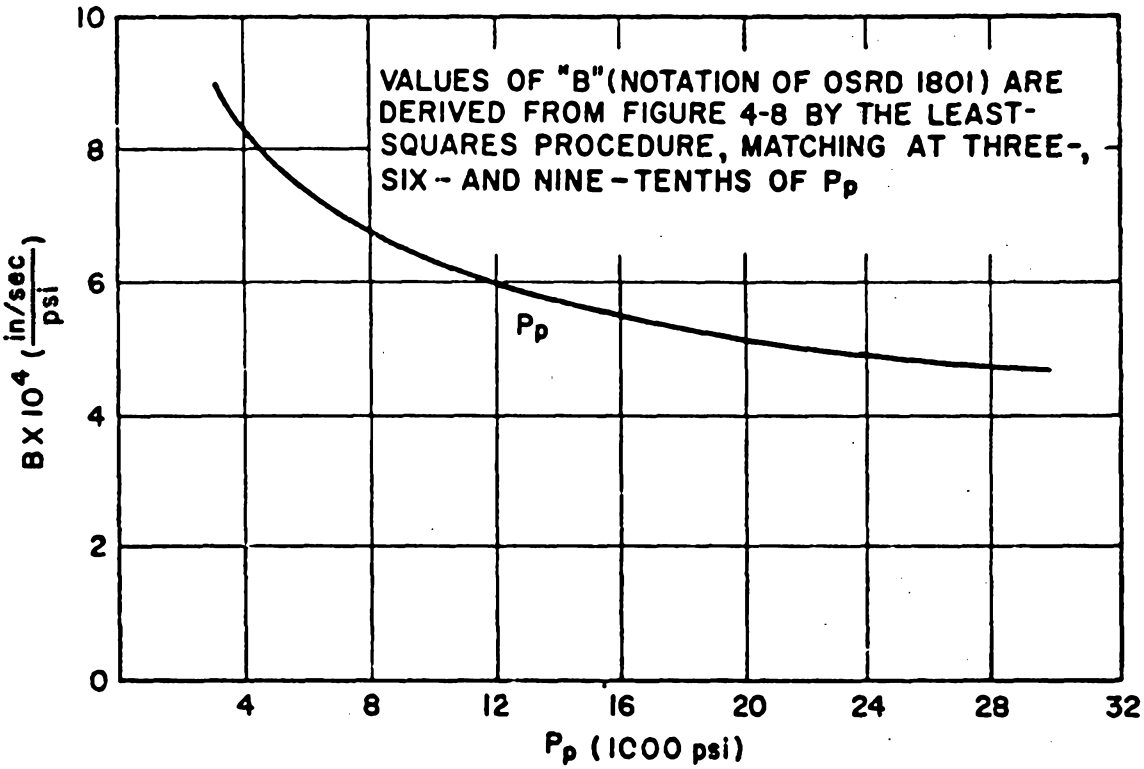

Figure 4-9. Values of B determined by least-squares fit

The most important dimension of the propellant grain is the web thickness. The web size of a multiperforated grain refers to its average web. Relatively slight changes in the average web of a propellant result in appreciable changes in the required weight of propellant charge and maximum pressure produced, for a given muzzle velocity of the projectile. Figure 4-11 illustrates the relation between surface area and weight percentage burned for various grain shapes.[10] When z (or N/C, the fraction burned), is zero, the ratio S/S_0 must be unity for all grain shapes.

4-17. The Form Function. It is assumed that all of the exposed surfaces recede at the same rate when propellant burns. Thus, there is a simple relation between the fraction of propellant burned and the distance that each surface has regressed. The mathematical expression of this relationship, for any particular propellant granulation, is called the form function for that granulation. In the following paragraphs we present two approaches to the solution of workable form functions, and show how the different systems may be correlated. Corner's[9] treatment is similar to the Hirschfelder[4] treatment, except that the former uses a form coefficient θ, based on experiment, whereas the latter uses a set of k's based on geometry.

4-18. Corner Form Coefficient, θ. If a long cord of propellant, of initial diameter D, burns under a pressure P, the rate of recession is uniform over the surface of the cord, and is expressed as 1/2B(P). The amount of gas generated up to time t is $C\phi(t)$, where C is the initial weight of the cord and ϕ goes from 0 to 1. The diameter of the cord remaining at the time t is fD.

Neglecting the small contribution from the burning of the ends of the cord, we have the geometrical relation

$$\phi = 1 - f^2 \qquad (23)$$

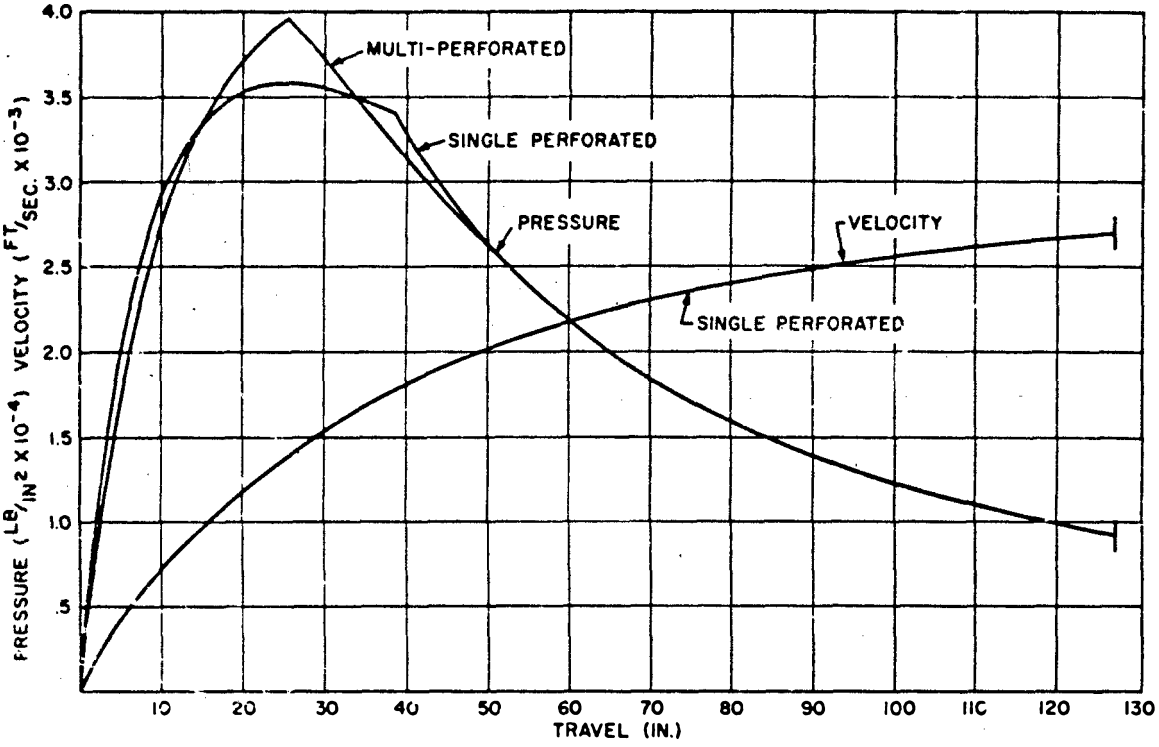

Figure 4-10. Pressure-travel and velocity-travel curves

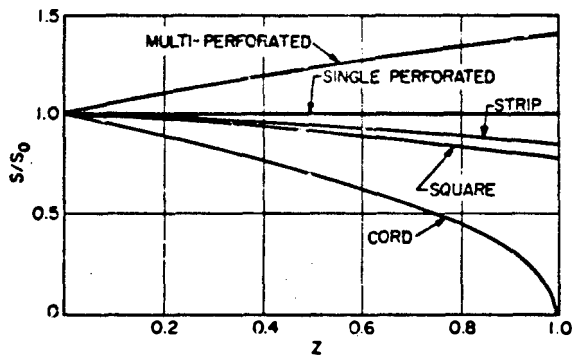

Figure 4-11. Surface area versus weight-percent burned for various grain shapes

and the expression of our definition of the rate of burning is

$$D\frac{df}{dt} = -B(P) \qquad (24)$$

In the solution of the equations of interior ballistics, f is a convenient variable, but as it appears only in these two equations and not in the other fundamental equations, we may eliminate f, giving

$$\frac{d\phi}{dt} = \frac{2B}{D}(1-\phi)^{1/2} \qquad (25)$$

These equations are true for any number of long cords. The web size (D) is the minimum distance between any two adjacent burning surfaces; for cord propellant, the web is equal to the diameter.

Analogous relations may be written down for other shapes. Single perforated grains of initial external and internal diameters d_1 and d_2, respectively, have $D = \frac{1}{2}(d_1 - d_2)$, and fD as the annulus remaining at time t. The geometrical relation is

$$\phi = 1 - f \qquad (26)$$

and the burning rate is still the same as in equation (24), leading to

$$\frac{d\phi}{dt} = \frac{B}{D} \qquad (27)$$

This assumes that the rate of burning is the same on all surfaces of the propellant, and that the inner and outer surfaces are coaxial.

Both cord and single-perforated grains may be brought into the same scheme by choosing the dimension of the grain along a direction normal to the surface at two points of intersection, where the direction is in one instance passing into, and at the other instance passing out of, the propellant. The smallest such diameter is called the web size.

Next, we define fD as the remaining web when a fraction ϕ of the propellant has been turned into gas. From the definition of the rate of burning, given in equation (24),

$$D\frac{df}{dt} = -B(P) \qquad (24)$$

For certain shapes, $\phi = 1$, when $f = 0$. For a still more restricted class of shapes, ϕ and f are related geometrically by

$$\phi = (1 - f)(1 + \theta f) \qquad (28)$$

where θ is a constant for a given shape. For example, $\theta = 0$ for single perforated grains, and $\theta = 1$ for long cords.

It is seen that D is defined by reference to a direction which will not exist for a shape chosen at random. For shapes of fairly high symmetry, D will have a meaning. The definitions of f and equation (24) then follow without exception. There is, however, no guarantee that when this dimension has been eaten away all the solid propellant will have turned into gas; only for simple shapes does this occur. Finally, equation (28) is a very special form. We shall discuss the most common shapes to illustrate the various possibilities.

With long cords and single perforated grains, there is no difficulty. The web is easily found, and equation (28) holds when $\theta = 1$ and 0, respectively. Equation (28) may be referred to as the "form function," with θ as the "form factor" or "form coefficient." θ is a measure of the change in the area of the burning surface as burning proceeds. The burning surface of a long tube remains constant ($\theta = 0$), and the surface area of a cord decreases to zero as the burning proceeds. The ratio of the initial and final surfaces is $(1 + \theta)/(1 - \theta)$. Thus, the larger the θ, the faster the decrease in surface and the faster the drop in the rate of evolution of gas at constant pressure. Shapes of positive θ are said to be "degressive," and those of negative θ to be "progressive." Shapes, such as tubes, with $\theta = 0$, are sometimes said to be "neutral."

The possible range of θ is restricted. θ cannot be less than -1, for otherwise ϕ would be negative for f near unity. Nor can θ be greater than unity, for then ϕ would be greater than unity for some accessible range of f. This does not mean that the cord, with its $\theta = 1$, is the most degressive shape possible. The sphere has a surface which decreases even more rapidly (figure 4-12). In this case, D comes out, by our prescription, as the diameter, and $\phi = 1$ when the remaining diameter is zero. Equation (28) cannot express precisely the relation between f and ϕ for every geometric shape, although a satisfactory approximation can often be made by a proper choice of θ. The true geometric form function is $\phi = 1 - f^3$ for a sphere. Although almost all grain shapes could be covered by writing ϕ as a cubic in f, this is not done because the analytical solutions of the ballistic equations would be much more difficult.

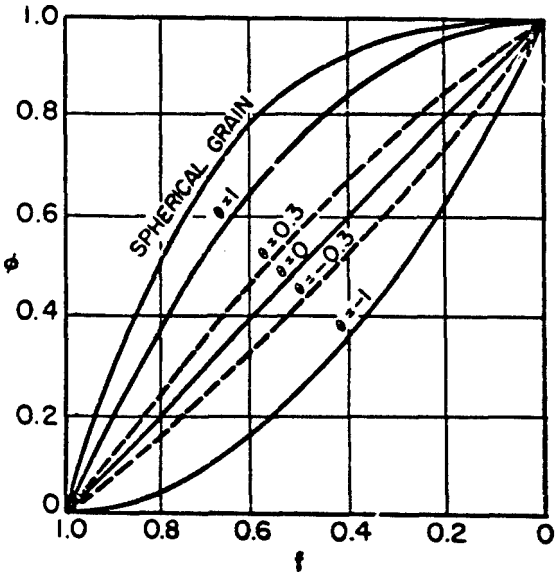

Figure 4-12. Relationship of form factor to rate of change of area of burning surface

4-19. Form Coefficient for OSRD 6468. Let N be the weight of propellant burned up to any time t, so that N/C is the fraction of propellant burned. Let W be the web thickness, which in the case of multiperforated grains is the minimum thickness before the grains splinter. Let f be the fraction of the web that remains unburned at any particular time. The OSRD 6468 ballistics are based on a form function that expresses N/C as a quadratic function in f; thus

$$N/C = k_0 - k_1 f + k_2 f^2 \qquad (29)$$

where k_0, k_1, and k_2 are all constants that depend on the granulation and grain shape. The form functions for all grain shapes, except the seven-perforated, can be expressed rigorously as cubic equations. However, since this would unnecessarily complicate the ballistics, and since the f^3-term is always quite small compared to the other terms, the quadratic approximation is used in practice. This approximation never differs from the exact expression by more than 0.05.

a. Constant Burning Surface. The form function for a grain with a constant burning surface is

$$N/C = 1 - f \qquad (30)$$

which is a simplification of equation (29). This is the simplest of all the form functions. Its use greatly simplifies our ballistic computations. It is derived from a consideration of a grain such as a sheet, whose web is so very small, compared to its length and width, that W/D and W/L can be considered equal to zero.

$$k_0 = 1$$
$$k_1 = 1$$
$$k_2 = 0$$

b. Strip Propellant. The web of this grain is its thickness and the k-coefficients are:

$$k_0 = 1$$

$$k_1 = 1 - \frac{W}{L} - \frac{W}{D} + \frac{W^2}{2LD}$$

$$k_2 = -\frac{W}{L} - \frac{W}{D} + \frac{W^2}{2LD}$$

c. Cord Propellant. Cord propellant is not used very much in the U. S. but is used extensively in Britain. The exact form function is

$$N/C = 1 - (1 - \frac{W}{L})f^2 - (\frac{W}{L})f^3 \qquad (30a)$$

but replacing f^3 by its approximate equivalent $(3/2)f^2 - (1/2)f$ gives the approximate form function

$$N/C = 1 + (\frac{W}{2L})f - (1 + \frac{W}{2L})f^2 \qquad (30b)$$

For cord propellant

$$k_0 = 1$$

$$k_1 = -\frac{W}{2L}$$

$$k_2 = -(1 + \frac{W}{2L})$$

For a very long cord, neglecting the burning of the ends of the cord, where W/4L is nearly zero, we can use

$$N/C = 1 - f^2 \qquad (31)$$

where

$$k_0 = 1$$
$$k_1 = 0$$
$$k_2 = -1.$$

d. Single-Perforated Grain. This granulation is in common use in the U. S. for small-caliber weapons. The web of this grain is one-half the difference between the outer and inner diameters. The form coefficients are

$$k_0 = 1$$

$$k_1 = 1 - \frac{W}{L}$$

$$k_2 = -\frac{W}{L}$$

No approximation was made here, but if W/L is quite small the form for constant burning surface may be used, and is recommended except for very accurate work.

e. Multiperforated Grain (Seven-Perforated). Form functions for the burning of this granulation, which is the most common in use in the U. S. for large-caliber weapons, are more complicated than those described above. The burning is considered to occur in two stages, a progressive stage, before the web burns

through to the formation of unburned splinters; and a regressive stage during the burning of the splinters. The burning in each stage is approximated by a separate quadratic form function.

1. Progressive Burning. The burning of the grain before splinter formation may be treated analytically. Values of k_0, k_1, and k_2, to be used in equation (29) for various values of the ratios D/d (grain diameter to web diameter) and L/D (grain length to diameter), are given in table 4-6. The curve of figure 4-13 (obtained from reference 4, based on reference 6) is a plot of the burning of a grain with D/d = 10, and L/D = 2.5. It will be noticed that the slope increases up to f = 0, where the splinters form.

2. Regressive Burning. After splintering, shown by the flex in the graph at f = 0, the slope decreases. This part of the curve is represented by another quadratic of the form

$$N/C = k_0' - k_1'f + k_2'f^2 \qquad (32)$$

This is actually a continuation of the curve to the left of f = 0. It is shown in reference 4 that if the curve is made to pass through the points ($f = f_0$, $N/C = 0$), ($f = 0$, $N/C = k_0$), and ($f = -0.5$, $N/C = 1$), the resulting expression is a satisfactory approximation to the form function in the regressive interval. Accordingly, the form function to use in the interval after splintering is given by the following equations.

Table 4-6

Form functions for seven-perforated propellant

D/d \ L/D		1.5	2.0	2.5	3.0	3.5
	k_0	0.8409	0.8362	0.8335	0.8316	0.8303
8	k_1	0.9111	0.9300	0.9414	0.9490	0.9544
	k_2	0.0702	0.0938	0.1079	0.1174	0.1241
	k_0	0.8498	0.8451	0.8423	0.8405	0.8391
9	k_1	0.9298	0.9507	0.9633	0.9717	0.9776
	k_2	0.0800	0.1056	0.1210	0.1312	0.1385
	k_0	0.8563	0.8516	0.8487	0.8468	0.8455
10	k_1	0.9447	0.9673	0.9808	0.9898	0.9963
	k_2	0.0884	0.1157	0.1321	0.1430	0.1508
	k_0	0.8612	0.8565	0.8536	0.8517	0.8503
11	k_1	0.9569	0.9809	0.9952	1.0048	1.0116
	k_2	0.0957	0.1244	0.1416	0.1531	0.1613
	k_0	0.8652	0.8603	0.8574	0.8554	0.8541
12	k_1	0.9673	0.9923	1.0073	1.0173	1.0245
	k_2	0.1021	0.1320	0.1499	0.1619	0.1704
	k_0	0.8682	0.8633	0.8604	0.8585	0.8571
13	k_1	0.9760	1.0020	1.0177	1.0281	1.0356
	k_2	0.1078	0.1387	0.1573	0.1696	0.1785

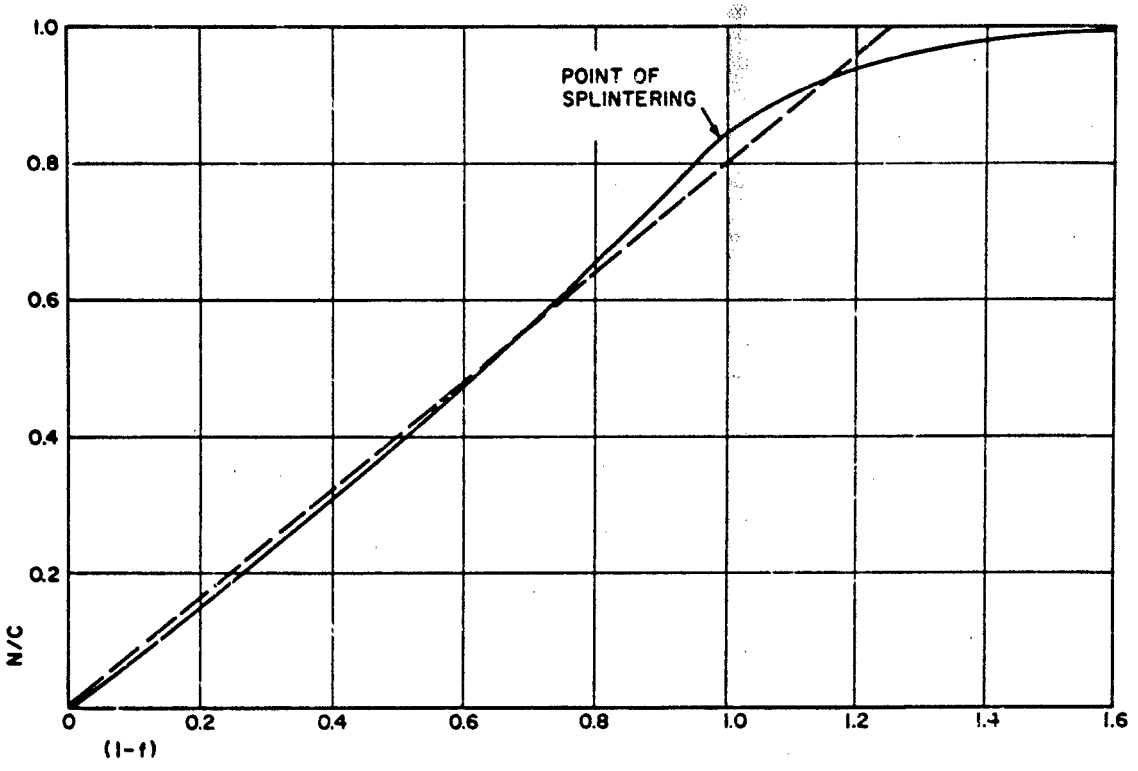

Figure 4-13. Actual versus theoretical burning curves

$$k_0' = k_0$$

$$k_1' = \frac{4f_0 (1 - k_0) + (k_0/f_0)}{2f_0 + 1}$$

$$k_2' = \frac{4 (1 - k_0) - 2 (k_0/f_0)}{2f_0 + 1}$$

3. Simplified Form Function for Seven-Perforated Propellant. It is often convenient for the purpose of rough calculations to consider the seven-perforated grains as having a constant burning surface throughout their entire burning. This approximation corresponds to replacing the true form function by the dotted line in figure 4-13, which is a graph of N/C = 1 - f with specific values. Since it is desired to vary f between unity at the beginning and zero when all of the propellant is burned, instead of between 1.0 and -0.25, as indicated by the dotted line in figure 4-13, we must define an adjusted web equal to 1.25 times the actual web thickness. With this adjusted web and the corresponding f,

$$\frac{N}{C} = 1 - f$$

Stating this another way, we may say that a seven-perforated propellant is ballistically equivalent to a single-perforated propellant of 1.25 times its web thickness. The factor 1.25 may vary somewhat between 1.23 and 1.28, depending on the conditions of firing, and on whether the ballistic equivalence of the two propellants is based on the same muzzle velocities or the same maximum pressures.

4-20. General Form Functions. The particular equations (form functions) used to describe the change in grain geometry during burning as a function of web or linear distance burned are determined by the ballistic method used. Paragraphs 4-18 and 4-19 have described the form functions used in the Corner and Hirschfelder systems. The form functions of the most common granulations, as used in the method of

subparagraph 4-12b, are included here along with their exact equivalents, since their derivation is time-consuming.[11] The symbols used in the various equations are listed below.

$\frac{N}{C}$ = fraction of charge burned
N = amount of charge burned
C = initial amount of charge
V_O = initial volume of grain
V_X = volume burned at any linear distance (X)
S_O = initial surface of grain
S_X = surface of grain burned at any linear distance (X)
$\frac{V_X}{V_O}$ = fraction of propellant remaining ($N/C = 1 - V_X/V_O$)
X = linear distance burned to flame front, perpendicular to burning surface
f = fraction of web remaining
$\frac{S_X}{S_O}$ = progressivity
R, r = larger and smaller radii, respectively, of grain geometry
W = web, or thickness
L = length
D = width
(Note that $Z = 1 - V_X/V_O$)

a. Equations for Strip Propellant. The exact formula for fraction of charge burned is

$$\frac{N}{C} = 1 + \frac{(LW + DW - LD - W^2)}{LD} f + \frac{(2W^2 - LW - DW)}{LD} f^2 - \frac{W^2}{LD} f^3$$

L and D are both assumed to be much greater than W, and the f^3 term is assumed negligible. With these assumptions, the Hirschfelder form can be shown to be

$$\frac{N}{C} = 1 - f$$

which is the Hirschfelder form function for a constant burning surface. The other equations are as follows.

$$\frac{S_X}{V_O} = \frac{2(LD + DW + LW) - 8(L + D + W)X + 24X^2}{Lwh}$$

$$Z = \frac{2(LD + DW + LW)X - 4(L + D + W)X^2 + 8X^3}{Lwh}$$

b. Equations for Cord Propellant. The exact equation for fraction of charge burned is

$$\frac{N}{C} = 1 + \frac{2R - L}{L} f^2 - \frac{2L}{L} f^3$$

where R is the radius of the cross section of the cord. The Hirschfelder approximation for this is

$$\frac{N}{C} = (1 - f)(1 + f) = 1 - f^2$$

on the basis that L is much greater than R, so that R becomes negligible by comparison. Since f is a decimal, it becomes insignificant when it is cubed, and the f^3 term drops out. The other equations, given without derivation, are as follows.

$$\frac{V_X}{V_O} = 1 - \frac{2(R^2 + RL)}{R^2L} X + \frac{4R + L}{R^2L} X^2 - \frac{2}{R^2L} X^3$$

$$\frac{S_X}{S_O} = \frac{2(R^2 + RL) - 2(4R + L)X + 6X^2}{R^2L}$$

$$Z = \frac{2(R + RL)X - (4R + L)X^2 + 2X^3}{R^2L}$$

c. Equations for Single-Perforated Propellant. The exact formula for N/C is

$$\frac{N}{C} = 1 + \frac{R - r - L}{L} f - \frac{R - r}{L} f^2$$

where the web (R - r) is assumed much less than the length (L), so that N/C becomes equal to (1 - f). This again is the Hirschfelder equation for a constant burning surface. The Hirschfelder equivalent, before simplification, is

$$\frac{N}{C} = 1 - k_1 f + k_2 f^2$$

where

$$k_1 = 1 - \frac{W}{L}$$

$$k_2 = \frac{W}{L}$$

(See subparagraph 4-19c.) The other equations are given below.

$$\frac{S_X}{V_O} = \frac{2(R - r + L) - 8X}{L(R - r)}$$

$$Z = \frac{2(R - r + L)X - 4X^2}{L(R - r)}$$

$$\frac{V_X}{V_O} = \frac{1 - 2(R - r + L)}{L(R - r)} X + \frac{4}{L(R - r)} X^2$$

d. Equations for Multiperforated Grain. The exact formula for N/C is

$$\frac{N}{C} = \frac{R^3 - R^2r - 5R^2r - 3r^3}{16(R^2 - 7r^2)} + \frac{14R^2L - 4RL - 114r^2L}{16(R^2 - 7r^2)}$$

$$+ \frac{9R^3 - 49R^2r + 35Rr^2 + 93r^3 - 20R^2L}{16(R^2 - 7r^2)}$$

$$+ \frac{40\ RrL + 60r^2L}{16(R^2 - 7r^2)} f$$

$$+ \frac{-13R^3 + 77R^2r - 111Rr^2 - 9r^3 + 6R^2L}{16(R^2 - 7r^2)}$$

$$+ \frac{-36RrL + 54r^2L}{16(R^2 - 7r^2)} f^2$$

$$+ \frac{3R^3 - 27R^2r + 81Rr^2 - 81r^3}{16(R^2 - 7r^2)} f^3$$

In the Hirschfelder system, the equivalent form function is represented by a cubic equation [see reference 4, p. 129, equations (14) and (15)] that is simplified to a pair of quadratics of the form

$$N/C = k_o - k_1 f + k_2 f^2$$

where the coefficients k_o, k_1, and k_2 are expressed in terms of grain diameter, grain length, and web. (See subparagraph 4-19d.) The other equations are

$$\frac{S_X}{V_O} = \frac{2\ [(R + 7r)L + (R^2 - 7r^2)]}{L(R^2 - 7r^2)} + \frac{-4\ [2(R + 7r) - 3L]X - 36X^2}{L(R^2 - 7r^2)}$$

$$Z = \frac{2\ [(R + 7r)L + (R^2 - 7r^2)]X}{L(R^2 - 7r^2)} + \frac{-2\ [2(R + 7r) - 3L]X^2 - 12X^3}{L(R^2 - 7r^2)}$$

REFERENCES AND BIBLIOGRAPHY

1. Jackson, W. F., "Closed Bomb Method of Powder Testing," E. I. Du Pont de Nemours & Co., Explosives Dept., Carney's Point Works, 1941.

2. Proof Directive-12, Rev. 3, Supplement to U. S. Army Specification 50-12-3, Powder, Cannon, Propellant.

3. Pallingston, A. O., and M. Weinstein, Method of Calculation of Interior Ballistic Properties of Propellants from Closed Bomb Data, Picatinny Arsenal Technical Report No. 2005, June 1954.

4. Interior Ballistics, A Consolidation and Revision of Previous Reports, Office of Scientific Research and Development Report No. 6468, July 1945.

5. Closed Bomb Burning of Propellants and High Explosives, Office of Scientific Research and Development Report No. 6329, January 1946.

6. Tschappat, W. H., "Textbook of Ordnance and Gunnery," John Wiley and Sons, New York, 1917.

7. Atlas, K., A Method for Computing Webs for Gun Propellant Grains from Closed-Vessel Burning Rates, Naval Powder Factory, R. and D. Dept., Indian Head, Md., Memorandum Report No. 73, January 1954.

8. Hughes, S. G., Summary of Interior Ballistics Theory for Conventional Recoilless Rifles, Frankford Arsenal, Report No. R-1140, September 1953.

9. Corner, J., "Theory of Interior Ballistics of Guns," John Wiley and Sons, Inc., New York, 1953, p. 30ff.

10. Hunt, Col. F. R. W., et al, "Internal Ballistics," Philosophical Library, New York, 1951, p. 52.

11. Julier, B. H., Form Functions for Use in Interior Ballistics and Closed Chamber Calculations, Naval Powder Factory, Indian Head, Md., Memorandum Report No. 3, February 1951.

Table 4-7
Table of symbols

Symbol	Unit	Definition
A	$in.^2$	Cross-sectional area of bore
a	$in.^3$ per lb.	$\eta - \frac{1}{\rho}$
a^o	...	$23{,}969\ (\frac{a}{F})$
B	$\frac{(in.\ per\ sec)}{(lb\ per\ in.^2)}$	Burning constant
b	ft^2 per sec^2	$\frac{2CF}{m'(\bar{\gamma} - 1)}$
C	lb	Charge weight
C_v	...	Specific heat (constant volume)
e_2	ft per sec	$\frac{j_1 CF(B/W)}{A}$
e_3	ft-lb per $in.^3$	$\frac{e_2^2\ m'}{v_c}$
F	ft	Powder impetus
f	...	Fraction of web remaining unburned
f_o	...	Initial value of f
g	ft per sec^2	Acceleration due to gravity
J	...	$\exp \int_o^z \frac{z\ dz}{q + z - uz^2}$
j_o	...	$\frac{N_o}{C}$
j_1	...	$k_1 - 2k_2 f_o$
j_2	...	$k_1 - \frac{1}{2}k_2$
k_o, k_1, k_2	...	Form-function constants
L	in.	Travel of the projectile
M	lb	Weight of projectile
m	slug	Effective mass of projectile
m'	slug	Modification of m
N	lb	Weight of powder burned
N_o	lb	Weight of powder burned when projectile begins to move
P	lb per $in.^2$	Space-average pressure

Table 4-7

Table of symbols (cont)

Symbol	Unit	Definition
P_o	lb. per in.^{2}	Initial value of P
p^o	lb. per in.^{2}	a^oP
P_r	lb. per in.^{2}	Pressure resisting projectile motion (friction)
P_x	lb. per in.^{2}	Pressure on base of projectile
Q	...	$\left(1 - \frac{\bar{\gamma} - 1}{2} J_1 f_o Z_b\right) \left(\frac{X_b}{X_o} - \eta\Delta_o\right)^{\bar{\gamma} - 1}$
q	...	$\frac{J_o Z_b}{J_1 f_o}$
R	$\frac{\text{energy}}{(\text{gm-mole}^o\text{K})}$	Gas constant
r	...	$\frac{a\Delta_o J_2 f_o}{Z_b}$
S	...	$J \int_o^Z \frac{dZ}{J}$
T	^{o}k	Absolute temperature of gas
T_o	^{o}k	Isochoric flame temperature
t	sec	Time from beginning of motion of projectile
u	...	$\frac{1}{2}(\bar{\gamma} - 1) - \frac{k_2 f_o}{J_1 Z_b}$
V	ft per sec	Velocity of projectile
V_c	in.^{3}	Chamber volume
W	in.	Web of powder
X	in.	Distance from the base of the projectile to a point fixed with respect to the gun
X_o	in.	Effective length of chamber = $\frac{V_c}{A}$
x	...	$\frac{X}{X_o} - \eta\Delta_o$
y	...	$\frac{X}{X_o} - a$
y'	...	$y - rZ$
Z	...	$\frac{V}{e_2}$
Z_b	...	Value of Z at the time the powder is all burned

Table 4-7

Table of symbols (cont)

Symbol	Unit	Definition
a	...	Geometric density of loading
Γ	...	Function of Z_b (or Z_s) and P_p^o
γ	...	Ratio of specific heats
$\bar{\gamma}$	...	Pseudoratio of specific heats
Δ	lb per in.^{3}	Average density of gas
Δ	gm per cm^3	Density of loading, $\Delta = 27.68\,\Delta_o$
δ	...	Constant depending on ratio of charge weight C to projectile weight M
η	in.^{3} per lb	Covolume of gas
μ	lb per in.^{3}	$\frac{100M}{AX_m}$
μ_1	...	$j_o - k_2 f_o \left(f_o - \frac{1}{2}\right)$
ξ	...	$\frac{a\Delta_o}{\left(\frac{X}{X_o} - \eta\Delta_o\right)}$
ρ	lb per in.^{3}	Density of solid powder
ϕ	...	$\frac{a}{\left(\frac{1}{\Delta_o} - \frac{1}{\rho}\right)}$

Table 4-8

Symbols proper to the RD38 method only

Symbol	Unit	Definition
D	in.^{2}	Initial web size
E	in.^{3}	Al (initial free space behind shot)
fD	in.	Remaining web
M'	...	Central ballistic parameter
RT_o	ft-lb	Force constant
λ	ft-lb per lb	Effective mean force constant

4-21. Introduction. When a gun is fired, the primer delivers energy in the form of hot gases to the individual propellant grains in the propelling charge, and initiates the decomposition reactions of the propellant. It is known that in many artillery rounds deficiencies of the ignition system cause nonuniform distribution of primer energy and, consequently, time differences in initiation of various parts of the charge. For ease of mathematical treatment, however, it is assumed that all grains are ignited on all surfaces instantaneously. The rate at which the solid propellant is transformed to gas depends on total exposed surface and on the pressure surrounding the grains. If there were no mechanism serving to increase the volume available for gas (chamber volume minus the volume taken up by the solid, unconsumed propellant), the pressure would rise at an increasingly high rate until the propellant was all transformed to gas. This is the action in a closed bomb, where the loading density (propellant weight divided by chamber volume) seldom exceeds 0.2 g/cc, and the pressure may be as high as 45,000 psi. At the loading densities usual in guns, however, if the volume did not increase during propellant burning the pressure would become excessively high. This increase in volume is provided by the forward motion of the projectile with an acceleration proportional to the force exerted by the chamber pressure on the projectile base. The projectile begins to move as soon as the force on its base is high enough to overcome the crimp and to inscribe the rotating band in the forcing cone. As the volume increases, the bulk gas temperature decreases, and the internal energy change of the gas is mostly accounted for by the kinetic energy acquired by the projectile. In the beginning, when the projectile is moving slowly, the pressure increases as a result of propellant burning. A proper balance of the factors that influence propellant burning and projectile motion determines the maximum attainable pressure. After this, the rate of volume increase more than compensates for the rate of gas production, and the pressure begins to drop. The point of maximum pressure occurs when the original volume has about doubled. After the propellant is completely transformed to gas, the pressure drops more rapidly. The projectile continues to increase in velocity, at an acceleration proportional to the pressure until it emerges from the muzzle of the gun. (See figure 4-14.)

4-22. Fundamental Equations of Interior Ballistics. Interior ballistics attempts to predict mathematically the effects described qualitatively above. The fundamental mathematical relations are: (a) equation (43), representing the rate of burning; (b) equation (33), representing the motion of the projectile; (c) equation (42), the energy balance equation; (d) equation (34), the equation of state of the powder gas; and (e) equation (47), an equation expressing the variation of weight fraction of propellant remaining with fraction of web burned.

Interior ballistics is concerned with the simultaneous solution of these equations, which are correctly modified to take into account projectile friction, the distribution of the gas, the heat lost to the bore, and other second-order effects.

The variety of systems of interior ballistics that have been proposed differ in the number of simplifying assumptions made in order to obtain a solution of these equations. If time is no object, or if automatic computing machines are available, it is possible to solve these equations by maintaining a strict analogy to the physical phenomena. A quick hand computational technique, however, requires some simplification. Two excellent compromises between exactness and ease of calculation are outlined in references 1 and 2. We reproduce below the method of reference 2, and two very much simpler techniques, one in use in the United Kingdom (RD38) and the other in considerable use by the U. S. Navy (Le Duc).

4-23. Basic Problems. The basic problems to which solutions are desired are of the following two general types.

a. Given the type, web (essentially a measure of available burning surface), and weight of the propellant; the weight of projectile; and the characteristics of the weapon, calculate the expected maximum pressure and muzzle velocity.

b. Given the characteristics of the weapon; the weight of the projectile; and the muzzle velocity and maximum permissible pressure, find the weight and web of propellant required (to this problem, there may be no practical solution).

In each of these cases it may be necessary to establish the point-to-point relationship among

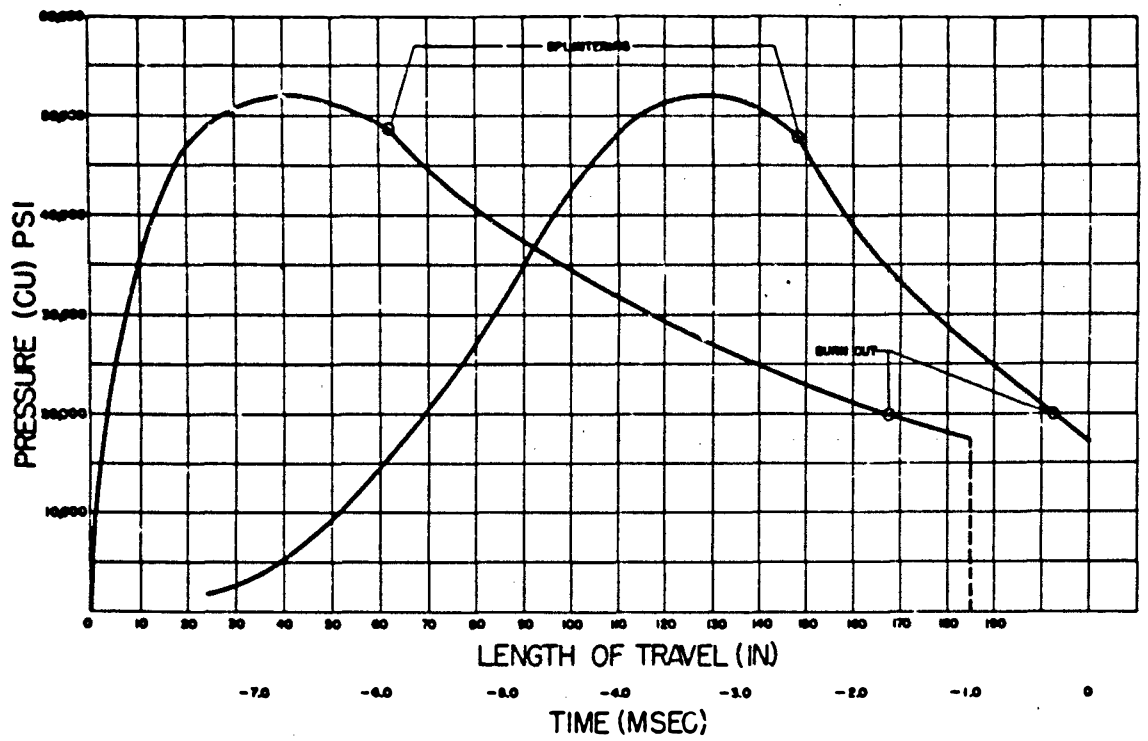

Figure 4-14. Pressure versus time and pressure versus travel curves

time, position of the projectile, velocity and pressure; or the muzzle velocity, maximum pressure, charge, and web may be the only values desired.

4-24. Development of the Fundamental Equations. The equation of motion of a projectile is one of Newton's laws. This equation states that the force is equal to the product of the mass and the acceleration. In the case of a gun, the force causing the acceleration of the projectile is the product of the pressure and the area on which it acts. Thus,

$$AP_x = \frac{M}{g}\frac{d^2X}{dt^2} = \frac{M}{g}V\frac{dV}{dX} \qquad (33)$$

where A is the cross-sectional area of the base at the beginning of motion of the projectile, and X is the distance the projectile has moved. M is the weight of the projectile, so that M/g is its mass (g is the acceleration due to gravity). P_x is the pressure on the base of the projectile, and t the time measured from the beginning of motion of the projectile. Normally, the cross-sectional area of the chamber is larger than that of the bore. It is convenient to define the zero point of X so that AX is the total volume behind the projectile available to gas and solid powder. However, the zero point may also be the position of the projectile base before motion occurs. In that case the distance traveled is denoted as X and the equation of motion is

$$AP_x = \frac{M}{g}\frac{d^2X}{dt^2} \qquad (33)$$

4-25. Equation of State. The equation of state of the powder gas is the relation among the pressure, the density, and the temperature of the gas. This equation is to some extent empirical. The virial equation of state is the most general form. This equation gives the pressure

in terms of a power series in the density. However, it is apparent that such an equation would considerably complicate the equations of interior ballistics. It can be shown that the Abel equation of state applies with sufficient accuracy under the conditions of the gas in the gun tube. The Abel equation of state is the van der Waals equation with the constant a omitted because it is negligible at the high temperature prevailing in guns. The Abel equation of state is

$$P\left(\frac{1}{\Delta} - \eta\right) = nRT \tag{34}$$

where Δ is the average gas density; η the covolume of the gas; P the space-average pressure; T the absolute temperature; n the number of moles of gas per unit weight; and R the usual gas constant.

The volume available to the propellant and the propellant gas is $V_c + Ax$, where V_c is the original volume (the volume of the cartridge case corrected for the volume occupied by the projectile extending into the case before firing). If ρ is the density of the solid propellant, then, since C - N is the amount of propellant remaining unburned, $\frac{C - N}{\rho}$ is the volume occupied by the solid propellant remaining. The volume available to the gas is

$$V_c + Ax - \left(\frac{C - N}{\rho}\right)$$

and the gas density is given by

$$\Delta = \frac{N}{V_c + Ax - \frac{C - N}{\rho}} \tag{35}$$

Let us define two constants characteristic of the powder.

$$a = \eta - \frac{1}{\rho} \tag{36}$$

$$F = n\,RT \tag{37}$$

The equation of state becomes

$$P\left[\frac{V_c + Ax - (C - N)/\rho}{N} - \eta\right] = F\,\frac{T}{T_o} \tag{38}$$

Simplifying, we get

$$P\left[V_c + Ax - \frac{C}{\rho} - aN\right] = NF\,\frac{T}{T_o} \tag{39}$$

4-26. Energy-Balance Equation. The energy-balance equation simply states that the loss of internal energy of the gas is equal to the kinetic energy of the projectile. Thus

$$N\int_T^{T_o} C_v\,dT = 1/2\,\frac{M}{g}V^2 \tag{40}$$

Where V is the velocity of the projectile, N the amount of powder that has been burned, T_o the flame temperature, and C_v the specific heat of the gas at constant density. We assume that C_v is constant in the region of temperatures involved, so that

$$NC_v\,(T_o - T) = 1/2\,\frac{M}{g}\,V^2 \tag{41}$$

Then the equation of energy balance becomes

$$\frac{NF}{\gamma - 1}\left(1 - \frac{T}{T_o}\right) = \frac{1m}{2g}V^2 \tag{42}$$

4-27. Burning Rate Equation. The equation of the rate of burning is the equation that gives the rate of regression of the surfaces. It has been found empirically that the rate of burning of the powder depends primarily on the pressure of the gas surrounding the burning grains. Other factors apparently affect the rate to only a small extent. It has been found that the dependence of the rate on the pressure can be given by an equation either of the form

$$\frac{dr}{dt} = a + bP \tag{43}$$

or

$$\frac{dr}{dt} = BP^n \tag{44}$$

where r is the distance the surface has regressed. It has been found that both forms fit the experimental data equally well. In the case of equation (43) it has been found that the constant a is small; and in the case of equation (44) the exponent n is near unity. An equation of the form

$$\frac{dr}{dt} = BP \tag{45}$$

therefore fits the existing data with reasonable accuracy over the range of high pressures existing in guns. In addition, the use of an equation of this type permits an analytic solution of the ballistic differential equation. For these reasons, we adapt the approximate equation for the rate of burning, equation (45). The web of the powder grain is defined to be the minimum distance between the surfaces of the grain, that is, the distance which must be burned before the grain is completely consumed (or in the case of seven-perforated grains, before the grain splinters). The equation of the rate of burning to be used in this ballistic system is

$$-W\frac{df}{dt} = BP \tag{46}$$

where B is the burning constant (a constant characteristic of the type of powder); W the web of the powder; and f the fraction of the web which remains unburned. The quantity f is related to the fraction of the powder burned by purely geometric relations based on the geometry of the grain. It is shown in section 52 of reference 2 that this relationship can usually be represented satisfactorily by a quadratic equation of the form

$$N/C = k_0 - k_1 f + k_2 f^2 \tag{47}$$

The values of coefficients k_0, k_1, and k_2 depend only on the shape of the grain.

Equation (47) is expressed in the RD38 method as

$$\frac{N}{C} = (1 - f)(1 + \theta f) \tag{48}$$

$$= 1 + (\theta - 1)f - \theta f^2 \tag{49}$$

4-28. The Second-Order Effects. In the previous section a necessary distinction was made between the pressure on the base of the projectile, and the space-average pressure. The gas must follow along behind the projectile, yet the breech element must remain stationary. This motion of the powder gas causes a pressure gradient to develop, in which the pressure on the base of the projectile is lower than that at the breech. The kinetic energy of the gas must be included in the energy-balance equation, and the existence of the pressure gradient must be taken into account in relating the motion of the projectile to the space-average pressure.

4-29. Equations of Motion and Energy Balance. The motion of the powder gas is represented by the usual partial differential equations of fluid flow. A solution of these equations applying to the motion of a gas in a gun tube with the powder burning has not been found. A solution under certain restricted conditions was developed by Love and Pidduck.[1] However, this solution involves the motion of waves of finite amplitude, and is entirely too cumbersome to use in the equations of interior ballistics. A solution developed by Kent represents a limiting condition, that is, a stable equilibrium situation. The development of this solution is described in section 57, reference 2.

According to this solution, the pressure on the base of the projectile is related to the average gas pressure by

$$P = P_x \frac{\left[M + \frac{C}{\delta}\right]}{M} \tag{50}$$

and the projectile base pressure is related to the breech pressure by P_{breech} =

$$\frac{P_x\left[M + \frac{C}{2}\right]}{M} \tag{51}$$

where δ is a constant depending on the ratio of the charge weight (C) to the projectile weight (M). In the usual cases, when the ratio $\frac{C}{M}$ is about 1/3, δ is about 3.1. (In RD38, the value of δ is taken as 3.) It is also shown in section 57 of reference 2 that the kinetic energy of the powder gas is given by $\frac{CV^2}{2g\delta}$

It becomes convenient to define an effective mass of the projectile,

$$m = \frac{(M + C/\delta)}{g} \tag{52}$$

In terms of this quantity the equation of motion, equation (1), becomes

$$AP_{av.} = m\frac{d^2X}{dt2} \tag{53}$$

and the equation of energy balance, equation (33) becomes

$$NC_v (T_o - T) = 1/2\ mV^2 \tag{54}$$

4-30. Energy Equation Including Heat Loss. The heat lost to the bore surface up to any instant is taken to be proportional to the square of the velocity. Thus if h is the amount of energy lost to the bore of the gun, then

$$h = 1/2\ (mV^2B) \tag{55}$$

where B is a constant. Some justification for this form is given in section 55 of reference 2.

This term is now included in the energy equation, equation (54) so that

$$\frac{NF}{\gamma - 1}\left(1 - \frac{T}{To}\right) = (1 + B)\ \frac{1}{2}\ mV^2 \tag{56}$$

4-31. Energy Equation Allowing for Friction. We take the friction of the projectile to be equivalent to a resisting pressure on the base of the projectile equal to a constant fraction of the actual average pressure. The resisting pressure is taken to be

$$P_r = \frac{c}{1 + c}\ P \tag{57}$$

Because of this friction, the equation of motion, equation (53) must be modified. Pressure causing acceleration is no longer P, but rather $P - P_r$. Thus

$$A\left(\frac{1}{1 + c}\right)P = m\ \frac{d^2X}{dt^2} \tag{58}$$

or

$$AP = m'\ \frac{d^2X}{dt^2} \tag{59}$$

where

$$m' = (1 + c)m \tag{60}$$

The work done against friction must be included in the energy-balance equation. This work is

$$A\int_{X_o}^{X} P_r\ dX = \frac{c}{1 + c}\ A\int_{X_o}^{X} P\ dX \tag{61}$$

where X_o is the effective length of the chamber, defined as the volume of the chamber divided by the cross-sectional area A. From equation (59) and $V = \frac{dX}{dt}$ this term becomes

$$1/2\ mV^2C$$

This correction term must be added to the right hand side of the energy-balance equation, equation (56), to give

$$\frac{NF}{\gamma - 1}\left(1 - \frac{T}{To}\right) = (1 + B)\ 1/2\ mV^2 + 1/2\ mV^2C \tag{62}$$

Equation (62) can be written in terms of m' as

$$\frac{NF}{\gamma - 1}\left(1 - \frac{T}{To}\right) = (1 + B)\ 1/2\ m'V^2 - 1/2\ C\beta\ mV^2 \tag{63}$$

The final term is dropped as negligible, to give as the modified equation of energy balance

$$\frac{NF}{\gamma - 1}\left(1 - \frac{T}{To}\right) = (1 + B)\ 1/2\ m'V^2 \tag{64}$$

4-32. Solution of Equations by the Scheme RD38. The simplifying assumptions are as follows.

a. There is no initial resistance to motion by cartridge-case crimp, or the need for engraving the rotating band.

b. The temperature of the gas during burning is constant, thereby reducing the simultaneous equations to be solved.

c. The covolume is assumed to be equal to the specific volume of the solid propellant. These assumptions permit an algebraic solution of the remaining simultaneous equations.

By assumption b the right hand side of equation (39) becomes λN, and by assumption c, a = o. The equation of state, equation (39), then becomes

$$P_{av.}\left[V_c + Ax - \frac{C}{\rho}\right] = \lambda N \tag{65}$$

or, in terms of breech pressure (P). See equations (50) and (51).

$$P\left[V_c + Ax - \frac{C}{\rho}\right] = \lambda C\frac{\left(1 + \frac{C}{2W_1}\right)}{\left(1 + \frac{C}{3W_1}\right)} \tag{66}$$

The assumption c introduces an error that may be considerable at high densities of loading, since η is about 1 g/cc, and $1/\rho$ is 0.6 g/cc. The result is that the peak pressure is higher than the calculations would predict. This can be compensated for by increasing either B or λ, which then becomes dependent on peak pressure. It is more convenient to hold λ constant, and to vary B as required to correspond with ballistics.

We can write

$$V_c - \frac{C}{\rho} = E \equiv A\ell \tag{67}$$

where E is the initial free space behind the shot. The length ℓ is a convenient measure. Hence, equation (66) becomes

$$P(x + \ell) = \frac{\left(\lambda N \left(1 + \frac{C}{2M}\right)\right)}{\left(1 + \frac{C}{3M}\right)} \tag{68}$$

The equation of motion of the shot is

$$M\frac{dV}{dt} = \frac{AP}{1 + \frac{C}{2W_1}} \tag{69}$$

neglecting resistances to motion, the recoil of the gun, and the rotational inertia of the shot. To include these we replace equation (40) by

$$M_1\frac{dV}{dt} = \frac{AP}{1 + \frac{C}{2M_1}} \tag{70}$$

where $M_1 = mM$ and

$$m = 1.02 \text{ (approximately)} \tag{71}$$

The fundamental equations are thus:

$$\frac{N}{C} = (1 - f)(1 + \theta f) = 1 - (\theta - 1)f - \theta f^2 \tag{72}$$

$$D\frac{df}{dt} = -BP \tag{73}$$

$$P(x + \ell) = \frac{\lambda N}{A}\frac{(1 + C/2M_1)}{(1 + C/3M_1)} \tag{74}$$

$$(M_1 + C/2)\frac{dV}{dt} = AP \tag{75}$$

with the initial conditions $x = 0$ at $f = 1$.

Eliminating P from equations (73) and (75) and integrating, we get

$$V = \frac{AD}{B(M_1 + C/2)}(1 - f) \tag{76}$$

If we use equation (76) in equation (75), and eliminate P by using equation (74), then

$$\frac{dx}{df} = -M'\left(\frac{x + 1}{1 + \theta f}\right) \tag{77}$$

where

$$M' = \frac{A^2D^2(1 + C/3M_1)32.2}{B^2M_1C\lambda(1 + C/2M_1)^2} \tag{78}$$

Integrating equation (46) with $\theta \neq 0$,

$$x + \ell = \ell\left(\frac{1 + \theta}{1 + \theta f}\right)^{M'/\theta} \tag{79}$$

whereas, if $\theta = 0$,

$$x + \ell = \ell e^{M'(1 - f)} \tag{80}$$

The pressure P can now be obtained from equations (39) and (48) as

$\theta \neq 0$: (81)

$$P = \frac{\lambda C(1 + C/2M_1)(1 - f)(1 + \theta f)}{E(1 + C/3M_1)}\left(\frac{1 + \theta f}{1 + \theta}\right)^{M'/\theta}$$

$$\theta = 0: P = \frac{\lambda C(1 + C/2M_1)}{E(1 + C/3M_1)}(1 - f)e^{-M'(1 - f)} \tag{82}$$

This completes the determination of x, V, and P as functions of the parameter f.

λ is an energy per unit mass, the square of a velocity; AD/BM_1 is a velocity. Hence M' is dimensionless, as it should be in order to be consistent with equation (77). M' is the "central ballistic parameter" of this method. M' or an equivalent can be identified in nearly all of the ballistic theories that lead to explicit solutions.

M' can be thought of as a dimensionless parameter showing the importance of the shot motion in reducing the pressure from the value that would be attained in a closed vessel.

4-33. Values at "All Burnt." The suffix B will be used to denote quantities at the instant at which the propellant is just burnt, $f = 0$. From equation (76),

$$V_B = \frac{AD}{B(M_1 + C/2)} \tag{83}$$

Integrating equation (77),

$$x_B + \ell = \ell(1 + \theta)^{M'/\theta} \quad (\theta \neq 0) \tag{84}$$

$$= \ell e^{M'} \quad (\theta = 0) \tag{85}$$

From equation (74),

$$P_B = \frac{\lambda C(1 + C/2M_1)}{E(1 + C/3M_1)\,(1 + \theta)^{M'/\theta}} \quad (\theta \neq 0) \tag{86}$$

$$= \frac{\lambda C(1 + C/2M_1)}{E(1 + C/3M_1)} e^{-M'} \quad (\theta = 0) \tag{87}$$

4-34. Values at "Maximum Pressure." Quantities here are denoted by the suffix m. Differentiating equations (48) and (49) gives

$$f_m = \frac{M' + \theta - 1}{M' + 2\theta} \tag{88}$$

for all θ. Also

$$\frac{N}{C}(m) = \frac{(1 + \theta)^2 (M' + \theta)}{(M' + 2\theta)^2} \tag{89}$$

$$X_m + \ell = \ell \left(\frac{M' + 2\theta}{M' + \theta}\right)^{M'/\theta} \quad (\theta \neq 0)$$

$$= \ell e \quad (\theta = 0) \tag{90}$$

and

$$P_m = \tag{91}$$

$$\frac{\lambda C(1 + C/2M_1)(1 + \theta)^2 (M' + \theta)^{1 + (M'/\theta)}}{E(1 + C/3M_1)\,(M' + 2\,)^{2 + (M'/\theta)}} \quad (\theta \neq 0)$$

$$= \frac{\lambda C(1 + C/2M_1)}{E(1 + C/3M_1)e^{M'}} \tag{92}$$

$(\theta = 0)$

The last equation (91) is simplified as

$$P_m = \frac{\lambda C(1 + C/2M_1)\,(1 + \theta)^2}{E(1 + C/3M_1)\,(eM' + 4\theta)} \tag{93}$$

This is exact for $\theta = 0$.

4-35. Solution After "Burnt."

Let $$r = \frac{x + \ell}{x_B + \ell} \tag{94}$$

At any travel x greater than x_B, the pressure is

$$P = P_B r^{-\gamma} \tag{95}$$

The velocity is given by

$$V2 = \frac{\lambda C(M + \phi)}{M_1 + C/3} \tag{96}$$

where $$\phi = \frac{2}{\bar{\gamma} - 1}(1 - r^{1 - \bar{\gamma}}) \tag{97}$$

where $\bar{\gamma}$ is the equivalent specific heat ratio, defined by equation (44).

For details on the derivations of the equations for the last three conditions, refer to reference 1, pages 138 and 139.

4-36. Summary of the Working Formulas. A solution of the equations given above leads to the expressions given below.

If $M' > (1 - \theta)$,

$$P_m = \frac{\lambda C(1 + C/2M_1)\,(1 + \theta)^2}{E(1 + C/3M_1)\,(eM' + 4\theta)} \tag{98}$$

Otherwise, the maximum pressure is

$$P_B = \frac{\lambda C(1 + C/2M_1)}{E(1 + C/3M_1)\,(1 + \theta)^{M'/\theta}} \quad (\theta \neq 0) \tag{86}$$

$$= \frac{\lambda C(1 + C/2M_1)}{E(1 + C/3M_1)e^{M'}} \quad (\theta = 0) \tag{87}$$

The position of "all burnt" is given by

$$x_B + \ell = \ell(1 + \theta)^{M'/\theta} \quad (\theta \neq 0) \tag{84}$$

$$= \ell e^{M'} \quad (\theta = 0) \tag{85}$$

If the muzzle is at travel x, and

$$r = \frac{x + \ell}{x_B + \ell} \tag{94}$$

and

$$\phi = \frac{2}{\bar{\gamma} - 1} (1 - r^{1 - \bar{\gamma}}) \tag{97}$$

$$V^2 = \frac{\lambda C(M^1 + \phi)}{M_1 + C/3} \tag{96}$$

4-37. Sample Solution by Use of the RD38 System. The equations developed include two constants whose value cannot easily be found except with experience obtained through the use of this scheme in the analysis of past firings. Since λ/RT_0 is equivalent to $\frac{T'}{T_0}$, where T' is the correctly averaged temperature assumed to exist during propellant burning, λ/RT_0 should be a fraction, probably between 0.8 and 1.0. θ can be assigned from considerations of geometry of the grain alone, but there are other factors such as nonideality of ignition and imperfect propellant grains that make a better value at θ to be 0.2 greater than the geometric value. The actual values have to be fitted in a particular problem to match the observed properties to calculated ones. When no results of firings are available for the particular case desired, it is necessary to obtain values of θ and λ from an analysis of a similar case where ballistic firings are available.

The burning constant B is of prime importance in determining the maximum pressure, as is clear from various equations. However, it is difficult to correlate values of B determined from closed-chamber firings with those obtained in guns. Hence, whenever possible, B should be determined from the observed maximum pressure or muzzle velocity in a ballistic firing of a similar case to the one under consideration. This can be done once values are assigned to λ and θ.

An illustrative example, of the manner in which this scheme may be used, follows. Table 4-22 contains the ballistics of reference propellants used in assessing charge for production lots of propellant for various weapons. In the problem worked out below, we will take item 21 (from table 4-22) as the one for which a solution is known. Then we will try to find the maximum pressure and muzzle velocity for items 10 and 14.

Knowing the value of the maximum pressure as given for item 21, we find the value of M' for item 21. We check this value of M' with the θ and λ/RT_0 used to see if the correct velocity will be obtained. The final value of θ and λ/RT_0 that we will use will be the one that will give us the correct velocity. Then, with the correct value of M' for item 21, we can calculate M' for items 10 and 14.

In the first set of calculations, we shall assume that $\theta = 0$, and then take various values for λ/RT_0 to see which of these will be correct for our problem.

In the standard calibration chart (table 4-22) it will be noticed that the maximum pressure is given as 39,500 psi, whereas the value used in this example, as well as for Hirschfelder and Le Duc is 45,400 psi. This is so as the pressure given in the charts is the copper gage pressure, which is a lower reading. To convert to the actual pressure, we must multiply the copper pressure by 1.15.

Using the basic formula for pressure, we have

$$P_m = \frac{\lambda C(1 + C/2M_1)\,(1 + \theta)^2}{E(1 + C/3M_1)\,(eM' + 4\theta)} \tag{98}$$

However, since $\theta = 0$, the formula can be slightly simplified.

Assuming $\theta = 0$, and $\lambda/RT_0 = 0.9$, we have

$$45{,}400 = \frac{(0.9)\,(3.18)\,(3.12)\,(1.15)\,(12)\,(10^5)}{(1.58)\,(1.1)\,eM'}$$

$$M' = 1.50$$

Checking the velocity with this value, we find that the velocity is 2,680 ft/sec, which is too low.

We then try a higher value of λ/RT_0. Trying $\theta = 0$ and $\lambda/RT_0 = 0.93$, we have

$$M' = 1.54$$

This value of M yields V as 2,710 ft/sec. Hence we raise the value of λ/RT_0 to 0.96, and obtain a velocity of 2,780. We try $\lambda/RT_0 = 0.98$, and obtain a velocity of 2,800. The value of M' that we choose for item 21 is 1.69. Using this value of M we can calculate the burning rate, using the formula

$$M' = \frac{A^2D^2\left[1 + C/3M_1\right] 32.2}{B^2M_1C\lambda\left[1 + C/2M'\right]^2} \qquad (78)$$

$$B^2 = \frac{102\ (2.97 \times 10^{-3})\ (1.1)\ (32.2)}{(1.69)\ (26.5)\ (8.12)\ (0.98)\ (3.18)\ (1.32)}$$

$$B^2 = 7.55 \times 10^{-8}$$

Using this value of B, we can find M' for items 10 and 14.

$$M'_{10} = \frac{(49.3)\ (1.76 \times 10^{-3})\ (1.08)\ (32.2)}{(7.55)\ (16.9)\ (3.82)\ (0.98)\ (3.18)\ (1.21)}$$

$$M_{10} = 1.59$$

$$M'_{14} = \frac{(49.3)\ (1.35)\ (1.07)\ (32.2)}{(7.55)\ (16.5)\ (3.39)\ (0.98)\ (3.18)\ (1.23)}$$

$$M'_{14} = 1.57$$

Calculating the pressure for items 10 and 14, we get

$$P_{m10} = \frac{(0.98)\ (3.18)\ (3.82)\ (1.12)\ (12)}{(73)\ (1.08)\ (3.94)}$$

$$P_{m10} = 49{,}400 \text{ lb per in.}^2$$

$$P_{m14} = \frac{(0.98)\ (3.18)\ (1.11)\ (12)\ (3.39)}{(130)\ (1.07)\ (3.40)}$$

$$P_{m14} = 26{,}400 \text{ lb per in.}^2$$

To calculate the velocities for both of these items, we have to obtain the values of ϕ.

ϕ for item 10 = 2.31

ϕ for item 14 = 1.62

$$V_{10}^2 = \frac{(0.98)\ (3.82)\ (3.18)\ (3.76)\ (32.2)}{18.2}$$

$$V_{10} = 2{,}560 \text{ ft per sec}$$

$$V_{14}^2 = \frac{(0.98)\ (3.39)\ (3.18)\ (2.87)\ (32.2)}{17.6}$$

$$V_{14} = 2{,}180 \text{ ft per sec}$$

We now assume a value of θ as 0.15, and then try various values of λ/RT_0 to see which is correct. We again use the formula for maximum pressure

$$P_m = \frac{\lambda C(1 + C/2M_1)\ (1 + \theta)^2}{E(1 + C/3M_1)\ (eM' + 4\theta)} \qquad (93)$$

Trying successively the values of λ/RT_0 as 0.85, 0.87, 0.90, and 0.92, we find that $\lambda/RT_0 = 0.88$ will yield the correct velocity for item 21. The correct value of M' for item 21, using $\theta = 0.15$ and $\lambda/RT_0 = 0.88$, is 1.79.

B^2 is obtained as 7.19×10^{-8}

$M'_{10} = 1.83$

$M'_{14} = 1.61$

$P_{m10} = 44{,}400$ lb per in.^{2}

$P_{m14} = 23{,}100$ lb per in.^{2}

Checking the velocities in these, we obtain

$\phi_{10} = 1.65$

$\phi_{14} = 1.24$

$V_{10} = 2{,}610$ ft per sec

$V_{14} = 2{,}230$ ft per sec

We again repeat the problem, but assume $\theta = 0.30$, and in the first case, that $\lambda/RT_0 = 0.95$. Using the formula

$$P_m = \frac{\lambda C(1 + C/2M_1)\ (1 + \theta)^2}{E(1 + C/3M_1)\ (eM' + 4\theta)} \qquad (93)$$

we get

$$45{,}400 = \frac{(0.95)(8.12)(3.18)10^5(1.15)(1.69)(12)}{(158)(1.1)(eM + 1.2)}$$

$$M' = 2.10$$

Trying this value of M' for velocity, we obtain

$$V = 2{,}950$$

which is too high.

We then try $\theta = 0.30$ and $\lambda/RT_o = 0.90$. With these values we obtain $M' = 2.06$ and the velocity $V = 2{,}850$, which is still too high.

Then we try $\theta = 0.30$, and $\lambda/RT_o = 0.88$. With these values $M' = 2.03$ and $V = 2{,}800$. This value of M is then correct for our θ and λ/RT_o. With this value of M' we can calculate B for M6 propellant. We can then use the value of B obtained for item 21, and use it for items 10 and 14 to obtain M' for these.

We obtain B from the formula for M'

$$M' = \frac{A^2D^2\left[1 + C/3M_1\right] 32.2}{B^2M_1C\left[1 + C/2M_1\right]^2} \qquad (78)$$

$$B^2 = \frac{(102)(2.97 \times 10^{-3})(1.1)(32.2)}{(2.03)(26.5)(8.12)(0.88)(3.18)(1.32)}$$

$$B^2 = 6.75 \times 10^{-8}$$

Hence, we obtain M_{10} from

$$M'_{10} = \frac{(49.3)(1.76)(1.08)(32.2)}{(6.75)(16.9)(3.32)(0.88)(3.18)(1.28)}$$

$$M'_{10} = 1.995$$

We obtain M_{14} from

$$M'_{14} = \frac{(49.3)(1.35)(10.7)(32.2)}{(6.75)(16.5)(3.39)(0.88)(3.18)(1.25)}$$

$$M'_{14} = 1.795$$

We can now use these values of M to calculate the pressure and velocity for both items 10 and 14.

$$P_{m10} = \frac{\lambda C(1 + C/2M_1)(1.69)(12)}{E(1 + C/3M_1)(eM' + 1.2)} \qquad (93)$$

$$P_{m10} = \frac{(0.88)(3.18)(3.82)(1.11)(1.69)(12)}{(73)(108)(5.12)}$$

$$P_{m10} = 46{,}400$$

$$P_{m14} = \frac{(0.88)(3.18)(3.39)(1.11)(1.69)(12)}{(140.6)(1.07)(4.70)}$$

$$P_{m14} = 25{,}300 \text{ psi}$$

$$V_{10}^2 = \frac{\lambda C(M' + e)}{M_1 + C/3}$$

$$V_{10}^2 = \frac{(0.88)(3.18)(3.82)(1.79 + 2.57)(32.2)}{18.2}$$

$$V_{10} = 2{,}590 \text{ fps}$$

$$V_{14}^2 = \frac{(0.88)(3.18)(3.39)(1.29 + 2.08)(32.2)}{17.6}$$

$$V_{14} = 2{,}300 \text{ fps}$$

4-38. Derivation of Equations by Method Outlined in OSRD 6468. For the tabular solution we assume that $\bar{\gamma} = 1.3$; and that the starting pressure is what is developed when one percent of the charge has burnt when the projectile begins to move. The covolume of the propellant is considered.

Equation of State. The equation of state (34), as derived in paragraph 4-25, is transformed by taking $V_c = AX_o$ and $AX = V_c + Ax$. The equation of state (34) then becomes

$$P\left[AX + \frac{C}{\rho} - aN\right] = NF\frac{T}{T_o} \qquad (99)$$

Multiplying this equation by v_c, dividing by its equivalent AX_o, and remembering that $C/V_c = \Delta_o$, we get

$$Pv_c\frac{C}{X_o} - \frac{\Delta_o}{\rho} - a\Delta_o\frac{N}{C} = NF\frac{T}{T_o} \qquad (100)$$

Equation of Motion. By equation (52), equation (33) can be expressed in terms of the average gas pressure as

$$AP = \frac{M}{g}\left(\frac{M + C/\delta}{M}\right)V\frac{dV}{dX} \qquad (101)$$

or

$$AP = mV\frac{dV}{dX} \qquad (102)$$

where

$$m = \frac{1}{g}\left(M + \frac{C}{\delta}\right) \qquad (103)$$

To account for frictional resistance, engraving resistance, etc., m' is substituted for m, the relation being m' = 1.02m. The quantity m' is defined as an effective mass.

The three equations, the energy of motion (33), the equation of state (34), and the energy balance equation (40), derived previously in paragraph 4-26, are combined to give one equation valid before and after the powder is all burned. The rate of burning will then be used to obtain a differential equation applicable only during the interval of burning of the powder.

First eliminate T/T_o between equation (34) and equation (40), and then eliminate P between this equation and equation (45). This gives

$$\frac{1}{2}m'V^2 = \frac{FN}{\bar{\gamma}-1} - \frac{V_c}{\bar{\gamma}-1}\left(\frac{X}{X_o} - \frac{\Delta_o}{\rho} - a\Delta_o\frac{N}{C}\right)\frac{m'}{A}V\frac{dV}{dX} \tag{104}$$

The equation for the rate of burning (43) may be rewritten in terms of velocity to give

$$-\frac{df}{dt} = \frac{m'}{A}\frac{B}{W}\frac{dV}{dt} \tag{105}$$

This equation is integrated to give

$$f_o - f = \frac{m'}{A}\frac{B}{W}V \tag{106}$$

where f_o is the value of f when the velocity is zero, that is, f_o is the fraction of the web that is unburned when the projectile begins to move. It is convenient to let N_o be the weight of the powder burned when the projectile begins to move (equation (47) evaluated at $f = f_o$). Equation (106) can be used to eliminate f from the form-function equation, equation (47), to give

$$\frac{N}{C} = \frac{N_o}{C} + (k_1 + 2k_2f_o)\frac{m'}{A}\frac{B}{W}V + k_2\left(\frac{m'}{A}\frac{B}{W}\right)^2V^2 \tag{107}$$

The value of N_o is related to the starting pressure P_o by the equation of state, equation (48), evaluated at the start of motion, that is, when $P = P_o$, $N = N_o$, $T/T_o = 1$, and $X/X_o = 1$, gives

$$\frac{N_o}{C} = \frac{P_o(1 - \Delta_o/\rho)}{\Delta_o(F + aP_o)} \tag{108}$$

Eliminating N in equation (104) by means of equation (107) gives the fundamental ballistic equation for the interval of burning

$$\frac{1}{2}(\bar{\gamma}-1)m'V^2 + \frac{m'}{A}V_c + \left[\frac{X}{X_o} - \frac{\Delta_o}{\rho} - a\Delta_o(k_1 - \frac{1}{2}k_2)\frac{m'}{A}\frac{B}{W}V - a\Delta_o\frac{N_o}{C}\right] + V\frac{dV}{dx} = CF\left[\frac{N_o}{C} + (k_1 - 2k_2f_o)\frac{m'}{A}\frac{B}{W}V + k_2\left(\frac{m'}{A}\frac{B}{W}\right)^2\right]V^2 \tag{109}$$

Here, in the term $a\Delta_o N/C$, which is a small correction term, we have approximated the value of N by replacing f^2 by $\frac{1}{2}f$. Thus

$$\frac{N}{C} \simeq k_o - (k_1 - \frac{1}{2}k_2)f \tag{110}$$

and, correspondingly, we have introduced

$$\frac{N_o'}{C} = k_o - (k_1 - \frac{1}{2}k_2)f_o$$

4-39. The Solution of the Differential Equation. Let us define the following:

$$j_o = \frac{N_o}{C} \tag{111}$$

$$j_1 = k_1 - 2k_2f_o \tag{112}$$

$$j_2 = k_1 - \frac{1}{2}k_2 \tag{113}$$

$$c = \frac{\Delta_o}{\rho} + a\Delta_o(k_o - j_2f_o) \tag{114}$$

and

$$Z_b = \frac{f_o A^2}{j_1 C F m' (B/W)^2} \tag{115}$$

In terms of these quantities, equation (109) becomes

$$X_o\left[\frac{X}{X_o} - c - a\Delta_o j_2\frac{m'}{A}\frac{B}{W}V\right]V\frac{dV}{dX} = \frac{CFj_o}{m'} + j_1\frac{CF}{A}\frac{B}{W}V - \left\{\frac{1}{2}(\bar{\gamma}-1) - \frac{k_2f_o}{j_1Z_b}\right\}V^2 \tag{116}$$

This is an equation relating the length of travel (X) of the projectile to its velocity (V). It now becomes convenient to define dimensionless variables related to the travel and velocity:

$$y = \frac{X}{X_o} - \alpha \tag{117}$$

and

$$Z = \frac{V}{e_2} \tag{118}$$

where

$$e_2 = \frac{j_1 C F (B/W)}{A}$$

In terms of these variables, equation (116) becomes

$$\left(y - a\Delta_o j_2 \frac{f_o}{Z_b} Z\right) Z \frac{dZ}{dy} = \frac{CFj_o}{e_2^2 m'} + Z - \left\{\frac{1}{2}(\gamma - 1) - \frac{k_2 f_o}{j_1 Z_b}\right\} Z^2 \tag{120}$$

Let us define the following:

$$r = \frac{a \Delta_o j_2 f_o}{Z_b} \tag{121}$$

$$u = \frac{1}{2}(\gamma - 1) - \frac{k_2 f_o}{j_1 Z_b} \tag{122}$$

and

$$q = \frac{j_o Z_b}{j_1 f_o} \tag{123}$$

In terms of these quantities, equation (120) becomes

$$(y - rZ) Z \frac{dZ}{dy} = q \tag{124}$$

which may be arranged to give

$$\frac{dy}{dZ} = \frac{Z(y - rZ)}{q + Z - uZ^2} \tag{125}$$

We define

$$y' = y - rZ \tag{126}$$

so that equation (125) becomes

$$\frac{dy'}{dZ} = \frac{Zy'}{q + Z - uZ^2} - r \tag{127}$$

Thus we obtain a linear first-order differential equation, with a solution as follows

$$y' = J\left(k - r\int_o^Z \frac{dZ}{J}\right) \tag{128}$$

Where k is the constant of integration,

$$J = \exp \int_o^Z \frac{Z\, dZ}{q + Z - uZ^2} \tag{129}$$

and

$$S = J \int_o^Z \frac{dZ}{J} \tag{130}$$

Then by using the definition of y' from equation (126) and of y from equation (117)

$$X/X_o = kJ + \alpha - r(S - Z) \tag{131}$$

The function J is elementary, but the expressions developed by the explicit integration are rather cumbersome from a computational point of view. The function S is, in general, not elementary, and must be calculated either by numerical integration or by some type of series expansion.

The integration constant k is obtained by use of the initial situation, $X/X_o = 1$ when $Z = 0$, $J = 1$, and $S = 0$.

This gives the following equation for X/X_o as a function of Z.

$$X/X_o = J - \alpha(J - 1) - r(S - Z) \tag{132}$$

This is the relation between the travel and the velocity of the projectile. It will be noted that in this equation the velocity is the independent variable and the travel is the dependent variable. This is not the choice that would have been desired. However, it is not possible to give a simple equation for the velocity in terms of the travel.

The pressure may be obtained as a function of the velocity as follows. From equation (45) and the definitions of Z and y in equations (117) and (118)

$$P = e_3 Z \frac{dZ}{dy} \qquad (133)$$

where

$$e_3 = \frac{e_2^2 m'}{V_c} \qquad (134)$$

The constant e_3 may be written in terms of more fundamental quantities as follows:

$$e_3 = \frac{F j_1 f_o A_o}{Z_b} \qquad (135)$$

Equations (124) and (133) may be combined to give

$$P = e_3 \frac{q + Z - uZ^2}{X/X_o - o - rZ} \qquad (136)$$

The relation between position and time can be obtained only by means of numerical integrals. This can be carried out by use of either of two equations

$$t = \int_{X_o}^{X} \frac{dX}{V} \qquad (137)$$

or

$$t = \frac{m'}{A} \int_{o}^{V} \frac{dV}{P} \qquad (138)$$

The first equation leads to an improper integral. For this reason, it is always convenient to begin the integration by use of equation (137). This equation leads to infinite times in the case $P_o = 0$. This is true because the ballistic equations give solutions for the case $P_o = 0$ only in a limiting sense. If the pressure is initially zero, the powder (according to the rate-of-burning equation used) will not burn. Therefore, the pressure will not rise, and the situation will remain unchanged.

4-40. The Maximum Pressure. The position of the maximum pressure is found by setting $\frac{dP}{dX} = 0$. Let a subscript p indicate that the quantity has been evaluated at the time of maximum pressure. The differentiation of equation (136), and the setting of $\frac{dP}{dX} = 0$, leads [see equation (117)] to

$$(dy/dZ)_p = \frac{(y_p - rZ_p)(1 - 2uZ_p)}{q + Z_p - u Z_p^2} \qquad (139)$$

If a position of true maximum pressure (that is, $\frac{dP}{dX} = 0$) occurs during the range of the equation (that is, during the burning of the powder), equation (137) may be combined with equation (125) to give

$$\frac{q + Z_p - uZ_p^2}{y_p - r Z_p} = \frac{(1 + 2u)Z_p - 1}{r} \qquad (140)$$

Thus, from equation (136) we obtain on rearrangement

$$Z_p = \frac{1 + \frac{r}{e_3} P_p}{1 + 2u} \qquad (141)$$

This is a relation between the value of Z, and the value of P at the time of maximum pressure. The numerical value of the term $(r/e_3)P_p$ is of the order of 0.1, so that the numerical value of Z_p is only slightly dependent on the value of P_p. This fact is made use of in a recursive method of obtaining Z_p and P_p numerically.

4-41. The Point at Which the Powder Is All Burned. The velocity at the time the powder is all burned is obtained from equation (106) by letting f, the fraction of the web left unburned, equal zero. Thus

$$V_b = \frac{A f_o}{m'\left(\frac{B}{W}\right)} \qquad (142)$$

It is convenient to let the subscript b indicate that the quantity has been evaluated at the time that the powder is all burned. From the definition of Z equations (117) and (118)

$$Z_b = \frac{f_o A^2}{j_1 C F m' (B/W)^2} \qquad (143)$$

Thus the quantity previously denoted by Z_b is seen to be simply the value of Z at the time the powder is all burned [equation (120)].

4-42. The Equations for the Period After All the Powder Is Burned. In the derivation (paragraph 4-38), it was stated that equation (104) is

applicable both before and after the powder is all burned. After the powder is all burned, N = C and equation (104) becomes

$$\frac{1}{2} m'V^2 = \frac{FC}{(\bar{\gamma} - 1)} \quad \frac{v_c m'}{A(\bar{\gamma} - 1)} \left(\frac{X}{X_o} - \eta\Delta_o \right) V \frac{dV}{dX} \tag{143}$$

Let

$$b = \frac{2CF}{m'(\bar{\gamma} - 1)} \tag{144}$$

and

$$x = \frac{X}{X_o} - \eta\Delta_o \tag{145}$$

Then, since

$$V \frac{dV}{dX} = \frac{V}{X_o} \frac{dV}{dX} = \frac{1}{2X_o} \quad \frac{dV^2}{dX} \tag{146}$$

equation (143) becomes

$$\frac{dV^2}{dX} + \frac{(\bar{\gamma} - 1)}{X} V^2 = \frac{b(\bar{\gamma} - 1)}{X} \tag{147}$$

This differential equation can be solved to give

$$V^2 = kX^{-(\bar{\gamma} - 1)} + b \tag{148}$$

where k is the constant of integration.

This constant is evaluated so that $V = V_b$ when $X = X_b$. Thus,

$$V^2 = \left(V_b^2 - b \right) \left(\frac{X_b}{X} \right)^{(\bar{\gamma} - 1)} + b \tag{149}$$

It is convenient to define

$$Q = \left(1 - \frac{\bar{\gamma} - 1}{2} j_1 f_o Z_b\right) (X_b/X_o - \eta\Delta_o)^{(\bar{\gamma} - 1)} \tag{150}$$

Then, by use of equations (142), (144), (145), and (149),

$$V^2 = \frac{2CF}{m'(\bar{\gamma} - 1)} \left[1 - Q(X/X_o - \eta\Delta_o)^{-(\bar{\gamma} - 1)} \right] \tag{151}$$

The pressure is found by combining equations (34), (146), and (147). Thus

$$P = \frac{m'(\bar{\gamma} - 1)}{2V_C} \quad \frac{(h - V^2)}{(X/X_o - \eta\Delta_o)} \tag{152}$$

It is convenient to introduce Q, as defined in equation (150), into this equation to give

$$P = \Delta_o FQ (X/X_o - \eta\Delta_o)^{-\bar{\gamma}} \tag{153}$$

4-43. Summary of Equations. The equations of interior ballistics developed previously can be summarized and rewritten in a form more suitable for use in the solution of problems. The equations are given in an order consistent with their use. The constants are expressed in a somewhat different manner, that is, in a manner which permits more direct calculation of their numerical values. Equations for the gas temperature and for the fraction of the powder burned are included. These equations are derived directly from equations (34) and (107). First we have the subsidiary quantities — functions of the form function constants k_o, k_1, and k_2, and the fraction of the powder burned to create the starting pressure, j_o:

$$j_1 = \left[k_1^2 - 4k_2 (k_o - j_o) \right]^{1/2} \tag{154}$$

$$j_2 = k_1 - \frac{1}{2} k_2 \tag{155}$$

$$f_o = \frac{(k_1 - j_1)}{2k_2} \text{ if } k_2 \neq 0$$

$$i_o = \frac{(k_o - j_o)}{k_1} \text{ if } k_2 = 0 \tag{156}$$

$$\mu_1 = j_o - k_2 f_o (f_o - \tfrac{1}{2}) \tag{157}$$

One of the important parameters is Z_b. This quantity introduces the burning rate, and is defined as

$$Z_b = f_o A^2 / j_1 CFm' (B/W)^2 \tag{158}$$

The quantity α, which is essentially the geometric density of loading, that is, the ratio of

the density of loading $\Delta_o = C/V_c$ to the density of the powder P, is defined by

$$\alpha = \frac{\Delta_o}{\rho} + a\Delta_o\mu_1 \qquad (159)$$

The quantity r introduces the covolume of the powder gas (η) through

$$a = \eta - \frac{1}{\rho} \qquad (36)$$

so that

$$r = \frac{aj_2f_o\Delta_o}{Z_b} \qquad (160)$$

The two parameters that enter into the functions J and S are q (related to the starting conditions) and u (related to the pseudo-ratio of specific heats, $\bar{\gamma}$):

$$q = \frac{i_oZ_b}{j_1f_o} \qquad (161)$$

$$u = \frac{1}{2}(\bar{\gamma} - 1) - \frac{k_2f_o}{j_1Z_b} \qquad (162)$$

The physical quantities for the interval before all the powder is burned (that is, $Z \leq Z_b$) are given in terms of the parameter Z. The travel of the projectile is given by

$$L = \frac{V_c}{A}(X/X_o - 1) \qquad (163)$$

where

$$\frac{X}{X_o} = J(1 - \alpha) - rs + \alpha + rZ \qquad (164)$$

The pressure is given by

$$P = \frac{12Fj_1f_o\Delta_o}{Z_b} \cdot \frac{q + Z - uZ^2}{J(1 - \alpha) - rs} \qquad (165)$$

The velocity is

$$V = \left(\frac{CFj_1f_o}{m'Z_b}\right)^{1/2} Z \qquad (166)$$

The time since the beginning of motion is given by

$$t = \frac{f_o}{Z_b\left(\frac{B}{W}\right)}\int_o^Z \frac{dZ}{P} \qquad (167)$$

The gas temperature is given by

$$T = T_o\left[1 - \frac{1/2(\bar{\gamma} - 1)Z^2}{(q + Z - uZ^2) + 1/2(\bar{\gamma} - 1)Z^2}\right] \qquad (168)$$

The fraction of the powder burned N/C is given by

$$\frac{N}{C} = \frac{j_1f_o}{Z_b}\left[q + Z - uZ^2 + 1/2(\bar{\gamma} - 1)Z^2\right] \qquad (169)$$

The point of maximum pressure is given by Z_p, where

$$Z_p = \frac{1}{1 + 2u}\left(1 + \frac{aj_2}{12Fj_1}P_p\right) \qquad (170)$$

unless $Z_p > Z_b$. If this is true, all the powder is burned before the pressure has risen to a point of zero slope. The maximum pressure then occurs at the time the powder is all burned, that is, at $Z = Z_b$. It will be noticed that Z_p depends on P_p. However, this is a weak dependence, so that a method of successive approximations converges quite rapidly.

4-44. Tables for the Calculation of Muzzle Velocity and Maximum Pressure. Tables 4-9 through 4-15 show the interdependence of the four functions Γ (a function related to the muzzle velocity, $P_p{}^o$ (a function related to the maximum pressure), δ (a function related to the density of loading), and Z_b (a function related to the burning rate or web). These tables permit the rapid solution of problems involving only the maximum pressure and muzzle velocity. The tables cannot be used to obtain the complete curves. The use of the tables is restricted somewhat by the fact that certain of the minor parameters are fixed; in general, this is not a serious restriction.

A new constant, dependent only upon the characteristics of the powder, is

$$a^o = 23{,}969\left(\frac{a}{F}\right) \qquad (171)$$

The numerical constant was chosen to make $a^o = 1$, for M-1 powder. A new pressure function is defined as

$$p^o = a^oP \qquad (172)$$

The travel function is

$$\xi = \frac{a\Delta_0}{\left(\frac{X}{X_0} - \eta_0\right)} \qquad (173)$$

and the density of loading function

$$\phi = \frac{a}{\left(\frac{1}{\Delta_0} - \frac{1}{\rho}\right)} \qquad (174)$$

As in the case of the other variables, a subscript p, b, or m on P^o or ξ indicates that the quantity is evaluated at the time of maximum pressure, when the powder is all burned, or when the projectile reaches the muzzle, respectively. In the case of seven-perforated grains, the subscript s refers to the instant the powder splinters. The use of two of these tables is shown in the solution of the problem worked out.

A function Γ has been defined so that

$$Vm^2 = \frac{2CF}{(\bar{\gamma} - 1)\, m'}\left(1 - \Gamma\xi^{\bar{\gamma}-1}\right) \qquad (175)$$

provided that

$$\xi_m(\bar{\gamma} - 1) \leqq \frac{(1 - uf_0Z_b)}{\Gamma}$$

or, in the case of the seven-perforated grain tables, provided that

$$\xi_m(\bar{\gamma} - 1) \leqq \frac{(1 - 0.2420Z_s)}{\Gamma}$$

(These conditions are necessary to ascertain that the powder is all burned when the projectile reaches the muzzle.)

Reference 2 has two sets of tables showing the interrelations of Γ, $P_p{}^o$, ϕ, and Z_b (or Z_s). One set applies to the problems involving the burning of constant-burning-surface grains. The other applies to the burning of seven-perforated grains. In this latter case, Z_s replaces Z_b as the variable in the tables.

There are three other fundamental parameters or auxiliary variables that enter into the simplified tables. They are:

a. The reduced velocity at the completion of burning, for constant-burning grains

$$Z_b = 0.99\,\frac{A^2}{CF}\,m\left(\frac{B}{W}\right)^2 \qquad (176)$$

for seven-perforated grains

$$Z_s = 1.369\,\frac{A^2}{CF}\,m\left(\frac{B}{W}\right)^2 \qquad (177)$$

b. The pressure function

$$P_o = \left(\frac{F}{a}\right)_{m'}\frac{a}{F}P = 2.3969 \times 10^4\,\frac{a}{F}\,P \qquad (178)$$

c. The velocity function for the period after burning is complete is

$$\Gamma(Z_b\, P_p{}^o) = (1 - 0.1485Z_b)\,\xi_b{}^{-0.3} \qquad (179)$$

Two of the minor parameters have been fixed by the tables. The starting pressure has been fixed by taking $j = 0.01$. The heat loss and ratio of specific heats has been fixed by taking $\bar{\gamma} = 1.30$. Provided that these quantities are not changed, the results obtained by use of these tables are numerically identical with those obtained by the cumbersome fundamental equations.

4-45. Solution by the Hirschfelder System. The example worked out by the RD38 System will now be worked out by the OSRD 6468 System, and the results will be compared in table 4-20. We again assume that item 21 is known, and will calculate the maximum pressure and muzzle velocity for items 10 and 14.

Knowledge of C, P_{max}, and type of propellant permits calculation of $P_p{}^o$ and ϕ. Table 4-11 provides the value of Z_s for the calculated values of $P_p{}^o$ and ϕ. From Z_s, B/W and therefore B can be calculated. B is dependent on the propellant formulation only, and may be used to estimate B/W for any other round (that is, items 10 and 14) using the same formulation. Z_s and ϕ may then be calculated for items 10 and 14, which are used to obtain values of $P_p{}^o$ and Γ. From $P_p{}^o$ and Γ the maximum pressure and muzzle velocity for items 10 and 14 are obtained.

The maximum pressure for item 21 is given as:

$$P_{max} = 45{,}400$$

From this we determine P_p by:

$$P_p = \frac{M + C/3}{M + C/2} P_{max}$$

$$P_{max} = 43{,}100 \text{ lb per in.}^2$$

The value of a, 12.98, is obtained from table 4-15. The value of a^o, also from table 4-15, is 0.991.

$$P_p{}^o = a^o P_p = 0.991\ (43{,}100) = 42{,}700$$

$$\phi = \frac{a}{(1/\Delta_o - 1/\rho)} = \frac{12.98}{19.5} = 0.665$$

$$\Delta_o = \frac{8.12}{300} = 0.027$$

$$Z_s = 1.5890 \text{ (from table 4-11)}$$

$$m' = \frac{(1.02)\ (24.1 + 8.12/3.1)}{32.17}$$

$$m' = 0.8467$$

$$\frac{B}{W} = \sqrt{\frac{(1.369)\ (102.1)}{(8\ 12)\ (3.18)\,10^5 (0.8467)\ (1.5890)}}$$

$$\frac{B}{W} = 0.00634$$

Therefore, B = 0.0003455.

Using this value of B, we may now calculate the ratio of B/W for items 10 and 14, since web sizes are known.

For item 10:

$$\frac{B}{W} = \frac{0.0003455}{0.0419} = 0.00825$$

$$\left(\frac{B}{W}\right)^2 = 6.81 \times 10^{-5}$$

$$Z_S = \frac{(1.369)\ A^2}{C F m'\ (B/W)^2} = 1.54$$

from table 4-11, we get $P_p{}^o = 46{,}000$ lb per in.^{2}. The value was obtained with a value of ϕ as 0.679.

$$P_p = \frac{46{,}000}{0.991} = 46{,}400 \text{ lb per in.}^2$$

$$P_{max} = 46{,}400 \left[\frac{15.4 + 3.82/2}{15.4 + 3.82/3}\right]$$

$$= 48{,}100 \text{ lb per in.}^2$$

For item 14:

$$\frac{B}{W} = \frac{0.0003455}{0.0367} = 0.00941$$

$$\left(\frac{B}{W}\right)^2 = 8.85 \times 10^{-5}$$

$$Z_S = 1.48$$

$$\phi = 0.313$$

hence, from table 4-11,

$$P_p{}^o = 19{,}010 \text{ lb per in.}^2$$

$$P_p = 19{,}200 \text{ lb per in.}^2$$

$$P_{max} = 19{,}800 \text{ lb per in.}^2$$

Checking the velocity, we use the basic formula

$$V_m = \sqrt{\left(1 - \Gamma \xi_m{}^{0.3}\right)\left(\frac{6.667CF}{m'}\right)}$$

For item 10:

$V_m =$

$$\sqrt{[1 - (1.3379)\ (0.3955)]\left[\frac{(6.667)\ (3.82)\ (3.18)\ 10^5}{0.528}\right]}$$

The value of Γ is obtained from table 4-13.

ξ_m is obtained from the formula

$$\xi_m = \frac{a\Delta_o}{(X_m/X_o - \eta\Delta_o)}$$

Hence

$$\xi_m = \frac{12.98\ (0.0273)}{8.63 - (30.49)\ (0.0273)}$$

$$\xi_m{}^{0.3} = 0.3955 \text{ (table 4-14)}$$

The value X_m/X_o is obtained from the formula

$$\frac{X_m}{X_o}\,\frac{V_c + AL}{V_c}$$

Hence

$$\frac{X_m}{X_o} = \frac{140 + (6.82)\,(156)}{140} = 8.63$$

$$V_m = 2{,}680 \text{ ft per sec}$$

The actual velocity is 2,600 ft per sec.

Checking for velocity in item 14:

$$\Gamma = 1{,}7813$$

$$m = 0.0336$$

$$m^{0.3} = 0.3613$$

$$\frac{X_m}{X_o} = 7.19$$

$$V = \sqrt{\left[\frac{1 - (1.7813)\,(0.361)}{0.509}\right]}\,(7.19)\,10^6$$

$$V = 2{,}340 \text{ ft per sec}$$

4-46. The Optimum Conditions.

a. Optimum Loading Density. Given a gun with its maximum rated pressure and the weight of the projectile to be fired from it, the question often is asked what is the maximum velocity that can be obtained. In most cases of guns encountered it turns out that the maximum velocity occurs at maximum loading density, that is, at the maximum charge that the case will hold. To avoid ignition difficulties, and as a consequence of the packing characteristics of propellants, this maximum loading density should seldom exceed 0.75 g/cc of chamber volume. The optimum loading density in the general case is dependent on pressure, however, and at low pressures, or with very light projectiles, the optimum loading density may leave a void in the cartridge can.

b. Optimum Gun. If the gun is in the design stage, with the required velocity and weight of the projectile known, the method of solution for the optimum gun corresponds to a trial and error solution for several assumed values of chamber volume and travel. A calculation is made for each of these values to determine optimum loading density (subparagraph 4-46a above) and velocity. The selection of these assumed values for chamber volume and travel is based upon the characteristics which are desired for the gun; for example, in tank guns it is desirable to keep gun length as short as possible. The desired characteristic could also be a light gun. The design should be a cooperative effort among the interior ballistician, the gun designer, and the man familiar with tactical requirements. As an example, if there is a maximum length limitation that cannot be exceeded, the initial calculation may be based on this maximum barrel length, and the velocity calculated for several assumed values of chamber volume. If the chamber volume at which the desired muzzle velocity is obtained is low enough, and it is desired to shorten the gun length at the expense of a larger chamber volume, the calculation may be repeated for a shorter barrel length. This relationship of chamber volume versus barrel length to obtain a given velocity at a given pressure is asymptotic to both axes, and there is a smallest practical chamber and shortest practical gun as shown in figure 4-15. Pressure enters into this problem by its effect on gun weight, and if the lightest gun is desired, the method outlined above has to be repeated for several pressure levels, and at each pressure level the lightest gun is selected. For tank guns, weight is not too important, and considerations of short length prescribe using the shortest possible gun, which implies working at the maximum pressure level permitted by practical considerations, such as cartridge case design.

Table XVII of OSRD 6468 has approximate solutions of velocity and loading density versus gun dimensions and pressure which may be used to restrict the number of trial calculations to be made as outlined above.

4-47. Example for Optimum Loading Density. In the example worked out below, there is a fixed gun-projectile combination, with one type of propellant. The loading density and quickness (B/W) are varied in order to attain maximum velocity at the required pressure.

In this example, we again use a 90-mm gun, but of different type. Also, we change the

Table 4-9 (OSRD 6468)

Table of Z_b as a function of τ and P_p^o, single-perforated grains

P_p^o \ τ	0.05	0.1	0.15	0.20	0.25	0.30
2000	2.4588					
4000	1.1748	2.4914				
6000	0.7767	1.6185	2.5242			
8000	0.5448	1.2047	1.8626	2.5574	3.2900	
10000	0.3591	0.9636	1.4819	2.0242	2.5906	3.1818
12000	0.2034	0.8058	1.2349	1.6810	2.1439	2.6241
14000	0.0691	0.6849	1.0618	1.4417	1.8342	2.2395
16000		0.5783	0.9338	1.2655	1.6071	1.9586
18000		0.4830	0.8354	1.1304	1.4334	1.7444
20000		0.3966	0.7543	1.0236	1.2964	1.5758
22000		0.3176	0.6803	0.9370	1.1856	1.4398
24000		0.2448	0.6121	0.8654	1.0941	1.3276
26000		0.1771	0.5488	0.8045	1.0174	1.2337
28000		0.1139	0.4897	0.7482	0.9520	1.1538
30000		0.0547	0.4343	0.6956	0.8958	1.0851
32000			0.3821	0.6460	0.8468	1.0253
34000			0.3329	0.5991	0.8018	0.9730
36000			0.2861	0.5547	0.7592	0.9266
38000			0.2417	0.5124	0.7187	0.8854
40000			0.1993	0.4722	0.6800	0.8480
42000			0.1588	0.4337	0.6432	0.8124
44000			0.1201	0.3969	0.6078	0.7783
46000			0.0829	0.3616	0.5740	0.7457
48000			0.0471	0.3277	0.5415	0.7143
50000			0.0127	0.2950	0.5102	0.6841
52000				0.2635	0.4800	0.6551
54000				0.2332	0.4509	0.6270
56000				0.2038	0.4228	0.5999
58000				0.1754	0.3956	0.5737
60000				0.1479	0.3693	0.5484
62000				0.1213	0.3438	0.5238
64000				0.0954	0.3190	0.4999
66000				0.0703	0.2950	0.4768
68000				0.0458	0.2716	0.4545
70000				0.0221	0.2489	0.4324
72000					0.2268	0.4111
74000					0.2052	0.3904
76000					0.1842	0.3702
78000					0.1637	0.3504
80000					0.1437	0.3312
82000					0.1242	0.3124
84000					0.1051	0.2941
86000					0.0864	0.2761
88000					0.0682	0.2586
90000					0.0503	0.2414
95000					0.0073	0.2001
100000						0.1608

Table 4-9 (OSRD 6168)

Table of Z_b as a function of ε and P_p^o, single-perforated grains (cont)

P_p^o \ ε	0.35	0.40	0.45	0.50	0.55	0.60
12000	3.1218					
14000	2.6578	3.0892				
16000	2.3291	2.6917	3.0737			
18000	2.0634	2.3905	2.7258	3.0694		
20000	1.8619	2.1515	2.4539	2.7601	3.0731	
22000	1.6995	1.9648	2.2357	2.5123	2.7946	3.0827
24000	1.5659	1.8089	2.0567	2.3094	2.5669	2.8293
26000	1.4541	1.6786	1.9073	2.1402	2.3773	2.6186
28000	1.3591	1.5681	1.7808	1.9971	2.2171	2.4407
30000	1.2776	1.4733	1.6722	1.8744	2.0799	2.2886
32000	1.2067	1.3910	1.5781	1.7682	1.9612	2.1570
34000	1.1446	1.3189	1.4958	1.6753	1.8574	2.0422
36000	1.0898	1.2553	1.4231	1.5934	1.7660	1.9410
38000	1.0409	1.1987	1.3586	1.5206	1.6848	1.8513
40000	0.9973	1.1480	1.3008	1.4556	1.6123	1.7711
42000	0.9579	1.1025	1.2489	1.3971	1.5472	1.6991
44000	0.9223	1.0612	1.2019	1.3443	1.4883	1.6341
46000	0.8899	1.0238	1.1592	1.2963	1.4349	1.5752
48000	0.8595	0.9896	1.1203	1.2525	1.3862	1.5214
50000	0.8303	0.9583	1.0846	1.2124	1.3416	1.4722
52000	0.8022	0.9295	1.0519	1.1756	1.3007	1.4271
54000	0.7750	0.9028	1.0217	1.1417	1.2630	1.3855
56000	0.7488	0.8774	0.9937	1.1103	1.2281	1.3470
58000	0.7234	0.8528	0.9678	1.0812	1.1957	1.3114
60000	0.6989	0.8289	0.9437	1.0542	1.1657	1.2783
62000	0.6751	0.8058	0.9211	1.0289	1.1377	1.2474
64000	0.6520	0.7835	0.8994	1.0054	1.1115	1.2186
66000	0.6296	0.7617	0.8782	0.9834	1.0870	1.1917
68000	0.6079	0.7406	0.8577	0.9627	1.0641	1.1664
70000	0.5867	0.7201	0.8377	0.9432	1.0425	1.1427
72000	0.5661	0.7001	0.8183	0.9243	1.0222	1.1203
74000	0.5461	0.6807	0.7994	0.9059	1.0031	1.0993
76000	0.5265	0.6617	0.7810	0.8879	0.9851	1.0794
78000	0.5075	0.6433	0.7631	0.8704	0.9679	1.0606
80000	0.4889	0.6252	0.7455	0.8534	0.9513	1.0428
82000	0.4708	0.6077	0.7285	0.8368	0.9351	1.0260
84000	0.4530	0.5905	0.7118	0.8205	0.9193	1.0100
86000	0.4357	0.5737	0.6955	0.8046	0.9038	0.9947
88000	0.4188	0.5573	0.6795	0.7891	0.8887	0.9800
90000	0.4022	0.5412	0.6639	0.7740	0.8739	0.9656
95000	0.3623	0.5026	0.6264	0.7375	0.8383	0.9309
100000	0.3244	0.4659	0.5908	0.7028	0.8046	0.8980

Table 4-9 (OSRD 6468)

Table of Z_b as a function of ε and P_p^o, single-perforated grains (cont)

P_p^o \ ε	0.65	0.70	0.75	0.80	0.85	0.90
24000	3.0967					
26000	2.8642	3.1112				
28000	2.6682	2.8293	3.1343			
30000	2.5006	2.7160	2.9347	3.1569		
32000	2.3559	2.5576	2.7624	2.9702		
34000	2.2295	2.4196	2.6123	2.8078	3.0059	
36000	2.1184	2.2982	2.4804	2.6651	2.8522	3.0418
38000	2.0198	2.1906	2.3636	2.5388	2.7163	2.8960
40000	1.9319	2.0947	2.2595	2.4263	2.5952	2.7662
42000	1.8529	2.0086	2.1661	2.3255	2.4867	2.6499
44000	1.7816	1.9309	2.0818	2.2345	2.3889	2.5451
46000	1.7170	1.8604	2.0055	2.1521	2.3004	2.4503
48000	1.6581	1.7963	1.9360	2.0772	2.2199	2.3641
50000	1.6042	1.7376	1.8724	2.0087	2.1463	2.2853
52000	1.5548	1.6838	1.8141	1.9458	2.0788	2.2132
54000	1.5092	1.6342	1.7605	1.8880	2.0167	2.1468
56000	1.4671	1.5885	1.7109	1.8346	1.9595	2.0855
58000	1.4281	1.5460	1.6650	1.7852	1.9064	2.0288
60000	1.3919	1.5066	1.6224	1.7393	1.8572	1.9762
62000	1.3582	1.4700	1.5828	1.6966	1.8114	1.9272
64000	1.3267	1.4357	1.5457	1.6567	1.7687	1.8816
66000	1.2972	1.4037	1.5111	1.6194	1.7287	1.8389
68000	1.2696	1.3737	1.4787	1.5845	1.6913	1.7989
70000	1.2437	1.3455	1.4482	1.5518	1.6562	1.7614
72000	1.2193	1.3190	1.4196	1.5209	1.6231	1.7262
74000	1.1963	1.2940	1.3926	1.4919	1.5920	1.6929
76000	1.1745	1.2704	1.3671	1.4645	1.5627	1.6616
78000	1.1540	1.2482	1.3430	1.4386	1.5350	1.6320
80000	1.1346	1.2271	1.3202	1.4141	1.5087	1.6040
82000	1.1162	1.2071	1.2986	1.3909	1.4839	1.5775
84000	1.0987	1.1881	1.2782	1.3689	1.4603	1.5524
86000	1.0821	1.1701	1.2587	1.3480	1.4379	1.5285
88000	1.0663	1.1529	1.2402	1.3281	1.4166	1.5057
90000	1.0512	1.1366	1.2225	1.3091	1.3963	1.4841
95000	1.0166	1.0990	1.1820	1.2655	1.3496	1.4343
100000	0.9844	1.0654	1.1458	1.2266	1.3080	1.3900

Table 4-9 (OSRD 6468)

Table of Z_h as a function of ϕ and P_p^o, single-perforated grains (cont)

P_p^o \ ϕ	0.95	1.00	1.10	1.20	1.30
38000	3.0780				
40000	2.9392	3.1143			
42000	2.8149	2.9819			
44000	2.7031	2.8628			
46000	2.6018	2.7550	3.0663		
48000	2.5098	2.6571	2.9563		
50000	2.4258	2.5677	2.8559		
52000	2.3488	2.4858	2.7639	3.0475	
54000	2.2780	2.4106	2.6795	2.9535	
56000	2.2127	2.3412	2.6016	2.8669	
58000	2.1523	2.2769	2.5296	2.7869	3.0488
60000	2.0962	2.2174	2.4629	2.7127	2.9699
62000	2.0441	2.1620	2.4008	2.6438	2.8910
64000	1.9955	2.1103	2.3430	2.5796	2.8202
66000	1.9500	2.0621	2.2890	2.5197	2.7541
68000	1.9075	2.0169	2.2384	2.4636	2.6923
70000	1.8675	1.9745	2.1910	2.4110	2.6344
72000	1.8300	1.9347	2.1465	2.3616	2.5800
74000	1.7947	1.8972	2.1045	2.3151	2.5289
76000	1.7613	1.8618	2.0650	2.2713	2.4807
78000	1.7298	1.8284	2.0277	2.2300	2.4352
80000	1.7001	1.7968	1.9924	2.1909	2.3922
82000	1.6718	1.7669	1.9590	2.1539	2.3515
84000	1.6451	1.7385	1.9273	2.1188	2.3129
86000	1.6197	1.7115	1.8972	2.0855	2.2763
88000	1.5955	1.6859	1.8686	2.0538	2.2415
90000	1.5725	1.6615	1.8414	2.0237	2.2085
95000	1.5196	1.6054	1.7788	1.9545	2.1324
100000	1.4724	1.5554	1.7231	1.8928	2.0647

Table 4-10 (OSRD 6468)

Table of Γ as a function of p and P_p^o, single-perforated grains

P_p^o \ p	0.05	0.10	0.15	0.20	0.25	0.30
2000	3.7334					
4000	2.9089	3.0370				
6000	2.7228	2.5375	2.6935			
8000	2.6248	2.3530	2.3380	2.4751	2.7762	
10000	2.5510	2.2567	2.1716	2.2007	2.3191	2.5382
12000	2.4922	2.1976	2.0748	2.0525	2.0964	2.2000
14000	2.4434	2.1541	2.0115	1.9595	1.9639	2.0128
16000		2.1170	1.9667	1.8955	1.8758	1.8935
18000		2.0847	1.9334	1.8487	1.8128	1.8104
20000		2.0562	1.9067	1.8130	1.7655	1.7492
22000		2.0307	1.8828	1.7849	1.7286	1.7021
24000		2.0076	1.8612	1.7622	1.6991	1.6648
26000		1.9866	1.8415	1.7431	1.6748	1.6344
28000		1.9673	1.8234	1.7258	1.6545	1.6091
30000		1.9494	1.8067	1.7099	1.6374	1.5879
32000			1.7911	1.6950	1.6227	1.5697
34000			1.7766	1.6811	1.6093	1.5539
36000			1.7630	1.6681	1.5967	1.5402
38000			1.7502	1.6559	1.5849	1.5281
40000			1.7381	1.6443	1.5737	1.5172
42000			1.7266	1.6334	1.5631	1.5069
44000			1.7157	1.6230	1.5531	1.4972
46000			1.7054	1.6131	1.5436	1.4879
48000			1.6956	1.6037	1.5345	1.4790
50000			1.6861	1.5947	1.5257	1.4705
52000				1.5860	1.5174	1.4624
54000				1.5777	1.5094	1.4546
56000				1.5698	1.5017	1.4471
58000				1.5621	1.4943	1.4399
60000				1.5548	1.4872	1.4330
62000				1.5477	1.4803	1.4265
64000				1.5408	1.4736	1.4198
66000				1.5341	1.4672	1.4136
68000				1.5277	1.4610	1.4076
70000				1.5215	1.4550	1.4017
72000					1.4491	1.3960
74000					1.4435	1.3905
76000					1.4380	1.3851
78000					1.4326	1.3799
80000					1.4274	1.3748
82000					1.4223	1.3699
84000					1.4174	1.3651
86000					1.4126	1.3604
88000					1.4079	1.3558
90000					1.4033	1.3513
95000					1.3923	1.3406
100000						1.3305

Table 4-10 (OSRD 6468)

Table of Γ as a function of ϕ and P_p^o, single-perforated grains (cont)

P_p^o \ ϕ	0.35	0.40	0.45	0.50	0.55	0.60
12000	2.3718					
14000	2.1050	2.2466				
16000	1.9437	2.0268	2.1477			
18000	1.8352	1.8850	1.9608	2.0670		
20000	1.7569	1.7856	1.8345	1.9048	1.9994	
22000	1.6978	1.7118	1.7428	1.7904	1.8559	1.9417
24000	1.6514	1.6548	1.6730	1.7051	1.7515	1.8131
26000	1.6140	1.6093	1.6180	1.6390	1.6718	1.7169
28000	1.5831	1.5721	1.5735	1.5860	1.6089	1.6420
30000	1.5573	1.5411	1.5368	1.5426	1.5578	1.5820
32000	1.5353	1.5149	1.5058	1.5063	1.5155	1.5327
34000	1.5163	1.4924	1.4794	1.4755	1.4798	1.4914
36000	1.4998	1.4729	1.4566	1.4491	1.4492	1.4563
38000	1.4853	1.4558	1.4366	1.4260	1.4227	1.4260
40000	1.4725	1.4407	1.4191	1.4058	1.3995	1.3996
42000	1.4610	1.4272	1.4035	1.3878	1.3791	1.3764
44000	1.4507	1.4151	1.3895	1.3718	1.3609	1.3558
46000	1.4415	1.4143	1.3770	1.3575	1.3446	1.3374
48000	1.4328	1.3945	1.3656	1.3445	1.3299	1.3208
50000	1.4245	1.3855	1.3553	1.3327	1.3165	1.3058
52000	1.4166	1.3773	1.3459	1.3220	1.3044	1.2922
54000	1.4090	1.3698	1.3372	1.3122	1.2933	1.2797
56000	1.4017	1.3626	1.3293	1.3031	1.2831	1.2683
58000	1.3946	1.3557	1.3220	1.2948	1.2737	1.2578
60000	1.3879	1.3491	1.3152	1.2871	1.2651	1.2481
62000	1.3813	1.3427	1.3088	1.2799	1.2570	1.2391
64000	1.3750	1.3365	1.3027	1.2733	1.2495	1.2308
66000	1.3689	1.3305	1.2968	1.2671	1.2426	1.2230
68000	1.3630	1.3247	1.2911	1.2613	1.2361	1.2157
70000	1.3572	1.3191	1.2856	1.2558	1.2299	1.2089
72000	1.3517	1.3136	1.2803	1.2505	1.2242	1.2025
74000	1.3463	1.3083	1.2751	1.2454	1.2188	1.1965
76000	1.3410	1.3032	1.2700	1.2404	1.2138	1.1909
78000	1.3359	1.2982	1.2651	1.2356	1.2089	1.1856
80000	1.3310	1.2933	1.2603	1.2309	1.2043	1.1805
82000	1.3261	1.2886	1.2557	1.2263	1.1998	1.1757
84000	1.3214	1.2840	1.2511	1.2218	1.1954	1.1712
86000	1.3168	1.2795	1.2467	1.2174	1.1911	1.1670
88000	1.3124	1.2751	1.2424	1.3132	1.1869	1.1628
90000	1.3080	1.2708	1.2382	1.2091	1.1828	1.1588
95000	1.2975	1.2605	1.2280	1.1991	1.1729	1.1490
100000	1.2876	1.2508	1.2185	1.1897	1.1636	1.1398

Table 4-10 (OSRD 646.)

Table of Γ as a function of ; and P_p^o, single-perforated grains (cont)

P_p^o \ ;	0.65	0.70	0.75	0.80	0.85	0.90
24000	1.8921					
26000	1.7752	1.8486				
28000	1.6859	1.7415	1.8102			
30000	1.6153	1.6581	1.7113	1.7762		
32000	1.5578	1.5911	1.6329	1.6841		
34000	1.5101	1.5360	1.5692	1.6101	1.6595	
36000	1.4699	1.4898	1.5162	1.5492	1.5893	1.6373
38000	1.4354	1.4505	1.4714	1.4981	1.5310	1.5704
40000	1.4054	1.4166	1.4330	1.4546	1.4817	1.5144
42000	1.3791	1.3869	1.3998	1.4171	1.4394	1.4667
44000	1.3559	1.3608	1.3703	1.3843	1.4026	1.4254
46000	1.3352	1.3376	1.3444	1.3553	1.3703	1.3894
48000	1.3166	1.3169	1.3213	1.3296	1.3417	1.3577
50000	1.2998	1.2982	1.3005	1.3066	1.3162	1.3294
52000	1.2846	1.2813	1.2818	1.2858	1.2933	1.3041
54000	1.2707	1.2659	1.2647	1.2670	1.2725	1.2812
56000	1.2580	1.2518	1.2491	1.2498	1.2536	1.2605
58000	1.2463	1.2388	1.2348	1.2341	1.2364	1.2416
60000	1.2356	1.2268	1.2217	1.2196	1.2206	1.2243
62000	1.2256	1.2158	1.2095	1.2063	1.2060	1.2084
64000	1.2163	1.2056	1.1983	1.1940	1.1925	1.1937
66000	1.2077	1.1961	1.1878	1.1825	1.1800	1.1801
68000	1.1996	1.1872	1.1780	1.1718	1.1684	1.1674
70000	1.1921	1.1789	1.1689	1.1618	1.1575	1.1556
72000	1.1850	1.1711	1.1604	1.1525	1.1473	1.1445
74000	1.1784	1.1638	1.1523	1.1438	1.1378	1.1342
76000	1.1721	1.1569	1.1448	1.1355	1.1288	1.1245
78000	1.1662	1.1504	1.1377	1.1278	1.1204	1.1154
80000	1.1606	1.1443	1.1310	1.1205	1.1125	1.1068
82000	1.1554	1.1385	1.1246	1.1135	1.1050	1.0986
84000	1.1504	1.1330	1.1186	1.1070	1.0978	1.0909
86000	1.1457	1.1278	1.1129	1.1008	1.0911	1.0836
88000	1.1412	1.1228	1.1075	1.0949	1.0847	1.0767
90000	1.1369	1.1181	1.1024	1.0893	1.0786	1.0701
92000	1.1271	1.1073	1.0906	1.0764	1.0647	1.0550
100000	1.1180	1.0977	1.0800	1.0650	1.0522	1.0416

Table 4-10 (OSRD 6468)

Table of Γ as a function of ϕ and P_p^o, single-perforated grains (cont)

P_p^o \ ϕ	0.95	1.00	1.10	1.20	1.30
38000	1.6171				
40000	1.5532	1.5987			
42000	1.4992	1.5375			
44000	1.4529	1.4854			
46000	1.4127	1.4404	1.5101		
48000	1.3774	1.4011	1.4612		
50000	1.3461	1.3664	1.4185		
52000	1.3182	1.3356	1.3808	1.4411	
54000	1.2931	1.3080	1.3473	1.4003	
56000	1.2703	1.2831	1.3173	1.3640	
58000	1.2496	1.2604	1.2903	1.3315	1.3854
60000	1.2307	1.2398	1.2657	1.3023	1.3503
62000	1.2134	1.2209	1.2433	1.2757	1.3187
64000	1.1974	1.2035	1.2228	1.2515	1.2901
66000	1.1826	1.1874	1.2039	1.2293	1.2640
68000	1.1688	1.1725	1.1864	1.2089	1.2401
70000	1.1560	1.1586	1.1702	1.1900	1.2181
72000	1.1440	1.1457	1.1552	1.1725	1.1977
74000	1.1328	1.1336	1.1411	1.1562	1.1789
76000	1.1223	1.1223	1.1280	1.1410	1.1614
78000	1.1125	1.1116	1.1156	1.1268	1.1450
80000	1.1032	1.1016	1.1040	1.1135	1.1297
82000	1.0944	1.0921	1.0931	1.1009	1.1153
84000	1.0861	1.0832	1.0828	1.0891	1.1018
86000	1.0782	1.0748	1.0730	1.0780	1.0891
88000	1.0707	1.0667	1.0638	1.0674	1.0771
90000	1.0636	1.0590	1.0550	1.0574	1.0657
95000	1.0474	1.0416	1.0349	1.0345	1.0397
100000	1.0329	1.0260	1.0171	1.0142	1.0167

Table 4-11 (OSRD 6468)

Table of Z_S as a function of ζ and P_p^o, seven-perforated grains

P_p^o \ ζ	0.05	0.10	0.15	0.20	0.25	0.30
2000	1.9949					
4000	1.0725	2.0177				
6000	0.7143	1.3927	2.0406			
8000	0.4493	1.0960	1.5684	2.0636		
10000		0.9038	1.2965	1.6844	2.0866	2.5031
12000		0.7432	1.1198	1.4400	1.7700	2.1096
14000		0.6048	0.9690	1.2695	1.5503	1.8380
16000		0.4829	0.8714	1.1438	1.3889	1.6394
18000			0.7721	1.0448	1.2655	1.4878
20000			0.6794	0.9564	1.1680	1.3684
22000			0.5947	0.8754	1.0884	1.2719
24000			0.5166	0.8010	1.0166	1.1923
26000			0.4442	0.7319	0.9501	1.1255
28000				0.6675	0.8880	1.0655
30000				0.6071	0.8299	1.0092
32000				0.5503	0.7753	0.9563
34000				0.4967	0.7236	0.9063
36000				0.4459	0.6748	0.8590
38000				0.3976	0.6283	0.8140
40000					0.5841	0.7712
42000					0.5418	0.7303
44000					0.5014	0.6912
46000					0.4626	0.6538
48000					0.4254	0.6178
50000						0.5832
52000						0.5498
54000						0.5177
56000						0.4867
58000						0.4566
60000						0.4275
62000						0.3993

Table 4-11 (OSRD 6468)

Table of Z_S as a function of ζ and P_p^o, seven-perforated grains (cont)

P_p^o \ ζ	0.35	0.40	0.45	0.50	0.55	0.60
12000	2.4591					
14000	2.1328	2.4344				
16000	1.8950	2.1559	2.4220			
18000	1.7142	1.9447	2.1791	2.4176		
20000	1.5720	1.7790	1.9891	2.2024	2.4188	
22000	1.4574	1.6456	1.8364	2.0297	2.2257	2.4241
24000	1.3630	1.5360	1.7111	1.8883	2.0676	2.2490
26000	1.2840	1.4443	1.6064	1.7702	1.9359	2.1032
28000	1.2169	1.3665	1.5176	1.6703	1.8244	1.9801
30000	1.1591	1.2996	1.4414	1.5846	1.7290	1.8747
32000	1.1076	1.2416	1.3754	1.5103	1.6464	1.7835
34000	1.0590	1.1907	1.3175	1.4453	1.5741	1.7038
36000	1.0130	1.1454	1.2664	1.3880	1.5104	1.6336
38000	0.9693	1.1028	1.2210	1.3370	1.4538	1.5713
40000	0.9278	1.0623	1.1803	1.2914	1.4032	1.5156
42000	0.8881	1.0236	1.1426	1.2505	1.3577	1.4656
44000	0.8501	0.9867	1.1065	1.2134	1.3166	1.4204
46000	0.8136	0.9512	1.0719	1.1794	1.2793	1.3794
48000	0.7788	0.9172	1.0387	1.1469	1.2452	1.3420
50000	0.7452	0.8845	1.0067	1.1157	1.2141	1.3077
52000	0.7128	0.8530	0.9760	1.0857	1.1847	1.2763
54000	0.6817	0.8227	0.9464	1.0567	1.1563	1.2472
56000	0.6515	0.7934	0.9178	1.0288	1.1289	1.2203
58000	0.6224	0.7650	0.8902	1.0018	1.1025	1.1944
60000	0.5943	0.7376	0.8634	0.9756	1.0769	1.1694
62000	0.5670	0.7110	0.8375	0.9503	1.0522	1.1451
64000	0.5405	0.6853	0.8124	0.9258	1.0282	1.1216
66000	0.5148	0.6603	0.7881	0.9020	1.0049	1.0988
68000	0.4899	0.6360	0.7644	0.8789	0.9823	1.0767
70000	0.4656	0.6125	0.7414	0.8565	0.9604	1.0552
72000	0.4419	0.5895	0.7191	0.8347	0.9390	1.0343
74000	0.4189	0.5672	0.6973	0.8134	0.9182	1.0139
76000	0.3964	0.5454	0.6761	0.7927	0.8980	0.9941
78000		0.5242	0.6554	0.7725	0.8783	0.9748
80000		0.5035	0.6353	0.7529	0.8591	0.9560
82000		0.4833	0.6156	0.7337	0.8403	0.9377
84000		0.4636	0.5965	0.7149	0.8220	0.9197
86000		0.4443	0.5777	0.6966	0.8041	0.9022
88000		0.4255	0.5594	0.6788	0.7867	0.8852
90000		0.4070	0.5414	0.6613	0.7696	0.8684
95000			0.4983	0.6192	0.7285	0.8283
100000			0.4573	0.5793	0.6895	0.7901

Table 4-11 (OSI 168)

Table of Z_S as a function of τ and P_p^o, seven-perforated grains (cont)

P_p^o \ τ	0.65	0.70	0.75	0.80	0.85	0.90
24000	2.4325					
26000	2.2723	2.4432				
28000	2.1372	2.2957	2.4558			
30000	2.0216	2.1698	2.3192	2.4698		
32000	1.9217	2.0610	2.2013	2.3427	2.4850	
34000	1.8345	1.9661	2.0986	2.2319	2.3662	2.5013
36000	1.7577	1.8825	2.0082	2.1346	2.2618	2.3897
38000	1.6895	1.8085	1.9281	2.0484	2.1694	2.2910
40000	1.6287	1.7424	1.8567	1.9716	2.0870	2.2031
42000	1.5740	1.6830	1.7926	1.9026	2.0132	2.1243
44000	1.5247	1.6295	1.7347	1.8404	1.9466	2.0533
46000	1.4799	1.5809	1.6823	1.7841	1.8863	1.9890
48000	1.4391	1.5366	1.6345	1.7328	1.8315	1.9305
50000	1.4017	1.4961	1.5909	1.6859	1.7813	1.8770
52000	1.3674	1.4589	1.5508	1.6429	1.7353	1.8280
54000	1.3358	1.4247	1.5139	1.6033	1.6930	1.7829
56000	1.3066	1.3931	1.4798	1.5667	1.6539	1.7413
58000	1.2796	1.3638	1.4482	1.5328	1.6177	1.7028
60000	1.2544	1.3365	1.4188	1.5014	1.5841	1.6670
62000	1.2306	1.3111	1.3915	1.4721	1.5528	1.6337
64000	1.2076	1.2875	1.3660	1.4448	1.5236	1.6027
66000	1.1852	1.2653	1.3422	1.4192	1.4964	1.5737
68000	1.1635	1.2440	1.3198	1.3952	1.4708	1.5465
70000	1.1424	1.2233	1.2988	1.3727	1.4468	1.5210
72000	1.1219	1.2032	1.2790	1.3516	1.4242	1.4970
74000	1.1020	1.1836	1.2598	1.3316	1.4030	1.4743
76000	1.0826	1.1646	1.2411	1.3128	1.3829	1.4530
78000	1.0637	1.1460	1.2229	1.2949	1.3639	1.4329
80000	1.0452	1.1279	1.2051	1.2775	1.3460	1.4138
82000	1.0272	1.1103	1.1878	1.2605	1.3290	1.3958
84000	1.0097	1.0931	1.1709	1.2439	1.3127	1.3786
86000	0.9926	1.0763	1.1545	1.2277	1.2968	1.3624
88000	0.9758	1.0599	1.1383	1.2119	1.2813	1.3469
90000	0.9595	1.0439	1.1226	1.1965	1.2661	1.3320
95000	0.9201	1.0053	1.0848	1.1593	1.2296	1.2961
100000	0.8828	0.9687	1.0489	1.1242	1.1951	1.2622

Table 4-11 (OSRD 6468)

Table of Z_s as a function of : and P_p^o, seven-perforated grains (cont)

P_p^o \ :	0.95	1.0	1.1	1.2	1.3
36000	2.5185				
38000	2.4133	2.5363			
40000	2.3197	2.4369			
42000	2.2359	2.3480			
44000	2.1604	2.2679	2.4642		
46000	2.0920	2.1954	2.4034		
48000	2.0298	2.1295	2.3299		
50000	1.9731	2.0694	2.2629	2.4576	
52000	1.9210	2.0143	2.2016	2.3899	
54000	1.8731	1.9636	2.1452	2.3276	
56000	1.8289	1.9168	2.0931	2.2703	2.4481
58000	1.7880	1.8735	2.0450	2.2172	2.3901
60000	1.7501	1.8334	2.0004	2.1681	2.3363
62000	1.7148	1.7960	1.9589	2.1224	2.2863
64000	1.6819	1.7612	1.9203	2.0798	2.2398
66000	1.6511	1.7287	1.8841	2.0400	2.1964
68000	1.6223	1.6982	1.8503	2.0028	2.1557
70000	1.5952	1.6696	1.8186	1.9680	2.1176
72000	1.5698	1.6427	1.7888	1.9352	2.0818
74000	1.5458	1.6174	1.7607	1.9043	2.0482
76000	1.5233	1.5935	1.7343	1.8753	2.0164
78000	1.5019	1.5710	1.7093	1.8478	1.9865
80000	1.4817	1.5497	1.6857	1.8219	1.9582
82000	1.4626	1.5295	1.6633	1.7973	1.9314
84000	1.4445	1.5103	1.6421	1.7740	1.9060
86000	1.4272	1.4921	1.6220	1.7519	1.8819
88000	1.4108	1.4748	1.6028	1.7309	1.8590
90000	1.3952	1.4584	1.5846	1.7109	1.8373
95000	1.3593	1.4205	1.5427	1.6650	1.7872
100000	1.3259	1.3867	1.5054	1.6241	1.7427

Table 4-12 (OSRD 6468)

Table of Γ as a function of Z_S and P_p^o, seven-perforated grains

P_p^o \ Z_S	0.5	0.6	0.7	0.8	0.9
2000	3.9415	3.8859	3.8306	3.7758	3.7213
4000	3.2004	3.1552	3.1103	3.0658	3.0215
6000	2.8328	2.7928	2.7531	2.7137	2.6745
8000	2.5976	2.5609	2.5245	2.4884	2.4525
10000	2.4285	2.3942	2.3602	2.3264	2.2929
12000	2.2984	2.2660	2.2338	2.2018	2.1700
14000	2.1937	2.1628	2.1320	2.1015	2.0712
16000	2.1008	2.0771	2.0476	2.0183	1.9892
18000	2.0329	2.0042	1.9758	1.9475	1.9194
20000	1.9639	1.9412	1.9136	1.8862	1.8590
22000	1.9127	1.8857	1.8590	1.8324	1.8060
24000	1.8627	1.8365	1.8104	1.7845	1.7588
26000	1.8179	1.7922	1.7668	1.7415	1.7164
28000	1.7772	1.7522	1.7273	1.7026	1.6781
30000	1.7402	1.7157	1.6913	1.6671	1.6431
32000	1.7062	1.6821	1.6583	1.6345	1.6110
34000	1.6748	1.6512	1.6278	1.6045	1.5814
36000	1.6457	1.6225	1.5995	1.5766	1.5539
38000	1.6186	1.5958	1.5732	1.5507	1.5284
40000	1.5933	1.5709	1.5486	1.5265	1.5045
42000	1.5696	1.5475	1.5255	1.5037	1.4821
44000	1.5472	1.5255	1.5038	1.4823	1.4610
46000	1.5262	1.5047	1.4833	1.4622	1.4411
48000	1.5062	1.4850	1.4640	1.4431	1.4223
50000	1.4873	1.4664	1.4456	1.4250	1.4045
52000	1.4694	1.4487	1.4282	1.4078	1.3875
54000	1.4523	1.4319	1.4116	1.3914	1.3714
56000	1.4360	1.4158	1.3957	1.3758	1.3560
58000	1.4204	1.4004	1.3806	1.3609	1.3413
60000	1.4055	1.3857	1.3661	1.3466	1.3273
62000	1.3912	1.3717	1.3522	1.3329	1.3138
64000	1.3775	1.3581	1.3389	1.3198	1.3008
66000	1.3643	1.3452	1.3261	1.3072	1.2884
68000	1.3517	1.3327	1.3138	1.2950	1.2764
70000	1.3394	1.3206	1.3019	1.2834	1.2649
72000	1.3277	1.3090	1.2905	1.2721	1.2583
74000	1.3163	1.2978	1.2794	1.2612	1.2431
76000	1.3053	1.2870	1.2687	1.2507	1.2327
78000	1.2947	1.2765	1.2584	1.2405	1.2227
80000	1.2844	1.2663	1.2484	1.2306	1.2130
82000	1.2744	1.2565	1.2387	1.2211	1.2036
84000	1.2647	1.2470	1.2293	1.2118	1.1945
86000	1.2554	1.2377	1.2202	1.2029	1.1856
88000	1.2463	1.2288	1.2114	1.1941	1.1770
90000	1.2374	1.2200	1.2028	1.1857	1.1687
95000	1.2163	1.1992	1.1823	1.1655	1.1488
100000	1.1966	1.1798	1.1631	1.1466	1.1301

Table 4-12 (OSRD 6468)

Table of Γ as a function of Z_S and P_p^o, seven-perforated grains (cont)

P_p^o \ Z_S	1.0	1.1	1.2	1.3	1.4
2000	3.3672	3.6154	3.5771	3.5520	3.5379
4000	2.9776	2.9351	2.9032	2.8821	2.8700
6000	2.6357	2.5978	2.5688	2.5494	2.5381
8000	2.4169	2.3819	2.3546	2.3363	2.3254
10000	2.2596	2.2267	2.2006	2.1829	2.1722
12000	2.1385	2.1073	2.0820	2.0647	2.0541
14000	2.0412	2.0113	1.9865	1.9695	1.9589
16000	1.9603	1.9317	1.9073	1.8904	1.8798
18000	1.8916	1.8639	1.8399	1.8231	1.8125
20000	1.8320	1.8053	1.7815	1.7648	1.7541
22000	1.7798	1.7538	1.7303	1.7136	1.7028
24000	1.7333	1.7080	1.6847	1.6680	1.6571
26000	1.6915	1.6668	1.6438	1.6271	1.6160
28000	1.6537	1.6296	1.6068	1.5900	1.5788
30000	1.6193	1.5956	1.5731	1.5562	1.5449
32000	1.5877	1.5645	1.5422	1.5252	1.5137
34000	1.5585	1.5357	1.5136	1.4966	1.4849
36000	1.5314	1.5091	1.4872	1.4701	1.4583
38000	1.5062	1.4843	1.4627	1.4454	1.4334
40000	1.4827	1.4611	1.4397	1.4223	1.4102
42000	1.4606	1.4393	1.4182	1.4007	1.3884
44000	1.4398	1.4189	1.3980	1.3804	1.3679
46000	1.4203	1.3996	1.3790	1.3612	1.3486
48000	1.4017	1.3813	1.3610	1.3431	1.3303
50000	1.3842	1.3640	1.3440	1.3260	1.3130
52000	1.3675	1.3475	1.3278	1.3097	1.2966
54000	1.3516	1.3319	1.3124	1.2943	1.2809
56000	1.3364	1.3169	1.2976	1.2795	1.2660
58000	1.3219	1.3027	1.2836	1.2655	1.2518
60000	1.3081	1.2890	1.2701	1.2520	1.2382
62000	1.2948	1.2759	1.2572	1.2392	1.2251
64000	1.2820	1.2634	1.2449	1.2268	1.2126
66000	1.2699	1.2513	1.2330	1.2150	1.2006
68000	1.2580	1.2397	1.2215	1.2037	1.1891
70000	1.2466	1.2285	1.2105	1.1928	1.1780
72000	1.2357	1.2177	1.1999	1.1822	1.1674
74000	1.2251	1.2073	1.1896	1.1721	1.1571
76000	1.2149	1.1972	1.1797	1.1624	1.1471
78000	1.2050	1.1875	1.1701	1.1529	1.1375
80000	1.1955	1.1781	1.1609	1.1438	1.1283
82000	1.1862	1.1690	1.1519	1.1349	1.1193
84000	1.1772	1.1601	1.1431	1.1263	1.1106
86000	1.1685	1.1515	1.1347	1.1180	1.1022
88000	1.1600	1.1432	1.1265	1.1099	1.0941
90000	1.1518	1.1351	1.1185	1.1020	1.0862
95000	1.1322	1.1158	1.0995	1.0833	1.0675
100000	1.1138	1.0977	1.0817	1.0658	1.0501

Table 4-12 (OSRD 6468)

Table of Γ as a function of Z_s and P_p^o, seven-perforated grains (cont)

P_p^o \ Z_s	1.5	1.6	1.7	1.8	1.9
2000	3.5333	3.5371	3.5483	3.5666	3.5916
4000	2.9657	2.8682	2.8769	2.8914	2.9112
6000	2 5338	2.5356	2.5429	2.5553	2.5725
8000	2.3209	2.3221	2.3284	2.3395	2.3550
10000	2.1676	2.1683	2.1738	2.1838	2.1980
12000	2.0493	2.0496	2.0545	2.0636	2.0768
14000	1.9540	1.9539	1.9582	1.9666	1.9789
16000	1.8746	1.8742	1.8781	1.8859	1.8974
18000	1.8071	1.8063	1.8098	1.8170	1.8279
20000	1.7485	1.7475	1.7505	1.7572	1.7675
22000	1.6970	1.6956	1.6982	1.7045	1.7143
24000	1.6511	1.6494	1.6517	1.6576	1.6668
26000	1.6098	1.6079	1.6098	1.6153	1.6241
28000	1.5724	1.5702	1.5718	1.5769	1.5853
30000	1.5383	1.5358	1.5371	1.5418	1.5498
32000	1.5069	1.5042	1.5052	1.5096	1.5172
34000	1.4779	1.4750	1.4757	1.4798	1.4870
36000	1.4510	1.4479	1.4483	1.4520	1.4589
38000	1.4260	1.4226	1.4227	1.4262	1.4327
40000	1.4026	1.3989	1.3988	1.4020	1.4082
42000	1.3806	1.3767	1.3764	1.3792	1.3851
44000	1.3599	1.3558	1.3552	1.3578	1.3634
46000	1.3404	1.3361	1.3352	1.3375	1.3429
48000	1.3219	1.3174	1.3163	1.3184	1.3234
50000	1.3044	1.2996	1.2983	1.3001	1.3049
52000	1.2878	1.2828	1.2812	1.2828	1.2873
54000	1.2719	1.2667	1.2650	1.2663	1.2705
56000	1.2568	1.2514	1.2494	1.2505	1.2545
58000	1.2424	1.2368	1.2346	1.2354	1.2392
60000	1.2286	1.2228	1.2203	1.2210	1.2245
62000	1.2154	1.2094	1.2067	1.2071	1.2104
64000	1.2027	1.1965	1.1936	1.1938	1.1968
66000	1.1905	1.1841	1.1810	1.1810	1.1838
68000	1.1788	1.1722	1.1689	1.1686	1.1712
70000	1.1675	1.1607	1.1572	1.1567	1.1591
72000	1.1567	1.1496	1.1460	1.1453	1.1474
74000	1.1462	1.1390	1.1351	1.1342	1.1361
76000	1.1361	1.1287	1.1246	1.1235	1.1252
78000	1.1263	1.1187	1.1144	1.1131	1.1146
80000	1.1168	1.1091	1.1046	1.1031	1.1044
82000	1.1077	1.0997	1.0951	1.0934	1.0944
84000	1.0989	1.0907	1.0858	1.0839	1.0848
86000	1.0903	1.0819	1.0769	1.0748	
88000	1.0820	1.0735	1.0682	1.0659	
90000	1.0739	1.0652	1.0598	1.0573	
95000	1.0547	1.0456	1.0397	1.0367	
100000	1.0369	1.0273	1.0210		

Table 4-12 (OSRD 6468)

Table of Γ as a function of Z_s and P_p^o, seven-perforated grains (cont)

P_p^o \ Z_s	2.0	2.1	2.2	2.3	2.4
2000	3.6229	3.6605	3.7044	3.7546	3.8115
4000	2.9363	2.9665	3.0018	3.0424	0883
6000	2.5944	2.6208	2.6518	2.6874	2.7278
8000	2.3747	2.3987	2.4269	2.4593	2.4961
10000	2.2162	2.2384	2.2645	2.2945	2.3287
12000	2.0937	2.1145	2.1390	2.1672	2.1994
14000	1.9949	2.0144	2.0376	2.0643	2.0948
16000	1.9125	1.9310	1.9530	1.9786	2.0076
18000	1.8422	1.8598	1.8809	1.9053	1.9332
20000	1.7811	1.7980	1.8182	1.8417	1.8685
22000	1.7270	1.7435	1.7629	1.7855	1.8114
24000	1.6793	1.6949	1.7136	1.7354	1.7604
26000	1.6360	1.6510	1.6691	1.6902	1.7145
28000	1.5967	1.6112	1.6287	1.6492	1.6727
30000	1.5608	1.5748	1.5917	1.6116	1.6345
32000	1.5277	1.5413	1.5577	1.5770	1.5993
34000	1.4972	1.5102	1.5262	1.5450	1.5667
36000	1.4687	1.4814	1.4969	1.5152	1.5364
38000	1.4422	1.4544	1.4695	1.4873	1.5080
40000	1.4173	1.4292	1.4438	1.4612	1.4814
42000	1.3939	1.4054	1.4197	1.4367	1.4564
44000	1.3718	1.3830	1.3969	1.4135	1.4328
46000	1.3510	1.3619	1.3754	1.3916	1.4105
48000	1.3312	1.3418	1.3550	1.3708	1.3893
50000	1.3125	1.3227	1.3355	1.3510	1.3691
52000	1.2946	1.3045	1.3170	1.3322	1.3499
54000	1.2775	1.2872	1.2994	1.3142	1.3316
56000	1.2612	1.2706	1.2825	1.2970	1.3140
58000	1.2456	1.2547	1.2663	1.2805	1.2972
60000	1.2307	1.2395	1.2508	1.2647	
62000	1.2163	1.2249	1.2359	1.2495	
64000	1.2025	1.2108	1.2216		
66000	1.1892	1.1973	1.2078		
68000	1.1764	1.1842			
70000	1.1641	1.1716			
72000	1.1522				
74000	1.1407				
76000	1.1295				

Table 4-13 (OSRD 6468)

Table of Γ as a function of ϕ and P_p^o, seven-perforated grains

P_p^o \ ϕ	0.05	0.10	0.15	0.20	0.25	0.30
2000	3.6211					
4000	2.9461	2.9413				
6000	2.7474	2.5387	2.6046			
8000	2.6162	2.3832	2.3213	2.3895		
10000		2.2916	2.1833	2.1726	2.2351	2.3685
12000		2.2199	2.1016	2.0515	2.0805	2.1167
14000		2.1613	2.0144	1.9739	1.9533	1.9709
16000		2.1119	1.9966	1.9200	1.8807	1.8752
18000			1.9554	1.8791	1.8282	1.8075
20000			1.9193	1.8438	1.7883	1.7569
22000			1.8872	1.8124	1.7568	1.7176
24000			1.8584	1.7842	1.7291	1.6863
26000			1.8322	1.7587	1.7039	1.6606
28000				1.7354	1.6810	1.6379
30000				1.7139	1.6599	1.6171
32000				1.6941	1.6404	1.5978
34000				1.6756	1.6223	1.5799
36000				1.6583	1.6053	1.5632
38000				1.6421	1.5894	1.5476
40000					1.5744	1.5328
42000					1.5603	1.5189
44000					1.5469	1.5057
46000					1.5342	1.4932
48000					1.5221	1.4813
50000						1.4699
52000						1.4591
54000						1.4487
56000						1.4387
58000						1.4291
60000						1.4199
62000						1.4111

Table 4-13 (OSRD 6469)

Table of Γ as a function of ε and P_p^o, seven-perforated grains (cont)

P_p^o \ ε	0.35	0.40	0.45	0.50	0.55	0.60
12000	2.2203					
14000	2.0216	2.1062				
16000	1.8967	1.9429	2.0145			
18000	1.8104	1.8338	1.8762	1.9385		
20000	1.7473	1.7555	1.7794	1.8187	1.8739	
22000	1.6989	1.6963	1.7077	1.7318	1.7684	1.8181
24000	1.6605	1.6500	1.6522	1.6655	1.6895	1.7239
26000	1.6294	1.6127	1.6079	1.6133	1.6280	1.6516
28000	1.6036	1.5820	1.5717	1.5710	1.5787	1.5942
30000	1.5818	1.5563	1.5416	1.5359	1.5382	1.5475
32000	1.5627	1.5344	1.5161	1.5064	1.5042	1.5086
34000	1.5450	1.5155	1.4942	1.4812	1.4754	1.4758
36000	1.5285	1.4990	1.4752	1.4594	1.4505	1.4476
38000	1.5130	1.4836	1.4585	1.4404	1.4289	1.4232
40000	1.4984	1.4692	1.4438	1.4236	1.4099	1.4018
42000	1.4847	1.4556	1.4303	1.4087	1.3930	1.3828
44000	1.4717	1.4427	1.4175	1.3954	1.3780	1.3660
46000	1.4593	1.4304	1.4054	1.3832	1.3645	1.3508
48000	1.4475	1.4188	1.3938	1.3718	1.3523	1.3372
50000	1.4363	1.4077	1.3828	1.3608	1.3412	1.3248
52000	1.4256	1.3971	1.3723	1.3504	1.3308	1.3136
54000	1.4153	1.3869	1.3622	1.3404	1.3209	1.3033
56000	1.4054	1.3771	1.3525	1.3308	1.3113	1.2937
58000	1.3960	1.3678	1.3432	1.3216	1.3022	1.2847
60000	1.3869	1.3588	1.3343	1.3127	1.2934	1.2759
62000	1.3781	1.3501	1.3257	1.3042	1.2849	1.2675
64000	1.3697	1.3417	1.3174	1.2960	1.2768	1.2594
66000	1.3615	1.3336	1.3094	1.2881	1.2689	1.2515
68000	1.3536	1.3258	1.3017	1.2804	1.2613	1.2439
70000	1.3459	1.3183	1.2942	1.2729	1.2539	1.2366
72000	1.3385	1.3109	1.2869	1.2657	1.2467	1.2295
74000	1.3314	1.3038	1.2799	1.2587	1.2398	1.2226
76000	1.3244	1.2970	1.2731	1.2520	1.2331	1.2159
78000		1.2903	1.2665	1.2454	1.2266	1.2095
80000		1.2837	1.2600	1.2390	1.2202	1.2032
82000		1.2774	1.2537	1.2328	1.2140	1.1970
84000		1.2712	1.2476	1.2267	1.2080	1.1910
86000		1.2652	1.2417	1.2208	1.2021	1.1852
88000		1.2594	1.2359	1.2151	1.1964	1.1795
90000		1.2537	1.2302	1.2094	1.1909	1.1740
95000			1.2166	1.1960	1.1775	1.1607
100000			1.2038	1.1833	1.1649	1.1482

Table 4-13 (OSRD 6468)

Table of Γ as a function of ; and P_p^o, seven-perforated grains (cont)

P_p^o \ ;	0.65	0.70	0.75	0.80	0.85	0.90
24000	1.7693					
26000	1.6841	1.7260				
28000	1.6174	1.6483	1.6872			
30000	1.5636	1.5863	1.6158	1.6523		
32000	1.5192	1.5357	1.5579	1.5862	1.6206	
34000	1.4819	1.4934	1.5100	1.5319	1.5590	1.5918
36000	1.4501	1.4575	1.4696	1.4864	1.5078	1.5341
38000	1.4226	1.4266	1.4351	1.4477	1.4646	1.4856
40000	1.3985	1.3998	1.4051	1.4144	1.4275	1.4443
42000	1.3774	1.3762	1.3789	1.3853	1.3953	1.4087
44000	1.3586	1.3553	1.3558	1.3597	1.3670	1.3775
46000	1.3417	1.3366	1.3351	1.3370	1.3420	1.3500
48000	1.3266	1.3198	1.3166	1.3166	1.3196	1.3255
50000	1.3128	1.3047	1.2999	1.2983	1.2996	1.3036
52000	1.3003	1.2909	1.2848	1.2817	1.2815	1.2838
54000	1.2889	1.2783	1.2710	1.2656	1.2650	1.2659
56000	1.2784	1.2668	1.2584	1.2528	1.2499	1.2495
58000	1.2688	1.2562	1.2468	1.2402	1.2362	1.2345
60000	1.2599	1.2464	1.2361	1.2285	1.2235	1.2208
62000	1.2516	1.2374	1.2262	1.2177	1.2118	1.2081
64000	1.2435	1.2290	1.2170	1.2077	1.2009	1.1963
66000	1.2357	1.2211	1.2084	1.1984	1.1908	1.1854
68000	1.2282	1.2136	1.2004	1.1897	1.1814	1.1753
70000	1.2209	1.2063	1.1930	1.1816	1.1726	1.1658
72000	1.2138	1.1993	1.1859	1.1740	1.1644	1.1569
74000	1.2069	1.1925	1.1791	1.1669	1.1567	1.1486
76000	1.2003	1.1859	1.1726	1.1602	1.1494	1.1408
78000	1.1939	1.1795	1.1662	1.1538	1.1426	1.1334
80000	1.1876	1.1733	1.1600	1.1476	1.1361	1.1265
82000	1.1815	1.1672	1.1539	1.1416	1.1300	1.1199
84000	1.1755	1.1613	1.1480	1.1357	1.1242	1.1137
86000	1.1697	1.1555	1.1423	1.1300	1.1185	1.1078
88000	1.1641	1.1499	1.1367	1.1245	1.1130	1.1022
90000	1.1586	1.1444	1.1313	1.1191	1.1076	1.0968
95000	1.1454	1.1313	1.1183	1.1061	1.0947	1.0839
100000	1.1330	1.1189	1.1059	1.0938	1.0824	1.0718

Table 4-13 (OSRD 6468)

Table of Γ as a function of ϕ and P_p^o, seven-perforated grains (cont)

P_p^o \ ϕ	0.95	1.00	1.10	1.20	1.30
36000	1.5653				
38000	1.5110	1.5410			
40000	1.4650	1.4896			
42000	1.4255	1.4458			
44000	1.3911	1.4079	1.4513		
46000	1.3609	1.3747	1.4112		
48000	1.3341	1.3454	1.3760		
50000	1.3102	1.3193	1.3450	1.3808	
52000	1.2886	1.2958	1.3172	1.3480	
54000	1.2691	1.2746	1.2923	1.3187	
56000	1.2514	1.2554	1.2698	1.2924	1.3232
58000	1.2352	1.2379	1.2494	1.2686	1.2954
60000	1.2203	1.2218	1.2307	1.2469	1.2703
62000	1.2066	1.2070	1.2136	1.2271	1.2475
64000	1.1939	1.1934	1.1978	1.2089	1.2266
66000	1.1821	1.1807	1.1831	1.1921	1.2074
68000	1.1712	1.1689	1.1696	1.1766	1.1896
70000	1.1610	1.1579	1.1570	1.1622	1.1732
72000	1.1514	1.1477	1.1452	1.1488	1.1580
74000	1.1424	1.1381	1.1342	1.1362	1.1438
76000	1.1340	1.1291	1.1239	1.1245	1.1305
78000	1.1261	1.1206	1.1142	1.1135	1.1180
80000	1.1187	1.1126	1.1050	1.1031	1.1063
82000	1.1116	1.1050	1.0964	1.0934	1.0953
84000	1.1049	1.0979	1.0883	1.0842	1.0850
86000	1.0986	1.0911	1.0806	1.0755	1.0752
88000	1.0926	1.0847	1.0733	1.0672	1.0659
90000	1.0869	1.0786	1.0663	1.0593	1.0571
95000	1.0738	1.0646	1.0504	1.0414	1.0370
100000	1.0617	1.0522	1.0363	1.0255	1.0192

Table 4-14 (OSRD 6468)

Values of $N^{0.3}$

N	0	2	4	6	8	Avg. Diff.
0.010	0.25119	0.25269	0.25416	0.25562	0.25706	146
0.011	0.25847	0.25988	0.26126	0.26263	0.26398	137
0.012	0.26531	0.26663	0.26793	0.26922	0.27050	129
0.013	0.27176	0.27301	0.27424	0.27546	0.27667	122
0.014	0.27787	0.27905	0.28023	0.28139	0.28254	116
0.015	0.28368	0.28481	0.28593	0.28704	0.28814	111
0.016	0.28923	0.29030	0.29138	0.29244	0.29349	106
0.017	0.29453	0.29557	0.29660	0.29761	0.29862	102
0.018	0.29963	0.30062	0.30161	0.30259	0.30356	98
0.019	0.30453	0.30549	0.30644	0.30738	0.30832	94
0.020	0.30925	0.31017	0.31109	0.31200	0.31291	91
0.021	0.31381	0.31470	0.31559	0.31647	0.31735	88
0.022	0.31822	0.31908	0.31994	0.32080	0.32165	85
0.023	0.32249	0.32333	0.32416	0.32499	0.32582	83
0.024	0.32664	0.32745	0.32826	0.32906	0.32986	80
0.025	0.33066	0.33145	0.33224	0.33302	0.33380	78
0.026	0.33457	0.33534	0.33611	0.33687	0.33763	76
0.027	0.33838	0.33913	0.33988	0.34062	0.34136	74
0.028	0.34210	0.34283	0.34355	0.34428	0.34500	72
0.029	0.34572	0.34643	0.34714	0.34785	0.34856	71
0.030	0.34925	0.34995	0.35064	0.35133	0.35202	69
0.031	0.35270	0.35338	0.35406	0.35474	0.35541	68
0.032	0.35608	0.35674	0.35741	0.35807	0.35873	66
0.033	0.35938	0.36003	0.36068	0.36133	0.36197	65
0.034	0.36261	0.36325	0.36389	0.36452	0.36515	63
0.035	0.36578	0.36641	0.36703	0.36765	0.36827	62
0.036	0.36888	0.36950	0.37011	0.37072	0.37133	61
0.037	0.37193	0.37255	0.37313	0.37373	0.37432	60
0.038	0.37492	0.37551	0.37610	0.37668	0.37727	59
0.039	0.37785	0.37843	0.37901	0.37958	0.38016	58
0.040	0.38073	0.38130	0.38187	0.38244	0.38300	57
0.041	0.38356	0.38412	0.38468	0.38524	0.38579	56
0.042	0.38634	0.38690	0.38744	0.38799	0.38854	55
0.043	0.38908	0.38962	0.39016	0.39070	0.39124	54
0.044	0.39177	0.39231	0.39284	0.39337	0.39390	53
0.045	0.39442	0.39495	0.39547	0.39599	0.39652	52
0.046	0.39702	0.39755	0.39807	0.39858	0.39909	51
0.047	0.39960	0.40011	0.40062	0.40113	0.40163	51
0.048	0.40214	0.40264	0.40314	0.40364	0.40413	50
0.049	0.40463	0.40513	0.40562	0.40611	0.40660	49
0.050	0.40709	0.40758	0.40806	0.40855	0.40903	49
0.051	0.40952	0.41000	0.41048	0.41096	0.41143	48
0.052	0.41191	0.41238	0.41286	0.41333	0.41380	47
0.053	0.41427	0.41474	0.41520	0.41567	0.41614	47
0.054	0.41660	0.41706	0.41752	0.41798	0.41844	46
0.055	0.41890	0.41935	0.41981	0.42026	0.42072	45
0.056	0.42117	0.42162	0.42207	0.42252	0.42297	45
0.057	0.42341	0.42386	0.42430	0.42474	0.42519	44
0.058	0.42563	0.42607	0.42650	0.42694	0.42738	44
0.059	0.42781	0.42825	0.42868	0.42912	0.42955	43
0.060	0.42998	0.43041	0.43084	0.43126	0.43169	43
0.061	0.43211	0.43254	0.43296	0.43339	0.43381	42
0.062	0.43423	0.43465	0.43507	0.43548	0.43590	42
0.063	0.43632	0.43673	0.43715	0.43756	0.43797	41
0.064	0.43838	0.43879	0.43920	0.43961	0.44002	41

Table 4-14 (OSRD 6468)

Values of $N^{0.3}$ (cont)

N	0	2	4	6	8	Avg. Diff.
0.060	0.44043	0.44083	0.44124	0.44164	0.44205	40
0.066	0.44245	0.44285	0.44325	0.44365	0.44405	40
0.067	0.44445	0.44485	0.44524	0.44564	0.44603	40
0.068	0.44643	0.44682	0.44722	0.44761	0.44800	39
0.069	0.44839	0.44878	0.44917	0.44955	0.44994	39
0.070	0.45033	0.45071	0.45110	0.45148	0.45187	38
0.071	0.45225	0.45263	0.45301	0.45339	0.45377	38
0.072	0.45415	0.45453	0.45491	0.45528	0.45566	38
0.073	0.45603	0.45641	0.45678	0.45715	0.45753	37
0.074	0.45790	0.45827	0.45864	0.45901	0.45938	37
0.075	0.45975	0.46011	0.46048	0.46085	0.46121	37
0.076	0.46158	0.46194	0.46230	0.46267	0.46303	36
0.077	0.46339	0.46375	0.46411	0.46447	0.46483	36
0.078	0.46519	0.46555	0.46590	0.46626	0.46661	36
0.079	0.46697	0.46732	0.46768	0.46803	0.46838	35
0.080	0.46873	0.46909	0.46944	0.46979	0.47014	35
0.081	0.47048	0.47083	0.47118	0.47153	0.47187	35
0.082	0.47222	0.47256	0.47291	0.47325	0.47360	34
0.083	0.47394	0.47428	0.47462	0.47497	0.47531	34
0.084	0.47565	0.47599	0.47632	0.47666	0.47700	34
0.085	0.47734	0.47767	0.47801	0.47835	0.47868	34
0.086	0.47902	0.47935	0.47968	0.48002	0.48035	33
0.087	0.48068	0.48101	0.48134	0.48167	0.48200	33
0.088	0.48233	0.48266	0.48299	0.48331	0.48364	33
0.089	0.48397	0.48429	0.48462	0.48494	0.48527	32
0.090	0.48559	0.48592	0.48624	0.48656	0.48688	32
0.091	0.48721	0.48753	0.48785	0.48817	0.48849	32
0.092	0.48881	0.48912	0.48944	0.48976	0.49008	32
0.093	0.49039	0.49071	0.49103	0.49134	0.49166	32
0.094	0.49197	0.49228	0.49260	0.49291	0.49322	31
0.095	0.49353	0.49385	0.49416	0.49447	0.49478	31
0.096	0.49509	0.49540	0.49570	0.49601	0.49632	31
0.097	0.49663	0.49694	0.49724	0.49755	0.49785	31
0.098	0.49816	0.49846	0.49877	0.49907	0.49938	30
0.099	0.49968	0.49998	0.50028	0.50058	0.50089	30

N	$N^{0.3}$
10	1.995262
10^2	3.981072
10^3	7.943282
10^4	15.84893
10^5	31.62278
10^6	63.09573
10^7	125.8925
10^8	251.1886
10^9	501.1872

Table 4-15 (OSRD 6468)

Nominal constants for typical American powders

Powder	T_o (°K)	C_v	n	F	γ	η	ρ	a	a^o
Pyro	2550 + 7/W	0.3710 - 0.00045/W	0.04178	296000 + 800/W	1.228	28.12	0.0560	12.14	0.930
FNH (85/10/5)	2480	0.3456	0.04482	310000	1.258	30.57	0.0567	12.93	1.000
NH (87/10/3)	2425 + 10/W	0.3520 - 0.00025/W	0.0461 - 0.0001/W	309000 + 500/W	1.256	30.49	0.0571	12.98	0.991
FNH-M2 (20% N.G.)	3560	0.3439	0.03873	384000	1.223	26.95	0.0596	10.17	0.635
IMR (small arms)	2800	0.3460	0.04301	334000	1.246	29.32	0.0578	12.02	0.863

powder to M2. The constants that we use in this evaluation are listed below.

M = 11 lbs
V_c = 457 in.^{3}
L = 185.2 in.
A = 10.1 in.^{2}
P_m = 59,800

Propellant Composition: M2
η = 26.95 in.^{3}/lb
ρ = 0.0596 lb/in.^{3}
F = 384,000 ft-lbs/lb
a = 10.17 in.^{3}/lb
a^o = 0.635
B = 0.5 x 10^{-3} (in./sec)/(lb/in.^{2})

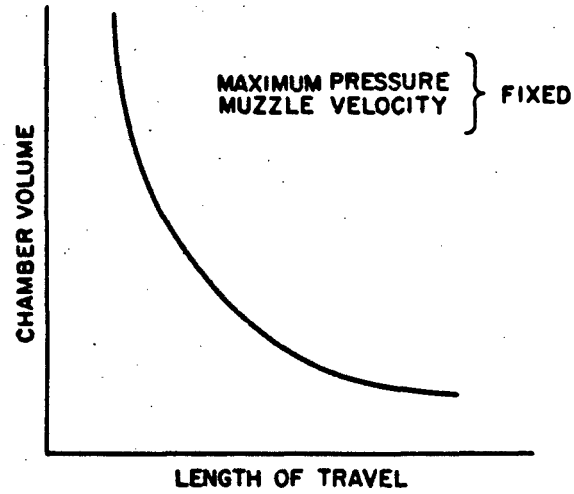

Figure 4-15. Optimum conditions

To start, we select three values for ϕ:

ϕ =		0.40	0.50	0.60
Δ_o =	$1/(a/\phi + 1/\rho)$	loading density, lbs/in.^{3}		
a/ϕ =		25.4	20.33	16.94
$1/\rho$ =		16.78	16.78	16.78
$1/\Delta_o$ =		42.18	37.11	33.72
Δ_o =		0.02372	0.02695	0.2968
Δ =	$27.68\Delta_o$	loading density, gms/cc		
Δ =		0.657	0.746	0.822
C =	$\Delta_o V_c$	charge, lbs		
V_c =		457	457	457
C =		10.84	12.33	13.56
P_{max} =		59,800	59,800	59,800
P_p^o =	$(P_{max})\left(\frac{M + C/\delta}{M + C/2}\right)(a^o)$			
M =		11	11	11
δ =		3.275	3.300	3.320
C/δ =		3.31	3.74	4.09
$M + C/\delta$ =		14.31	14.74	15.09
M =		11	11	11
$C/2$ =		5.42	6.16	6.78
$M + C/2$ =		16.42	17.16	17.78
$\frac{M + C/\delta}{M + C/2}$ =		0.872	0.858	0.849
$P_{max}\left(\frac{M + C/\delta}{M + C/2}\right)$ =		52,200	51,300	50,800
P_p^o =		33,200	32,600	32,200
X_m/X_o =	$(V_c + AL)/V_c = 1 + AL/V_c$			
V_c =		457	457	457
AL =		1852	1852	1852
$V_c + AL$ =		2309	2309	2309
X_m/X_o =		5.05	5.05	5.05

$\xi = a\Delta_o/(X_m/X_o - \eta\Delta_o)$				
X_m/X_o =		5.05	5.05	5.05
$\eta\Delta_o$ =		0.640	0.726	0.800
$X_m/X_o - \eta\Delta_o$ =		4.41	4.32	4.25
$a\Delta_o$ =		0.2412	0.2740	0.3015
ξm =		0.0545	0.0632	0.071

Use table 4-14 for values of $N^{0.3}$

$\xi m^{0.3}$ =	0.41775	0.43673	0.45225

Use table 4-9 or 4-11 for Z and tables 4-10 and 4-13 for Γ as indicated.

Γ =	1.5250	1.4988	1.5043
Z_s or Z_b =	1.2110	1.4908	1.7755

$$V_m = \sqrt{(1 - \Gamma\xi m^{0.3}) \frac{2CF}{0.3m'}}$$

$$m' = \frac{1.02(M + C/3.1)}{32.174}$$

M =	11	11	11	11
C/3.1 =	3.31	3.74	4.09	3.88
M + C/3.1 =	14.31	14.74	15.09	14.88
m' =	0.454	0.467	0.478	0.472
0.3m' =	0.1361	0.1385	0.1434	
2CF =	8330000	9470000	10420000	
2CF/0.3m' =	6120000	6840000	7260000	
CF =	4665000	4732000	5210000	
$\Gamma\xi m^{0.3}$ =	0.636	0.654	0.681	
$1 - \Gamma\xi m^{0.3}$ =	0.364	0.346	0.319	
V_m^2 =	22.2×10^6	23.68×10^6	23.18×10^6	
V_m =	4710	4865	4810	

When using a multiperforated propellant, follow this method:

$\xi m^{0.3}$ $(1 - 0.242Z_s)/\Gamma$			
$0.242Z_s$ =	0.293	0.361	0.43
$1 - 0.242Z_s$ =	0.707	0.639	0.57
$(1 - 0.242Z_s)/\Gamma$ =	0.464	0.426	0.379

The point of optimum efficiency is when $\xi m^{0.3}$ and $(1 - 0.242Z_s)/\Gamma$ are equal, hence we use

$$B/W = \sqrt{\frac{1.369A^2}{CFm'Z_s}}$$

A^2 = 100

$1.369A^2$ = 136.9

$CFm'Z_s = (12.05)(384{,}000)(0.472)(1.4315) = 3.19 \times 10^{+6}$

$(B/W)^2 = 43.7 \times 10^{-6}$

$B/W = 6.61 \times 10^{-3}$

Now, having all the values, we plot the curve for $\zeta_m^{0.3}$ and for $(1 - 0.242\ Z_s)/\Gamma$. The value of Δ (and therefore C and V_m) selected should be the one corresponding to the point of intersection of these curves, or the one corresponding to the highest velocity, whichever occurs first. Values of Δ beyond the point of intersection are undesirable because they imply unburnt propellant released at the muzzle. The graph is shown in figure 4-16.

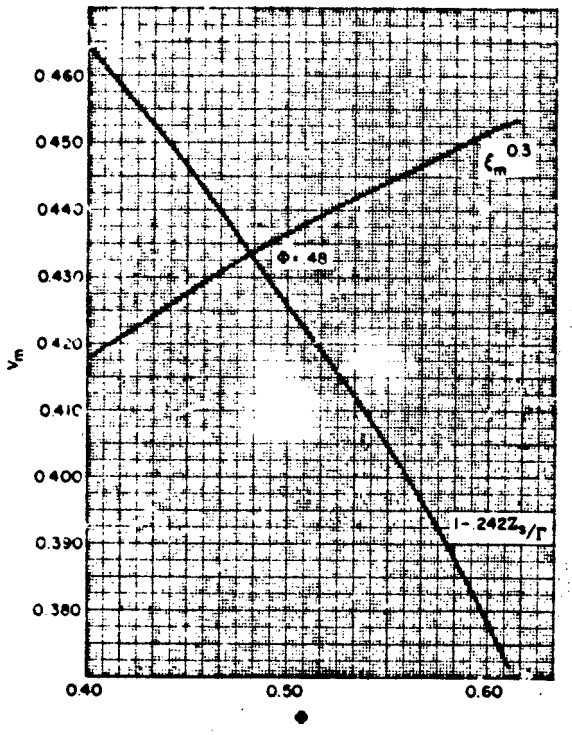

Figure 4-16. Optimum value of Δ

The constants calculated are listed below.

$C = 12.05$ lbs
$\Delta = 0.725$ gms/cc
$V_m = 4{,}855$ ft/sec
$Z_s = 1.4315$

4-48. The Complete Solution for a Pressure-Time Trace. Utilizing the formulas of the preceding derivation for the OSRD 6468 System, we shall make a complete solution, and plot the resultant pressure-time curve. Our gun is again the 90-mm, WTV-F1951, the same as in the example for the optimum conditions.

From the example for the optimum loading density, we found B/W to be

$$6.61 \times 10^{-3}$$

We shall use this value of B/W for our calculations below. As explained previously, the pressure-time trace is divided into three intervals — before splintering, after splintering, and after burnt. There are different formulas for each interval; accordingly the problem worked out below is done in three sections.

We know the value of Z_s to be 1.4315, and Δ to be 0.462. We break our interval before splintering into increments of Z of 0.2, starting with 0.2, and going up to 1.4315, omitting 1.40. The form function constants for this first interval are

$k_0 = 0.8487$

$k_1 = 0.9808$

$k_2 = 0.1321$

Also, we have

$J_0 = 0.01$
$\bar{\gamma} = 1.30$
$J_1 = 0.72028$
$J_2 = 0.91475$
$f_0 = 0.98607$
$\mu_1 = -0.53315$
$\Delta_0/\rho = 0.439$
$a\Delta_0\mu_1 = -0.01422$
$a = 0.42478$
$a J_2 f_0 \Delta_0 = 0.2405$
$\Gamma = 0.1679$
$J_0 Z_s = 0.014315$
$J_1 f_0 = 0.711$
$q = 0.02014$
$\frac{1}{2}(\bar{\gamma} - 1) = 0.15$
$k_2 f_0 = 0.1302$
$J_1 Z_s = 1.03$
$k_2 f_0 / J_1 Z_s = 0.1264$

Using the formula

$$u = \tfrac{1}{2}(\bar{\gamma} - 1) - k_2 f_0 / J_1 Z_s$$

we get $u = +0.0236$.

With our values of q, u, and Z we can get the values of J and S from tables. These values are given here in table 4-16.

Table 4-16

Values of J and S for values of Z

Z	0.2	0.4	0.6	0.8	1.0	1.2	1.4315
J	1.1647	1.4065	1.7082	2.0812	2.5427	3.1131	3.9327
S	0.2180	0.4834	0.8082	1.2064	1.6945	2.2951	3.1633

We then find the pressure for each interval from the formula

$$P = \frac{12F\, j_1 f_o \Delta_o}{Z_s} \cdot \frac{q + Z - uZ^2}{J(1-a) - rs}$$

The steps in the calculation are tabulated below.

Z	0.2	0.4	0.6	0.8
$12FJ_1f_o\Delta_o/Z_b$	59,900	59,900	59,900	59,900
Z^2	0.04	0.16	0.36	0.64
uZ^2	0.000936	0.00374	0.00842	0.01497
$q + Z - uZ^2$	0.2192	0.41640	0.61172	0.80517
$J(1-a)$	0.669	0.809	0.982	1.195
$J(1-a) - rS$	0.6324	0.7273	0.8463	0.990
$\frac{q + Z - uZ^2}{J(1-a) - rS}$	0.3405	0.573	0.723	0.813
P	20,700	34,300	43,300	48,700

Z	1.0	1.2	1.4315
$12FJ_1f_o\Delta_o/Z_b$	59,900	59,900	59,900
Z^2	1.0	1.44	2.043
uZ^2	0.023	0.0337	0.0478
$q + Z - uZ^2$	0.99674	1.1864	1.4038
$J(1-a)$	1.462	1.789	2.260
$J(1-a) - rS$	1.1775	1.404	1.7297
$\frac{q + Z - uZ^2}{J(1-a) - rS}$	0.846	0.845	0.812
P	50,700	50,600	48,600

This is the space average pressure. To convert to maximum pressure, we multiply by

$$\frac{M + C/2}{M + C/3}$$

We get

20,900 34,700 43,800 49,300
51,500 51,400 49,200

We find the time before splintering by the equation

$$t = \frac{f_o}{Z_s(B/W)} \int_0^Z \frac{dZ}{P}$$

To solve this integral, we plot Z versus 1/P, and find the areas under the curve for the various intervals. These values of the area give us the value of the time. The curve is shown in figure 4-17. The outline of the calculations for the curve is given below.

Z	0.2	0.4	0.6
$f_o/Z_s(B/W)$	104.2	104.2	104.2
$1/P \times 10^4$	0.483	0.292	0.231
$\int_0^Z \frac{dZ}{P}$	1.2×10^{-5}	0.744×10^{-5}	0.512×10^{-5}
t	1.648	2.022	2.554

Z	0.8	1.0	1.2	1.4315
$f_o/Z_s(B/W)$	104.2	104.2	104.2	104.2
$1/P \times 10^4$	0.2052	0.1972	0.1976	0.2060
$\int_0^Z \frac{dZ}{P}$	0.432×10^{-5}	0.400	0.392	0.460
t	3.003	3.419	3.827	4.306

The plot of the P - t curve for the interval from t = 0, to t = 4.306 (splintering), can be seen on figure 4-18 as part of the complete curve.

The equations used in the solutions for the interval before splintering no longer apply. From the point of splintering to the point when all the powder is burned, the following values apply. The form function constants for the burning of splinters are

$$k_1' = 0.49037$$
$$k_2' = -0.3755$$
$$j_1' = 1.231$$
$$j_2' = 0.39648$$
$$\mu_2 = 0.45774$$
$$\mu_3 = 0.66817$$
$$\mu_4 = 0.24197$$
$$\Delta_0/\rho = 0.439$$
$$a\Delta_0\mu_2 = 0.122$$
$$a' = 0.561$$
$$a\Delta_0\mu_3 = 0.179$$
$$r' = 0.125$$
$$\tfrac{1}{2}(\bar{\gamma} - 1) = 0.15$$
$$k_2' f_0 = -0.370$$
$$j_1 Z_s = 1.03$$
$$k_2' f_0/j_1 Z_s = -0.359$$

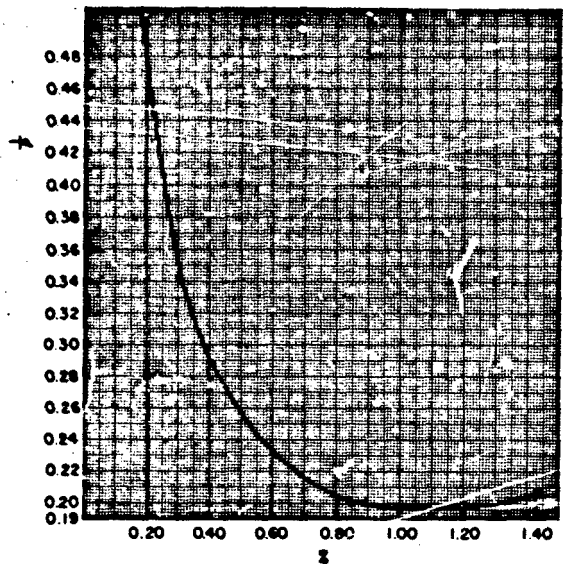

Figure 4-17. Evaluation of time integral in interval before splintering

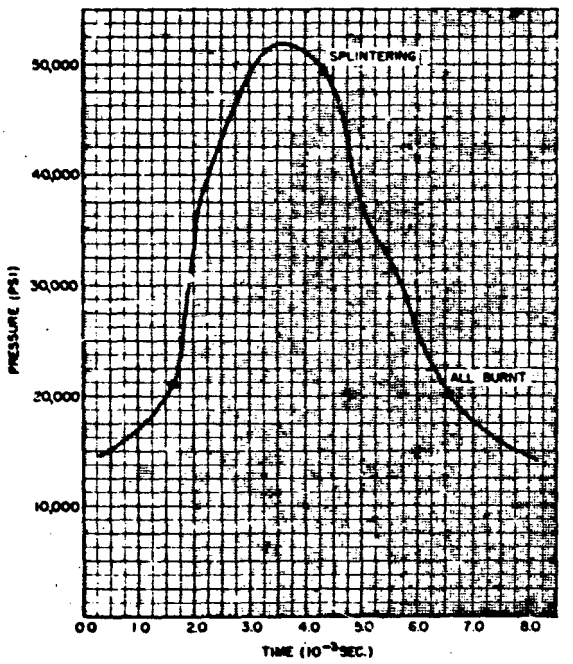

Figure 4-18. Pressure-time curve

Using the formula

$$u' = \tfrac{1}{2}(\bar{\gamma} - 1) - k_2' f_0/j_1 Z_s = 0.68751$$

The physical quantities for the interval of burning of the splinters are given in terms of the parameter Z' in the region

$$Z_s' \leq Z' \leq Z_b'$$

where $Z_s' = j_1 Z_s/j_1' = 0.837$, and $Z_b' = (f_0 + \tfrac{1}{2})\, Z_s'/f_0 = 1.262$.

In addition, we use the following two quantities:

$$J_s' = (1 - u' Z_s')^{-1/u'} = 2.98$$

$$K = \frac{1}{J_s'}\left[\frac{X_s}{X_0} - a' - \frac{r'}{1 + u'}\,(1 + Z_s')\right] = 0.62299$$

where X_s/X_0 is the value of X/X_0 at the end of the previous interval (2.3848).

We take our interval during burning from $Z_s' \leq Z' \leq Z_b'$. Hence, we break this interval into four parts, as shown in the calculations below. To calculate J', we use the formula

$J' = (1 - u'Z')^{-1/u'}$. The values for the various intervals are given in table 4-17.

Table 4-17

Values of J'

Z	0.837	0.900	1.000	1.100	1.262
u'Z'	0.426	0.458	0.509	0.560	0.632
1 - u'Z'	0.574	0.542	0.491	0.440	0.367
1/J'	0.336	0.3095	0.247	0.199	0.140
J'	2.973	3.230	4.050	5.020	7.140

For this interval, S is absorbed in the equations. To calculate the pressure, we use the formula

$$P = \frac{12F\,j_1'\,f_o\,\Delta_o}{Z_s'} \cdot \frac{Z'(1 - u'Z')}{k\,J' + \frac{r'}{1+u'}(1 - u'Z')}$$

The outline of the values for the increments is given in table 4-18.

The value of the time from the beginning of motion is given by

$$t = t_s + \frac{f_o}{Z_s'(B/W)} \int_{Z_s'}^{Z'} \frac{dZ'}{P}$$

We again solve this integral by plotting Z' versus 1/P, and finding the area under the curve for the increments. The values are given in table 4-19.

The equations for the interval after all the powder is burned are in general the same as those for the interval after splintering. First, we find Q, as

$$Q = (1 - \mu_4 Z_s)\left(\frac{X_b}{X_o} - \eta\Delta_o\right)^{\bar{\gamma}-1}$$

The values that we have are

$$\mu_4 = 0.24197$$
$$Z_s = 1.4315$$
$$\mu_4 Z_s = 0.346$$
$$(1 - \mu_4 Z_s) = 0.654$$
$$\eta\Delta_o = 0.706$$
$$\frac{X_b}{X_o} - \eta\Delta_o = 3.992$$
$$\left(\frac{X_b}{X_o} - \eta\Delta_o\right)^{0.3} = 1.515$$
$$Q = 0.991$$

The physical quantities for the interval after all the powder is burned are given in terms of X/X_o as the parameter. The pressure is given by

$$P = 12\,F\Delta_o\,Q\,(X/X_o - \eta\Delta_o)^{-\bar{\gamma}}$$

Table 4-18

Maximum pressure in interval after splintering

Z	0.837	0.900	1.000	1.100	1.244
KJ'	1.67	1.814	2.270	2.820	4.01
$r'/1+u'$	0.0829	0.0829	0.0829	0.0829	0.0829
$12FJ'_1 f_o\Delta_o/Z_s'$	175,000	175,000	175,000	175,000	175,000
$Z'(1 - u'Z')$	0.4805	0.4880	0.4910	0.484	0.458
$\left[\frac{r'}{(1+u')(1-u'Z')}\right]$	0.0476	0.0449	0.0407	0.0365	0.0305
$P_{space\ av.}$	49,000	46,000	37,100	29,650	19,840
P_{max}	49,700	46,800	37,700	30,200	20,100

Table 4-19

Time in interval after splintering

Z'	0.837	0.9	1.00	1.10	1.244
$f_o/Z'_s(B/W)$	178.2	178.2	178.2	178.2	178.2
$1/P \times 10^4$	0.204	0.2175	0.2695	0.338	0.503
$\int \frac{dZ}{P}$	0.136×10^{-6}	0.245	0.300	0.597	
t	4.306	4.548	4.984	5.518	6.578

For our X/X_o values, we take the value X_b/X_o, and X_m/X_o. We have $X_b/X_o = 4.698$, $P_m = 19{,}740$; and $X_m/X_o = 5.05$, $P_m = 17{,}700$.

The time is found from the integral

$$t = t_b + \frac{V_C}{12a} \int_{X_b/X_o}^{X_m/X_o} \frac{d(X/X_o)}{V}$$

To find the value of V, we use the formula

$$V^2 = \frac{2CF}{(\bar{\gamma} - 1)m'} \left[1 - Q\,(X/X_o - \eta\Delta_o)^{1-\bar{\gamma}}\right]$$

$$V_b^2 = 2.754 \times 10^6 \left[1 - 0.991\,(4.698 - 0.706)^{-0.3}\right]$$

$$V_b = 976 \text{ ft/sec}$$

$$V_m^2 = 2.754 \times 10^6 \left[1 - 0.991\,(4.344)^{-0.3}\right]$$

$$V_m = 1{,}012 \text{ ft/sec}$$

$$t = 6.578 + \frac{45.7}{12} \int_{4.698}^{5.05} \frac{d(X/X_o)}{V}$$

$$\frac{1}{V_b}(10^3) = 1.025$$

$$\frac{1}{V_m}(10^3) = 0.988$$

$$t = 6.578 + 0.352 = 6.930$$

LE DUC SYSTEM

4-49. Introduction. The Le Duc System is almost completely empirical, deriving little support from theory. The system depends on assuming a simple algebraic relation between velocity and shot travel.

The basic assumption of the Le Duc System is that the velocity space curve for the travel of the projectile up the bore of any gun can be represented by the hyperbolic function

$$v = \frac{ax}{b + x} \qquad (180)$$

This curve passes through the origin, rises steeply at first, and gradually flattens out. This curve resembles the velocity-space curve in general form, but the equation is not always accurate.

To determine the significance of a, it will be noticed that as x tends to infinity, $\frac{x}{b + x}$ tends to unity, and v thus tends to a. Therefore, a is the theoretical velocity of a projectile fired from a gun with the given loading conditions, but from a gun of infinite length. Under these conditions the kinetic energy of the projectile is expected to be $\frac{1}{2}\frac{wa^2}{g}$. However, by consideration of the energy equation

$$\frac{FC_Z}{\gamma - 1} = \frac{PC_Z(v - b)}{\gamma - 1} + A\int_o^x P_s\,dx \qquad (181)$$

it is seen that the energy released by the burning propellant is $FC/\gamma - 1$. Neglecting losses, and equating the two energy expressions, we get

$$\frac{FC}{(\gamma - 1)} = \frac{1}{2}\frac{wa^2}{g} \qquad (182)$$

or

$$a = \left[\frac{2gF}{(\gamma - 1)}\frac{C}{w}\right]^{1/2} \qquad (183)$$

Adapted for American naval pyro powder, the formula becomes

$$a = 6823(C/w)^{\frac{1}{2}}\,(27.68C/K_o) \qquad (184)$$

with

$$\gamma = \frac{7}{6}$$

C and w are in lb, K_o is in cubic inches.

For other propellants, the constant term is modified in the ratio of $\left[\frac{F}{(\gamma - 1)}\right]^{\frac{1}{2}}$.

By consideration of the equation of motion of a projectile, the formula for maximum pressure is derived as

$$P_m = \frac{4.48\, wa^2}{27Agb} \qquad (185)$$

It can be shown that b is travel to maximum pressure.

It is assumed that the shot travel to maximum pressure is proportional to some function of the quickness of the propellant, to initial air space, and to some power, positive or negative, of the chamber volume and of the weight of the projectile, that is

$$b = q(K_o - C/\delta)K_o^{a} - 1_w^{-k}$$

$$= q(1 - C/\delta K_o)K_o^{a} w^{-k} \qquad (186)$$

where q is a constant depending on the composition and ballistic size of the propellant. For American pyro powders, a and k have been determined as approximately 2/3. Hence the formula becomes

$$b = q(1 - C/\delta K_o)\,(K_o/w)^{2/3} \qquad (187)$$

4-50. Example by Le Duc System. The four basic equations that are used in our calculations are given below.

$$v = \frac{ax}{b + x} \qquad (188)$$

$$a = \left[\frac{2gF}{\gamma - 1}\,\frac{C}{w}\right]^{1/2} \qquad (189)$$

$$P_m = \frac{4.48\, wa^2}{27Agb} \qquad (190)$$

$$b = q\left(1 - \frac{C}{K_o\delta}\right)\left(\frac{K_o}{w}\right)^{2/3} \qquad (191)$$

By the Le Duc system, we first calculate the value of a, directly from equation (189). With this value of a, and by use of equation (190), with the known maximum pressure of item 21, we can calculate the value of the constant b. We can use the computed value of a in either the formula for pressure or the formula for velocity. With the constant b, however, we can only use the b value calculated from maximum pressure in the formula for maximum pressure. The b value which is calculated from the velocity formula can be used only in computing velocity. This is explained by the fact b takes somewhat different values in each case. In our example, we will first calculate the value of a for item 21. With this, we will calculate the values of b from the pressure formula and from the velocity formula. We then calculate the value of a for items 10 and 14, and by changes in equation (191), we can calculate the b value for velocity for items 10 and 14. Then, with our values of b and a for items 10 and 14 a simple calculation yields the velocity.

To calculate the maximum pressure in items 10 and 14, we use the a values computed for 10 and 14 and make the proper changes in the b from pressure in item 21 to obtain the b value for pressure in items 10 and 14. With these values, the maximum pressure can be calculated directly.

For item 21

$$a = \frac{(64.4)\,(318{,}000)\,(8.12)}{(0.258)\,(24.1)}$$

$$a = 5{,}189$$

Finding the b value for maximum pressure, we obtain

$$45{,}400 = \frac{(0.1659)\,(24.1)\,(2.692)\,10^7}{(10.7)\,(32.2)\,b}$$

$$b = 7.126 \text{ ft}$$

b_{10}(for pressure) =

$$\frac{(1 - C/\delta K_o)_{10}\,(K_o/w)_{10}^{2/3}}{(1 - C/\delta K_o)_{21}\,(K_o/w)_{21}^{2/3}} \qquad (7.126)$$

$$b_{10} = \frac{\left[1 - \frac{3.82}{(0.0571)\,(140)}\right]\left(\frac{140}{15.4}\right)^{2/3}}{\left[1 - \frac{8.12}{(0.0571)\,(300)}\right]\left(\frac{300}{24.1}\right)^{2/3}}$$

$$b_{10} = 5.74 \text{ ft}$$

To get the value of b for item 14 that is needed for pressure, we solve in the same manner, and obtain

$$b_{14} = \frac{\left[1 - \frac{3.39}{(0.0571)\ (200)}\right]\left(\frac{200}{15}\right)}{28.2} \qquad (7.126)$$

$$b_{14} = 10.1$$

The a value for item 10 is

$$a = \left[\frac{(64.4)\ (3.18 \times 10^5)}{0.256}\ \frac{3.82}{15.4}\right]^{1/2} = 4,455$$

$$a^2 = 19.85 \times 10^6$$

The a value for item 14 is

$$a = \left[\frac{(64.4)\ (3.18)\ 10^5}{0.256}\ \frac{3.39}{15.0}\right]^{1/2} = 4,250$$

$$a^2 = 18.08 \times 10^6$$

$$P_{10} = \frac{(0.166)(15.4)(19.85)10^6}{(7.02)(32.2)(5.74)} = 39,100 \text{ lb per in.}^2$$

$$P_{14} = \frac{(0.166)(15)(18.1)}{(7.02)(32.2)(10.1)} = 19,800 \text{ lb per in.}^2$$

Checking for velocity in items 10 and 14, we first have to obtain the b value for velocity in item 21.

$$b = \frac{(5,189)(156)}{2,800} - 156 = 133 \text{ in.}$$

Applying this value of b to find the values of b in 10 and 14, we obtain

$$b_{10} = \frac{(0.522)(4.36)(133)}{(0.526)\ (5.36)} = 107 \text{ in.}$$

$$b_{14} = \frac{(0.703)(5.61)(133)}{2.82} = 186 \text{ in.}$$

$$V_{10} = \frac{(4,455)(136)}{107 + 136} = 2,490 \text{ ft per sec}$$

$$V_{14} = \frac{(4,250)(158)}{186 + 158} = 1,980 \text{ ft per sec}$$

4-51. Comparison of Results. Since the same problems have been worked out by the three systems, a comparison of the results may be made. This is done in table 4-20. Since only two problems have been worked out, a general comment cannot be made as to the relative accuracy of the three systems, although it seems that both the RD38 (Corner system) and Hirschfelder (OSRD 6468) systems give results which are about the same in value.

Table 4-20

Comparison of results

Value	RD38 method			OSRD 6468	Le Duc	Firing values
	$\theta = 0$	$\theta = 0.15$	$\theta = 0.30$			
$P_{m_{10}}$	43,600	44,400	46,400	48,100	39,100	48,640
V_{10}	2,560	2,610	2,590	2,680	2,490	2,600
P_{14}	21,800	23,100	25,300	19,800	19,800	33,000
V_{14}	2,180	2,280	2,300	2,340	1,980	2,400

REFERENCES AND BIBLIOGRAPHY

1. Corner, J., "Theory of Interior Ballistics of Guns," John Wiley and Sons, New York, 1950.

2. Curtiss, C. F., and J. W. Wrench, Jr., Interior Ballistics, Division 1, OSRD, NDRC Report No. A-397, Washington, D. C.

3. Hypervelocity Guns and the Control of Gun Erosion, Summary of Technical Report of Division 1, NDRC, Vol. 1, Washington, D. C., 1946.

4. Hayes, T. J., "Elements of Ordnance," John Wiley and Sons, New York, 1938.

5. "Internal Ballistics," Philosophical Library, New York, 1951.

GENERAL PROBLEMS OF PROPELLANT IGNITION

4-52. The standard method of igniting fixed and semifixed rounds of ammunition is by the long artillery primer; usually the longest primer allowed by the cartridge case and round lengths is used, in the hope of distributing the igniter gases uniformly in the propelling charge. Few conventional primers justify this intent (see references 1, 2, and 3), because the black powder charge within the narrow primer tube imposes a resistance to rapid flow of gases within the tube. For a simplified analysis of the action of the primer gases, see reference 4; for design information regarding standard primers, see reference 7.

Manifestations of improper ignition vary from misfires and hangfires to sporadic high pressures and poor velocity uniformity. Theoretical analysis indicates, and experience confirms, that problems of ignition are more severe under the following conditions:

1. High propellant loading density (over 0.7 gm/cc)
2. Long cartridge cases
3. Small granulations of propellant
4. Low flame temperature propellants
5. Low ambient temperatures
6. Low projectile sectional densities and starting forces.

These conditions are met more frequently in modern ammunition, because there is a need to attain high velocities and to extend gun life.

There is still much to be learned about ignition of propellants and there may be disagreement among workers in the field on the principles to follow. There appears to be no difference of opinion, however, that in artillery rounds the index of satisfactory ignition is a pressure-time record of the firing that exhibits no discontinuities. There has been general acceptance of this rule, which was first proposed by British workers in 1942, and most proving grounds are equipped to record the pressure-time relationship in experimental firings.

It is obvious that the ignition interval is complete when the pressure in the gun has reached some high value. It follows that the primer must have discharged its igniter gases by that time. If the primer used does not accomplish this, only part of its black powder charge is effective. This is the explanation of why some primers with a small black powder charge perform better than larger primers in certain rounds.

As a consequence of the nonuniform distribution of black powder gases along the axis of the primer or the time delay which exists in many primers before any gases emerge from the forward vent holes, some parts of the propellant bed start burning, and increase the pressure locally, earlier than others. This is believed to be conducive to sporadic high pressures under the several conditions listed earlier. For an alternate hypothesis, see reference 5.

During the past few years there have been several proposals made for overcoming the deficiencies of the conventional long artillery primers.

a. The fraction of the black powder charge emitted from each section of the primer can more nearly be equalized by using small vents where the pressure normally is highest and large vents where pressure is low. An example of this is the T88E1 primer.

b. An empty channel can be built into the primer, so that the percussion element flash is transmitted rapidly along the whole primer axis.

c. Some correction is effected if the black powder charge is positioned forward, rather than in close contact with the percussion element. The distance forward has to be precisely determined in order to prevent hangfires.

d. The igniter charge may be placed in a closed magazine at the rear, from which the gases then issue into a highly vented, empty forward section. Since room for the igniter material is limited in such an arrangement, something with a higher heat of reaction than black powder must be used. In a practical device designed by the Canadians, a propellant with high nitroglycerine content is used.[6]

e. The resistance to flow along the axis, characteristic of haphazardly packed black powder granules, can be drastically reduced by using an igniter material in the form of long sticks. A proper rate of burning is provided by inducing porosity in the igniter sticks during manufacture.[7]

Practical considerations often dictate the design of the ignition system on terms directly

opposed to the requirement for optimum ignition. As an example, there was one experimental, fin-stabilized round whose fin extended within a few inches of the cartridge-case base, leaving no room for a primer. Fortunately for the engineers responsible for the ignition system, the project was cancelled. The problem is present to a varying extent in other finned ammunition.

In separate-loading ammunition (no cartridge case), no primer is used. The ignition system consists of pancake bags loaded with black powder and positioned along the charge. An attempt is made to allow a free channel for passage of igniter gases by using propelling charges of smaller diameter than the chamber. There is evidence to indicate that the loading density must be very low to prevent sporadic high pressures.

REFERENCES AND BIBLIOGRAPHY

1. Ekstedt, E. E., and D. L. Wann, The Discharge Characteristics of Certain Artillery Primers, BRL Report No. 972, November 1955.

2. Vest, D. C., et al, On the Performance of Primers for Artillery Weapons, BRL Report No. 852.

3. Unpublished experimental data available at Picatinny Arsenal on several standard and special primers.

4. Hicks, B. L., Some Characteristics of the Practical Ignition of Propellants, BRL Memorandum Report No. 640, December 1952.

5. Frazer, J. d., et al, One View of the Ignition Process for Nitrocellulose Propellants, Bulletin of the First Symposium on Solid Propellant Ignition.

6. McLennan, D. E., Studies in Ignition, Part VIII: Further Experiments with the "Hot Gas" Primer, CARDE Report No. 296/54, April 1954.

7. Vest, D. C., A General Discussion of Extruded Igniter Compositions, BRL Memorandum Report No. 894.

8. Price, J. R., Experiments on the Ignition of Cool Granular Propellants in the Q. F. 3" 70 cal Gun, CARDE Memorandum (P) 14/55.

CALCULATION OF THERMODYNAMIC PROPERTIES OF PROPELLANTS

4-53. Introduction. From a knowledge of the composition of propellants, the thermochemical properties of their constituents, and of the products of explosion, it is possible to calculate the ballistic properties of propellants. Because the propellant is a colloid rather than a compound, the individual contributions of the constituents are additive. The following methods of calculation, based on reference 1, use the summation of tabulated values of these additive properties.* Gun performance depends, essentially, on three properties of the propellant gas: n, the number of moles of gas formed per gram of propellant burned (reciprocal of the mean molecular weight of the gas); C, the mean heat capacity of the combustion gases in the range of temperatures and densities attained in the gun; T_V, the adiabatic (constant volume) flame temperature (the temperature a gas would attain if all the energy of the propellant were used to heat the gas, without energy loss to surroundings). Auxiliary quantities are defined in terms of these three. The constituent properties of propellants that are calculated by these methods are:

Heat of explosion	Q	cal per gm
Gas volume	n	moles per unit mass
Relative energy in gas	E	cal per gm
Mean heat capacity	C	cal per gm per deg
Force	F	ft-lbs/lb
Unoxidized carbon	UC	percent in gas
Density	D	gms per cc

4-54. Heat of Explosion. Calculations are based on the assumption that the carbon, hydrogen, nitrogen, and oxygen of the solid propellant are transformed into CO or CO_2, H_2 or H_2O, and N_2; and that no free oxygen or dissociation results.

a. The heat of explosion (Q) is calculated for an organic chemical constituent by the formula

$$Q = \frac{(-\Delta H_C) - 67{,}421\ (2C + \frac{1}{2}H - 0)}{\text{molecular weight}}$$

where ΔH_C = heat of combustion, in cal per mole.

Example. Ethylene diamine dinitrate ($C_2H_{10}N_4O_6$):

$$Q = \frac{377{,}580 - 67{,}421\ (4 + 5 - 6)}{186}$$

$$= 945 \text{ cal per gm}$$

b. The heat of explosion (Q) is calculated for a propellant composition (the colloid) by obtaining the algebraic sum of weighted values for all constituents.

Example. Calculation for a propellant containing 20 percent nitrocellulose (13.15 N), 30 percent triethylene glycol dinitrate, and 50 percent ethylene diamine dinitrate is as follows:

1033* x 0.20 = 206.2
619 x 0.30 = 186.
945 x 0.50 = 473.
Q = 865.2 cal per gm

4-55. Gas Volume (Volume of Products of Explosion). Calculations are based on the assumed complete reaction to yield maximum volume. Below 3,000°K, n is additive (by this method; values are given in table I of reference 1). Above 3,000°K, dissociative equilibrium becomes important, but does not affect values of n at densities encountered in guns.

a. The gas volume (n) is calculated for an organic chemical constituent by the formula

$$n = \frac{C + \frac{1}{2}H + \frac{1}{2}N}{\text{molecular weight}}$$

Example. Triethylene glycol dinitrate ($C_6H_{12}N_2O_8$):

$$n = \frac{6 + 3 + 1}{240} = 0.0542 \text{ moles per gm}$$

b. The gas volume (n) is calculated for a propellant composition by obtaining the sum of weighted values for all constituents.

Example. For composition as in subparagraph 4-54b, above:

0.0392 x 0.20 = 0.00784
0.0542 x 0.30 = 0.01625
0.0484 x 0.50 = 0.02420
n = 0.04829 moles per gm

*These are simplified equations. For more detailed methods, see paragraph 4-64 and associated references.

*The Q value for nitrocellulose is obtained from reference 19, p. 276.

4-56. Energy Released (Relative Energy) is the change in internal energy of the propellant gases when they cool from the adiabatic flame temperature to the temperature at which the relative energy is being calculated (in this case, 2,500°K). (See paragraph 4-59.)

a. The relative energy in the gas is calculated for an organic chemical constituent by the formula:

$$E = \frac{(-\Delta E) - 132{,}771\,C - 40{,}026\,H}{\text{molecular weight}} + \frac{51{,}819\,O - 6{,}724\,N}{\text{molecular weight}}$$

where $-\Delta E$ is the heat of combustion.

Example. Ethylene diamine dinitrate ($C_2H_{10}N_4O_6$):

	-132,771 x 2 =	-265,542
	- 40,026 x 10 =	-400,260
ΔE = 377,580		
	- 6,724 x 4 =	- 26,896
6 x O = 310,914		-692,698
+688,494		+688,494
		- 4,204

$$E = \frac{4204}{186} = 22.59 \text{ cal per gm}$$

b. The relative energy is calculated for a propellant composition by obtaining the algebraic sum of weighted values for all constituents.

Example. For composition as in subparagraph 4-54b, above:

283.1 x 0.20 =	+56.6
-169 x 0.30 =	-50.5
- 22.6 x 0.50 =	-11.3
	- 5.2 cal per gm

4-57. Mean Heat Capacity (see reference 2, p.19 ff).

a. The mean heat capacity is calculated for an organic chemical constituent by the formula:

$$C = \frac{1.62\,C + 3.265\,H + 5.193\,O + 3.384\,N}{\text{molecular weight}}$$

b. The mean heat capacity is calculated for a propellant composition by obtaining the sum of weighted values for all constituents.

4-58. The Ratio of Specific Heats.

$$\gamma = \frac{\text{Sp. Ht. Constant Pressure}}{\text{Sp. Ht. Constant Volume}} = \frac{C_p}{C_v}$$

where

$$\gamma = 1 + \frac{nR}{C_v}$$

$$\gamma = 1 + 1.987\frac{n}{C_v}$$

where the units of R are BTU per lb-mole per °R, or cal per gm-mole per °K.

4-59. Isochoric Adiabatic Flame Temperature. (See reference 2, pp. 19-22.) This value (T_v) = 2,500 + E/C_v. If T_v is found to be over 3,000°K, a better approximation can be obtained from the formula:

$$T_v = 3000 + 6046\left\{-(C_v + 0.01185) + \left[(C_v + 0.01185)^2 + 3.308 \times 10^{-4}(E - 500C_v)\right]^{\frac{1}{2}}\right\}$$

4-60. Isobaric Adiabatic Flame Temperature. This value (T_p) = T_v/γ.

4-61. Force. This term is a property of a propellant composition that is convenient for use in interior ballistic systems. It is defined as

$$F = nRT_v$$

For the composition given in subparagraph 4-54b above,

$$F = (0.04823)\,(1543)\,(2490)\,(1.8) \quad \text{ft-lbs/lb}$$

where 1.8 x 1543 is the gas constant.

Experimental values of force for a new composition relative to a known composition may be obtained as the ratio of maximum pressures obtained in the closed bomb upon firing equal weights of propellant. This is justified as follows.

The equation of state of satisfactory assuracy under closed bomb conditions is

$$P(V - \eta) = nRT_v = F$$

where η is the covolume and T_v (neglecting cooling) is the adiabatic flame temperature. For equal covolumes,

$$\frac{P_1}{P_2} = \frac{(nRT_v)_1}{(nRT_v)_2}$$

Note that the cooling of the system affects the results, if widely different granulations (see paragraphs 4-7 and 4-8) are tested.

4-62. Unoxidized Carbon.

a. This value is determined for the purpose of estimating by calculation the amount of carbonaceous smoke produced from propellants in ballistic tests. For the purpose of simplicity in calculations, the following assumptions are made:

1. Propellant gases consist only of CO_2, CO, H_2O, H_2, and N_2.

2. N_2 is not involved in smoke and related oxidations.

3. All CO_2 and H_2 which are formed can be considered as equivalent amounts of additional CO and H_2O formed, without affecting fuel-oxygen balance.

4. All H_2 burns to H_2O; all remaining O_2 burns some C to CO; remaining unoxidized C represents carbonaceous smoke.

b. The excess (or deficiency) of oxygen in an organic chemical compound, for rearrangement of the atoms to CO and H_2O, can be calculated by the formula.

$$\text{Oxygen deficiency percent} = \frac{\text{deficient no. atoms oxygen} \times 16}{\text{molecular weight}} \times 100$$

Example. Ethylene diamine dinitrate:

$$\text{Oxygen deficiency} = \frac{16}{186} \times 100 = -8.6 \text{ percent}$$

The value of this estimation is that it allows a comparison to be made between a new formulation and a known formulation whose smoke characteristics are favorable.

c. The percentage oxygen deficiency of the products of combustion of a propellant composition can be calculated by obtaining the algebraic sum of weighted values for all constituents.

Example. For the composition (given in subparagraph 4-54b, above:

+0.81 x 0.20 =	0.162	(20% NC; 13.15% N)
-26.7 x 0.30 =	- 8.01	(30% TEGN)
- 8.6 x 0.50 =	- 4.30	(50% EDDN)
Oxygen deficiency =	-12.15%	

d. Unoxidized Carbon. This value can be obtained by multiplying the oxygen deficiency by 12/16. In the example in subparagraph 4-62c, above:

$$-12.15 \left(\frac{12}{16}\right) = 9.12\% \text{ unoxidized}$$

4-63. Density. The density of a propellant composition can be calculated by obtaining the sum of weighted values for all constituents. This is the density of the solid propellant.

4-64. Alternate Methods of Calculation. Some important quantities used to determine the thermochemical characteristics of propellants and explosives are heat of combustion (ΔH_c), heat of explosion (Q), heat of formation (ΔH_f), and heat of reaction (ΔH_r). These quantities are all interrelated and are usually determined by some form of calorimetric test. The detailed descriptions of the many methods of calculating these quantities are given in the references (see bibliography at end of this section). The exact definition of each term is given in the glossary.

The calorimetric quantities are related by the formula:

$$\Delta H = \Sigma H_f(\text{products}) - \Sigma \Delta H_f(\text{reactant}) \quad (192)$$

where

ΔH = heat (energy) evolved

$\Delta H_f(\text{products})$ = heat of formation of the products of the reaction

$\Delta H_f(\text{reactant})$ = heat of formation of the reactant (explosive).

The principal methods of calculating these properties are described in references 4, 5, 6, 7, and 10.

To calculate the heat of explosion (Q) for any explosive or propellant, it is necessary to know the heat of formation (ΔH_f), or the heat of combustion (ΔH_c), of the substance, as well as the products of explosion.

a. Methods for Calculating ΔH_f. Based on chemical structure of the molecue, it is possible to estimate the heats of formation of compounds by the following methods:

1. Kharasch method, references 4 and 8;

2. Bond, group, and atomization energies, references 5, 6, and 9;

3. Group contribution method, reference 7.

A simpler, but generally satisfactory, method (for heat of combustion) consists of adding the contribution of the various structural groups, as given in table 4-21. Special experimental studies have been made on heats of formation of nitrocellulose, reference 11, and nitroglycerin, reference 12.

b. Calculation of ΔH_c. Heat of combustion, H_c, may be calculated by (1) a modification of formula (192),

$$\Delta H_c = \Sigma \Delta H_f(\text{products}) - \Sigma \Delta H_f(\text{reactant})$$

or (2) by direct summation of heats of combustion of the molecular structural units (if the values are known). Substituting the known values from table 4-21 for TNT ($C_7H_5O_6N_3$), ΔH_c may be calculated thus:

Structural feature	Heat liberated (kcal per mole)
3 C=C	3 x 116.43
4 C–C	4 x 49.79
5 C–H	5 x 52.44
3 C–NO_2 (Aromatic)	3 x 16.66
Resonance of benzene nucleus	-40.00
H_c calculated	820.6 kcal per mole
H_c experimental	820.7 kcal per mole

c. Calculation of Q. The heat of explosion cannot be predicted as accurately as the heat of combustion because the products of explosion are uncertain. Various procedures have been advanced for estimating the products of explosion. See subparagraph 4-54b and references 2, 13, 14, 15, 16, 17, and 18.

Table 4-21

Heat of combustion values from structural features

(H_2O is calculated as a liquid; see reference 6.)

C–H	52.44
C–C	49.79
C–O (Aliphatic)	13.96
C–O (Aromatic)	4.16
C–N (Aliphatic)	27.91
C–N (Aromatic)	33.70
O–H	-14.28
N–H	21.34
C=C	116.43
C=O (Ketone)	11.25
C=O (Amide)	16.15
C=O (Aldehyde)	19.09
O–NO_2	-12.90
C–NO_2 (Aliphatic)	10.76
C–NO_2 (Aromatic)	16.66
N–NO_2	6.55
Resonance of benzene nucleus	-40.00
Resonance of naphthalene nucleus	-77.00
Resonance of amide	-27.00

REFERENCES AND BIBLIOGRAPHY

1. Hirschfelder, J. O., and J. Sherman, Simple Calculation of Thermochemical Properties for Use in Ballistics, Office of Scientific Research and Development Report No. 935, October 1942.

2. "Internal Ballistics," Philosophical Library, New York, 1951.

3. Hirschfelder, J. O., et al., Interior Ballistics, Office of Scientific Research and Development Report No. 6468, July 1945.

4. Kharasch, S., Heats of Combustion of Organic Compounds, Bu. Std. Jr. Res., RP 41, vol. 2, p. 359, 1929. This paper gives determined and calculated values for hundreds of compounds.

5. Springall and Roberts, ARD Explosives Report No. 614/44, Bristol Research Report No. 126, July 1944.

6. Report on Study of Pure Explosive Compounds, Arthur D. Little, Inc., 2 April 1947.

7. Anderson, Beyer, and Watson, National Petroleum News, vol. 36, May-August 1944.

8. Selected Values of Physical and Thermodynamic Properties of Hydrocarbons and Related Compounds, American Petroleum Institute Research Project 44, 1953, Carnegie Press.

9. Pauling, "Nature of Chemical Bond," Cornell University Press, 1948.

10. Laidler, K. J., Progress Report, Catholic University of America, NORD 10260, December 1949.

11. Jessup and Prosser, National Bureau of Standards Report RP 2086, vol. 44, April 1950.

12. Taylor and Hall, Journal of Physical Chemistry, p. 593, 1947.

13. Kistiakowsky and Wilson, NDRC Report No. 1352.

14. Robinson, C. S., "Thermodynamics of Firearms," McGraw-Hill Book Co., New York, p. 41 ff

15. Corner, J., "Theory of Interior Ballistics of Guns," John Wiley and Sons, New York, 1950, p. 89 ff.

16. "Handbook of Chemistry and Physics," 34th ed., Chemical Rubber Pub. Co., Cleveland, Ohio, pp. 1631-1640, 1952-53.

17. Perry, J. H., ed., Chemical Engineer's Handbook," 3rd ed., McGraw-Hill Book Co., New York, 1950, pp. 236-246, 344, 345.

18. Gilman, Henry, ed., "Organic Chemistry," John Wiley and Sons, New York, 1953, vol. IV, p. 953 ff.

19. Hickman, C. M., Rocket Fundamentals, Office of Scientific Research and Development Report No. 3992, 29 December 1944 (CONFIDENTIAL).

20. Tomlinson, W. R., Properties of Explosives of Military Interest, Picatinny Arsenal Technical Report No. 1740, 20 June 1949 (CONFIDENTIAL).

21. Garner, W. E., and C. L. Abernathy, Heats of Combustion and Formation of Nitro Compounds (Benzene, Toluene, Phenol and Methylaniline Series), Chemical Abstracts, vol. 15, 3748, 1921.

22. Blatt, A. H., Compilation of Data on Organic Explosives, Office of Scientific Research and Development Report No. 2014, 29 February 1944 (CONFIDENTIAL).

23. Stegeman, G., Heat of Combustion of Explosive Substances, Office of Scientific Research and Development Report No. 5306, 4 July 1945 (CONFIDENTIAL).

24. Sheffield, O. E., Long range Basic Research Leading to the Development of Ideal Propellants — Compounds of High Nitrogen Content in Propellant Powders, Picatinny Arsenal Technical Report No. 1694, 26 May 1948 (CONFIDENTIAL).

25. Taylor, J., C. R. Hall, and H. Thomas, Thermochemistry of [illegible] pellant Explosives, J. Phys. & Colloid Chem., vol. 51, 580-592, 1947.

26. Helf, S., Long Range Research Leading to the Development of Ideal Propellants — Compounds of High Nitrogen Content in Propellant Powders, Picatinny Arsenal Technical Report No. 1752, 7 November 1949 (CONFIDENTIAL).

27. Castarina, T. C., Long Range Research Leading to the Development of Ideal Propellants — Explosives Plasticizers for Nitrocellulose, Picatinny Arsenal Technical Report No. 1755, 30 December 1949 (CONFIDENTIAL).

28. Second Report on Synthesis and Testing of High Explosives to Office of the Chief of Ordnance, Arthur D. Little, Inc., 1 March 1951 (CONFIDENTIAL).

29. Picatinny Arsenal Technical Report No. 1841.

30. Jessup, R. H., and E. J. Prosen, Heats of Combustion and Formation of Cellulose and Nitrocellulose, National Bureau of Standards Research Paper, Report No. 2086, vol. 44, 3 January 1950.

31. J. Soc. Chem. Ind., vol. 55, 291-2T, 1936.

32. Stohmann, F., Colorimetrische Untersuchungen, Journal Praktische Chemie (2), vol. 55, 263, 1897.

33. Karrer, P., and W. Fioroni, Heats of Combustion of Carbohydrates, Chemical Abstracts, vol. 17, 2416, 1923.

34. Picatinny Arsenal Physical Chemistry Laboratory reports.

PROPELLANT CHARACTERISTICS AND TEST* METHODS[1]

4-65. Sensitivity is a measure of the ease with which an explosive material can be made to burn or explode. Propellants, as manufactured, are relatively insensitive to shock and friction. However, they are required to be sufficiently sensitive to ignition by flame so that initiation may be positive and burning may be uniform (see paragraph 4-52).

4-66. Stability is a measure of the period of time that an explosive material can be safely stored before it begins to decompose. Propellant stability is concerned primarily with the stability of nitrocellulose, which, being hygroscopic, is the most vulnerable component of propellant compositions. Tests for stability are made during the manufacture of the propellant, immediately after the completion of each lot, and as long as the lot remains in service. After propellants are issued for service use, it is not possible to subject them to the heat tests described here; therefore, visual checks, such as the methyl violet test, are used.

4-67. Methyl Violet Test. This test is used as an acceptance test for both nitrocellulose and finished propellant. The test prevents acceptance of improperly stabilized nitrocellulose and detects deterioration of the propellant in service. It consists of heating the sample with methyl violet test paper in a glass tube while the temperature is maintained at a constant 134.5±0.5°C, or 120°C, and noting the time required for the test paper to turn salmon pink, and for the onset of NO_2 fumes; in addition, the sample must not explode in less than five hours. Actual minimum time requirements of individual propellants are given in the propellant specifications. This test is run at 135°C for single-base propellants, and at 120°C for double-base propellants. A related test (for nitrocellulose) is the Bergmann-Junk test, in which a quantitative determination is made of the amount of gas liberated.

4-68. KI-Starch Test. This test is used as an acceptance test to prevent acceptance of nitrocellulose containing traces of oxidizing impurities that tend to accelerate the decomposition. It is a test for traces of impurities that might cause deterioration, rather than a test of inherent instability. After being properly prepared and dried, the sample is heated (nitrocellulose to 65.5°C, nitroglycerin to 82.2°C) in a glass tube maintained at constant temperature, into which is suspended a potassium iodide- and starch-impregnated paper. The test is continued until the paper becomes discolored. The minimum time required for discoloration of the paper is considered to be the test value of the sample. This test is gradually being eliminated from general use.

4-69. 65°C Surveillance Test. This test is applied only to finished propellants. It consists of placing the samples in sealed bottles in a magazine kept at a constant temperature of 65°C. The end point is reached when red fumes of nitrous oxide appear in the bottles. Minimum times of appearance of the fumes are stated for each size of granulation.

4-70. 115°C Heat Test. This test applies only to finished propellant. It consists of exposing whole grains of the propellant to a temperature of 115°C for six 8-hour days and noting the weight loss. The loss in weight must be less than a specified limit for each size of granulation. This test is not in general use.

4-71. Compression Test. Propellant grains should be designed to withstand the stresses to which they may be subjected during the firing of a gun. Little has been done to determine what theoretical factors are involved, but it is known that the chamber pressure builds up too sharply if the grains fracture (exposing more burning surface). Therefore, it is desired that the grains do not fracture during firing. The compression test is a routine test for measuring the percent compression to failure under static load. It is a very simple test, and unsatisfactory as a measure of the propellant's ability to withstand stresses imposed by the gun. In the test, the grains are cut to form cylinders whose lengths are equal to their diameters, and are then compressed between parallel surfaces until the first crack appears on the cylindrical surface. Specification JAN-P-270 requires that the average compression of a grain at the point of cracking be not less than 30 percent. Nitroguanidine propellants are excepted.

*See Section 2 for tests applicable to high explosives.

4-72. Maximum Pressure (see Glossary, under "PERMISSIBLE INDIVIDUAL MAXIMUM PRESSURE"). Proof firings are made to determine the pressure developed by a propellant. The easiest way to measure this pressure is by the use of a device called a crusher gage, which is inserted in the gun chamber. In this type of gage the gas pressure developed is transmitted, by means of a piston, to a copper cylinder contained within the body of the gage, and the amount of deformation of the copper cylinder is used as a measure of the maximum gas pressure to which the gage has been subjected.[2] The crusher gage is used in two forms: a fixed gage, which is threaded into the breech block, and a loose gage, which is loaded loosely with the propellant charge. Because of the high strain rate of the gage, the deformation of the copper cylinder is smaller than the deformation that would be obtained for the same stress under static conditions. Accurate piezoelectric measurements indicate that the true pressure stressing the gage is approximately 1.2 times the static pressure required to produce the measured strain of the copper cylinder. Although the crusher gage does not record true pressure levels, it is still of value as an indicator of relative pressure.

Crusher gages can only measure the maximum pressure developed at the position of the gage in the gun. The piezoelectric gage is used to obtain a history of the way pressure builds up. This device operates on the principle that pressure applied to certain types of crystals will produce a charge which is proportional to that pressure. A piezoelectric gage can be used in conjunction with an oscilloscope and sweep generator to measure, as the projectile travels through gun, the variation of pressure with time, producing a photographic time-pressure record.

4-73. Hygroscopicity is the tendency of the propellant composition to absorb moisture, thereby decreasing its effectiveness. It is determined by routine chemical analysis.

4-74. Total volatiles is a measure of the incorporated solvents. The tests and requirements for specific propellants are as per specifications.

Vacuum stability tests have been found suitable for determining the compatibility of propellants or explosives with each other. (See table 4-27 and Section 2.) This is accomplished by testing the stability of the proposed mixture of materials under vacuum and determining whether the volume of gas liberated is significantly greater than the sum of the gas volumes liberated by the materials when tested separately. When used for this purpose, the test generally is made at 100°C, 120°C, or 150°C. or any other desired temperature, but 100° or 120°C are most commonly used. Vacuum stability tests yield reproducible values; and when a material is subjected to this test at two or more temperatures, a rather complete picture of its chemical stability is obtained. In some cases, tests at two or more temperatures are required to bring out significant differences with respect to stability between explosives, but a test at 100°C is sufficient to establish the order of stability of an explosive.

4-75. Taliani Test (110°C). One gram of finely ground propellant is placed in a sample tube-helix combination with constant volume of 6 ml. This assembly is placed in an aluminum block heater maintained at 100 ± 0.1°C and attached to a mercury manometer equipped with a leveling device. The system is evacuated and then infused with nitrogen or oxygen. The mercury is leveled to a fiducial mark on the helix, and at progressive readings at 30-minute intervals, the mercury is leveled to this mark. With temperature and volume constant, the evolution of gas is reflected as increased pressure. The series of readings is plotted as pressure versus time and the resulting curve is examined for slope.

REFERENCES AND BIBLIOGRAPHY

1. Purchase Description and General Specification for Methods of Inspection, Sampling and Testing, MIL-P-11960, 24 April 1952.

2. "Internal Ballistics," Philosophical Library, New York, 1951, pp. 98, 99.

Table 4-22

Standard propellant calibrati

(TANKS AND ARTILLERY WEAPONS)

Cannon	Item No.	Projectile Type	Projectile Weight (pounds)	Fuze type	Primer Type	Primer Grains	Cart case Type	Cart case Pull lbs	Propellant Lot	Propellant Type	Propellant Web	L
76mm G, M1A2, M1A1C	9	HE, M42A1 WP, M312	12.80	Dummy, M73	M28B2	300	M26	Min of 1800	17636-R	M6	.0419-MP	Lo
	10	APC-T, M62A1	15.40	BD, M66A1	M40A1	270	M26	"	17636-R	M6	.0419-MP	Lo 1/2 lea on pro
	11	AP-T, T166E2, TP-T304	14.60	None	M49B2	400	M26	2000 to 8500	35718-S	M17	.0547-MP	Lo
	12	HVAP-T, M93	9.30	None	M28B2	300	M26	2000 to 8500	18891-R	M2	.0598-MP	Lo
	13	HVTP-T, M315A1	9.30	None	M28B2	300	M26	2000 to 8500	18891 R	M2	.0598-MP	Lo
76mm G, T91, T124	14	HE, T64	15.00	PD, M51A5	M58	400	T19E1B1	5000 to 11000	35036-S	M6	.0367-MP	Ba Gr. sil 19
									12479-R	M6	.0377-MP	Lo
	15	WP, T140E2	15.71	PD, M51A5	T70	300	T19E1B1	5000 to 11000	35036-S	M6	.0367-MP	Di
	16	AP-T, T128E6 TP-T, T212	14.50	None	M58	400	T19E1B1	2000 to 8500	38313-R	M17	.0615-MP	Lo
	17	HVAP-T, T66E4, HVTP-T, T74E1	7.0	None	M62	300	T19E1B1	2000 to 8500	16050	M6	034-MP	Lo
	18	HVAP-DS-T, M331A2	8.22	None	T88E1	300	T19E1B1	5000 to 11000	34482-R	M17	.0495-MP	Lo

Item No. 9 - Data valid in assessment for Shell, WP, M312; test rounds M42A1 loaded to 12.80 lbs., std. rds. loaded to 12.80 lbs.
12 - Std. rds. loaded to 9.30 lbs. and test rds. loaded to 9.38 lbs. Assessment of prop. to be made for M93A1 shot weighing 9.38 lbs.
14 - Prop. to be std'z. with distance wadding if authorized by 000.
18 - Prop. lot 34700, M17, MP, web size .0448" to be std'z. in the near future.
Bullet pull requirements have not been established, a minimum of 5000 lbs. is recommended, however, the maximum of 11000 lbs. will need further investigation

A.

ble 4-22

t calibration data chart

Revision 3, dated: 1 April 1954

Web	Loading	Standard charge: Desig.	Standard charge: Zone	Standard charge: Weight (ounces)	Calibration values: Vel. fps	Calibration values: Press psi	Gun rated max. press psi	Press gages used	Last check fired date	Valid data	STDZ FR NO.
9-MP	Loose			60.40	2700	36600	43000	2-M3	To be std w. M40A1 primer, Jan 45 Check due w/Shell Lot LOP-500-2	Yes (R)	JP0109261
9-MP	Loose w. 1.2 oz. pure lead foil on top of prop.			61.17	2600	42300	43000	2-M3	Feb 53 Lot LM-3 (a) Check Firing due	Yes (R)	JP0124847
7-MP	Loose			57.84	2700	39500	43000	2-M3	Estb. Aug 53	Yes (S)	P57020
6-MP	Loose			61.73	3400	39800	43000	2-M3	June 52 Lot CM-72 CHK w/GP-1-35(a)	Yes (R)	P37413
8-MP	Loose			61.98	3400	39500	43000	2-M3	June 52	Yes (R)	P51796 P51797
7-MP	Bag, Sleeve Gr. "E" silk 19" x 3"			54.21	2400	28700	46000 Shell RMP 30000	2-M3	Std-Aug 52 To be Re-Stdz w/ Dist. Wad + T70 Primer. Prop Lot 60105	No (S)	P52483
7-MP	Loose			55.94	2400	28109		2-M3		Yes (R)	P49108
7-MP	Dist. Wad				2400		46000 Shell RMP 30000	2-M3	To be Stdz w/Dist. Wad. + T70 Primer, Prop Lot 60105, Web .0365"		
5-MP	Loose			89.43	3200	44200	46000	2-M3	Estb. Jan 53 Incomplete. Pdr. To be std'z. JPG conducted Temp. Ref.	Yes (R)	JPG172685
MP	Loose			84.64	4135	44700	46000	2-M3	Estb. Mar 52	No (A)	P48982
4-MP	Loose			91.05	4125	43800	46000	2-M3	Estb. Jan. 54 Prop Lot to be std'z.	Yes (R)	P58583

ns.

(S) - Valid Standard
(R) - Valid Reference
(A) - Not valid, limited reference
(a) - Proj. lot used in latest check

B.

Table 4-22

Standard propellant calibration data

(TANKS AND ARTILLERY WEAPONS)

Cannon	Item No.	Projectile: Type	Projectile: Weight (pounds)	Projectile: Fuse type	Primer: Type	Primer: Grains	Cart case: Type	Cart case: Pull lbs	Propellant: Lot	Propellant: Type	Propellant: Web	Load
90mm G, M1, M1A1, M2, M3, T8	19	HE, M71 TP, M71 WP, M313	23.40	PD, M51A5	M28B2	300	M19	Min of 5000	17665-S	M6	.0496-MP	Loose
									8799-S	M6 + K_2SO_4	.0491-MP	Loose
	20	HE, M71 TP, M71 WP, M313	23.40	PD, M51A5	M49	400	M19	"	38422-S	M15	.0550-MP	Loose
	21	APC-T M82	24.10	BD, M68	M49	400	M19	"	10632-R	M6	.0545-MP	Dist. Wad. 2 oz. Ign. on top of chg.
	22	HVAP-T M304	16.75	None	M40A1	270	M19	5000 to 11000	14677-R	M6	.0469-MP	Dist. Wad. 2 oz. Ign. on top of chg.
	23	HVTP-T M317A1	16.75	None	M40A1	270	M19	5000 to 11000	14677-R	M6	.0469-MP	"
	24	HVAP-T, M332A1 HVTP-T, M333A1	12.44	None	M49	400	M19	5000 to 11000	3571B	M17	.0547-MP	Dist. Wad.
	25	HEAT T108E45 T108E40	14.60 16.20	PI-BD. T209	T69	400 approx. in boom.	T27	Not Est.	35258 + K_2SO_4	M1	.0344-MP	Loose
	26	Canister M336	23.29	None	M49	400	M19	5000 to 11000	33840-R	M2	.0924-MP approx.	Loose
90mm Gun, T119, T139	27	RE, T91 WP, T92	18.60	PD, M51A5	T70	300	T24B1	5000 to 10000	38740-S	M1	.0267-MP	Dist. Wad.
	28	AP-T, T33E7 TP-T T225	24.10	None	M58	400	T24	5000 to 11000	34478	M17	.073-MP	Loose 2 oz. Ign. on top of chg.
	29	HVAP-DS-T, T137										
	30	HEAT T108E40	16.20	PI-BD, T209	T69	400	T27	Not Est.	35258-R + K_2SO_4	M1	.0344-MP	Loose

Item No. 22 and 23 - Differences in band materials result in different prop. charges for M304 and M317A1 Shell.
25 - Present production round is T108E40.
26 - Shell, HE, M71 loaded to 23.29 lbs. used to simulate Canister, M336. Chg. based on tube have 9 prev. rds.
27 - Standardized with M28B2, screw head primer (T70 primer was not available at the time of test). Fired also with various lots modified T10 Brass cases. Comparison test with T24B1 cases were conducted. 12 fps less vel. with steel case.
23 - Standard rounds loaded to 16.75 lbs., test rounds (M317A2) fired at 16.31 lbs.

A.

Table 4-22

mt calibration data chart (cont)

Revision 3, dated: 1 April 1954

ant Web	Loading	Standard charge Design	Zone	Weight lbs	oss	Calibration values Vel. fps	Press psi	Gun rated max. press psi	Press gages used	Last check fired date	Valid data	STDZ FR NO.
.0496-MP	Loose			7	3.13	2700	36600	38000	2-M3	Oct 51 Lot DDW-79 CHK w/EGS-1-13 (a)	Yes (S)	P-41910
.0491-MP	Loose			7	1.7	2700	36200	38000	2-M3	To be replaced w/Prop. Lot 63215	Yes (S)	P-6429
.0550-MP	Loose			7	1.81	2700	36200	38000	2-M3	Estb. Aug 1953	Yes (S)	P-56830
.0545-MP	Dist. Wad. 2 oz. Ign. on top of chg.			8	2.1	2800	39500	41500	2-M3	June 48 BS-36 (a)	Yes (R)	P32409
.0469-MP	Dist. Wad. 2 oz. Ign. on top of chg.			8	5.22	3350	40600	41500	2-M3	June 52 Lot HCO-7 and CAA-1-8 (a)	Yes (R)	P37523
.0469-MP	"			8	3.10	3350	41100	41500	2-M3		Yes (R)	P51784
.0547-MP	Dist. Wad.			8	0.27	3875	41400	41500	2-M3	Chg. Est. conducted March 1954	Yes (R)	P58912
.0344-MP	Loose			5	8.38	2800	22700	41500	2-M1		No (A)	P47615
				5	13.34	2800	28700	41500	2-M1		Yes (R)	P58913
.0924-MP approx.	Loose			7	11.2 8.58	2870	39200	41500 Shell RMP 41500	2-M3	Estb. Mar. 1954	Yes (R)	P59166
.0267-MP	Dist. Wad.			4	8.46	2400	26500	47000 Shell RMP 30000	2-M3	Stdz. Sept. 1953	Yes (S)	P57202
.073-MP	Loose 2 oz. Ign. on top of chg.			8	4.21	3000	47400	47000	2-M3	Prop. Gran. Tests to be continued	No (A)	P53277
								47000	2-M3	Dev. incomplete		
.0344-MP	Loose			5	13.34	2800	28700	47000	2-M1	Estb. Dec. 1953	Yes (R)	P58913

(S) - Valid standard
(R) - Valid Reference
(A) - Not valid, limited reference
(a) - Proj. lot used in latest check

B.

Table 4-22.

Standar propellant calibration

(TANKS AND ARTILLERY WEAPONS)

Cannon	Item No.	Projectile Type	Projectile Weight (pounds)	Fuze type	Primer Type	Primer Grains	Cart case Type	Cart case Pull lbs	Propellant Lot	Propellant Type	Propellant Web
105mm How. M2, M2A1, M4.	31	HE, M1	33.00	PD, M51A5	M28B2	300	M14B1	None	61050-S 31080-S 61180-S 61180-S 61180-S 61180-S 61180-S	M1 M1 M1 M1 M1 M1 M1	.0143-SP .0143-SP .0262-MP .0262-MP .0262-MP .0262-MP .0262-MP
	32	HEAT-T M67	28.80	BD, M91	M1B1A2	100	M14	None	6658-S	M1	.0146-SP
	33	HEAT T131E31	24.00	PI-BD T208	(Mod) M23A2	700	(Mod) M14	Not Estb.	3328	M6	.0240-MP
105mm How. M3.	34	HE, M1	33.00	PD, M51A5	M28B2	300	M14(I)	None	9525-S	M1	.0154-SP
	35	HEAT, M67	28.80	BD, M91	M28B2	300	M14(II)	None	9525-S	M1	.0154-SP
105mm Gun, T140	36	AP-T-T182, TP-T, T79	35.0	None	T48	400	T6	None	EXA-6905	M17	.0852-MP
120mm Gun, M1	37	HE, M73	50.000	MT, M61	M1B1A2	100	M24	None	38470-S	M6	.0674-MP
120mm, Gun, T123	38	HE, T15E2 WP, T16E2	50.40	PD, M51A5	M57 or M67	1000	M54 or T25E3	None	38723-S	M15	.034-SP
	39	AP-T, T116E5 TP-T, T147E3	50 0	None	M67	1000	T25E1	None	EXA 7069	M17	.1123-MP Approx.
	40	HEAT T153E8	32.0		M57 Mod	800	M34 Mod 18 1/2" Length	None		M6	.0469-MP

Item No. 33 - Charge weight in primer includes the amount of black powder obtained in primer and shell boom.
32 - Standardization conducted with prop. loose in case and crimped. Test rounds should be fired in bag and standard loose in case when firing for calibration. New values will be set for standard using Gr. "E" silk bag if requirement exists.
31 - Propellants recently made the new standard by matching the velocity levels of propellant lots 36172/17395.
40 - Data shown is approximate.

A.

Table 4-22

nt calibration data chart (cont·

Revision 3, dated 1 April 1954

ant Web	Loading	Standard charge Design	Zone	Weight lbs	Weight ozs	Calibration values Vel fps	Calibration values Press psi	Gun rated max. press psi	Press gages used	Last check fired date	Valid data	STDZ FR NO
.0143-SP	Dualgran	Zone	1		8.55	650	6600			Stdz Mar.	Yes (S)	P58846
.0143-SP	Rayon	1 + 2	2		9.98	710	8200			1954		
.0262-MP	Bag 1, 3	SP Pdr.	3		12.51	780	9000					
.0262-MP	oz. 60/	MP all	4		16.31	875	11000					
.0262-MP	40 lead	other	5		22.98	1020	14300					
.0262-MP	foil	zones.	6		30.85	1235	19800					
.0262-MP	sewed to Zone 5 Bag		7		45.24	1550	31000	32500	2-M3			
.0146-SP	Bag	Single Sect. Gr. "E" Silk Bag			24.42	1250	23500	32500 Shell RMP 26000	2-M3	Jan 48 Lot RA-3-6 (a) Chk firing due	Yes (S)	M14542
.0240-MP	Loose				60.50	1750	20600	32500 Shell RMP approx. 25000	2-M1	To be stdz if require-ments exist.	No (A)	P49276
.0154-SP	Bag	Gr. "E" Silk			9.75	650	7800	25000	2-M3	Apr 47	Yes (S)	M23114
					11.38	710	9100					
					13.34	780	10800					
					16.23	875	13800					
					21.24	1020	19900					
.0154-SP	Bag	Gr. "E" Silk 1 pc sleeve			24.42	1020	17400	25000	2-M3	Apr 47	Yes (S)	M22294
.0852-MP	5 oz. ign. on top of chg.				274.90	3500	45500	48000	2-M3	Cont. dev. on Chg. to be done	No (A)	P49350
.0674-MP	8 oz. ign. Dist. Wad, M2E2 closing plug, no retainer	M15E1		23	5.97	3100	37200	38000	2-M3	Stdz. Nov. 53	Yes (R)	P577168
.034-SP	T23 Plug, Bag Silk "E" 25 x 5" + Dist. Wad.	T21E1 Chg.		12	3.82	2500	38500	48000	2-M3	Additional firings to be conducted to establish Prop. as Standard	Yes (R)	P58630
.1123-MP Approx.	Loose 4 oz. on ign. top of chg.	T38E1 Chg.		29	5.0	3500	45600	48000	2-M3	Dev. Prop. incomplete	No (A)	P55152
.0469-MP	Loose, Plastic Plug	T41 Chg.		18	8.0	3450	33000	48000	2-M3	Dev. incomplete		

exists.

(S) - Valid Standard
(R) - Valid Reference
(A) - Not valid, limited reference
(a) - Proj. lot used in latest check

B.

(TANKS AND ARTILLERY WEAPONS)

Cannon	Item No.	Projectile Type	Projectile Weight (pounds)	Fuse type	Primer Type	Primer Grains	Cart case Type	Cart case Pull lbs	Propellant Lot	Propellant Type	Propellant Web	
155mm Gun, M1, M2A1 and M2	41	HE, M101	95.0	PD, M51A5	MK IIA4	17	None	None	32809-S	M6	.0552-MP	Gr Co
155mm How, M1 and M2	42	HE, M107	95.00	PD, M51A5	MK IIA4	17	None	None	3742-S	M1	.0165-SP	Gr Co
	43	HE, M107	95.0	PD, M51A5	MK IIA4	17	None	None	38250-S + K_2SO_4	M1	.0334-MP	Gr Co
8" Gun, M1	44	HE, M103	240.0	PD, M51A5	MK IIA4	17	None	None	8501-S	M6	.0691-MP	M9
	45	HE, M103	240.0	PD, M51A5	MK IIA4	17	None	None	16697-R	M6	.0839-MP	M1
8" How., M1	46	HE, M106	200.0	PD, M51A5	MK IIA4	17	None	None	8295-S	M1	.0161-SP	M1
	47	HE, M106	200.0	PD, M51A5	MK IIA4	17	None	None	10567-S	M1	.0414-MP	M2
240mm How., M1	48	HE, M114	360.0	PD, M51A5	MK IIA4	17	None	None	17014-S	M6	.0691-MP	M2
280mm Gun, T131	49	HE, T122	600.0	VT, T27 or PD, M51A5	MK 15 Mod. 1 Elec.	30	None	None	38834-R 30271-R 30271-R 30271-R	M6 + 1 M6 M6 M6	.0703-MP .0993-MP	T4

Item No. 44 and 45 - Check firings due, however, no firings will be conducted due to propellant being of limited standard.

A.

Table 4-22

nt calibration data chart (cont)

Revision 3, dated: 1 April 1954

Web	Loading	Standard charge Design	Zone	Weight lbs	Weight ozs	Calibration values Vel. fps	Calibration values Press psi	Gun rated max press psi	Press gages used	Last check fired date	Valid data	STDZ FR NO.
.0552-MP	Gr. "C" Cotton	Normal Super M19 Chg.		20	4.8	2100	17300	40000	2-M3	June 48 Lot OSW-1-32 (a) to be fired with Lot JBC-1 62 Check due	Yes (S)	P36803
				30	10.8	2800	38400	40000	2-M3			
.0165-SP	Gr. "B" Cotton	M3 C[illegible]	1	1	15.2	630	4800			Jan 52, Aide-I and NCC-15 (a) Chk. firing due w/Lot USH-1-26	Yes (S)	M3 1803
			2	2	7.10	770	6200					
			3	3	1.40	880	8400					
			4	3	15.70	1020	12000					
			5	5	8.0	1220	18900	32000	2-M3			
.0334-MP	Gr. "A" Cotton	M4A1 Chg	3	4	4.00	860	5200		2-M3	Est. Mar 53	Yes (S)	P55650
			4	5	7.04	1020	7000					
			5	7	3.20	1220	10100					
			6	[illegible]	0.64	1520	17000					
			[illegible]	13	[illegible]4	1850	29700	32000				
0691-[illegible]	M9 Chg.	Reduced		530	0.0	2100	18700	38000	4-M3	Apr 46 HC-2-4 (a) Check due w/LR-9	Yes (S)	M26648
		Normal Gr. "D" Cotton		740	8.0	2600	33500	38000	4-M3			
.0839-MP	M10 Chg.	Normal		800	14.25	2600	29300	38000	4-M3	May 46 HC-2-9 (a) Check due w/LR-9	Yes (R)	P37233
		Super Gr. "D" Cotton		920	4.25	2850	37600	38000	4-M3			
.0161-SP	M1 Chg	Green Bag Gr. "B" Cotton	1	50	5.3	820	7600	33000	4-M3	Aug 47 OWS-1-49 (a) Check due	Yes (S)	P31800
			2	60	4.5	900	9600					
			3	70	8.3	1000	12400					
			4	90	8.6	1150	17100					
			5	130	2.5	1360	27000	33000				
0414-MP	M2 Chg	White Bag Gr. "E" Silk	5	160	10.0	1380	12900			Aug 47 OWS-1-49 (a) Check due	Yes (S)	P31800
			6	210	13.4	1640	19800					
			7	280	0.8	1950	32000	33000	4-M3			
[illegible]-MP	M23 Chg	Gr. "D" Cotton	1	420	2.0	1500	10900			June 48 ACF-55-23145 (a) Check due	Yes (S)	M31889
			2	520	10.0	1740	15100					
			3	650	7.0	2020	23100					
			4	780	10.0	2300	34600	36000	4-M3			
[illegible]03-MP .0993-MP	T44 Chg.	Silk Class "B"	1		53.7#	1380	8700	36000	4-M3	Est. Nov 1952	Yes (R)	P53814
			2		90.05#	1780	16000					
			3		118.26#	2100	22700					
			4		156.76#	2500	35200					

(S) - Valid Standard
(R) - Valid Reference
(a) - Proj. lot used in latest check

B.

Table 4-23

Calculated thermochemical values for standard prop
(including residual volatiles)

Use	Artillery								Recoil	
Propellant	M1	M2	M5	M6	M14	M15	M17	T20	M10	T18
Specification	JAN-P-309	JAN-P-323	JAN-P-323	JAN-P-309	JAN-P-309	PA-PD-26	PA PD-26		PA-PD-123	PA-PD-329
Nitrocellulose	85.0	77.45	81.95	87.0	90.0	20.0	22.0	20.0	98.0	72.0
% Nitration	13.15	13.25	13.25	13.15	13.15	13.15	13.15	13.15	13.15	13.15
Nitroglycerin	...	19.50	15.00	...	...	19.0	21.5	13.0	...	19.75
Barium nitrate	...	1.40	1.40	...	...	...	...	...	...	0.75
Potassium nitrate	...	0.75	0.75	...	...	...	...	...	...	0.70
Potassium perchlorate	...	...	...	...	...	...	...	...	...	...
Nitroguanidine	...	...	...	...	...	54.7	54.7	60.0	...	...
Dinitrotoluene	10.0	...	...	10.0	8.0	...	...	...	...	...
Dibutylphthalate	5.0	...	...	3.0	2.0	...	...	5.0	...	...
Diethylphthalate	...	...	...	...	...	...	...	...	...	...
Potassium sulfate	...	...	...	...	...	...	...	...	1.0	...
Tin	...	...	...	...	...	...	...	...	...	...
Diphenylamine	1.0*	...	...	1.0*	1.0*	...	...	...	1.0	...
Ethyl centralite	...	0.60	0.60	...	...	6.0	1.5	2.0	...	6.50
Graphite	...	0.30	0.30	...	...	...	0.1†	...	0.10†	0.30
Carbon black	...	...	...	...	...	...	...	...	...	...
Cryolite	...	...	...	...	...	0.3	0.3	...	...	...
Ethyl alcohol (Residual)	0.75	2.30	2.30	0.90	1.00	0.30	0.30	0.30	1.50	1.20
Water (residual)	0.50	0.70	0.70	0.50	0.25	0.00	0.00	0.00	0.50	0.30
Lead carbonate	...	...	...	...	...	...	...	1.0*	...	...
Isochoric flame temp, °K	2417	3319	3245	2570	2710	2594	3017	2388	3000	2938
Force, ft-lbs/lb, x 10^{-3}	305	350	355	317	327	336	364	314	339	346
Unoxidized carbon, %	9.6	0	0	6.8	5	9.5	3.9	11.6	4	3.4
Combustibles, %	65.3	47.2	47.4	62.4	58.9	51.0	38.7	53.1	54.5	59.1
Heat of explosion, cal/gm	700	1080	1047	758	809	796	962	712	936	910
Gas volume, moles/gm	0.04533	0.03900	0.03935	0.04432	0.04338	0.04645	0.04336	0.04794	0.04068	0.04219
Ratio of specific heats	1.2593	1.2238	1.2258	1.2543	1.2496	1.2557	1.2402	1.2591	1.2342	1.2421
Isobaric flame temp, °K	1919	2712	2647	2050	2168	2066	2433	1897	2431	2365
Density, lbs/in.^{3}	0.0567	0.0597	0.0596	0.0571	0.0582	0.0600	0.0603	...	0.0602	1.0583
Covolume, in.^{3}/lb	30.57	27.91	27.52	29.92	29.54	31.17	29.50	30.41	27.76	29.13

*Added †Glazed ‡Coating Added

A.

Table 4-23

Thermochemical values for standard propellants (including residual volatiles)

			Recoilless				Mortar			Small arms		
	M17	T26	M10	T19	T25	T29	M7	M8	M9	IMR	M12	M18
D-	PA-PD-26		PA-PD-123	PA-PD-329	PA-PD-329	PA-PD-329	JAN-P-659	JAN-P-381	MIL-P-20306	JAN-P-733	JAN-P-528	FA-PD-26A
0	22.0	20.0	98.0	72.0	73.25	67.25	54.6	52.15	57.75	100.0	97.7	80.0
15	13.15	13.15	13.15	13.15	13.15	13.15	13.15	13.25	13.25	13.15	13.15	13 15
0	21.5	13.0	...	19.75	20.00	25.00	35.5	43.00	40.00	...	...	10.0
	...	...	...	0.75	0.75	0.75	...	...	...	...	...	...
	...	...	...	0.70	0.70	0.70	...	1.25	1.50	...	...	...
	...	...	...	...	...	...	7.80	...	...	...	...	...
7	54.7	60.0	...	...	...	...	.	...	...	...	...	...
	...	...	...	...	...	...	...	...	...	8.0‡	...	...
	...	5.0	...	...	...	...	...	...	...	...	...	9.0
	...	...	...	...	...	...	...	3.00	...	...	...	...
	...	...	1.0	...	...	...	...	...	...	1.0*	0.75	...
	...	...	...	...	...	...	...	...	...	...	0.75	...
	...	...	1.0	...	...	...	...	...	0.75	0.7*	0.80	1.0
0	1.5	2.0	...	6.50	5.00	6.00	0.90	0.60	...	...	...	...
	0.1†	...	0.10†	0.30	0.30	0.30	...	...	...	...	...	...
	...	...	...	...	...	...	1.20	...	...	...	...	...
3	0.3	...	...	...	..	...	...	...	...	...	...	...
30	0.30	0.30	1.50	1.20	1.20	1.20	0.80	0.40	0.50	0.60	1.50	0.50
00	0.00	0.00	0.50	0.30	0.30	0.30	0.00	0.00	0.00	1.00	1.00	0.00
	...	1.0*	...	...	...	...	...	...	...	...	...	...
34	3017	2388	3000	2938	3071	3081	3734	3695	3799	2827	2996	2577
36	364	314	339	346	353	356	368	382	382	325	336	319
5	3.9	11.6	4	3.4	1.8	2.2	0	0	0	1.9	6	6.8
1	38.7	53.1	54.5	59.1	...	...	55.4	37.2	32.8	59.2	53.66	66.6
96	962	712	936	910	962	966	1255	1244	1295	866	933	772
45	0.04336	0.04794	0.04068	0.04219	0.04133	0.04157	0.03543	0.03711	0.03618	0.04137	0.04037	0.04457
57	1.2402	1.2591	1.2342	1.2421	1.2373	1.2383	1.2100	1.2148	1.2102	1.2400	1.2326	1.2523
96	2433	1897	2431	2365	2482	2488	3085	3042	3139	2280	2431	2058
00	0.0603	...	0.0602	1.0583	0.0585	0.0585	...	...	...	...	...	...
17	29.50	30.41	27.76	29.13	28.66	29.77	...	26.63	25.97	28.87	27.91	30.21

‡Coating Added

B.

Table 4-24

Characteristics of propellant compositions*

Composition	Heat of combustion† (cal per gm)	Products‡ of explosion		Burning rate¶ (at 25°C)	Force (1,000 ft-lb per lb)
		Heat (cal per gm)	Gas (ml per gm)		
M1	2,975	744	858	15	314
M2	2,275	1,138	685	29	368
M3	2,830	820	904	12	310
M4	2,945	797	783	...	325
M5	2,389	1,032	729	...	362
M6	2,780	796	842	14	328
M7	...	1,262	587	59	370
M8	...	1,225	671	67	380
M9	...	...	...	43	384
M10	...	949	762	38	352
M12	...	950	760	38	356
M13	...	1,244	640	55	390
M14	...	879	...	...	337
M15	...	800	836	18	337
T2	...	935	821	31	353
T3	...	798	874	...	...
T5	...	1,259	610	...	...
T6	...	873	842	28	338
T8	...	752	864	20	306
T9	...	...	...	65	...
Pyrocellulose	...	861	792	19	339
Cordite MD	...	1,025	940	...	...

* For units, meaning, and methods of determination see paragraphs 4-53 through 4-64.
† At constant volume.
‡ Water produced in liquid form.
¶ In. per sec per lb per sq in. x 10^{-5}

Table 4-25

Thermochemical characteristics of nitrocellulose

Characteristics	Nitrogen content, percent			
	12.60	13.15	13.35	14.0
Heat of combustion (cal per gm)				
At constant volume	2,415	2,345	2,320	2,237
At constant pressure	2,409	2,336	2,313	2,228
Heat of formation (cal per gm)				
At constant volume	616.7	575.5	560.9	512.5
Heat of explosion (cal per gm)				
At constant volume, with				
Water, liquid	936	1,017	1,046	1,140
Water, gaseous	855	935.5	965	1,058
Gas produced (ml per gm)				
At constant volume, with				
Water, liquid	744	721.6	713.5	687
Water, gaseous	918.5	892.7	883.2	853

Table 4-26

Thermochemical properties of propellant constituents

Constituent	Formula		Molecular weight	Heat of combustion (cal/mole)	N (moles/gm)	C (cal/gm/d
Acetone		C_3H_6O	58	426,800	.10345	.5111
5-Amino Tetryl		CH_3N_5	85	254,500	.05882	.3333
Acid Ammonium Tartrate		$C_4H_9NO_6$	167	341,700	.05389	.4216
Ammonium Alum (Anhyd)		$AlH_4NS_2O_8$	237		.020	.2400
Ammonium Nitrate	NH_4NO_3	NH_4NO_3	80	49,200	.03750	.4426
Ammonium Picrate		$C_6H_6N_4O_7$	246	677,130	.04472	.3219
Ammonium Thiocyanate		NH_4SCN	76	340,100	.05260	.2830
Barium Nitrate	$Ba(NO_3)_2$	$BA(NO_3)_2$	261		.00765	.1574
Barium Sulfate	$BaSO_4$	$BaSO_4$	233		.00430	
N-Bensoylalanine		$C_{10}H_{11}NO_3$	193	1,168,100	.08390	.3683
Butane Triol Trinitrate		$C_4H_7N_3O_9$	241	522,480	.03734	.3578
Butyl Malonate		$C_{11}H_{20}O_4$	216	1,484,400	.09722	.4810
Butyl Stearate	BS	$C_{22}H_{44}O_2$	340	3,342,330	.12941	.5579
Camphor		$C_{10}H_{16}O$	152	1,411,000	.11842	.4844
Carbon Black	CB	C	12		.08333	.1350
Cellulose Acetate		$C_{10}H_{14}O_7$	246	1,196,000	.06911	.3994
Cyanuric Trihydrazide		$C_3H_9N_9$	171	623,979	.07018	.3784
Cyclohexane Hexanone $\cdot 8H_2O$		$C_6H_{16}O_{14}$	312	366,000	.04487	.3718
Cyclotetramethylene Tetranitramine	HMX	$C_4H_8N_8O_8$	296	666,610	.04054	.3419
Diamylphthalate		$C_{18}H_{26}O_4$	306	2,359,000	.10131	.4406
Dibutylphthalate	DBP	$C_{16}H_{22}O_4$	278	2,056,000	.09712	.4263
Dibutyltartrate		$C_{12}H_{22}O_6$	262	1,533,000	.08779	.4673
Diethanolnitrameninediniti ate	DINA	$C_4H_8N_4O_8$	240	576,060	.04167	.3653
Diethyldiphenylurea	EC	$C_{17}H_{20}N_2O$	268	2,266,700	.10448	.3910
Diethyleneglycoldinitrate	DEGN	$C_4H_8N_2O_7$	196	548,400	.0459	.3862
Diethylphthalate	DEP	$C_{12}H_{14}O_4$	222	1,432,000	.08559	.3870
Diethylmalonamide		$C_7H_{14}N_2O_2$	158	994,800	.09494	.4696
Dimethyldiphenylurea		$C_{15}H_{16}N_2O$	240	1,950,000	.10000	.3688

A.

Table 4-26

nochemical properties of propellant constituents

Molecular weight	Heat of combustion (cal/mole)	N (moles/gm)	C (cal/gm/deg)	E (cal/gm)	Q (cal/gm)	Oxygen balance	N ($In.^3/lb$)	Density	Heat of combustion reference
58	426,800	.10345	.5111	-2756	-1911	-138			4
85	251,500	.05882	.3333	-376	360	-47.1			28
167	341,700	.05389	.4216	-1470	-578	-21			4
237		.020	.2400	-600					
80	49,200	.03750	.4426	365	1458	20	22.83	1.725	17
246	677,130	.04472	.3219	-97	560	-13			23
76	340,100	.05260	.2830	445	926	-42.1		1.30	35
261		.00765	.1574	131	1139		15.34	3.240	
233		.00430			234				
193	1,168,100	.08390	.3683	-2338	-1808	-104			4
241	522,480	.03734	.3578	653	1469	10		1.52	20
216	1,484,400	.09722	.4810	-2635	-1867	-126			
340	3,342,330	.12941	.5579	-3636	-2861	-198	58.91	.855	6
152	1,411,000	.11842	.4844	-3324	-2693	-179			4
12		.08333	.1350		-3330	-133			
246	1,106,000	.06911	.3994	-1704	-985	-65	42.10		34
171	623,979	.07018	.3784	-1141	-491	-70.2			24
312	366,000	.04487	.3718	-1117	-123	0			6
296	666,610	.04054	.3419	595	1341	0		1.92	23
306	2,359,000	.10131	.4406	-2824	-2206	-141	58.81	1.022	31
278	2,056,000	.09712	.4263	-2667	-2063	-132	56.97	1.05	31
262	1,533,000	.08779	.4673	-2404	-1611	-104			6
240	576,060	.04167	.3653	469	1277	0			23
268	2,266,700	.10448	.3910	-2808	-2360	-155	62.60	1.11	25
196	548,400	.0459	.3862	237	1078	-8.2			22
222	1,432,000	.08559	.3870	-2315	-1749	-108			4
158	994,800	.09494	.4696	-2561	-1811	-122			4
240	1,950,000	.10000	.3688	-2682	-2269	-147			25

B.

Table 4-26

Thermochemical properties of propellant constituents (co

Constituent	Formula		Molecular weight	Heat of combustion (cal/mole)	N (moles/gm)	C (cal/gm/
Dimethylphthalate	DMP	$C_{10}H_{10}O_4$	194	1,119,700	.07732	.3589
Dinitrodimethyl Oxamide	DD Oxam	$C_4H_6N_4O_6$	206	511,910	.04369	.3435
Dinitroethylbenzene	DNEB	$C_8H_8N_2O_4$	196	1,011,800	.06633	.3399
Dinitrotoluene	DNT	$C_7H_6N_2O_4$	182	855,200	.06043	.3213
Diphenylamine	DPA	$C_{12}H_{11}N$	169	1,536,200	.10651	.3476
Diphenylurea		$C_{13}H_{12}N_2O$	212	1,614,500	.09434	.3406
Diphenylurethane		$C_{15}H_{15}NO_2$	241	1,866,090	.09544	.3612
Ether (Dimethyl)		C_2H_6O	46	347,600	.10870	.6092
Ether (Diethyl)		$C_4H_{10}O$	84	660,300		
Ethyl Alcohol	ETOH	C_2H_6O	46	327,600	.10870	.6092
Ethylene Diamine Dinitrate	EDDN	$C_2H_{10}N_4O_6$	186	374,700	.04839	.4332
Ethylenedinitramine	HALEITE	$C_2H_6N_4O_4$	150	371,690	.04667	.3809
Food Meal					.06785	.4215
Glucose		$C_6H_{12}O_6$	180	673,000	.06667	.4148
Glucose Pentaacetate (Insol.)		$C_{16}H_{22}O_{11}$	390	1,726,300	.06923	.3971
Glycine		$C_2H_5NO_2$	75	233,400	.06667	.4445
Graphite	G	C	12	94,272	.08333	.1350
Guanidine Nitrate		$CH_6N_4O_3$	122	209,230	.01918	.4125
Guanylnitrourea (Stab. Insol.)		$C_2H_5N_5O_3$	147	288,900	.04080	.3540
Guanylurea nitrate (Stab. Soluble)		$C_2H_7N_5O_4$	165	296,500	.04840	.3860
Hexanitroethane	HEXANE	$C_2N_6O_{12}$	300	130,000	.01666	.2862
Hexanitro oxanilide	HNO	$C_{14}H_6N_8O_{14}$	510	1,421,030	.04118	.2785
Hydrazine Nitrate		$H_5N_3O_3$	95	112,200	.04210	.4427
Hydrazine Hydrogen Oxalate		$C_2H_6N_2O_4$	122	189,100	.04920	.4120
Hydroxylamine Nitrate	HYDROX N	$NH_2OH.HNO_3$	96	49,740	.03125	.4229
Lead Carbonate	$PbCO_3$	$PbCO_3$	267		.00374	.0644
Melamine		$C_3H_6N_6$	126	478,926	.07143	.3552
Metriol Trinitrate		$C_5H_9N_3O_9$	255	673,710	.04314	.3701

A.

Table 4-26

hemical properties of propellant constituents (cont)

Molecular weight	Heat of combustion (cal/mole)	N (moles/gm)	C (cal/gm/deg)	E (cal/gm)	Q (cal/gm)	Oxygen balance	N_3 (In.^{3}/lb)	Density	Heat of combustion reference
194	1,119,700	.07732	.3589	-2067	-1527	-91			4
206	511,910	.04369	.3435	120	849	-7.76			22
196	1,011,800	.06633	.3399	-911	-342	-65.3	43.0	1.32	6
182	855,200	.06043	.3213	-662	-117	-52.7	40.44	1.27	21
169	1,536,200	.10651	.3476	-2988	-2679	-166	65.41	1.16	20
212	1,514,500	.09434	.3406	-2610	-2243	-136			4
241	1,866,090	.09544	.3612	-2609	-2188	-136			6
46	347,600	.10870	.6092	-2310	-1238	-139			4
84	660.300			-2610	-1141				4
46	327,600	.10870	.6092	-2715	-1672	-139	56.35	.789	4
186	374,700	.04839	.4332	-38.1	927	-8.6		1.59	23
150	371,690	.04667	.3809	309	1130	-10.6	33.90	1.71	22
		.06785	.4215	-1303					
180	673,000	.06667	.4148	-1628	-756	-53.3			4
390	1,726,300	.06923	.3971	-1517	-1105	-66			4
75	233,400	.06667	.4445	-1901	-933	-55.3		1.60	4
12	94,272	.08333	.1950	-3208	3370	-133	60.53	2.10	
122	209,230	.04918	.4125	-288	610	-13.1			22
147	285,900	.04080	.3540	-374	360	-16.3		1.93	26
165	296,500	.04840	.3860	-457	367	-14		1.54	20
300	130,000	.01666	.2862	1486	2231	53.3			4
510	1,421,030	.04118	.2785	-12	539	-9.4			
95	112,200	.04210	.4427	499	1536	-13 1			29
122	189,100	.04920	.4120	-1007	-108	-13.1			27
96	49,740	.03125	.3229	855	1923	33.3			17
367		.00374	.0644	618				.315	
126	473,926	.07143	.3552	-1587	-1015	-76.2		1.57	24
255	673.710	.04314	.3701	375	1188	-3.1		1 47	20

B.

Table 4-26

Thermochemical properties of propellant constituents

Constituent	Formula		Molecular weight	Heat of combustion (cal/mole)	N (moles/gm)	(cal/
Mineral Jelly (Vistanex)		$C_{30}H_{62}$	423	4,695.000	.14421	.
Nitrocellulose 11.1%N	NC	$C_6H_9N_2O_9$	252	657.000	.04390	.
Nitrocellulose 11.2%N	NC				.04129	.
Nitrocellulose 11.6%N	NC	$C_6H_{7.5504}N_{2.4496}O_{9.8992}$	272	651.800	.04041	.
*Nitrocellulose 13.15%N		$C_6H_{7.3645}N_{2.6700}O_{10.2710}$	281	651,700	.03920	.
Nitrocellulose 13.25N	NC	$C_6H_{7.3300}N_{2.6726}O_{10.3400}$	282	650,000	.03898	.
Nitrocellulose 13.35%N	NC				.03876	.
Nitrocellulose 13.45%N	NC	$C_6H_{7.2604}N_{2.7396}O_{10.4792}$	285	649,000	.03854	.
Nitrocellulose 14.14%N	NC	$C_6H_7N_3O_{11}$	297	647,000	.03704	.
Nitrodicyanodiamidine					.04761	.
2-Nitrodiphenylamine	2NDPA	$C_{12}H_{10}N_2O_2$	214		.08400	.
Nitroglycerin	NG	$C_3H_5N_3O_9$	227	370,237	.03084	.
Nitroguanidine	NGua	$CH_4N_4O_2$	104	211,300	.04808	.
4-Nitro-N-Methylanaline	4NNMA	$C_7H_8N_2O_2$	152	925,200	.07887	.
Oxalic Acid		$C_2H_2O_4$	90	60,200	.03333	.
Oxamic Acid		$C_2H_3NO_3$	89	128,600	.0450	.
Oxamide		$C_2H_4N_2O_2$	88	203,280	.05682	.
Paracyanogen		$(C_2N_2)X$	(52)X	250,000	.05769	.
Pentaerythritol Tetranitrate	PETN	$C_5H_8N_4O_{12}$	316	619,360	.03481	.
Potassium Aluminum Flouride	CRYOLITE	K_3ALF_6	258			
Potassium Nitrate	KNO_3	KNO_3	101		.00989	.
Potassium Sulfate	K_2SO_4	K_2SO_4	174		.00574	.
Potassium Perchlorate	$KC10_4$	$KC10_4$	139		.00722	.
Sodium Aluminum Flouride	CRYOLITE	Na_3ALF_6	210			
Starch					.06785	.
Sucrose		$C_{12}H_{22}O_{11}$	342	1,349,600	.06725	.

* The values for nitrocellulose depend linearly on the degree of nitration.
$X = A + B\ (13.15 - \%N_B)$; N_B = % Nitrogen of component B

NC-B N = .00218 C = .0060 E = -153 Q = -140

A.

Table 4-26

Thermochemical properties of propellant constituents (cont)

	Molecular weight	Heat of combustion (cal/mole)	N (moles/gm)	C (cal/gm/deg)	E (cal/gm)	Q (cal/gm)	Oxygen balance	N (In.^{3}/lb)	Density	Heat of combustion reference
	423	4,695,000	.14421	.5935	-4184	-3405	-231	63.64	0.92	6
	252	657,000	.04390	.3545	-27.4	734	-6.3	29.61		11
			.04129	.3478				28.51		11
1.4496^{O}9.8992	272	651,800	.04041	.3454	183	941	0.77	28.11		11
1.6700^{O}10.2710	281	651,700	.03920	.3421	268.4	1024	3.4	27.56	1.66	11
1.6726^{O}10.3400	282	650,000	.03898	.3415	278.5	1034	3.95	27.46		11
			.03876	.3409	291		4.4	27.36		11
1.7396^{O}10.4792	285	649,000	.03854	.3403	305	1061	4.8	27.26		11
	297	647,000	.03704	.3362	407.2	1160	8.3	26.57		11
			.04761	.3541	-252					
	214		.08400	.3240	-1960	-1575	-112	53.73		
	227	370,237	.03084	.3439	960	1779	24.7	22.78	1.601	22
	104	211,300	.04808	.3712	-46.5	735	-15.4	31.77	1.50	22
	152	925,200	.07387	.3560	-1671	-1141	-94.6			21
	90	60,200	.03333	.3393	-868	-80	17.8		1.65	4
	89	428,600	.0450	.3600	-1222	-449	-9			4
	88	203,280	.05682	.3801	-1502	-755	-36.4	36.26	1.67	24
	(52)X	250,000	.05769	.1925	-5575	-3785	-61.5			4
	316	619,360	.03481	.3483	729	1533	15.2	24.88		22
	258									
	101		.00989	.2158	25	1434		23.61	2.109	
	174		.00574	.1250	-800	300		9.36	2.662	
	139		.00722	.2467	891	1903	46.1			
	210									
			.06785	.4215	-1606					
	342	1,349,600	.06725	.4339	-1620	-785	-56		1.59	4

tration.

40

B.

Table 4-2b

Thermochemical properties of propellant constituents

Constituent		Formula	Molecular weight	Heat of combustion (cal/mole)	N (moles/gm)	C (cal/gm
Tetranitro Diphenyleneimine	TNC	$C_{12}H_5N_5O_8$	347	1,332,250	.04899	.27
Tetranitro Oxanilide	TNO	$C_{14}H_8N_6O_{10}$	420	1,492,590	.05000	.28
Triacetin		$C_9H_{14}O_6$	218	1,100,620	.07339	.41
Tricresyl Phosphate	TCP	$C_{21}H_{21}PO_4$	368	2,539,568		
Triethyleneglycol	TEG	$C_6H_{11}O_4$	150	857,800	.08667	.44
Triethyleneglycol Dinitrate	TEGN	$C_6H_{12}N_2O_8$	240	822,270	.05417	.40
Trimethylenetrinitramine	RDX	$C_3H_6N_6O_6$	222	507,270	.04054	.34
Trinitrotoluene	TNT	$C_7H_5N_3O_6$	227	816,900	.04846	.30
Urea		CH_4N_2O	60	151,600	.06667	.44
Water	HOH	H_2O	18		.05556	.65

A.

Table 4-2b

hermochemical properties of propellant constituents (cont)

	Molecular weight	Heat of combustion (cal/mole)	N (moles/gm)	C (cal/gm/deg)	E (cal/gm)	Q (cal/gm)	Oxygen balance	N ($In.^3/lb$)	Density	Heat of combustion reference
	347	1,332,250	.04899	.2716	-231	245	-30.0			6
	420	1,492,590	.05000	.2882	-497	22	-30.5			6
	218	1,100,620	.07339	.4195	-1577	-827	-73	43.77	1.161	6
	368	2,539,568								
	150	857,800	.08667	.4427	-1146	349	-96			32
	240	822,270	.05417	.4051	-223	-617	-26.7	33.60	1.33	20
	222	507,270	.04054	.3419	628	1374	0	28.51	1.816	22
	227	816,900	.04846	.3039	-96	480	-24.6	34.31	1.654	22
	60	151,300	.06667	.4440	-1715	-844	-53.3			4
	18		.05556	.6513	-1568	0	0	24.60	1.00	

B.

Table 4-27

Propellant stability test values

Composition	Surveillance test (Days to red fumes)		120°C heat test		134.5°C heat test		Vacuum stability tes (Ml gas per 5 grams p 40 hours)	
	At 65.5°C	At 80°C	SP, min	Expl, min	SP, min	Expl, min	At 90°C	At 100°C
IMR	550	150	...	300+	50	300+	0.8	2.5
WC Ball	1,000	...	85	300+	25	300+	1.2	6.5
M1	1,700	400	...	...	50	300+	0.2	3.5
M2	500	90	105	300+	...	...	1.0	2.0
M5	600	100	110	300+	...	..	2.0	...
M6	1,700	400	...	...	55	300+	0.5	5.0
M7 (DPA)*	400	75	85	300+	...	...	7.5	...
M7 (EC)*	800	200	115	300+	...	...	2.0	...
M8 (DPA)*	200	40	50	300+	15	90	7.0	...
M8 (EC)*	370	75	60	300+	...	...	4.0	...
M9	210	...	50	300+	20	85	6.5	...
M10	500	150	...	...	90	300+	1.0	5.0
M12	800	...	...	...	50	300+	...	2.5
M15	1,000†	...	100	300+	35	300+	2.0	...
M17	1,000†	...	150	300+	35	100	1.3	6.0
T18	...	...	60	300+	25	300+	6.5	...
T20	...	...	95	300+	...	...	...	...
ECBF	800	...	150	300+	40	240+	...	6.0

*Stabilizers: diphenylamine (DPA); ethyl centralite (EC).

† Surveillance Test of nitroguanidine propellants does not produce red fumes by normal procedure. Fumes appear on opening of test bottle after approximately 1,000 days.

Table 4-27

Propellant stability test values

heat test	134.5°C heat test		Vacuum stability test (Ml gas per 5 grams per 40 hours)		Taliani test (110°C)			
Expl, min	SP, min	Expl, min	At 90°C	At 100°C	Medium	Slope at 100 .nm	Min to 100 mm	Slope at 100 min
300+	50	300+	0.8	2.5	Nitrogen	0.30	400	0.25
300+	25	300+	1.2	6.5	Nitrogen	0.90	175	0.35
. . .	50	300+	0.2	3.5	Nitrogen	0.25	500	0.10
300+	. . .	. . .	1.0	2.0	Nitrogen	0.95	145	0.70
300+	. . .	. . .	2.0	. . .	Nitrogen	1.54	139	0.85
. . .	55	300+	0.5	5.0	Nitrogen	0.34	324	0.25
300+	. . .	. . .	7.5	. . .	Nitrogen	2.22	52	1.95
300+	. . .	. . .	2.0	. . .	Nitrogen	0.60	200	0.60
300+	15	90	7.0	. . .	Nitrogen	3.45	44	2.50
300+	. . .	. . .	4.0	. . .	Nitrogen	0.80	250	0.65
300+	20	85	6.5	. . .	Nitrogen	2.38	76	2.50
. . .	90	300+	1.0	5.0	Nitrogen	1.47	43	0.95
. . .	50	300+	. . .	2.5	Nitrogen	0.30	360	0.25
300+	35	300+	2.0	. . .	Nitrogen	0.75	170	0.50
300+	35	100	1.3	6.0	Nitrogen	0.55	245	0.50
300+	25	300+	6.5	. . .	Nitrogen	1.41	74	1.38
300+	. . .	. . .	. . .	. . .	Nitrogen	. . .	. . .	. . .
300+	40	240+	. . .	6.0	. . .	. . .	. . .	. . .

lite (EC).

loes not
es appear on
days.

B.

4-76. Introduction. The primary function of a cartridge case is to facilitate the handling of the propellant charge. When the projectile and charge are short enough and light enough to be handled as a unit, and when adjustment of the charge is not required, fixed ammunition is used. When provision for adjustment of the charge is required, semifixed ammunition is used. When the combined overall length or total weight of a case and projectile is too great to permit both to be handled as a unit, and there is no need for adjustment of the charge, separated ammunition is used. In very large guns, where the weight of a case for the propellant charge would be a liability, separate loading ammunition is used. (See paragraphs 1-1 through 1-12, "Types and Classification of Complete Rounds," for a description of these types of ammunition.)

In a separate loading gun, the chamber must be designed for a volume determined by the interior ballistician. This volume must be sufficient to hold the propellant charge and provide the desired loading density (see paragraphs 4-21 through 4-51, "Theoretical Methods of Interior Ballistics"). The shape of the chamber is determined, within the limitations of this volume, by the gun designer. From the latter's standpoint, the diameter of the chamber should be kept low to reduce the diameter and weight of the breech of the gun. A further limitation is set, however, by the fact that the diameter must not be so small as to cause the breech of the gun to be excessively long or to require the use of powder bags that are difficult to handle.

In separated, fixed, and semifixed ammunition, the propellant charge is not loaded directly into the gun, but is contained in a cartridge case which may or may not be attached to the projectile. This cartridge case must be designed so that it has the volume desired by the propellant designer. The shape of the case is subject to the same limitations as the shape of the chamber, in addition to the limitation that it must be capable of being extracted from the chamber of the gun. Moreover, the case is expected to protect the propellant charge during storage and handling, and to provide effective obturation during the firing of the gun.

BRITISH PRACTICE

4-77. Design of Drawn Cartridge Cases — British Practice. The report by the British Armaments Design Department of the Ministry of Supply on the design of drawn cartridge cases is acknowledged by both the Picatinny and Frankford Arsenals to be the best assemblage of design material available for this type of cartridge case. Paragraphs 4-78 to 4-93 are taken directly from this report. The only changes that have been made are changes in nomenclature, where British nomenclature differs from American, and the insertion of a few parenthetical remarks to indicate some points where American practice is at variance with the British.

It is highly probable that other variations than those indicated exist between American and British practice. This must be borne in mind when making use of this information.

4-78. Requirements in Design. The requirements for the production of a cartridge case are that:

1. It shall be easy and cheap to manufacture.
2. It shall effectively protect the propellant charge against flash and moisture during the storage.
3. It shall not be corroded by moisture.
4. It must not develop cracks or split during storage or undergo dimensional changes.
5. It must be strong enough to withstand rough usage and the force of the gun extractors after firing, and in the instance of fixed ammunition rigid enough to carry the projectile without distortion in handling.
6. It shall withstand the high temperatures and pressures encountered during firing.
7. It shall be of suitable hardness to ensure that it will expand to the chamber and obturate satisfactorily during firing, but will be resilient enough to recover after firing to allow free extraction.

8. It shall preferably be capable of being reformed to size a number of times after firing.

The following paragraphs (4-79 to 4-93) consider the above requirements and attempt to cover those points in cartridge case design, which can, to some degree, be standardized. It is emphasized, however, that successful case design involves experience and a knowledge of the methods of manufacture and of the functioning of the case during firing.

4-79. Theory of Functioning. Figure 4-19 shows a typical cartridge case with the names of the various parts. The closed end of the case is known as the "base" or the "head" but the term "base" is more consistent with the names of the other parts.

When firing a cartridge case in a gun, the case is supported by the gun and the metal of the case is subject to plastic flow; therefore, strength calculations by elastic theories do not apply.

When a gun is fired, the propellant charge is ignited and the resultant internal gas pressure causes the case to expand to the diameter of the chamber, after which case and gun expand together. The gun expands elastically; the metal of the case will be stretched beyond its yield point and plastic strain will occur. For the case to extract freely, the recovery of the case from firing strain must exceed that of the gun, or in other words, the permanent expansion of the case after firing must not exceed the initial clearance in the chamber. This is illustrated in figure 4-20, which shows a stress-strain curve for the material (brass) of the case wall. AB represents the initial clearance between the case and chamber, and BC represents the elastic expansion of the gun on firing. Stress and strain are proportional up to the yield point Y, and hence the graph follows a straight line, whose slope is a measure of Young's modulus for the material. Beyond the yield point, plastic extension takes place up to a point E; on release of the pressure, elastic recovery takes place along line ED (which may be assumed to be parallel to YA).

AD then represents the permanent expansion of the case. Provided that the expansion of the gun is completely elastic, the chamber will return to B after firing; the distance BD thus represents the clearance between chamber and case after firing. The dotted line AF represents a case made from material of the same

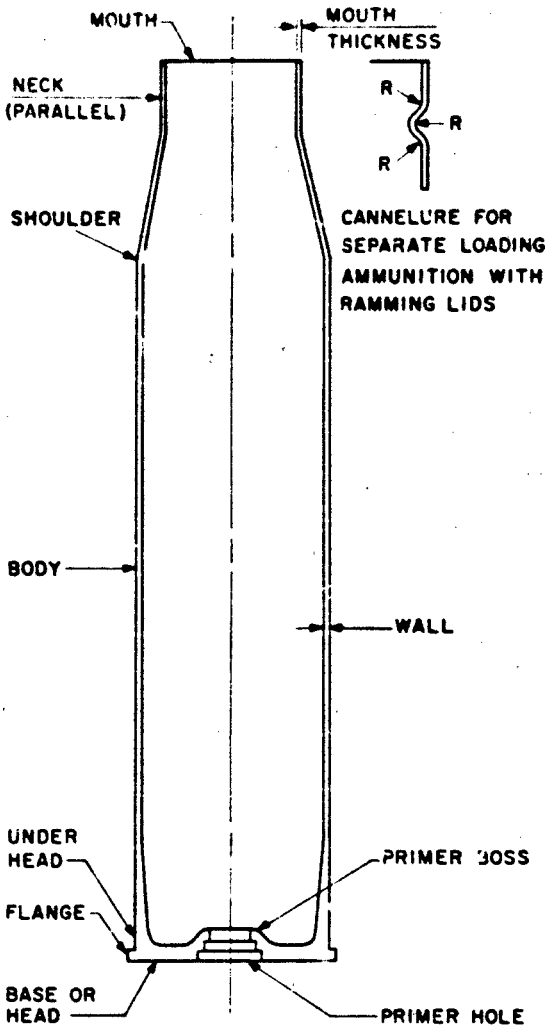

Figure 4-19. Cartridge case

modulus but lower yield. It will be seen that this case would, on recovery, follow the line FG, which would result in an interference between case and chamber (represented by BG), causing stiff extraction.

The factors, then, influencing the freedom of extraction represented by distance BD in figure 4-20 are:

1. Yield stress of material, indicated by point Y;
2. Young's modulus of elasticity for the material (given by the slope of the straight portion AY of the stress-strain curve and assumed to be also the slope of the recovery line (ED);

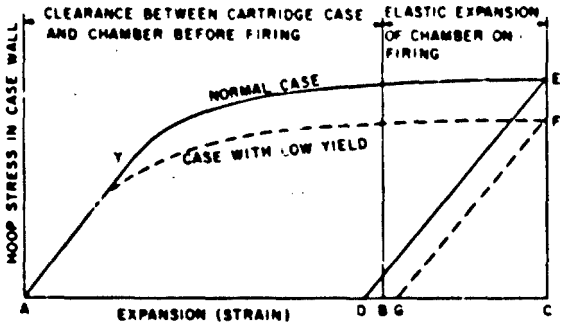

Figure 4-20. Functioning of cartridge case

3. Elastic expansion of the gun (BC),

4. Initial clearance of the case in the chamber (AB).

With brass, there is a good correlation between hardness and yield stress, so in cartridge case manufacture great importance is attached to the hardness. It is emphasized, however, that the factor influencing extraction is yield stress and not hardness, the latter being merely a convenient method of measuring the former.

The elastic expansion of the gun for a given pressure will depend on the materials and design of the gun. Higher gun pressures or guns with a reduced factor of safety will lead to higher elastic expansion, with accompanying extraction difficulties. It will be seen from figure 4-20 that the initial clearance of the case in the chamber has little influence on extraction conditions.

Figure 4-21 gives two further diagrams to amplify the theory of extraction. Figure 4-21a shows the effect of an increased elastic expansion of the gun, due to raising the pressure or reducing the factor of safety. It will be seen that a case which extracts freely on the normal chamber expansion will be hard to extract with increased expansion. Figure 4-21b shows a comparison of steel and brass cases. It will be seen that the steel case, owing to its higher modulus, will require a much higher yield stress than the brass to give the same recovery. With steel cases, a small increase in the elastic expansion of the gun would necessitate a relatively large increase in the yield stress of the case, and a condition is eventually reached when the necessary yield stress is unobtainable by work-hardening during manufacture, and a heat-treated steel becomes necessary.

4-80. Effect of Gun on Extraction The preceding theory is based only on the behavior of the case across a plane perpendicular to the axis, and would be true for a chamber with a very smooth surface finish, no extractor pockets, and no longitudinal expansion. In these circumstances, a case made as thin as manufacturing considerations permit would be expected to extract freely. In British practice, however, the gun usually has extractor pockets, and during the war the surface finish of chambers was permitted to deteriorate. This has resulted, on occasions, in stiff extraction of cartridge cases. The precise reason for this is a little obscure, but is probably due to the internal gas pressure expanding the mouth of the case to the chamber. The chamber expands longitudinally, and the pressure forces back the base of the case, together with the breech. Owing to the roughness of the gun chamber, the mouth of the case will not slide, and the case is thus stretched. In this condition the case expands into the extractor pockets, and when the gun recovers after firing the bulged portion of the case is longer than the extractor pocket and the edge becomes jammed in the chamber. Similar trouble will be experienced if the radius at the junction of chamber and breech face is too small. Shots striking this edge during loading will bruise it and form small projections in front of it, which the case will upset on firing, causing stiff extraction. A further possible cause of stiff extraction occurs when the gun is recovering after firing and the breech travels forward relative to the barrel, pushing the cartridge case in front of it. The gas pressure may be sufficient to hold the mouth of the case against the rough chamber, preventing sliding. In these circumstances the case will be subjected to a longitudinal compressive force, which may cause "barrelling" and stiff extraction. If the breech-block face is rough or if the firing-hold bushing sets back on firing, the pressure of the expanded case thereon will make operation of the sliding block very difficult.

The Ordnance Board has now recommended the adoption of the following design policy:

1. To provide full support for the cartridge cases (no breakthrough extractor pockets).

2. The provision of breech blocks without firing-hole bushings when possible.

3. The specification of a smooth finish to the chamber and front face of the breech block.

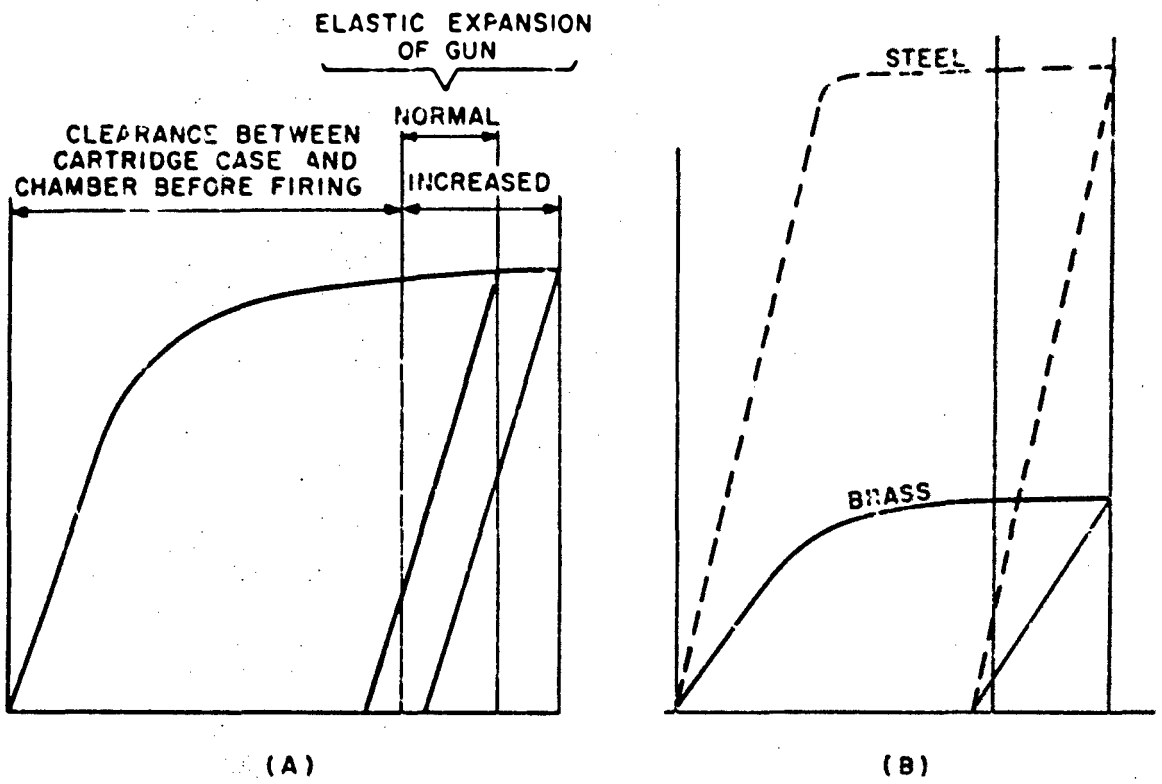

Figure 4-21. Functioning of cartridge case

If pressures in new designs of guns are raised appreciably, with a corresponding increase in elastic chamber expansion, it is unlikely that a brass case or work-hardened, low-carbon steel case will have sufficient elastic recovery to extract freely. In that case the only solution (for a solid-drawn metal case) would probably be a case made of alloy steel of high yield obtained by a combination of work-hardening and heat treatment.

4-81. Effect of Case Manufacture on Extraction. A further cause of stiff extraction is the use of different length cases in the same gun. With the shorter cases, constant firing will cause an annular depression to be eroded in the chamber near the mouth of the case. When a longer case is fired in the same gun, the mouth of the case will expand into the depression and stiff extraction will result.

4-82. Summary of Causes of Case Failure. The causes of "case failures" can be summarized as follows:

a. Failures Due to Case.

1. Cases too soft (yield stress too low), resulting in hard extraction (see figure 4-20).
2. Cases too hard, resulting in splitting caused by the low percentage elongation of the material.
3. Cases with inherent metal faults or folds, causing "blow-throughs" and gas wash.
4. The use of cases of different lengths in the same gun, causing stiff extraction.

b. Failures Due to Gun Causing Hard Extraction.

1. Extractor pockets.
2. Rough chamber and/or breech-block face.
3. Setback of firing-hole bushing.
4. Burrs at junction of chamber and breech face, caused by the shot striking on an insufficient radius.

4-83. Data Required to Design a Cartridge Case. Before a design can be initiated, the following data will be required:

1. Details of gun chamber

2. Details of projectile and rotating band
3. Gun pressure.

With regard to the details of the gun chamber, dimensions of the gun chamber should not be finalized until the cartridge-case designer has confirmed that a case to suit the chamber is a manufacturing proposition.

The gun designer is not always permitted a free hand in the shape of chamber. Often there is a complete round length restriction to suit stowage or other special conditions. For a specified chamber capacity, then, it may become necessary to design a chamber with a large back end; but this is objectionable from the gun designer's point of view, as it results in a large breech and heavy gun. Such a design also causes difficulties, in cartridge-case manufacture; it is difficult to taper the case from the large back end to the comparatively small emergent caliber.

To ensure ease of extraction, it is desirable that the main body taper should not be less than 0.02 inch per inch on diameter. The tapered portion of the case, between shoulder and parallel, should not have a taper in excess of 0.3 inch per inch on diameter, or manufacturing difficulties will be encountered.

When designing new equipment, a "basic design," showing the chamber and rifling with the cartridge case and projectile in position, ensures close cooperation between the various design sections, which is obviously very desirable.

4-84. Length of Cartridge Case. On fixed ammunition the mouth of the cartridge case should be in contact with a projection on the projectile known as the "case stop," controlling the overall length of the round. On conventional projectiles, the rear face of, or a step on, the rotating band forms the case stop.

The length of case should be calculated by assuming a minimum run-up of 0.015 in. in a new gun; that is, with a high length of case and high rotating band in a low chamber the projectile should have a travel of 0.015 in. before the rotating band contacts the taper portion (known as the forcing cone) at the front of the chamber. The tolerance of the length of the case, for fixed or semifixed ammunition, may be taken approximately as 0.01 inch per inch of caliber, but this tolerance can be reduced, if necessary, without causing serious manufacturing problems.

For separated ammunition, the length of the case should be calculated so that after ramming the projectile there is a minimum clearance of 0.075 in. between the base of the projectile and the closing plug of the case.

4-85. Clearance in Case in Chamber. With fixed ammunition, and separated ammunition (closed with plastic plug), the clearance should be constant along the body taper and the tapered portion in front of the shoulder. An exception to this rule occurs with fixed ammunition, when it is necessary to increase the length of parallel to improve shot attachment, which may be done, for a given length of case, by increasing the taper of the portion of the case in front of the shoulder. The clearance has hitherto been obtained by assuming minimum clearance of 0.004 in. on diameter per inch of caliber. This is excessive for the larger calibers; figure 4-22 shows a suggested clearance curve. (American practice for 37-mm to 120-mm calibers is to allow 0.006 in. clearance on diameter for brass cases, and 0.008 in. on diameter for steel cases. The larger clearance for steel is specified to allow 0.002 in. for the varnish coat.)

When estimating the clearance at the parallel portion of fixed-ammunition cases, it must be borne in mind that the projectile is an interference fit in the case, and hence the mouth of the case expands upon assembly.

The parallel portion of the gun chamber must be designed to give the correct clearance over the rotating band. Once the case mouth thickness has been fixed, therefore, the case designer has no means of controlling the clearance in the chamber at the mouth of the case. The clearance between the gun chamber and the parallel portion of the case (after insertion of the projectile) should not be less than 0.01 in. on diameter per inch of caliber; if this cannot be achieved, the chamber and projectile dimensions should be reconsidered. At this point it is better to err on the side of too much rather than too little clearance, as maltreatment of a

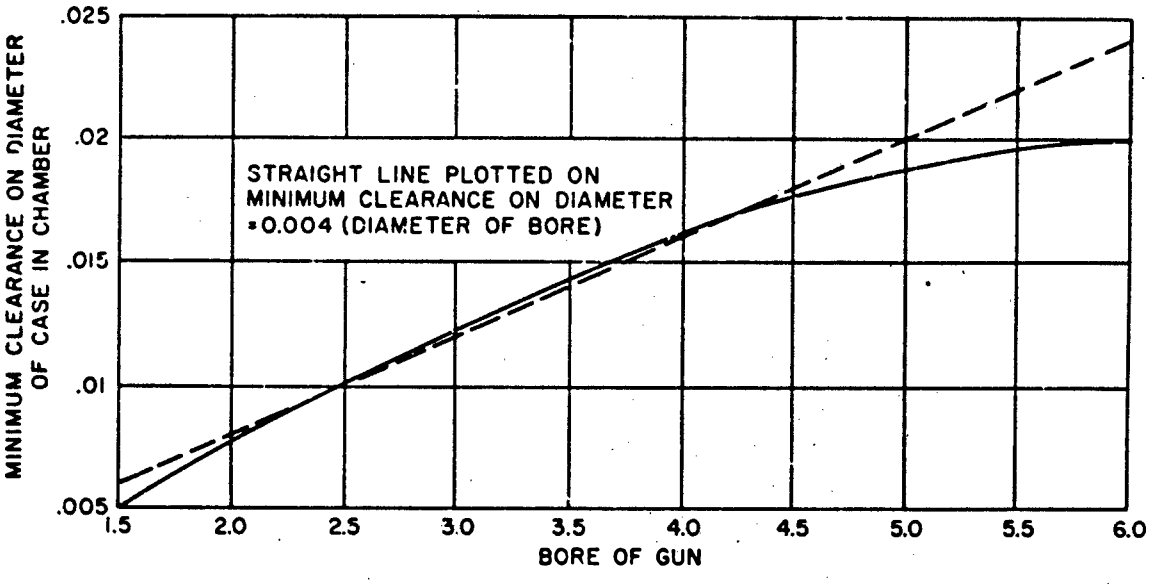

Figure 4-22. Clearance of cartridge case in chamber

fixed round will sometimes cause a slight bolling of the mouth of the case, and if the clearance is too small troubles in loading may be experienced.

In separated ammunition closed with a white metal plug, the clearance at the "under head" position should be on the lines outlined above. The clearance should then decrease uniformly along the taper toward the mouth, so that the high mouth diameter of the case is equal to the low chamber diameter at that point.

With a plastic plug, however, the mouth of the cartridge case after closing is very rigid and will not "give" to the chamber, as would a case closed with a white metal plug, should slight discrepancies (due, for instance, to ovality) be present. Therefore, with a plastic plug it is necessary to allow clearances of the case within the chamber in the same manner as for fixed ammunition, except that the clearance at the short parallel portion should be approximately the same as at the taper.

4-86. Crimping Groove Design. With separated ammunition, where the projectile is rammed before the loading of the cartridge (as is the case in howitzers), the cartridge case is normally closed with a simple glazed-board cup. When the projectile is rammed by means of the cartridge, however, the latter is closed with a white metal or plastic plug. In such cases it is now common practice to strengthen the mouth of the case, and to increase the support for the plug, by rolling a crimping groove into the mouth of the case (see figure 4-19). For the 3.25-in. case the radius (R) is 0.2 inch, and for other sizes the radius should be adjusted in the ratio of the calibers.

For white metal plugs, the empty case is slotted at the mouth to form tangs which may be bent over the recesses in the plug to secure the latter.

The present tendency is to close with a plastic plug, this being secured by "coining," no tangs being required.

4-87. Flange Design. The flange (figure 4-19) performs the dual function of acting as a stop when loading the round, and providing a projection on the case against which the gun extractors operate to eject the case after firing. The force exerted by the extractors when a case is tight may be considerable, and flange strength is therefore of importance.

Figure 4-23 shows several types of flanges. With any type of flange the cartridge head space (the clearance between the base of the case and

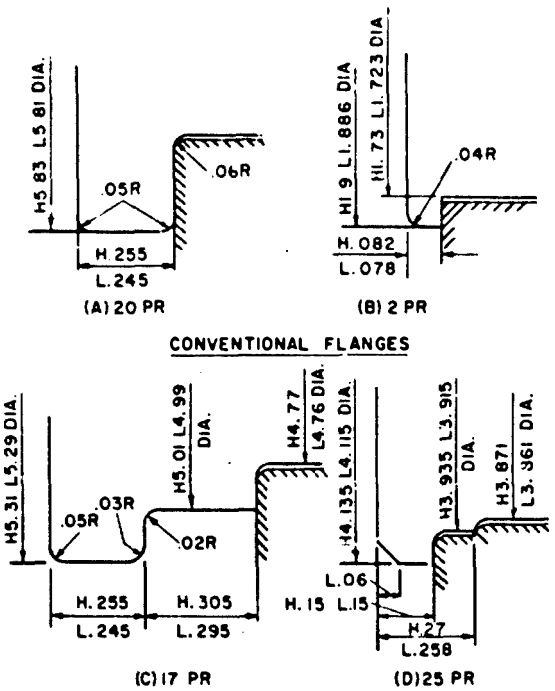

Figure 4-23. Flange design

the face of the breech block when the case is pushed right home into the chamber) should be low* 0.005 in. - high† 0.015 in. with a high thickness flange. When designing ammunition for a new gun, the case designer is usually permitted a free hand on flange thickness, and the breech is then designed to give the correct cartridge head space.

*Low refers to the minimum dimension.
†High refers to the minimum dimension.

With a simple flange without step (figure 4-23, a and b) the extractors are usually located in recesses at the mouth of the chamber. These pockets leave small areas of cartridge case unsupported; when there is insufficient thickness under the head, the case is likely to expand into the pockets, causing hard extraction. (See paragraphs 4-79 through 4-82.) German designs for Q.F. guns incorporate a lip at the rear of the chamber (see figure 4-23e), which obviates extractor pockets; it is understood that extraction troubles with German cases are very rare.

With a stepped flange (figure 4-23c), the step acts as a stop in loading, and positions the flange proper at a fixed distance from the chamber face. The extractors are located in the space so formed, leaving a portion of the case unsupported and necessitating a rather heavier base. A few early case designs have a step located in the chamber. This step appears to serve no useful purpose, and the design is not likely to be repeated.

4-88. Design of Mouth of Cartridge Case. From a functional aspect, the internal surface of the mouth of the case is quite satisfactory "as drawn." In production, however, forming the mouth within the specified tolerances, particularly with fixed ammunition, could only be effected at the expense of repeated tool replacements.

It is usually considered more economical to thicken the cases at the mouth when tapering and necking, and to bore on a lathe to within the specified tolerances. (In American practice, this is not usually done; instead, the case is used "as drawn.")

To obtain a rigid fixed round, there must be adequate interference between the cartridge case and the projectile. Excessive interference is objectionable as it causes stretching of the cartridge-case mouth in the plastic range without giving additional strength of attachment, and increases the work necessary to insert the projectile.

The interference depends on the diameters and tolerances of both the case mouth and the base of the projectile; it is often necessary to compromise. Figure 4-24 shows recommended maximum and minimum interferences. The

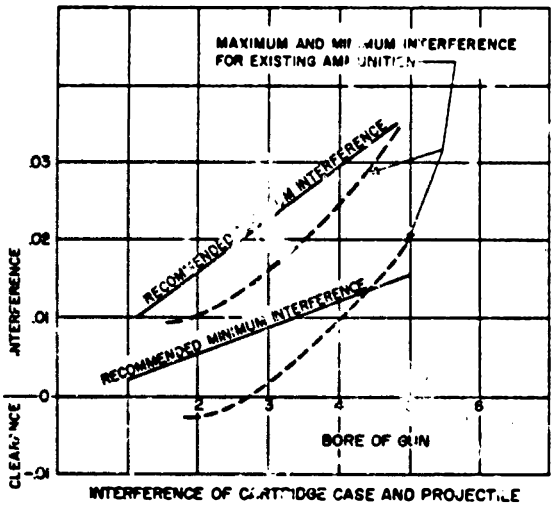

Figure 4-24. Interference of cartridge case and projectile

dotted curves show the maximum and minimum interferences for selected existing ammunition.

The thickness of the case mouth is governed by two considerations:

1. Strength of attachment of the cartridge case to the projectile
2. Sealing in the chamber upon firing.

For a given hardness, a thin mouth would be expected to seal better than a thick mouth, but the thickness must be adequate for the strength of attachment. It should be borne in mind that once the dimensions of the chamber have been fixed, the mouth thickness can only be increased at the cost of reduced clearance in the chamber.

The length of the parallel mouth of the cartridge case is controlled by the shape of the chamber and the width of the rotating band. However, to give the maximum possible strength of attachment, it is desirable that the case parallel be at least as long as the portion of projectile to the rear of the rotating band.

For conventional projectiles, the surface finish after mouth boring is unimportant, but for skirt-banded projectiles (for example, discarding-sabot shot) and for projectiles where the case is attached over the rotating band a smooth case mouth is essential; the case design should carry a note to the effect that the "mouth of case may be bored, but a smooth finish is essential."

Reference should be made here to the method of dimensioning the mouth of the case. With separate-loading ammunition, the internal diameter of the mouth of the case is not critical, and the mouth is usually controlled by an external high and low diameter and a high and low wall thickness. The wall thickness tolerance also controls the eccentricity of the mouth boring.

Assuming an internal diameter tolerance of 0.005 in. and a wall thickness tolerance of 0.01 in. the above method of dimensioning would permit a tolerance on the internal diameter of 0.025 in., which would in general be acceptable for separate-loading ammunition.

With fixed ammunition, however, the internal mouth diameter is critical as it controls the interference of the case on the projectile; and the wall thickness is critical because it controls the strength of attachment as well as the clearance of the assembled round in the gun chamber.

Having fixed these two dimensions, one cannot logically add external high and low dimensions, but the manufacturing and inspection departments insist on a control at this point. A rather unsatisfactory compromise has therefore been agreed, of giving a high (only) external diameter calculated from the additions of two high wall thicknesses to the low internal mouth diameter.

4-89. Internal Contour of Case. After drawing and before tapering, a cartridge case is parallel externally, but to facilitate stripping the case from the punch the inside of the case will have a constant taper from the mouth to a point where the thickening for the base commences.

The internal contour in the base must be considered in conjunction with the gun design and working conditions, but the general trend is indicated in figure 4-25. The contour of figure 4-25a is favored for the smaller sizes of case, but in the larger sizes (over about 3 in.) the contour of figure 4-25b is preferred.

The distance to points x and y is stated on the design. The radius (R) is invariably left open, but is virtually fixed by being centered on a line through x parallel to the base and drawn tangential to xy and to the base thickness line.

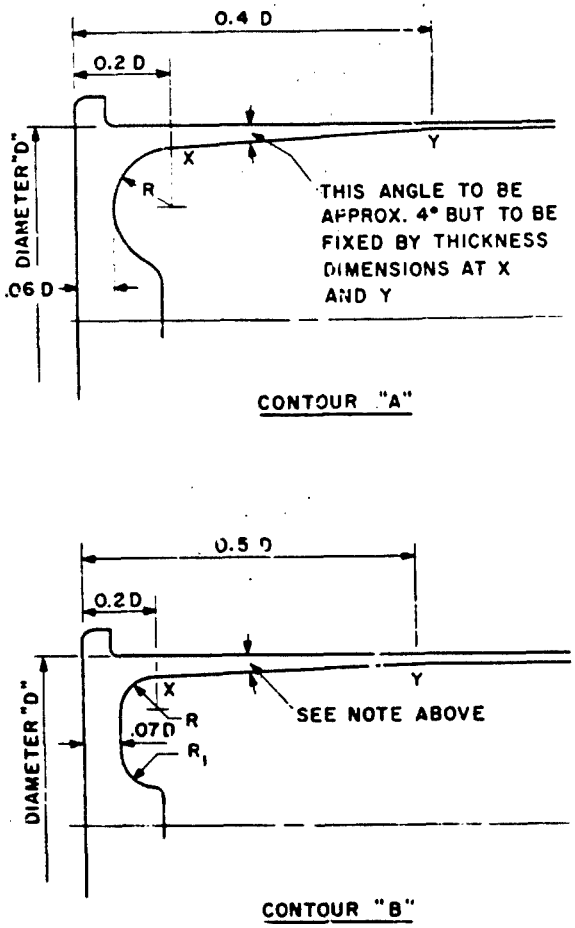

Figure 4-25. Internal contour of cartridge cases

Radius R can be fixed, but as it is not critical it is usually left to the manufacturer's discretion. These radii will affect the flow of metal, and hence the hardness under the flange, and it is undesirable to restrict the manufacturer unnecessarily.

The question of a blending radius at point y or of a large radius joining point y to radius R has caused some controversy. Each manufacturer usually has a definite opinion on what he considers the best contour to avoid a hard spot at the junction of the wall and base (point y). It is usual therefore to allow, as an alternative to contour figure 4-25a, a blending radius at point y equal approximately to 2 1/2 times the inside diameter of the case at that point.

Early designs of the case showed a radius approximately equal to the internal diameter of the case, connecting point y to radius R. This contour, while possibly permitting a better flow of metal in drawing, gave a very thick wall in the region of point x. The contour has been replaced in new designs by the contour shown in figure 4-25a or b, except for an occasional case design for medium- or low-pressure guns.

The base thickness and wall thickness at points y and x are at present controlled by low dimensions only. The high dimensions have previously been controlled by specifying the maximum weight of the case.

In estimating the minimum chamber capacity, it may be assumed that the base thickness will be low* +10 percent and the high wall thickness low +20 percent for sizes up to and including 6 pounder, and the low +40 percent for sizes larger than 6 pounder. The high figures are not, however, specified at present.

4-90. Additional Notes on Cartridge Case Designs.

a. Number of Draws. The minimum number of draws and anneals required during manufacture used to be stated on the design with the object of controlling, to some extent, the work hardening of the final product, but this practice has been discontinued as unsatisfactory since the case is now fully annealed between draws. An insufficient number of draws may result in overworking the brass and producing a case which would split upon firing, but this would be brought to light at proof.

b. Hardness of Cartridge Case. The hardness figures of the finished case are quoted in the relevant inspection department specifications, but as a rough guide, the hardness of the mouth for fixed ammunition should be 60 to 75 D.P.N., and the "underhead" approximately 160 D.P.N. Between these two points the hardness should approximate to a straight line gradient.

The hardness of the case (see paragraphs 4-79 to 4-82) is particularly critical for certain high-pressure guns having a large elastic setback of the breech block; the gas pressure tends to hold the mouth of the case to the chamber while the

*See notes to paragraph 4-87.

base of the case is being forced back. The case then must stretch, and if the metal will not stretch sufficiently separation will occur. This type of failure is more common in small arms than in larger calibers. Too high a hardness will result in a high yield stress but low ductility. To insure correct functioning in such guns, it is desirable to work to both high and low hardness figures on the case.

c. Notes on Experimental Case Design Drawings. On experimental cartridge-case designs, the following information should be given, in order that a complete history of the design can be referred to:

1. Chamber design number and date
2. Projectile design number and date
3. Rotating band design number and date
4. Diagram showing clearance of cartridge case in chamber
5. Volume of projectile to the rear of the rotating band (case stop)
6. Effective chamber capacity with projectile in position. (In the case of separate-loading or separated ammunition this will include the space around the base of the projectile.)

d. Control of Flatness of Base. Inaccuracies and wear in the lathes may produce concavity or convexity of the base in machining. Concavity will reduce the thickness of the base toward the center and will increase the distance between the primer and the breech block, thus reducing the effective striker blow when percussion firing is being used. Convexity will result in a reduced cartridge head space toward the center of the base, which if excessive may cause difficulty in closing the breech.

4-91. Marking on Bases of Cartridge Cases. Marking is one of the last operations in manufacture, and is usually carried out with a group stamp on a light power press. During stamping the case must be supported on a bolster which is small enough to pass through the mouth of the case. It is therefore very desirable (though not always practical) that all stamping should be within the diameter of the bolster (that is, the diameter of the mouth); otherwise, tilting of the case and distortion of the base may occur during stamping.

4-92. Effective Chamber Capacity. For a given weight of propellant, the resultant ballistics are influenced by the volume of the chamber; an accurate estimation of this volume is therefore necessary. The effective chamber capacity for fixed ammunition is the volume contained by the cartridge case, up to the base of the shot, less the volume of the empty primer (American practice considers the filled primer). The volume of an empty rather than a filled primer is subtracted, as the primer magazine contains gunpowder which may be considered part of the propellant charge. The internal volume of the primer thus becomes part of the effective chamber capacity.

The effective chamber capacity for separated ammunition is the same as for fixed ammunition, except that the volume of the gun chamber around the base of the projectile to the rear of the rotating band must be added, and the volume of the plug with which the cartridge case is closed must be deducted.

To determine the internal volume of the cartridge case, the case is drawn accurately to scale and divided up into frustums of cones, and an irregular portion in the base of the case. The volume of the frustums may be calculated by the usual formulas. The volume of the irregular portion in the base of the case may be obtained by the use of an integrator or by mensuration. In capacity calculations it is necessary to assume a thickness for the tapered portions of the wall to the rear of the mouth parallel, and for this purpose the thickness at the junction of the taper and the parallel is taken as being equal to the high mouth thickness.

When a new gun is designed, the effective chamber capacity (E.C.C.) is first obtained by the gun designer, who calculates the gross capacity of the chamber and subtracts an estimated amount for the volume of the cartridge case. This preliminary E.C.C. can only be regarded as an approximate figure that is subject to correction after the cartridge case has actually been designed. A small variation in the final figure from the original estimate of chamber capacity is not serious, as the charge is determined with the cartridge case to give the required ballistics. Once the charge has been determined, however, it is important that the case-to-case variation of the actual volume of metal shall be within a defined percentage tolerance.

4-93. Typical Calculations for a Cartridge Case Design to Suit a Given Chamber.* Figure 4-26

*See notes to paragraph 4-87.

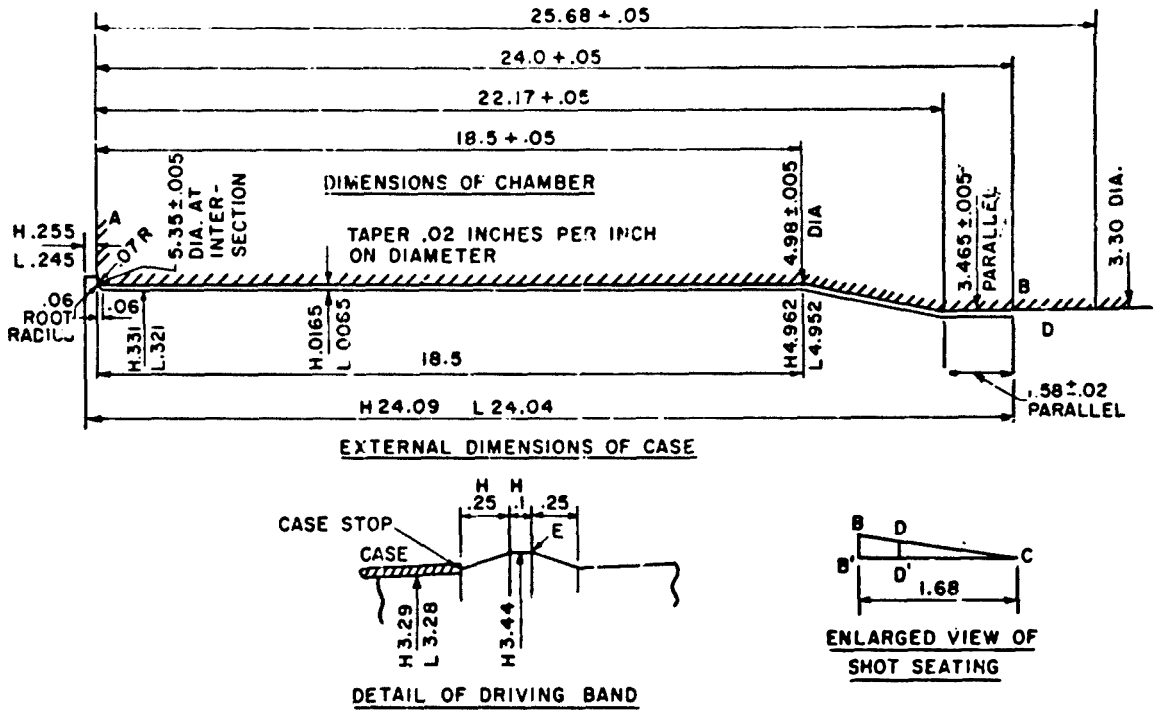

Figure 4-26. Typical chamber and details of rotating band

shows a typical chamber together with details of the rotating band.

Assuming a minimum run-up to be 0.015 inches and supposing D to be the point at which the front edge E of the rotating band first meets the forcing cone,

Then

$$\text{Distance from mouth of case to point E} = \text{high } 0.35 \qquad (193)$$

(See detail of rotating band in figure 4-26.)

$$\text{High length of case (from chamber face)} + 0.35 + 0.015 = \text{low distance of D from chamber face (AD)} \qquad (194)$$

$$\text{Axial length of forcing cone BC} = 25.68 - 24.0 = 1.68 \qquad (195)$$

(Note that subtracting high AB from low AC would give a shorter length for BC, but we require the shortest length AD to ensure that a high length case will not foul. See figure 4-27.)

$$\text{Low BB'} \; 1/2\,(3.465 - 0.005) - 3.3 = 0.08 \qquad (196)$$

$$DD' = 1/2\,(3.44 - 3.3) = 0.07 \qquad (197)$$

Then by ratio we get that

$$B'D' = \frac{1.68 \times 0.01}{0.08} = 0.21 \qquad (198)$$

$$\text{Low distance of D from chamber face (AD)} = 24.0 + 0.21 = 24.21 \qquad (199)$$

Substituting in equation (194) gives

$$\text{High length of case from chamber face} = 23.845$$

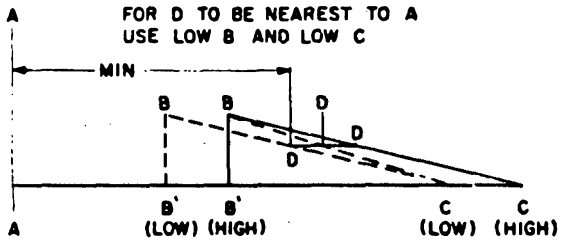

Figure 4-27. Slope of forcing cone

*Assuming low thickness of flange = 0.245

High overall length of case = 24.09 (200)

Allowing a tolerance of 0.05 gives

Low overall length of case = 24.04 (201)

Clearance on Main Taper. This should be a parallel clearance (see figure 4-22) of low 0.013 on diameter = low 0.0065 on radius.

Diameter of chamber at rear face
= 5.35 ± 0.005

Taper of chamber = 0.02 inches per inch on diameter

Diameter of chamber at 0.07 inches from chamber face
= 5.35 - (0.02 x 0.07) ± 0.005 = 5.349 ± 0.005
= H.5.354 L.5.344

High diameter of case under head
= low chamber - low clearance
= 5.344 - 0.013 = H.5.331 (202)

Allowing a tolerance of 0.01 gives the low diameter of case = L.5.321 (203)

(For calibers less than 3-inch, tolerance should be reduced to 0.005 inch.)

Then

High clearance = high chamber - low case
= 5.354 - 5.321
= H.033 on diameter
= H.0165 on radius (204)

*The length of a cartridge case is invariably taken from the base to the mouth, that is, including the flange. Had the high thickness of the flange been used in the above calculation, then in manufacture it would be possible to obtain a high length of case from the chamber face in excess of 23.845.

Length from flange to shoulder of case

= low length of chamber = 18.5

(As the precise position of the shoulder is somewhat indeterminate, tolerances are not given for this dimension.)

Diameter of chamber at shoulder
= H.4.985 L.4.975

High case diameter at shoulder
= low chamber - low clearance
= 4.975 - 0.013
= H.4.962 (205)

Low case diameter at shoulder
= high chamber - high clearance
= 4.985 - 0.003
= L.4.952 (206)

Assume mouth thickness of case after boring = H.06 L.05

Diameter of rear end of projectile
H.3.29 L.3.28

External diameter of neck of case after projectile is inserted:

High = 3.29 + 0.12 = H.3.41
Low = 3.28 + 0.10 = L.3.38

Diameter of chamber parallel = 3.465 ± 0.005
= H.3.47 L.3.46

Low clearance on diameter = 3.46 - 3.41
= L.0.05

High clearance on diameter = 3.47 - 3.38
= H.0.09

Assume interference of L.0.01 H 0.025 (See figure 4-24.)

Mouth bore diameter (high) = 3.28 - 0.01
= 3.27H

Mouth bore diameter (low) = 3.29 - 0.025
= 3.265L

High external diameter of mouth
= low mouth bore diameter + 2 (high mouth thickness)
= 3.265 + 0.12 = H.3.385 (209)
(See paragraph 4-88.)

To Obtain Length of Parallel Mouth. The clearance of the conical portion of the case above the shoulder within the chamber should be constant and equal to the clearance on the main body taper.

Using mean dimensions

$$\text{Taper of coned portion of chamber} = \frac{4.98 - 3.465}{3.67} = 0.4128 \text{ in. per in. on diameter} \quad (210)$$

Mean diameter of shoulder of case = 4.957

Mean diameter of neck case after insertion of shot = 3.395

$$\text{Length of coned portion of case} = \frac{4.957 - 3.395}{0.4128} = 3.783 \quad (211)$$

Theoretical length of parallel mouth of case

= High overall length of case
- (low flange thickness + length to shoulder
+ length of coned portion case)
= 24.09 - (0.245 + 18.5 + 3.783) = 1.56

To obviate fouling in the chamber this must be regarded as a low dimension; allowing a tolerance of ±0.02 inch gives a dimension of

$$1.58 \pm 0.02 \quad (212)$$

NOTES ON AMERICAN PRACTICE

4-94. Design Procedure for Cartridge Cases. In order to design a cartridge case, the required internal volume and the maximum length of the case must be specified. The external volume of the case is determined by adding to the required interior volume the volume of the metal in the case, the volume occupied by the portion of the projectile that projects into the case, and the volume of the primer. (The primer charge is not considered to add to the effectiveness of the propellant, hence the volume of the primer tube is considered as if it were a solid rod.) When determining the length of the case, the maximum length permissible is usually used in order to obtain minimum body diameter.

The volume of metal contained in the case is ordinarily obtained by using the volume of a similar, previously designed, case for an approximation. When possible, Frankford Arsenal solves the design problem by finding a case already manufactured and having approximately the same volume as the required case, but which takes a larger caliber projectile. By necking this case down to the required size, a satisfactory new design can be established. This procedure not only simplifies the design problem, but also expedites manufacture, since, with the exception of the tapering dies, existing dies may be used.

4-95. Trend in Specifications for Cartridge Cases. Frankford Arsenal recommends that the major reliance of quality in the production of cartridge cases be placed upon functional tests. They feel that the fewer the restrictions placed upon a manufacturer, the more likely he is to find it possible to reduce the cost of producing a satisfactory product. It is recognized that in some instances the effect of changes in accepted methods may not be immediately perceptible. One example of this type was the high notch sensitivity of the bases of non-heat-treated steel cartridge cases at low temperatures. This high notch-sensitivity was not predictable, and did not show up until low-temperature firing tests were performed. In instances of this sort, it is necessary, of course, to make definite specifications for heat treating.

Figure 4-28 shows the format used for drawings of steel cartridge cases. Figure 4-29 shows the format for brass cases.

4-96. Bullet Pull. Bullet pull refers to the straight pull necessary to remove the projectile from the crimped case in a round of fixed ammunition. Correct bullet pull is required in order to obtain proper internal ballistic characteristics. Propellant pressure must be allowed to build up to a minimum value before the projectile leaves the case. Excessive variations in bullet pull from round to round may cause the muzzle velocity of the projectile to vary accordingly, and consequently may result in excessive dispersion of the rounds. Bullet pull is also highly important in rounds used in automatic weapons. If insufficient bullet pull exists, the case may become detached from the projectile during the loading cycle.

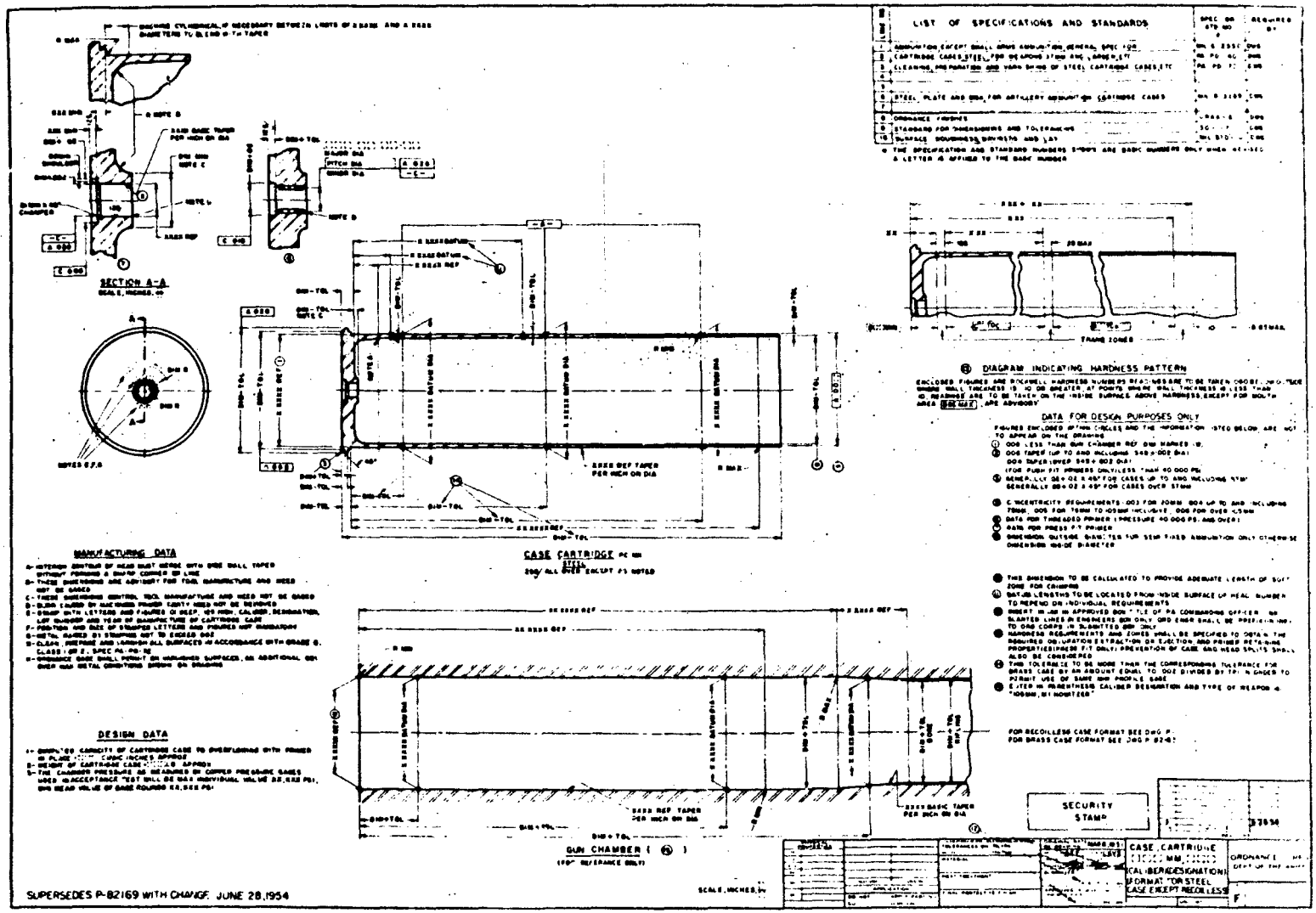

Figure 4-28. Steel cartridge case.

Figure 4-29. Brass cartridge case

4-97. Methods of Achieving Desired Bullet Pull. The desired bullet pull may be obtained by means of (1) press fitting of the projectile in the cartridge case and (2) by machining a crimping groove into the projectile and crimping the case into this groove.

a. Press Fit. The amount of bullet pull that may be obtained by means of the press fit is limited by two considerations. Both considerations are dependent on the fact that, for a metal of a given modulus of elasticity, the tangential force that can be applied by the press fit is determined by the thickness of the neck of the cartridge case. These limitations are:

1. The absolute limit is set by the fact that the outside diameter of the case at the neck must be less than the outside diameter of the rotating band.

2. The manufacturing process (drawing) imposes a practical limit on the thickness of the neck; this practical limit is usually well below the absolute limit.

b. Crimping. The amount of bullet pull required, beyond that obtained by means of the press fit, must be obtained by crimping the case to the projectile. The amount of pull obtained depends upon (1) the physicals of the metal of the case, (2) the length of the crimping groove, (3) the depth of the crimp, (4) the width of the crimping groove, and (5) the number of crimping grooves.

1. The physicals of the metal are not ordinarily controlled in order to affect the bullet pull. In the case of steel cases, however, the mouth must be soft enough to permit the crimp to be made without cracking the metal. For that reason, cases that have been overall heat-treated must be mouth-annealed before crimping.

2. The length of the crimp may vary from a full crimp, around the entire periphery of the case, to an interrupted crimp that makes use of only a small portion of the available circumferential length. An interrupted crimp can be used only when press-type crimping is employed.

3. The depth of the crimping groove is limited, for any given width of groove, by the physicals of the metal. Depth is further limited by the requirement that the crimping groove must not be so deep that it weakens the wall of the projectile.

4. Excessively wide crimping grooves have been found to cause extraction difficulties. Under the action of the propellant gases, the metal in the crimp expands to the wall of the chamber and, due to the highly strained condition of this metal, sufficient recovery does not take place.

4-98. Effect of Method of Crimping. Two methods of crimping are in use: (1) press-type crimping, and (2) rubber-die crimping.

a. In press-type crimping, the case is crimped to the shell by means of a form tool in a mechanical or hydraulic press. This method has an inherent difficulty in that the tool must be properly alined with the crimping groove. Since the projectile is inside the case, the alinement cannot be done visually but must be done by means of an alining jig. Variations in the position of the crimping groove may result in the tool's not falling at the exact position required. This results in the metal of the case being excessively strained in the area where the crimping tool forces it against the edge of the crimping groove. This effect is not easily noticed during inspection, but has given rise to extraction difficulties during firing.

b. In rubber-die crimping, the projectile is placed inside the case and a closed rubber bag or a solid rubber ring is fitted over the neck of the case. In the use of the rubber bag, hydraulic pressure applied on the inside of the bag forces the metal of the case into the crimping groove. In the use of the solid rubber ring, compressing the ring by a mechanical or hydraulic press forces the case into the groove. Rubber-die crimping does not present the alinement difficulties that press-type crimping does. It is difficult, however, to make an interrupted crimp by this process.

4-99. Materials for Cartridge Cases. Brass strips or disks of 70/30 composition were used almost exclusively in the manufacture of cartridge cases prior to World War II. Present specifications allow:

68.5 to 71.5 percent copper
0.07 percent maximum of lead
0.05 percent maximum of iron
0.15 percent other materials but not over 0.006 percent bismuth and 0.0001 percent mercury; remainder, zinc.

In the annealed state, the minimum tensile strength may vary between 40,000 and 45,000 pounds per sq in. (depending upon the thickness

of the sheet or disk) with corresponding minimum elongation of from 60 to 40 percent. In the cold-worked state, the tensile strength may vary from about 50,000 to about 100,000 pounds per sq in. Cold work produces plastic deformation which not only increases the tensile strength, but also increases the yield strength while decreasing the percent of elongation. Cold working sets up stresses whose magnitude depends upon the amount of plastic deformation. these stresses may cause surface cracks or, in the case of thin sections, complete cracks in the finished cartridge case. The stresses are relieved by low-temperature annealing.

Steel had long been considered as a substitute for brass in the manufacture of cartridge cases; not until World War II, however, did the shortage of copper and zinc force an acceleration of the development of steel cartridge cases.

Present specifications (1955) advise the use of MIL-5-3289, generally in the spheroidized annealed condition. This steel has a carbon content of 0.25 to 0.35 percent. It may contain a maximum of 0.045 percent phosphorous and 0.055 percent sulfur. Steels with lower carbon or manganese content cannot be properly heat treated.

4-100. Base Rupture of Steel Cartridge Cases. It has been found that base rupturing of steel cases at low temperatures is almost always the result of small folds or discontinuities produced on the inside of the base during the heating process. Discontinuities, which under ordinary conditions would cause no trouble, may cause trouble when the notch sensitivity of the steel is increased at lower temperatures. It has been found that this increased notch sensitivity at low temperatures is a property of non-heat-treated steels. The notch sensitivity of heat-treated steels is relatively unaffected by temperature. Frankford Arsenal heat treats the inner section of the base and sidewall of the case at a temperature of 1,650°F, followed by a quench in brine and a 750°F draw, to prevent these low-temperature base ruptures.

DIMENSIONING OF CARTRIDGE CASE AND CHAMBER

4-101. Head Thickness. In table 4-29 the column headed R shows the nominal head thickness for certain representative service cartridge cases. The height of the primer boss is shown in column P; P - R is the height of the primer boss above the bottom of the cavity of the case. This dimension (P - R) is determined entirely by the dimensions of the heading mandrel. To allow for wear and recovery of the metal after pressing, a rather generous tolerance is usually allowed. But, because the outside of the head is machined, the tolerance of the head thickness may, if necessary, be held quite close. However, 0.01 in. is usually allowed for the smaller calibers, while as much as 0.05 in. may be allowed for the larger ones.

4-102. Flange Thickness affects the seating of the complete round when it is loaded into the gun. This thickness is obtained by machining, so that a fairly close tolerance is practicable. It rarely exceeds 0.01 in.

4-103. Primer Hole. In cases designed for use at chamber pressures in excess of 40,000 psi, a screwed-in primer is used; for pressures below 40,000 psi a forced fit is used to hold the primer in place.

4-104. Thickness at Mouth. In the taper drawing operations, the walls of the case will thicken; the amount of thickening depending on the amount of taper: the greater the taper, the greater the thickening will be. Usually, the friction of the die will prevent any appreciable increase in the overall length of the case. This thickening of the wall cannot be directly controlled, and the final wall thickness at the mouth depends on (1) thickness of the walls before the taper draw, (2) diameter of the final taper draw die at the mouth of the case, and (3) recovery or spring of the walls after leaving the die. Experience indicates that a tolerance of 0.01 in. is necessary for mass production.

The thickening of the mouth that takes place during taper drawing is the primary factor limiting the amount of necking the case may undergo. The body of the case is rarely made more than 1.5 calibers in diameter.

4-105. Chamber Dimensions. Once the cartridge case has been designed, the gun chamber may readily be laid out by adding the clearance to the outside dimensions of the cartridge case. The length of the chamber is determined by adding to the length of the case contained in the chamber (1) the width of the rotating band, and (2) the allowable travel necessary for the

rotating band to engage the rifling. As smooth a finish as is consistent with production is necessary if obturation and extraction difficulties are to be avoided.

4-106. Chamber Tapers. In guns using cartridge cases the taper of the chamber is made the same as that of the cartridge case. In some chambers, the part that accommodates the straight portion of the case is given a taper of 0.005 in. per in. on diameter. This taper has been found to facilitate the extraction of drawn steel cases. In guns using bagged charges, the chamber is not tapered.

4-107. Protective Coating must be controlled, and tests must be prescribed by the designer of the steel cartridge case to ensure the ability of the coating to resist corrosion and abrasion. Thickness of the coating should not exceed 0.001 in.

4-108. Neck of Case and Obturation. Obturation, as well as ease of extraction, tends to dictate the physical properties of the metal at the neck of the cartridge case. Capability of holding projectile firmly is also important in the case of fixed ammunition.

Hot propellant gases must not escape between the walls of the neck of the cartridge case and the walls of the chamber. To prevent escape, the walls of the neck of the case must expand outward and begin to press firmly against the walls of the chamber before there is any appreciable forward movement of the projectile. This desired expansion is possible because of the impact nature of the propellant pressure. The inertia of the projectile causes the immediate initial action of the propellant gases to stress the base of the projectile and the walls of the case. If the yield strength of the metal in the neck of the case is not too high, this metal in the neck will be strained sufficiently to press firmly against the walls of the chamber during the short interval of time when the base of the projectile is elastically deforming and before the projectile moves forward out of the neck of the case.

If the yield strength of the neck metal is too high, the straining of the walls of the case will lag behind the propellant pressure. In this instance, the projectile will have begun to move out of the case before the walls of the neck are pressed firmly enough against the walls of the chamber to prevent escape of hot gases. Similarly, if the build-up of propellant pressure is too slow, there also may be escape of gases.

If the yield strength of the neck metal is too low, satisfactory recovery will not take place and extraction will be difficult.

Compromise between the conflicting requirements for extraction and obturation is therefore necessary in specifying the physical properties of the metal in the neck of the cartridge case. Brass cases (modulus of elasticity, 15,000,000 psi), according to experience, should have tensile strength at the mouth up to a maximum of about 55,000 psi. Steel cases (modulus of elasticity, 30,000,000 psi), according to experience, may have a Rockwell hardness up to a maximum of B85 at the mouth. This corresponds to a tensile strength of 82,000 psi.

4-109. The Obturating Problem in Howitzers. The use of zoned charges in howitzers creates a unique problem in obturation. A cartridge case, designed (and heat-treated) to obturate successfully when the greatest powder charge is used, may not obturate at the lower zone charge. Two methods have been tried by Frankford Arsenal to eliminate this difficulty. The first of these (figure 4-30a) was to use an inverted bead placed in the straight portion of the case at a point slightly below the base of the shell. It was hoped that this inverted bead would act as a labyrinth seal and permit effective obturation. Tests of cases modified in this manner revealed that, although obturation was improved, extraction difficulties were experienced. The second method involved the use of two obturating beads in the straight portion of the case (figure 4-30b). These beads filled up most of the clearance space between the case and the chamber. Successful obturation was achieved with this design and no extraction difficulty was experienced.

4-110. Hardness Requirements. Hardness values of various parts of the case for certain representative steel cartridge cases are shown in table 4-28. In general, it has been found by Frankford Arsenal that extraction difficulties can be minimized by overall heat treating.

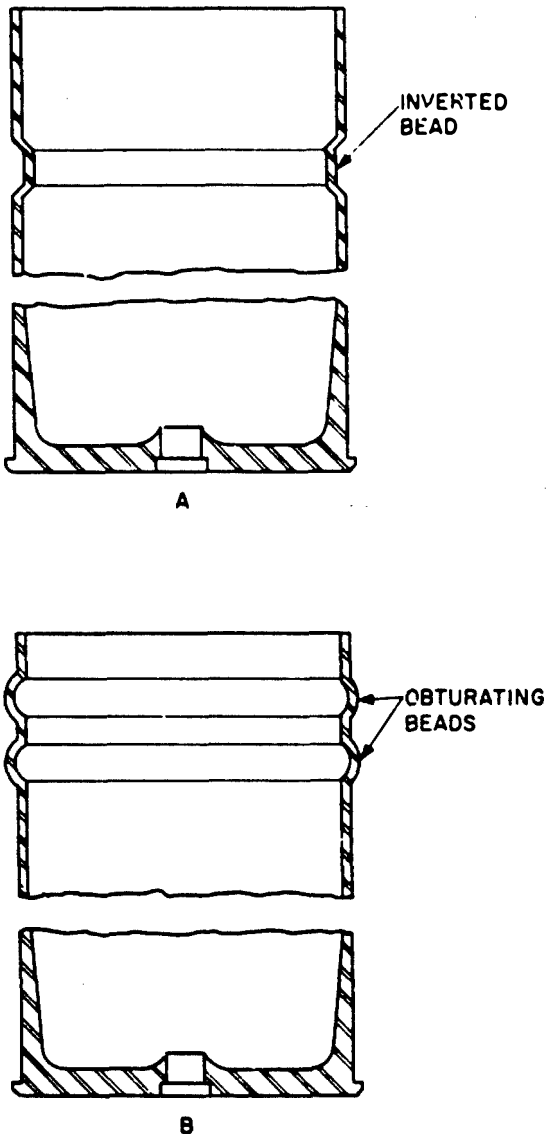

Figure 4-30. Obturating beads

4-111. Elongation. Minimum elongations at the C and D sections (table 4-28) are usually specified to assure sufficient ductility to permit expansion without rupture. Experience indicates that the minimum elongation in the C section should be not less than 6 percent in one inch; in the D section, 4 percent in one inch.

Hardness requirements, except at the mouth, are furnished by the designer to the manufacturer for the latter's guidance in controlling manufacture. Hardness requirement at the mouth is mandatory for acceptance.

4-112. Tensile Strength, Brass. Required tensile strength of walls of brass cartridge cases at the important sections are given in the specifications for manufacture of brass cartridge cases.

a. Head. At the head, the minimum tensile strength varies from 57,000 psi to 60,000 psi, depending upon the particular cartridge case.

b. Mouth. At the mouth, the maximum values range from 44,000 psi to 54,000 psi, depending on the particular cartridge case.

c. Shoulder. At the shoulder, the minimum values range from 47,000 psi to 50,000 psi.

d. Body. At the body, the minimum values range from 62,000 psi to 67,000 psi.

4-113. Stress-Relief Anneal, Steel Cases. The final taper draw gives the walls their "as drawn" hardness and sets up stresses in the steel that, if not relieved, may result in splitting or rupturing of the cases. These stresses are relieved by a stress-relieving anneal. The temperature of the anneal varies from 600° to 800°F, depending on the composition of the steel. Fortunately, the anneal raises the yield strength and, at the same time, increases the elongation slightly.

WRAPAROUND CARTRIDGE CASES

4-114. Wraparound Steel Cartridge Case. The wraparound process for forming a steel cartridge case has been studied along two lines, one a spiral wrap (not too satisfactory) and the other (more successful) a trapezoidal wrap. The spiral-wrapped design employs a strip of sheet steel wound helically around a mandrel. In the more successful design, a steel sheet in the shape of a trapezoid is wrapped around a mandrel and firmly pressed.

A double thickness of metal is usually provided at the neck and a triple thickness at the head. The end of the case toward the head is spun over and joined to the head (a separate piece).

The wraparound design is to be preferred for cartridge cases that have a relatively small shoulder taper, that is, whose body diameter is not much greater than the mouth diameter.

4-115. Trapezoidal-Wrapped Steel Case. This type of case has several advantages over the

Table 4-28

Hardness requirements, steel cartridge cases

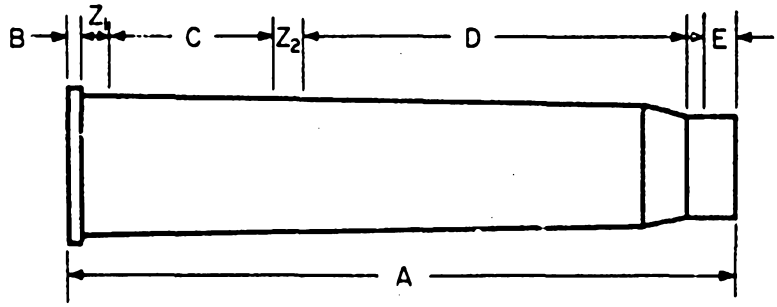

Cartridge case	Dimension		Rockwell hardness
75mm T6B1	A	21.30 in. max.	
	B	0.05 in. approx.	B-92 min.
	C	3.5 in. approx.	C-35 to C-42
	D	16 in. approx.	B-95 to B-102
	E	1 in. approx.	B-78 max.
	Z_1*	3/8 in. max.	
	Z_2*	1/4 in. max.	
76mm T19E1B1	A	22.830 max.	
	B	0.40 in. approx.	B-92 min.
	C	4.5 in. approx.	C-35 to C-42
	D	13 in. approx.	B-95 to B-102
	E	1.3 in. approx.	B-85 max.
	Z_1*	0.125 in. max.	
	Z_2*	0.25 in. plus 0.25 in.	
90mm T24B1	A	23.30 in. max.	
	B	0.40 in. approx.	B-95 min.
	C	6 in. approx.	C-36 to C-44
	D	15 in. approx.	B-95 to B-102
	E	1.2 in. approx.	B-85 max.
	Z_1*	0.125 in. max.	
	Z_2*	0.25 in. plus 0.25 in.	

*Z_1 and Z_2 represent transition zone.

drawn case: it may be made by using commercial materials; no large-capacity presses are required; and the body may be formed by conventional pyramid rolls available in commercial sheet-metal shops. Extraction difficulties and obturation difficulties are minimized.

The body may be rolled from 1010 to 1020 steels with a Rockwell B hardness of 65 to 80. Softer steels also have been found to perform satisfactorily. The minimum percentage elongation required is 8 percent, but 15 percent is ordinarily specified. The base may be forged from steels having a yield stress as low as 30,000 psi, with 35,000 psi the recommended minimum. Free-machining steels have also been used successfully for manufacture of bases.

Rigid specifications have not been found necessary. All physicals are advisory, and all dimensions other than those directly affecting fit or interchangeability are advisory. For the most part, functional tests can be relied upon to indicate the acceptability of these cases.

The interior edges of the sheets are ordinarily chamfered so that an extremely sharp bend is not formed where the sheet overlaps. In order to prevent the overlap at the mouth from causing eccentricity of the projectile in the case, the upper edges of the trapezoid, which form the mouth, are scarfed where overlap takes place. Additional information on this type of case may be found in Section 6.

4-116. Characteristics of Present Cartridge Case and Chamber Designs. Table 4-29 and figures 4-31 to 4-47 are taken from a Franklin Institute report.[1] The portion of the report from which this material was abstracted was an attempt to extrapolate the dimensions of existing cartridge cases to obtain advisory dimensions for future designs.

Flange diameter, case diameter at the breech, outside diameter at the neck of the case, length of the case, maximum thickness at the base of the case, thickness of the base flange, wall thickness of the case near the base, wall thickness of the case at start of forward slope, thickness of the case at throat diameter, outside diameter at the start of forward slope, volume of the case, length of chamber slope, length of forward slope, length of the case neck, length of the base reinforcement, curve of chamber slope, and curve of forward slope were plotted separately against the caliber of the projectile for each of the current designs. In each instance, a straight line or curve was fitted to the data by eye. Where a large amount of dispersion was present in the data, the slopes were drawn in such a manner as to favor the conservative values. The equations of these curves were then determined, and the suggestion was made that future designs could be based on these equations.

It is felt by both Picatinny Arsenal and Frankford Arsenal that these equations may have some value in indicating trends. Inspection of many of the curves, however, reveals that the dispersion of the data is so great as to preclude reasonable extrapolation. In several cases, correlations have been drawn between projectile diameter and design parameters that can have no real relationship to the size of the projectile. One example of this is the volume curve of the case versus the projectile diameter. The volume of the case is determined by the internal ballistician, and is obtained from a consideration of the type of propellant to be used, the allowable pressure in the gun, and the required muzzle velocity. Given a series of guns with similar muzzle velocities, some correlation with projectile diameter might be expected, and actually was obtained in this case. It will be noted, however, that the greatest deviation from the mean takes place for the three howitzers that have the lower muzzle velocities.

REFERENCES AND BIBLIOGRAPHY

1. Cartridge Case and Chamber Design, Report No. 307 Part II, Franklin Institute.

2. Notes on the Design of Solid Drawn Q.F. Cartridge Cases, Technical Report No. R5030-48, Armaments Design Department, Ministry of Supply, Fort Halstead, Kent, December 1946.

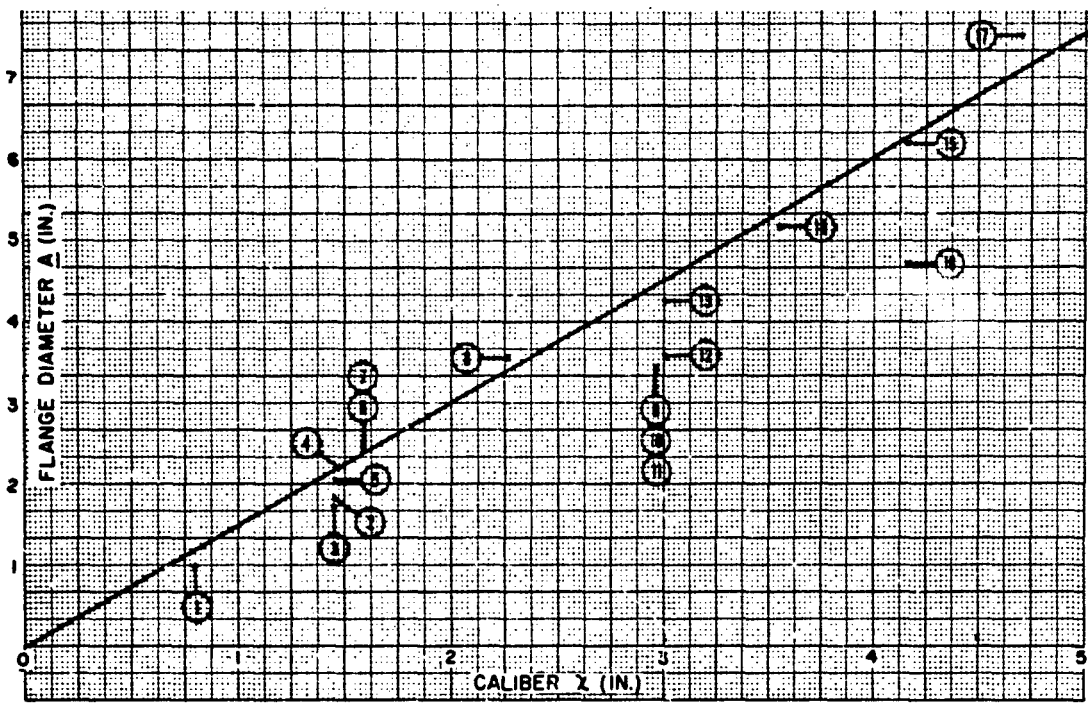

Figure 4-31. Flange diameter

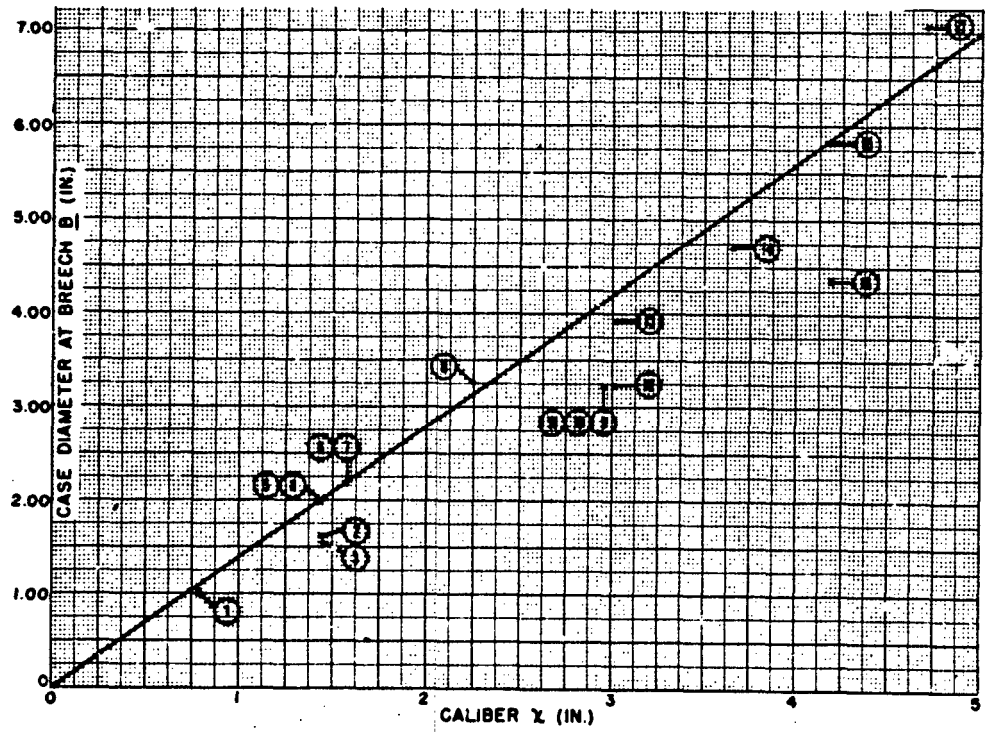

Figure 4-32. Case diameter

BLANK PAGE

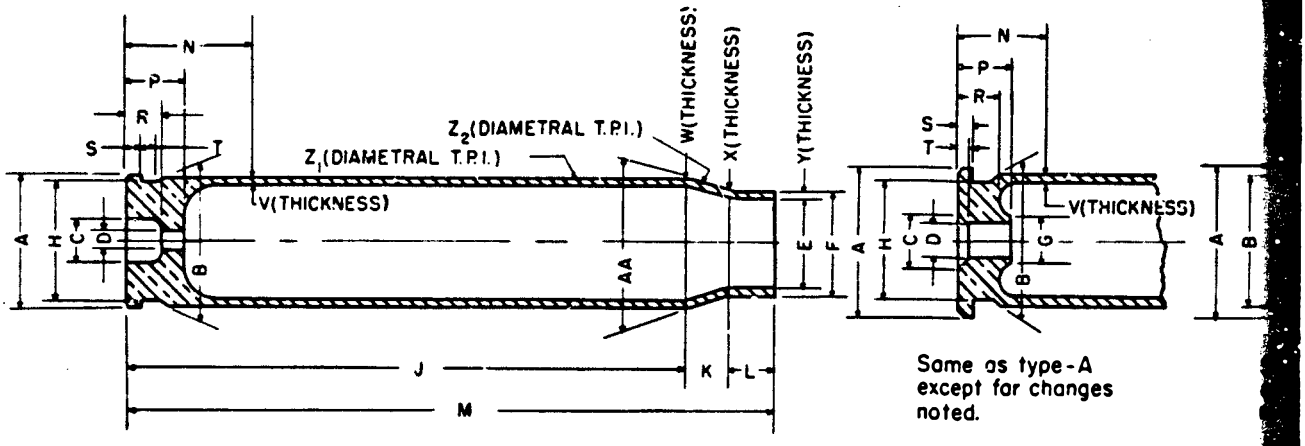

Case Type-A

Same as type-A except for changes noted.

Type-B

NO	CALIBER	Case & Chamber	Type Case	A	B	C	D	E	F	G	H	J	K	L	M	N	P
1	20MM, M21A1	71-2-119	A	.976	.990	.328	.135	.766	.816	–	.886	3.732	.250	.360	4.342	.846	.375
2	37MM, MARK 3 A2 AND MARK 3 A2B1	71-2-48	C	1.775	1.60	.630	.549	1.430	1.470	.670	–	4.352	.430	.908	5.69	.770	.320
3	37MM, MARK 1 A2 AND MARK 1 A2B1	71-2-73	C	1.735	1.565	.630	.549	1.430	1.470	.670	–	2.922	.120	.598	3.640	.600	.320
4	37MM, M16 & M16B1	71-2-96	C	2.190	1.970	.630	.549	1.430	1.490	.718	–	5.960	1.28	1.51	8.75	1.010	.390
5	37MM, M17 & M17B1	71-2-100	B	2.035	1.970	.630	.549	1.430	1.490	.718	1.870	5.960	1.28	1.51	8.75	1.010	.390
6	40MM, M2S	71-2-122	B	2.441	2.196	.630	.549	1.541	1.615	780	1.983	9.74	1.770	.730	12.24	1.378	.600
7	40MM, M2SB1	71-2-130	B	2.441	2.196	.630	.549	1.541	1.615	.750	2.008	9.74	1.770	.730	12.24	1.378	.750
8	57MM, M23A2	71-2-120	C	3.540	3.230	.630	.540	2.229	2.319	.787	–	14.20	1.950	1.250	17.40	1.250	.490
9	75MM, M18 & M18B1	71-2-71	D	3.426	3.193	.630	.549	2.918	2.998	.787	3.237	11.504	.590	1.726	13.82	1.811	.490
10	75MM, M5A1, TYPE 1-2 HOWITZER	71-2-91	D	3.426	3.193	.630	.549	2.958 2.913	3.018 2.993	.787	3.237	7.259	.750	2.681	10.69	1.811	.490
11	75MM, M5A1B1, TYPE 1-2 HOWITZER	71-2-129	D	3.426	3.193	.630	.549	2.998 2.918	3.018 2.993	.787	3.237	7.259	.750	2.681	10.69	1.811	.490
12	76MM, M26 & M26B1	71-2-123	C	3.566	3.266	.630	.549	2.970	3.086	.787	–	20.11	–	1.186	21.30	1.750	.600
13	3 INCH, MARK 2M2	71-2-95	D	4.270	3.900	.630	.549	2.970	3.080	.820	4.020	20.27	1.000	1.810	23.08	1.780	.450
14	90MM, M19 & M19B1	71-2-112	D	5.150	4.700	.630	.549	3.534	3.654	1.000	4.850	17.97	3.50	2.23	23.70	2.200	.700
15	105MM, M6	71-2-97	D	6.25	5.80	.630	.549	4.115	4.235	.875	.595	24.37	3.75	2.25	30.37	2.51	.790
16	105MM, M14 & M14B1 HOWITZER	1-2-101	C	4.70	4.35	.630	.549	4.143	4.223	.650	–	12.29	–	1.35	14.64	1.77	.560
17	120MM, M24	71-2-113	D	7.55	7.05	.630	.549	5.434	5.546	1.10	7.20	17.60	12.17	3.03	32.8	2.55	.800
	DIMENSION FORMULA FOR APPARENT PRESENT STD.			A = 1.5 X	B = 1.4 X				F = 1.1 X			J = 5 X	K = .66 X	L = .64 X	M = 7 X	N-P = .38 X	P = 28+12 X
	FIGURE NO. 4 -			31	32				33			42	43	44	5	45	35

A.

Table 4-29
Characteristics of present cartridge case and chamber design

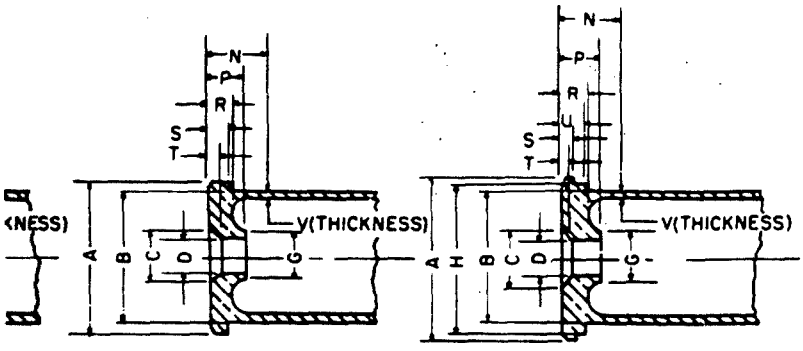

Same as type-A except for changes noted.

Type-C

Same as type-A except for changes noted.

Type-D

NOTES:
1- Taper computed on basic dimensions.
2- Max. and min. diameter of rotating band used in computing allowance. Rotating band assumed to strike chamber at crest of bevel.

N	P	R	S	T	U	V	W	X	Y	Z_1	Z_2	AA	Case Volume Cu. In.	Proj. Weight Pounds	Std. Muzzle Velocity	Dim.-A Max.	Dim.-A Min.	Taper-B Gun	Taper-B Case	Taper-B Taper
.846	.378	.233	.098	.118	-	.049	.034	.025	.025	.00878	.5359	.950	2.40	.28	2850			.00393	.00439	.00046
.770	.320	.160	.082	.079	-	.050	.023	.020	.020	.01148	.1884	1.551	9.30	1.52	2900	.0085	.005	.00642	.00571	.00063
.600	.320	.160	.082	.079	-	.050	.020	.020	.020	.00496	.6841	1.551	5.60	1.91	2050	.0105	.005	.00355	.00248	.00107
1.010	.390	.250	.100	.079	-	.055	.032	.030	.030	.00681	.3438	1.930	20.90	1.91	1276	.010	.015	.00341	.00341	-
1.010	.390	.250	.100	.079	-	.055	.032	.030	.030	.00681	.3438	1.930	20.2	1.34	1276	.010	.005	.00341	.00341	-
1.378	.600	.380	.240	.079	-	.067	.037	.037	.037	.03485	.1452	1.874	31.98	7.27 A.P.C.	2870			.01752	.01742	.0001
1.378	.750	.240	.240	.079	-	.070	.037	.037	.037	.03485	.1452	1.874	31.98	7.27 A.P.C.	2870			.01752	.01742	.0001
1.250	.490	.320	.200	.079	-	.070	.045	.045	.045	.03000	.2518	2.810	104.0	1.953 H.E.	2970			.01500	.01500	-
1.611	.490	.315	.115	.079	.229	.057	.040	.040	.040	.00975	.1449	3.083	94.2	12.44	1778	.014	.008	.00493	.00487	.00005
1.811	.490	.315	.115	.079	.229	.057	.040	.040	.040	.00967	.1427 .1760	3.125	97.56	18.76	705 1270	.014	.008	.00512	.00483	.00801
1.811	.490	.315	.115	.079	.229	.057	.040	040	.040	.00967	.1427 .1760	3.125	72.56	13.76	705 1270			.00512	.00483	.00801
1.750	.600	.380	.225	.079	-	.070	.058	-	.058	.00900	-	3.068	149.0	12.87	2800			.00395	.00450	.00055
1.780	.450	.320	.150	.079	.280	.080	.055	.055	.055	.02521	2.000 Radius	-	212.0	12.87	2800	.308	.072	.01239	.012605	.00021
2.200	.700	.390	.200	.079	.350	.130	.060	.060	.060	.01703	.2131	4.40	322.0	23.4	2700	.2095	.003	.00825	.008515	.00026
2.51	.790	.560	.300	.079	.450	.120	.060	.060	.060	.01672	.3107	5.40	638.0	32.77	2800	.0105	.003	.00806	.00836	.00029
1.77	.560	.360	.180	.079	-	.090	.040	-	.040	.00968	-	4.223	191.0	33.00	650	.0105	.003	.00450	.00484	.00033
2.55	.800	.550	.300	.079	.450	.100	.080	.056	.056	.01283	.1120	6.830	1014.5	69.53				.00612	.006415	.00029
N-P=.38X	F=.28+.12X		S=.05+.06X			V=.018X+.03	W=.12X+.10		Y=.0126X +.015	Z_1=.0038X	$Z_2=\frac{48+X}{X}$	AA=1.3X	VOL=2X³							
45	35		36			37	38		39	46	47	40	41							

B.

on basic dimensions.
meter of rotating
mputing allowance.
sumed to strike
of bevel.

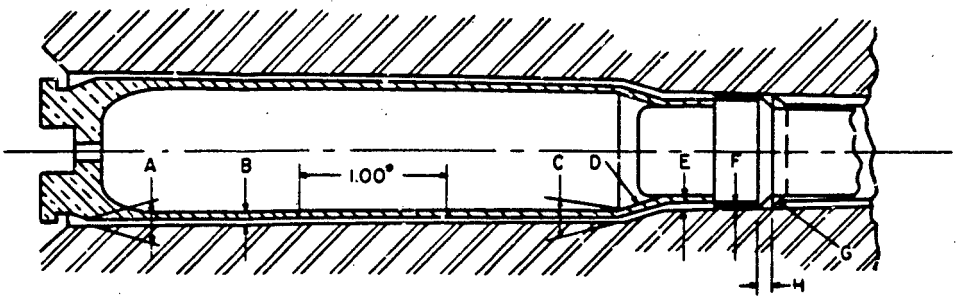

le ity	Dim.-A		Taper-B			Dim.-C		Taper-D			Dim.-E		Dim.-F		Taper-G		Travel-H	
	Max.	Min.	Gun	Case	Taper	Max.	Min.	Gun	Case	$\Delta\beta$	Max.	Min.	Max.	Min.	Gun	E.A.I.	Max.	Min.
)			.00393	.00439	.00046				.26795		.018	.009	.013	.006	.08393			
)	.0085	.005	.00642	.00571	.00063	.007	.002	.05235	.0942	.04185	.019	.011	.0115	.0075	.04206		.261	.093
)	.0105	.005	.00355	.00248	.00107	.009	.002	.0924	.34205	.24965	.0225	.0115	.0125	.0065	.03615		.532	.290
)	.010	.015	.00341	.00341	-	.0125	.005	.16795	.1718	.00385	.015	.0045	.014	.003	.0757		.1375	.004
)	.010	.005	.00341	.00341	-	.0125	.005	16795	.1718	.00385	.115	.0045	.010	.0045	.0757		.1375	.000
)			.01752	.01742	.0001			.0689	.0726	.0037	.0178	.0075	.010	.001	.10325		.044	.024
)			.01752	.01742	.0001			.0689	.0726	.0037	.0178	.0075	.010	.001	.10325		.044	.024
)			.01500	.01500	-			.11975	.1259	.00615	.047	.027	.044	.031	.1515		.0602	.0472
)	.014	.008	.00493	.00487	.00005	.0138	.0075	.0662	.07245	.00635	.023	.006	.0095	.0045	.06835		.188	.0065
)	.014	.008	.00512	.00483	.00801	.0095	.0025	.0600	.07135 .0880	.01135 .0280	.033	.016	.0195	.0145	.0750		.172	.0075
)			.00512	.00483	.00801			.0600	.07135 .0880	.01135 .0280	.050 .075	.026 .051	.039	.029	.0750		.157	.013
)			.00395	.00450	.00055	-	-	-	-				.013	.022	.1000		.348	.298
)	.008	.002	.01229	.012605	.00021	.0105	.006				.0225	.005	.0065	.001	.1000		.136	.004
)	.0095	.003	.00825	.008515	.00026	.014	.0075	.10545	.10605	.0006	.0245	.010	.022	.017	.1340		.111	.0168
)	.0105	.003	.00806	.00836	.00029	.0175	.010	.02027	.022	.00173	.0245	.010	.017	.012	.1675		.170	.042
)	.0105	.003	.00450	.00484	.00033	-	-	-	-		.028	.0135	.011	.006	.12625		.125	.013
			.00612	.006415	.00029			.05612	.05600	.00012					.0666			

c.

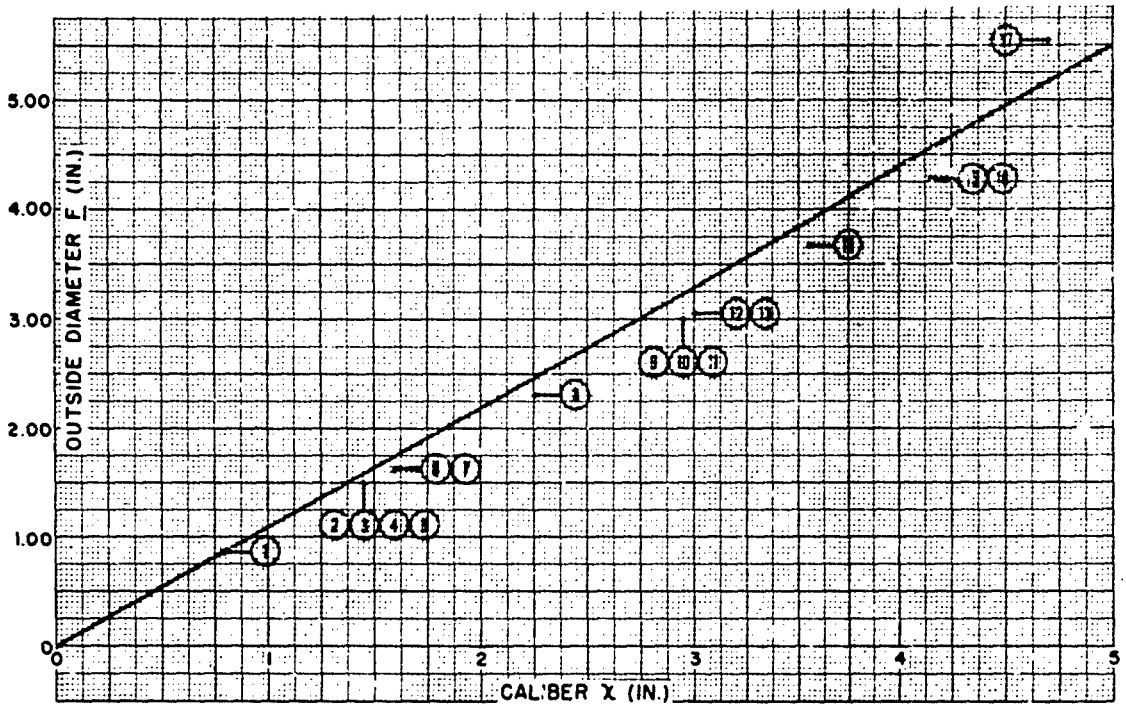

Figure 4-33. Outside diameter

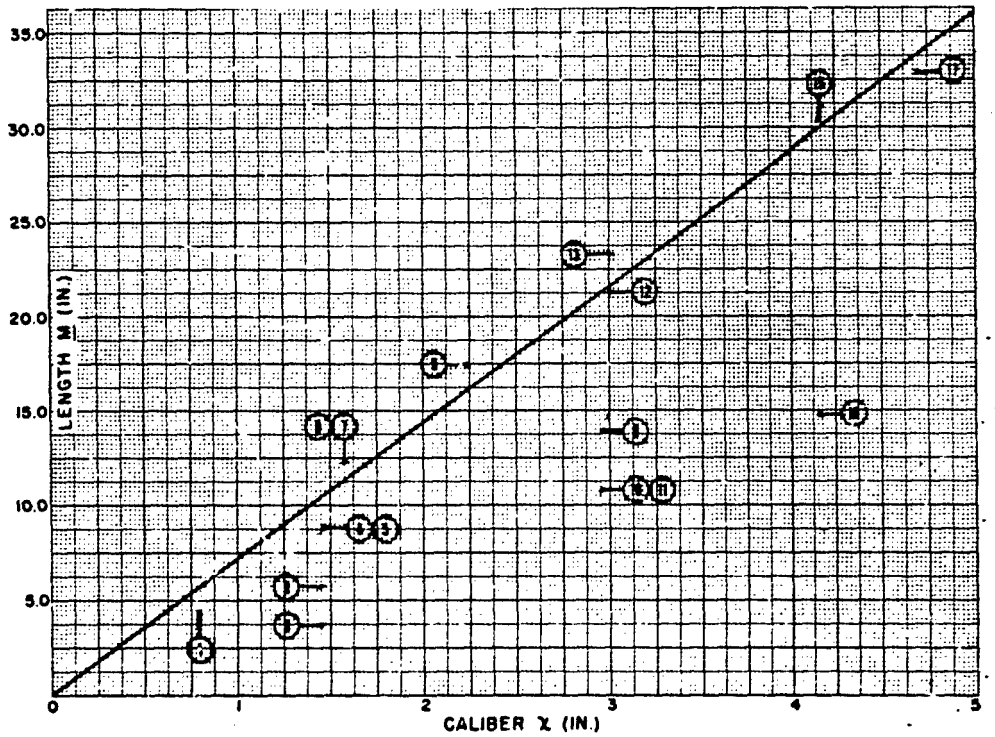

Figure 4-34. Length of case

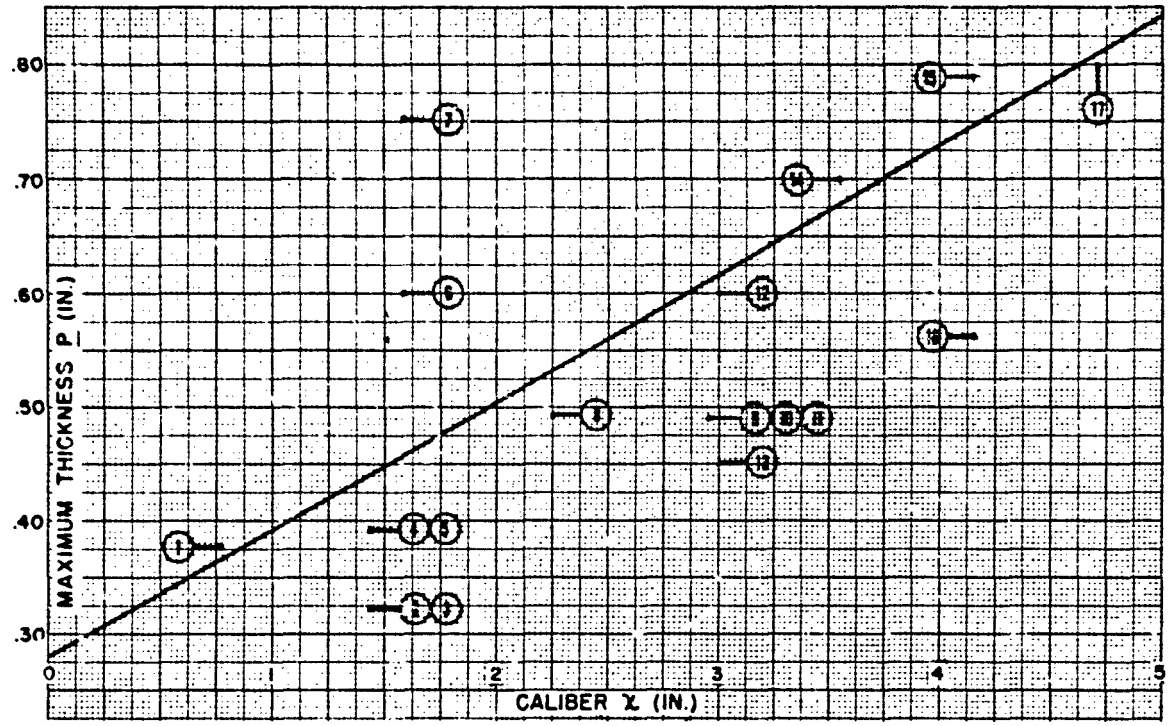

Figure 4-35. Thickness of base of case

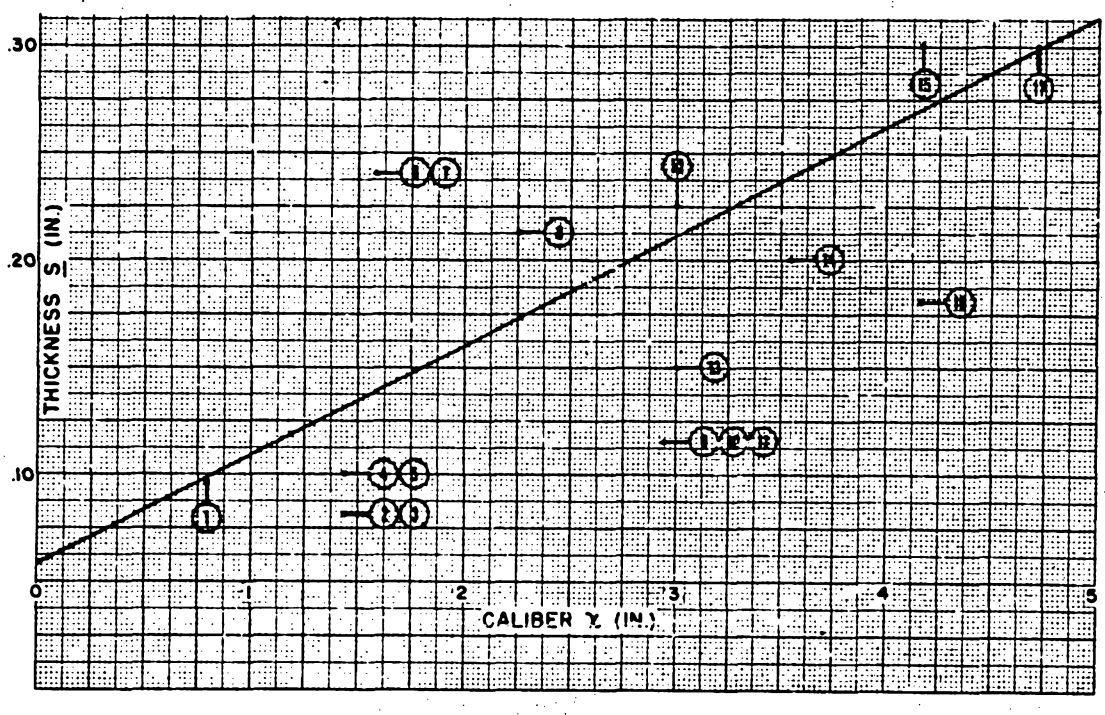

Figure 4-36. Thickness of base flange

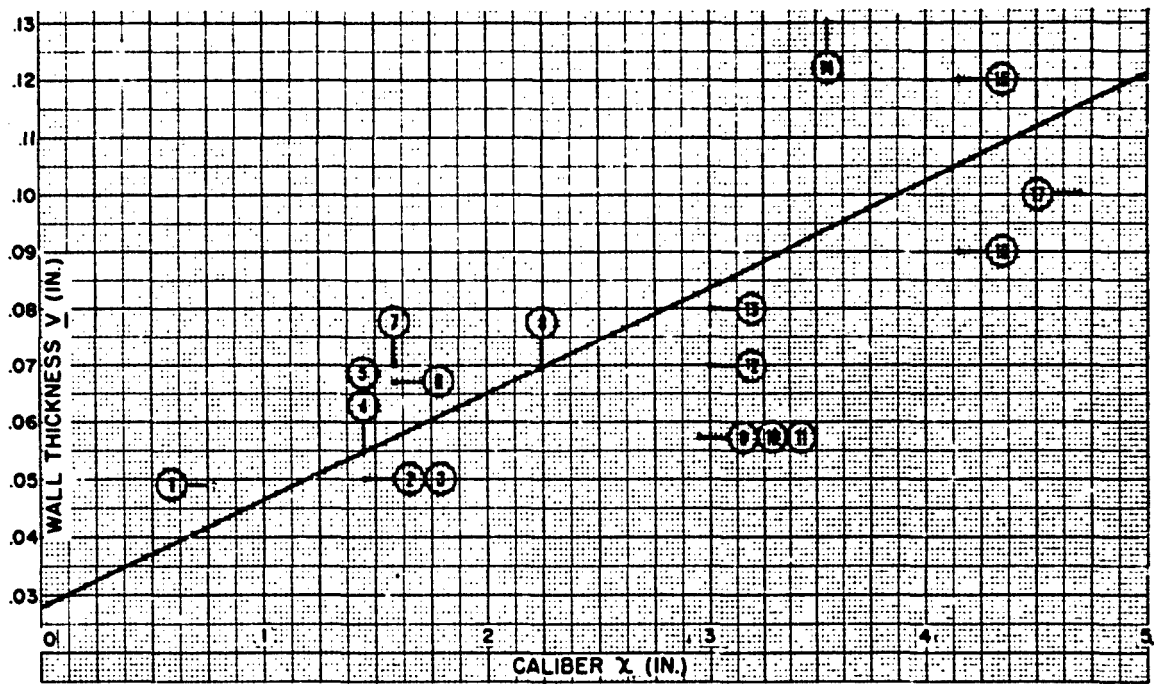

Figure 4-37. Thickness of case near base

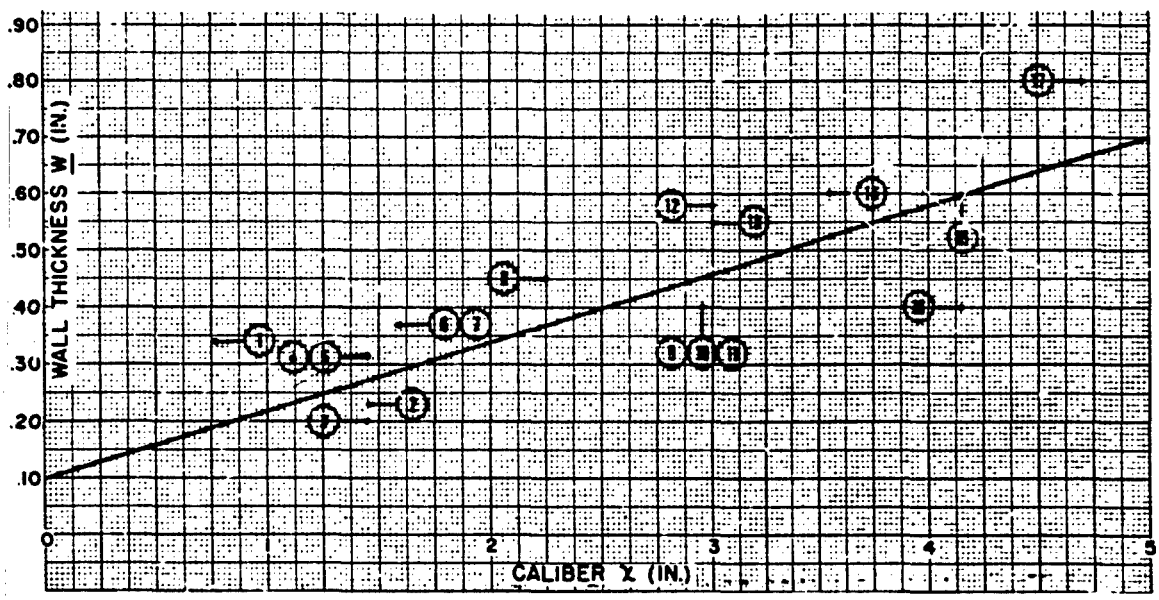

Figure 4-38. Wall thickness at start of forward slope

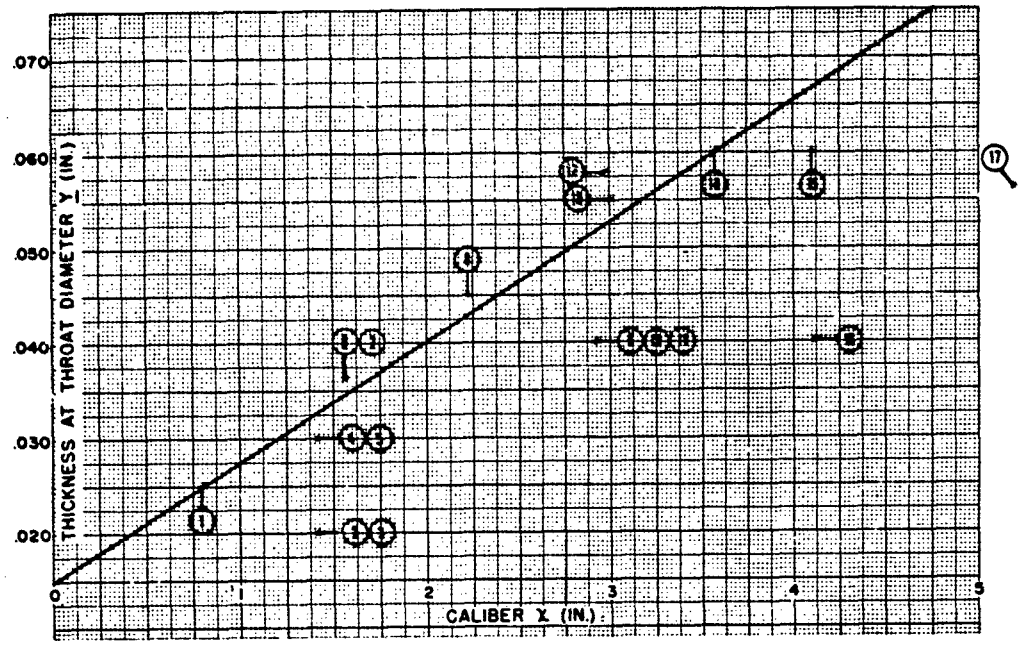

Figure 4-39. Throat diameter of case

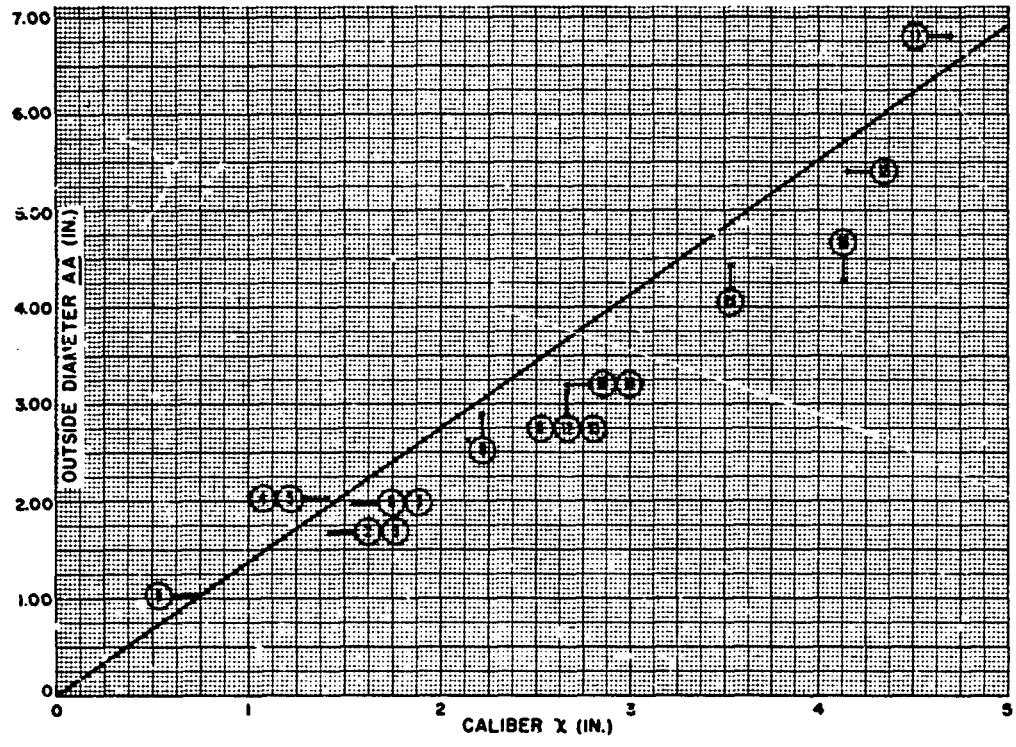

Figure 4-40. Outside diameter at start of forward slope

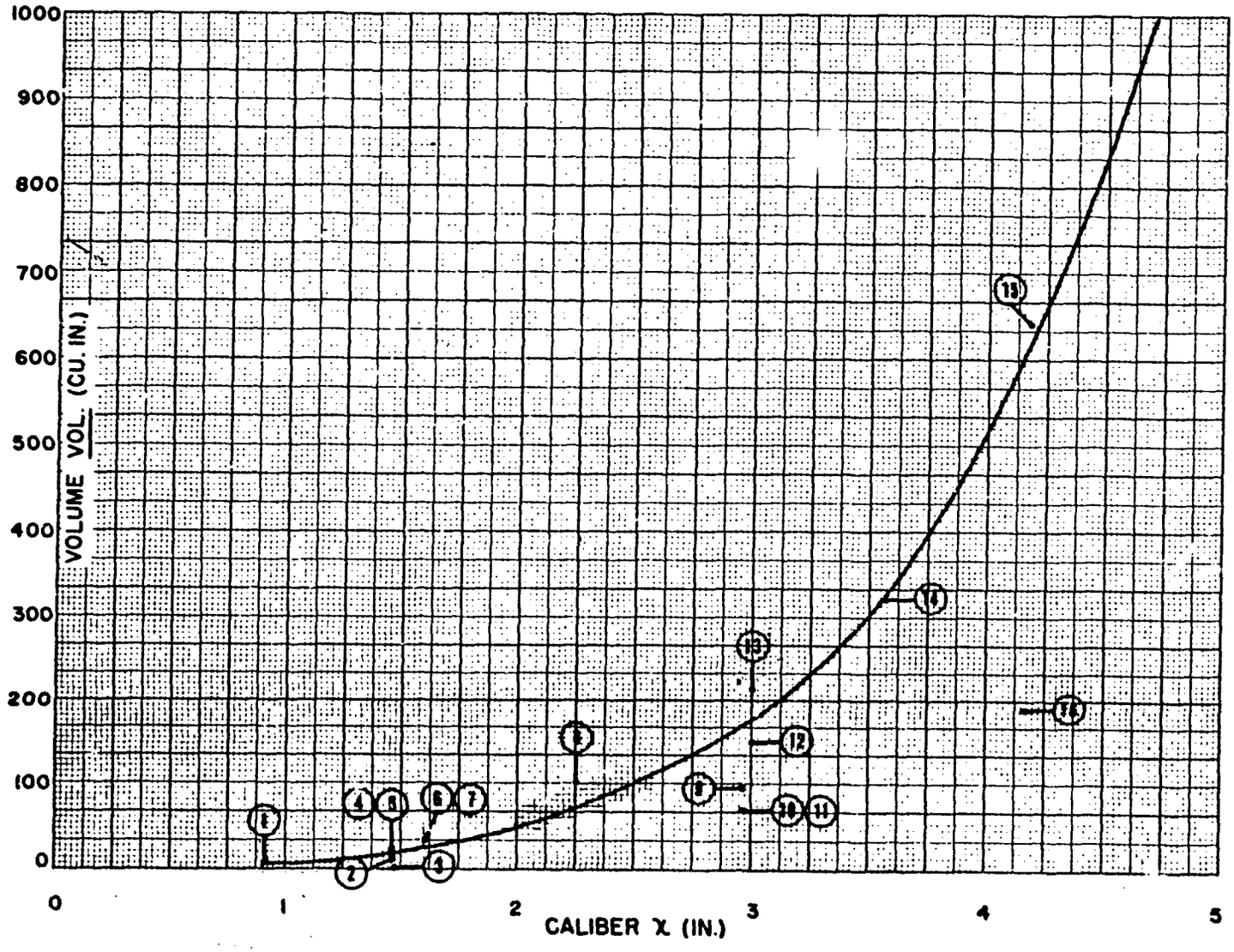

Figure 4-41. Volume of case

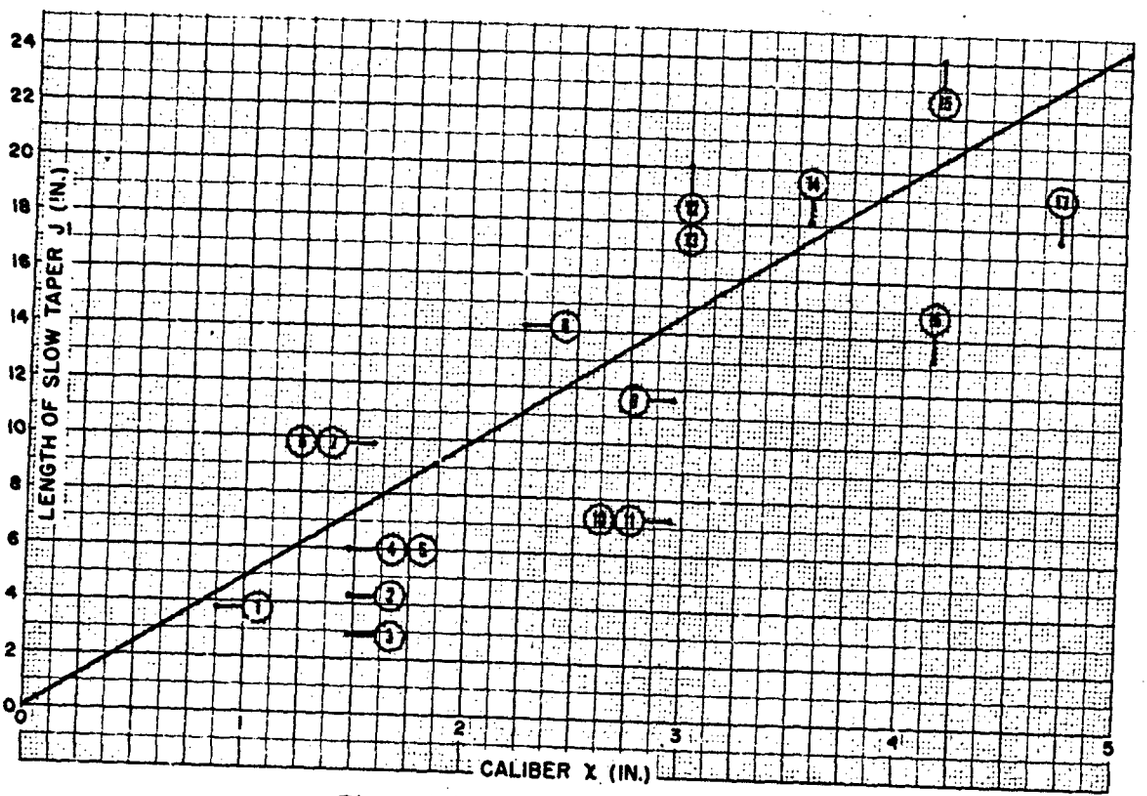

Figure 4-42. Length of chamber slope

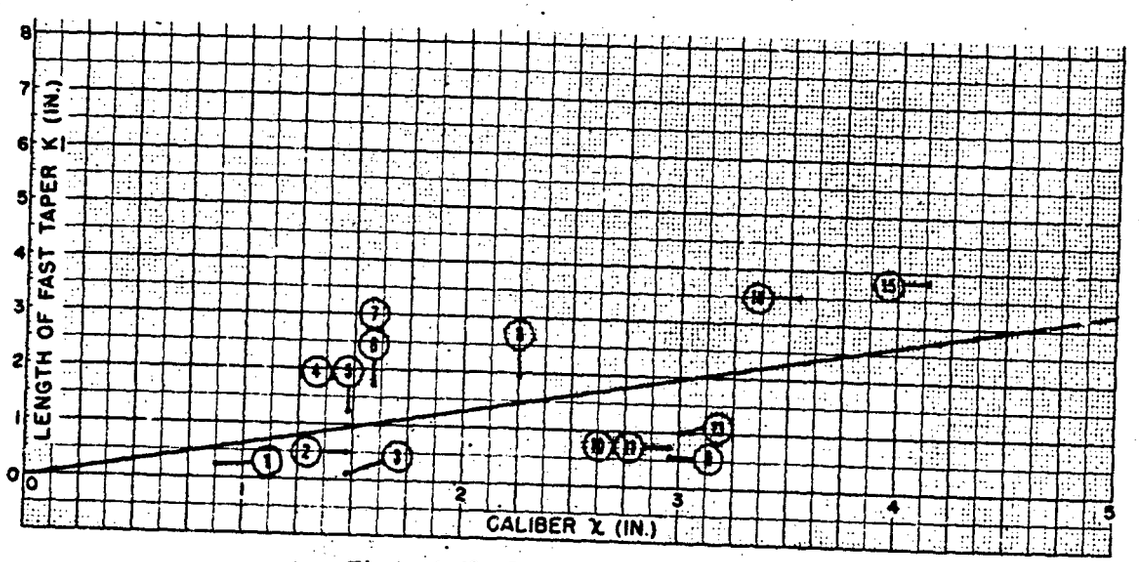

Figure 4-43. Length of forward slope

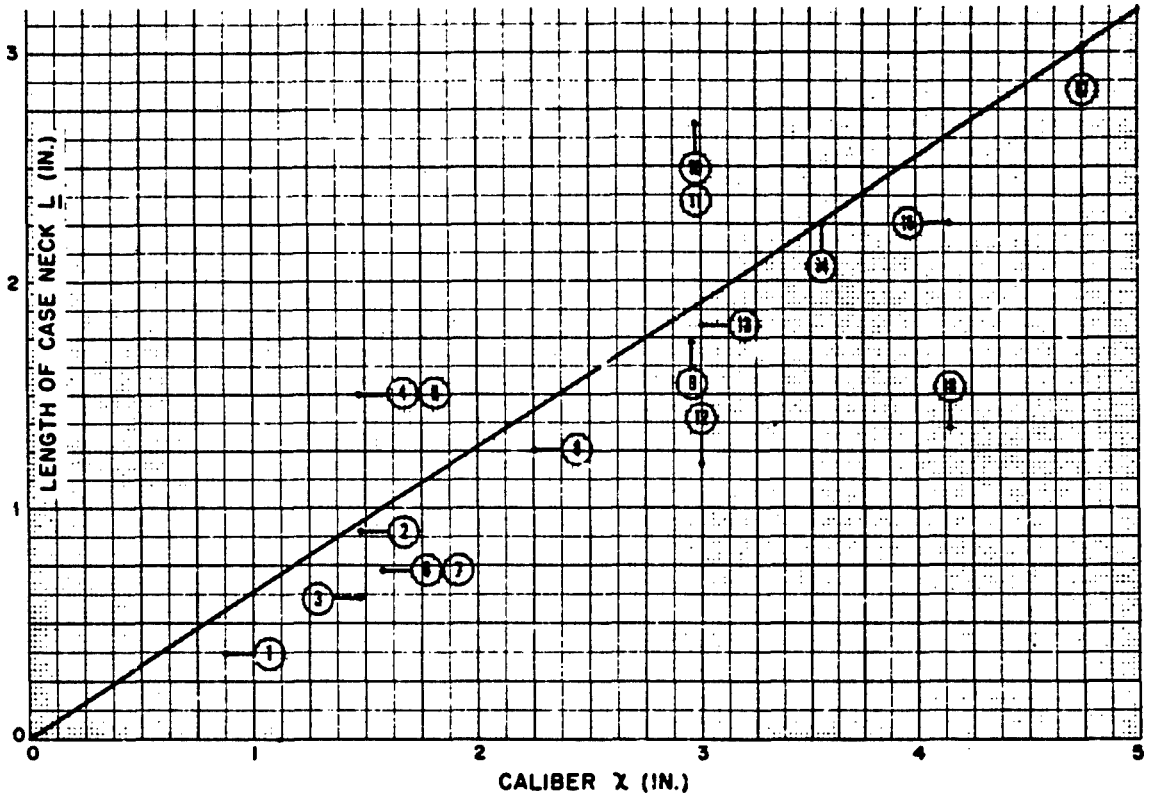

Figure 4-44. Length of case neck

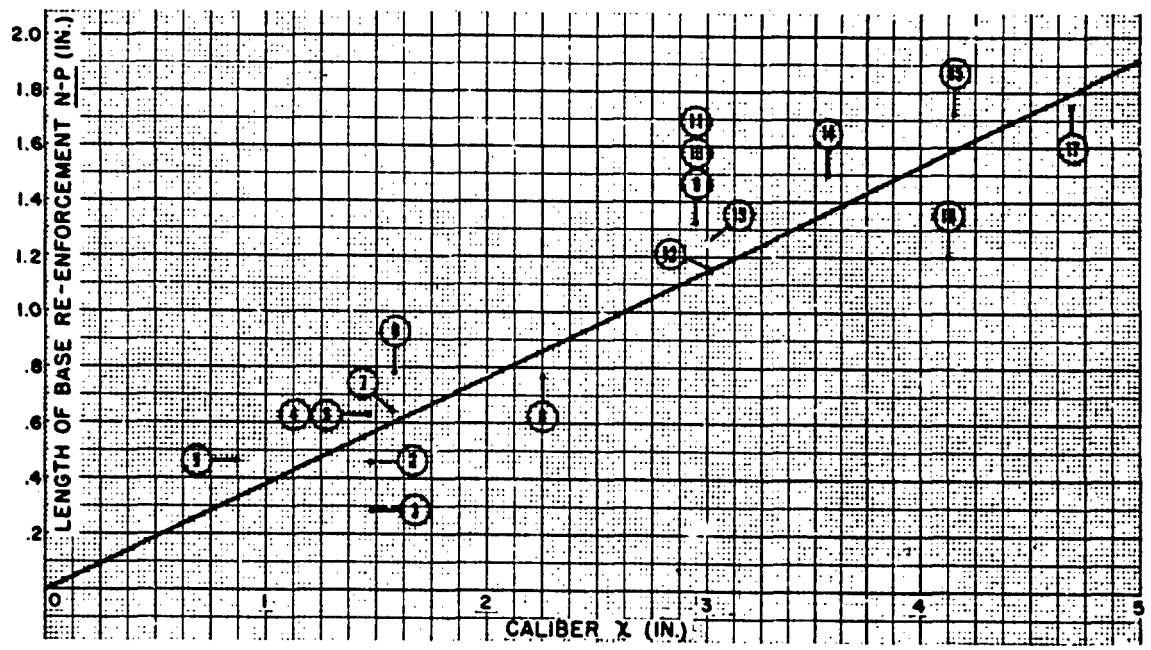

Figure 4-45. Length of base reinforcement

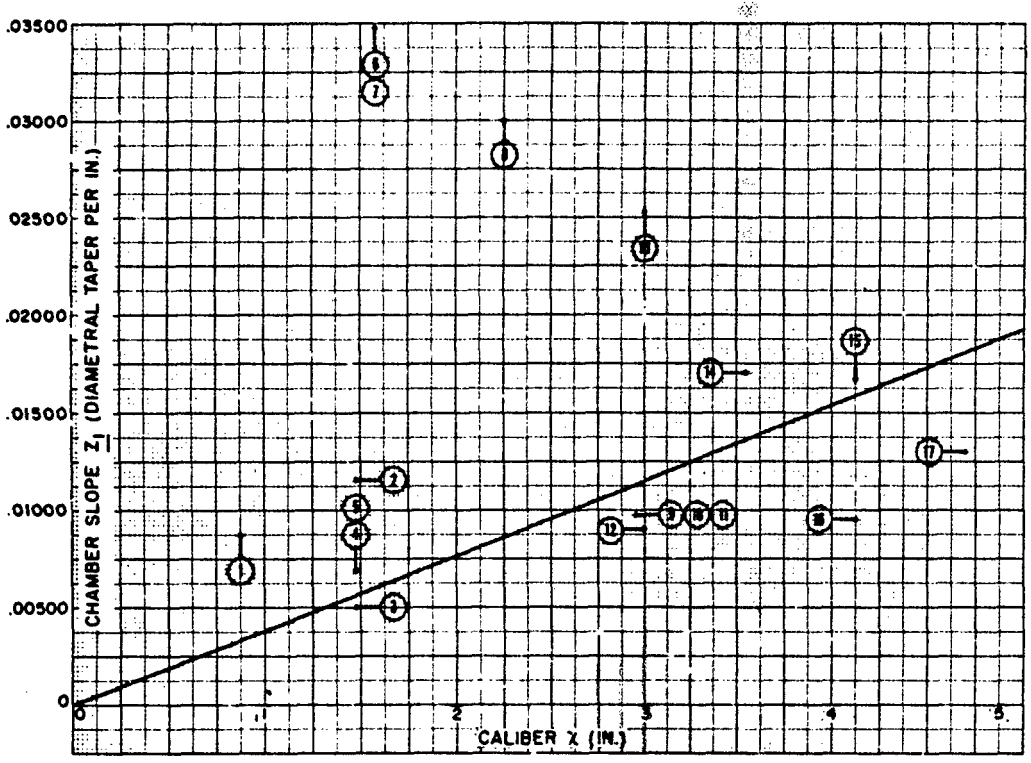

Figure 4-46. Curve of chamber slope

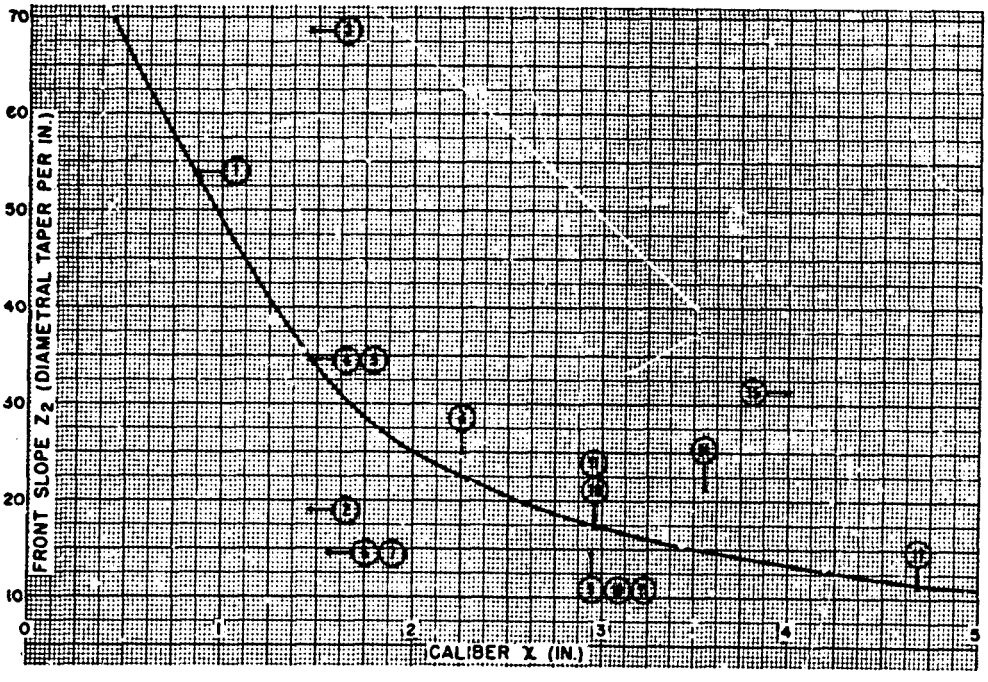

Figure 4-47. Curve of forward slope

ROTATING BAND DESIGN

4-117. Rotating Band. The rotating band is a ring of easily engraved material, whose primary purpose is to engage the rifling in the gun tube in order to impart spin to the projectile. Materials used for rotating bands include gilding metal, copper, sintered iron, soft (Armco) iron, nylon, and other plastics. Rotating bands either may be pressed into a seat machined in the shell body or, in the case of the welded overlay type of band, they may be welded or brazed to the body. When the band is pressed on, the seat is knurled or machined with wavy grooves to prevent the band from slipping on the body. The seat may be straight-sided or undercut. The undercut assists in preventing the band from flying off when subjected to the centrifugal stresses induced after the projectile leaves the gun. The use of the welded overlay band obviates the need for concern with either fly-off or slipping of the band.

4-118. Function of Rotating Band. In addition to its primary function of imparting spin to the projectile, the rotating band is also required (1) to provide obturation; (2) to center the projectile in the bore in order to limit yaw of the projectile inside the gun (initial yaw of the projectile as it leaves the muzzle is a function of the yaw inside the gun); (3) in the case of separate-loading ammunition, to hold the projectile in the rammed position when the gun is elevated; (4) to provide a uniform initial (shot start) pressure at which the projectile will begin its travel through the tube. This characteristic enables consistent performance of the propelling charge to be obtained. A successful rotating band will perform all of these functions adequately in either a new or a worn gun tube.

4-119. Other Methods of Imparting Rotation. In some special types of ammunition, use has been made of canted fins or jets to provide spin in lieu of the rotating band and rifling.

4-120. Properties Required of Materials Used in Rotating Bands.

a. The material must have a yield stress sufficiently low to permit it to be engraved easily by the rifling and yet high enough to prevent fly-off. Ideally, this would require an anisotropic material. An anisotropic rotating-band material should have a low yield strength in the radial direction and a high yield strength in the tangential if the band is long, in the axial direction if the band is short, or in both axial and tangential directions if the band is of intermediate length.

b. It must be soft enough to obturate effectively without wearing the gun tube excessively; at the same time, it must not be so soft that particles will adhere to the rifling and cause excessive metal fouling.

c. The material should not be subject to age-hardening, nor should its properties be greatly affected by changes in temperature.

4-121. Rotating Band Design. After selection of the material, the design of a rotating band may be broken down into the following procedures.

1. Determination of band outside diameter.
2. Determination of band inside diameter
3. Determination of equivalent width of band
4. Determination of profile of rotating bands, including cannelures and front and rear chamfers, and true width
5. Check the design for a possibility of fly-off under centrifugal stresses, which may dictate the necessity for an undercut band seat, or the use of welded overlay
6. Determine location of the rotating band with respect to the base of the projectile.

4-122. Band Outside Diameter. Experience seems to indicate that a good seal is provided if the diameter of the band is made 0.02 inch greater than the diameter of the grooves. However, recent experiments indicate that the high radial band pressure (paragraph 4-126) that may be induced as a result of excessive positive interference between band and groove diameter tends to cause rapid wear of the rifling.

During engagement of the band with the rifling, some elastic deformation occurs in the radial, tangential, and axial directions. A properly de-

signed band would utilize the elastic deformation to provide continuously a new band surface to replace the one that wears away. Thus, if one could predict the amount of wear that will occur, the amount of elastic deformation that will exist in the band, and the axial flow of the band material, then it would be possible to design a band that would obturate perfectly.

These factors, however, defy theoretical prediction at present. In the absence of the ideal solution, Watertown Arsenal suggests that best results might be achieved by designing the band so that the volume of the material in the unengraved band is just sufficient to flow into and completely fill the rifling grooves after engraving. Such practice could result in poor obturation, and the Watertown Arsenal further suggests that a short sealing lip, with a diameter greater than that of the rifling-groove diameter, be included in the band to provide the necessary obturation.

Another practice that shows considerable promise is the use of expanding cups attached to the base of the projectile. These cups, which may be made of metal, rubber, or plastics, expand into the rifling under the pressure of the propellant gases and provide effective obturation. They may be used either as a supplement to the rotating band, in which case the cup provides obturation and the band provides spin, or as a substitute for the rotating band, in which case the cup must perform both functions. This type of rubber cup has been applied experimentally to several models of canister round (see paragraphs 2-266 through 2-278) and has been found very effective.

4-123. Determination of Band-Seat Diameter. Past practice indicates that the depth of the band seat should always be greater than the height of the band above the body or, if present, the rear bourrelet of the projectile. Table 4-30 lists these dimensions for several representative projectiles.

Plasticity theory indicates that the minimum thickness of band material below the lands should be no less than $0.354W_\ell$, where W_ℓ is the width of the land. This will ensure that the engraving pressure, before the grooves are filled, will be no greater than $1/2(2+\pi)K$, where K is the yield strength, in pure shear, of the band material. As the thickness of band material decreases below the given value, the radial band pressure (paragraph 4-126) rises very rapidly, even before the grooves have filled.

4-124. Determination of Effective Width of Band. The effective width of the rotating band is defined as the bearing area of the band divided by the average bearing height. The width selected must be sufficient to ensure that (1) the band will not wear excessively during its travel through the bore of the gun, (2) the band will not fail in shear, and (3) the band will not fail in bearing.

The following procedure is suggested:

1. Determine the effective band width on the basis of the British wear factor (paragraph 4-125).
2. Determine the radial band pressure for this width (paragraph 4-126).
3. Using the radial band pressure and the width determined above, compute the force on the driving edge of the band (paragraph 4-128).
4. From the driving edge force and the band and rifling geometry, determine the bearing stress (paragraph 4-129) and the shear stress (paragraph 4-130). If these stresses are below the yield strengths in bearing and in shear of the material, the width is great enough; if these stresses are above the appropriate yield strengths, choose a greater band width and repeat steps 2 through 4.
5. Using the radial band pressure determined for the final band, check to be sure that excessive stresses are not developed in the shell wall or the gun tube.

4-125. British Wear Factor. The British wear factor method for computing band width assumes that wear of the rotating band is proportional to the rotational muzzle energy of the projectile.[1] It is a wholly empirical method and requires a value for the wear factor that has been previously computed for a rotating band for use in a weapon similar to that under design. The wear factor (F_w) is defined as

$$F_w = \frac{E}{Nhb\ell}$$

where

- E = rotational muzzle energy of the projectile, ft-tons
- N = number of lands
- h = groove depth
- b = groove width
- ℓ = effective width of band.

Table 4-30

Rotating band characteristics

Caliber	Projectile	Shape of band	Width of band width tol.	Diameter of band	Diameter of body	Diameter of band seat	Width of band seat	Cannelure	Dist. to base
37-mm	M51		0.74 -0.02	1.507 -0.006	1.441 -0.008	1.320 -0.008	0.72 +0.02	none	0.58 +0.02
40-mm	Mk 2		0.345 -0.02	1.630 -0.004	1.547 -0.005	1.45 -0.01	0.342 +0.02	1	0.618 +0.015 (to nose)
75-mm	M48		0.49 -0.02	3.011 -0.006	2.933 -0.015	2.75 -0.02	0.47 +0.02	none	2.26 -0.03
76-mm	APC M62A1		1.02 -0.02	3.098 -0.006	2.980 -0.01	2.76 -0.02	1.00 +0.02	2	0.79 -0.02
90-mm	M71		1.20 -0.02	3.64 -0.006	3.520 -0 015	3.28 -0.02	1.18 +0.02	2	2.65 -0.03
105-mm	M1		0.81 -0.02	4.223 -0.006	4.10 -0.02	3.94 -0.02	0.79 +0.02	none	3.08 -0.03
120-mm	M73	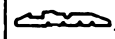	2.25 -0.04	4.980 -0.006	4.67 -0.02	4.49 -0.02	2.29 +0.04	2	3.53 +0.02
155-mm	M101		2.02 -0.04	6.320 -0.008	6.07 -0.02	5.80 -0.02	1.98 +0.04	1	3.48 -0.03
8-in.	M106		2.02 -0.04	8.254 -0.008	7.98 -0.02	7.53 -0.02	1.98 +0.04	3	6.06 -0.06
240-mm	M114	...	2.52 -0.04	9.820 -0.008	9.39 -0.02	9.00 -0.02	2.48 +0.04	...	6.64 -0.06

$$E = \frac{\ell}{2{,}000} Mk^2 \left(\frac{\pi}{n}\right)^2 \left(\frac{V}{d}\right)^2$$

where

- n = twist of the rifling, calibers per turn
- V = muzzle velocity of the projectile, ft per sec
- d = caliber of the projectile, ft
- M = mass of the projectile, lbs
- k = radius of gyration of the projectile, ft (The approximations of paragraph 4-128 may be used to determine k^2; the value of d used must be in feet.)

For most guns, the wear factor should be kept in the range of 20 to 25 ft-tons per cu. in.; for howitzers, it may be as high as 30. These values are for gilding metal. Values for other materials are not available at this time.

4-126. Theoretical Prediction of Radial Band Pressure. An approximate theoretical estimate of the radial band pressure at the instant of complete engraving has been made by Watertown Arsenal.[1]

Case I: Interference Ratio (IR) < 0 (that is, incomplete obturation after engraving)

$$\frac{P_b}{Y} = \left[\frac{2}{\sqrt{3}}\left(1 + \frac{\pi}{2}\right)\right]\left[\frac{W_L}{W_L + W_G}\right]\left[1 - \frac{IR}{(IR)_o}\right]$$

where

P_b = radial band pressure (averaged over the lands and grooves of the rifling)

Y = yield stress of the band material (refer to "Discussion of Equations" following)

IR = interference ratio

$$= \frac{\text{band dia. before engraving - aver. bore dia.}}{\text{average bore diameter}}$$

$$(IR)_o = \frac{\text{rifling diameter - average bore dia.}}{\text{average bore diameter}}$$

(The rifling diameter is measured from groove to groove of the gun. The average bore diameter may be obtained by dividing the entire bore area — including grooves — by $\pi/4$ and taking the square root of the result.)

W_L = land width

W_G = groove width.

The formula was arrived at from the following considerations: the first bracketed factor corresponds to the indentation pressure on the tops of the lands, assuming the rifling is a rigid material pressing into an ideal plastic (rotating band) material.[2] The second bracketed factor averages the pressure acting on the lands over the entire bore surface. The final bracketed term is inserted to compensate for the flexibility of the gun tube and shell wall and incomplete bottoming of the band. It is assumed that the band pressure is linear with respect to IR up until the time of complete obturation.

Case II: Interference Ratio (IR) ≥ 0 (that is, complete obturation)

$$\frac{P_b}{Y} = \left[\frac{2}{\sqrt{3}}\left(1 + \frac{\pi}{2}\right)\frac{W_L}{W_L + W_G}\right] + \frac{L}{2\sqrt{3}\,t}$$

where

L = final band width = the width of the band, with an IR of zero, having the same volume of band material as the original band. For instance, "L" can be readily derived if one considers the projectile to be completely pushed through a smooth-bore cylinder having the same inside cross-sectional area at the rifled tube. As a result, the band material will flow to the rear, increasing its length. The new length is defined as "L."

t = band thickness = average band diameter after engraving, minus band-seat diameter, all divided by two.

For complete obturation, the band pressure is assumed to be due to the pressure required to fill the grooves, plus additional pressure causing the backward flow of the excess band material. The bracketed portion of the formula represents the first effect (see case I) and the additional term corresponds to the average pressure exerted by two rigid plates squeezing an ideal plastic material.[3]

Discussion of Equations

a. Since these equations are derived for an ideal plastic material, they do not take into account the effects of strain-hardening. In other words, they are applicable to a material that has a flow stress which, at any portion of the plastic deformation region of the true stress-strain curve, is equal to the yield stress. Engineering materials do not behave in this manner. The strain-hardening effect causes the flow stress, which may be defined as that stress at which plastic flow will take place, to increase with increase in strain. If the yield stress for a nonideal material is used in these equations, the band pressure obtained will err on the low side. This effect may be compensated for by choosing as the yield stress the value of the flow stress for the average strain under the land. The strain may be computed from consideration of the band and rifling geometry. It is equal to the band outside diameter minus the rifling land diameter, all divided by the band diameter minus the band seat diameter. The flow stress may then be found by reference to the true stress-strain curve in compression.

b. These formulas should be used with caution until sufficient experimental evidence attests to their validity. Several factors, such as

strain-hardening, strain rate effect, temperature, and effect of gas pressure, have not been taken into account in these approximations. In particular, though the formula for band pressure for IR < 0 was based upon the best information available at the time, current investigations would appear to indicate that the last bracketed term should be taken as unity.

c. These equations apply to an uncannelured band. Recent investigations indicate that band pressures may be considerably reduced by the use of cannelures.[4] In effect, if the cannelure is sufficiently wide, so that it will not fill up during engraving, the results obtained will be equivalent to those that could be expected if the band were actually made as several smaller bands, rather than merely being divided by the cannelures.

4-127. Driving Face Force — No Friction. The force on the driving face of each land of the engraved rifling may be closely approximated for a tube with uniform twist rifling by the following expression.[1] This equation does not take into account the effect of friction between the rotating band and the rifling as the projectile passes through the gun. It is, however, quite satisfactory for the range of accuracy presently required in rotating band design.

$$R = \frac{\pi^2 k^2}{nN} p$$

where

R = driving face force
k = radius of gyration of the projectile about its longitudinal axis
n = rifling twist, calibers per turn
N = number of lands.

The following approximate values of k^2 may be used.

For HVAP projectiles, $k^2 = 0.100d^2$
For AP shot, $k^2 = 0.115d^2$
For HE shell, $k^2 = 0.140d^2$

4-128. Driving Face Force — With Friction. The force on the driving face of each land of the engraved rifling may be closely approximated for a tube with uniform twist rifling by the following expression, which, in addition to the force required to cause rotation of the projectile, also takes into consideration the force needed to overcome friction on the driving edge and on the top of the land and the bottom of the groove.[1] Values for coefficients of friction under the conditions experienced during the firing of a gun are not available at present. Until satisfactory values are obtained, the simpler formula given in the preceding paragraph may be used.

$$R = \frac{2\pi \left[k^2 G(1 + \tan\theta)^{\frac{1}{2}} + \mu \tan\theta \, F_b(r^2 - k^2)\right]}{\left[hr(\tan\theta - \mu) + 2\pi k^2(\mu \tan\theta + 1)\right] N}$$

where

G = propellant force on the projectile [maximum pressure (psi) x area of the bore, in.2]
k = radius of gyration about the longitudinal axis, in.
μ = coefficient of friction between band and rifling
$\tan\theta$ = tangent of angle made by rifling with plane perpendicular to bore
r = radius of projectile, in.
h = distance along bore for one complete turn of rifling (twist in calibers per turn x caliber in in.)
F_b = force resulting from the radial band pressure (radial band pressure x effective band length x band circumference)
N = number of lands.

The following approximate values k^2 may be used.

For HVAP projectiles, $k^2 = 0.100d^2$
For AP shot, $k^2 = 0.115d^2$
For HE shell, $k^2 = 0.140d^2$

The term $k^2G(1 + \tan\theta)^{1/2}$ in the numerator represents the portion of the force which results from consideration of the driving face; the term $\tan\theta \, F_b(r^2 - k^2)$ results from consideration of the friction acting at the top of the lands and the bottom of the grooves.

4-129. Bearing Stress. The bearing stress (S_b) on the driving face of the rotating band is

$$S_b = \frac{R}{\ell h}$$

where ℓ is the effective width of the band (in.) and h is the average height of the band land (in.).

4-130. Shear Stress. The shear stress across the base of the land of the rotating band is

$$S_s = \frac{R}{\ell b}$$

where ℓ is the effective width of the band and b is the transverse width of the rotating band land.

4-131. Profile. Table 4-30 illustrates the shapes of finish-machined rotating bands used on certain representative projectiles. The following characteristics merit special notice.

a. Most bands are tapered toward the front to match the taper of the forcing cone.

b. In order to allow space for part of the metal displaced by the lands during engraving, cannelures are provided. The cannelures are circumferential grooves cut in the band, into which part of the excess metal ahead of the cannelure may flow. Theoretically, the cannelure should provide sufficient space to accommodate the metal displaced to the rear during engraving; the purpose is to avoid an objectionable fringe and to lower radial band pressure (paragraph 4-126). Actually, the width, depth, and profile of the cannelure are determined empirically or experimentally. As a general rule, the depth of a cannelure measured below the top of the metal immediately to its rear should not be greater than the depth of the band metal beneath the cannelure. Cannelure root diameter should not be less than rifling land diameter, to minimize possibility of band flyoff.

c. Approximately the maximum metal displaced ahead of a cannelure during engraving V_E is

$$V_E = \left(\frac{\pi}{4} D_{ba}^2 - A_b\right) \ell_1$$

where

D_{ba} = maximum band diameter
A_b = maximum bore area
ℓ_1 = width of a band, ahead of a cannelure, the volume of which is equal to the actual band but which has rectangular cross section.

4-132. Band Retention. Band retention refers to the ability of the rotating band to remain attached to the projectile throughout its flight. During flight, the centrifugal forces caused by the rotation of the projectile tend to cause it to leave its seat, rupture, and fly off. This tendency is opposed by the strength properties of the material itself. In addition, the method of attaching the band to the projectile may aid retention. In a projectile that has a nonundercut seat, the friction at the ends aids retention. In one that has an undercut seat, the undercut itself constrains the band. Special methods have been used to prevent fly-off. One of these, which has been used in connection with plastic bands that are cast into place on the projectile, is to machine ridges into the seat. These ridges are rolled, so that their tops mushroom and provide dovetails, which hold the band in place. Another is the use of the welded overlay band, which is applied primarily to very thin-walled shell that either are too thin to take an effective seat or that might collapse under the pressure applied in a banding press or "tire-setter." Paragraphs 4-134 to 4-140, following, deal only with the problem of calculating for retention of the rotating band by the straight-sided and by the undercut band seat.

4-133. Calculation for Band Retention.[5] The following method may be used to determine whether or not a given band will be retained in flight. It may also be used to determine whether a long band, which calculations indicate will not be retained, may be retained by dividing it into two shorter bands.

The rotating band is analyzed as a shell acted upon by centrifugal forces. The action of end friction or undercut is considered to impose simple constraint on the ends of the band. This analysis is then compared to two simpler analyses: one for short bands on the basis of a simple beam formula; and one for long bands on the basis of a "boiler" formula, which considers the band to be a simple unconstrained shell. A length parameter (γ) is developed, and values of γ are determined such that the value of γ may be used to predict whether the simpler beam or boiler formulas may be satisfactorily used to determine the retention of the band. Limiting values of γ are chosen to permit calculation by either of the simpler methods when the error introduced by so doing is no greater than 10 percent.

4-134. Suggested Procedure for Calculation.

1. Determine geometry of equivalent rotating band for analysis (paragraph 4-135).
2. Calculate length parameter γ (paragraph 4-136).
3. If γ is less than 0.63, use the beam analysis (paragraph 4-137).
4. If γ is greater than 3.03, use the boiler analysis (paragraph 4-138).
5. If γ has an intermediate value, use the constrained shell analysis (paragraph 4-139).

6. If calculations indicate that the band will not be retained, consideration may be given to dividing the band into two shorter bands equivalent to the single long band. This procedure ordinarily will be found effective only for long (γ greater than 3.03) or intermediate length bands. In any case, the redesigned band should be checked. (See paragraph 4-126 for effect of this procedure on radial band pressure.)

4-135. Equivalent Rotating Band Geometry. The equivalent rotating band geometry for band retention computation may be determined as follows:

1. The band will be considered to have been engraved by the rifling.
2. The outside, band land, radius will be equal to the radius of the rifling grooves.
3. The band groove radius will be equal to the rifling land diameter.
4. The inside, band seat, radius will not take into consideration the depth of the band that is penetrated by the knurling on the seat. That is, it will be equal to the radius over the knurling.
5. The band width will not take into account front and rear chamfers. It will be considered that the band extends radially from the outer edge of the band seat.
6. Where the long or intermediate band length analyses are used, the section of band considered will extend from the center of one band groove to the center of the next.
7. The profile of the rifling will be considered to be straight-sided in the analysis of the intermediate length band. Appropriate stress concentration factor to account for the true fillet radius will be used when calculating the stress at the root of the band land.

4-136. Calculation of Length Parameter.

$$\gamma = \sqrt[4]{\frac{12t_1\,(1-\nu 2)}{D^2H}}\,\frac{\ell}{2}$$

where

t_1 = thickness of equivalent band from seat to band groove, in.
ν = Poisson's ratio (about 0.3 for most materials)
D = mean band diameter, in.
= 1/2 (seat diameter + band groove diameter)
≈ shell diameter

$$H = \frac{t_1^4 + 4kt_1^3t_2 - 6kt_1^2t_2^2 + 4kt_1t_2^3 + k^2t_2^4}{(1+k)\,(t_1 + kt_2)}$$

$$= t_1^3\left[\frac{1 + 4kT - 6kT^2 + 4kT^3 + k^2T^4}{(1+k)\,(1+kT)}\right]$$

where

$$T = \frac{t_2}{t_1}$$

t_2 = thickness of equivalent band from seat to band land, in.

$$k = \frac{\text{band land width}}{\text{band groove width}} = \frac{a_2}{a_1}\left(\frac{\text{in.}}{\text{in.}}\right)$$

ℓ = band width, in.

For the case where k = 1 (land width equals groove width) the value of θ may be obtained from the plot at the center of figures 4-48 and 4-49. Curves are given for values of θ ranging from -0.2 to +0.5447.

4-137. Beam Analysis. The beam analysis is made by means of the following equation. The maximum permissible velocity or minimum permissible yield stress may be solved for

$$\left(\frac{V}{n}\right)_i^2 \quad \frac{2}{3\pi^2 144}\left(\frac{\sigma_L g}{\rho}\right)\left(\frac{D\tau}{\ell^2}\right)$$

where

V = velocity, fps
n = rifling twist, calibers per turn
σ_L = longitudinal stress at outer fiber, lb per in.^{2}
g = acceleration of gravity, in. per sec^2
ρ = density of band material, lb per in.^{3}
D = mean band diameter, in.
= 1/2 (seat diameter + band groove diameter)
≈ shell diameter
ℓ = band width, in.
τ = quasi-equivalent rotating band thickness parameter

$$= \frac{2(t_1^4 + 4kt_1^3t_2 - 6kt_1^2t_2^2 + 4kt_1t_2^3 + k^2t_2^4)}{(t_1+t_2)\,(2t_1t_2 + kt_2^2 - t_1^2)\,(1+k)}$$

where

t_1 = thickness of equivalent band from seat to band groove, in.
t_2 = thickness of equivalent band from seat to band land, in.

$$k = \frac{a_2}{a_1}$$

a_2 = band land width, in.
a_1 = band groove width, in.

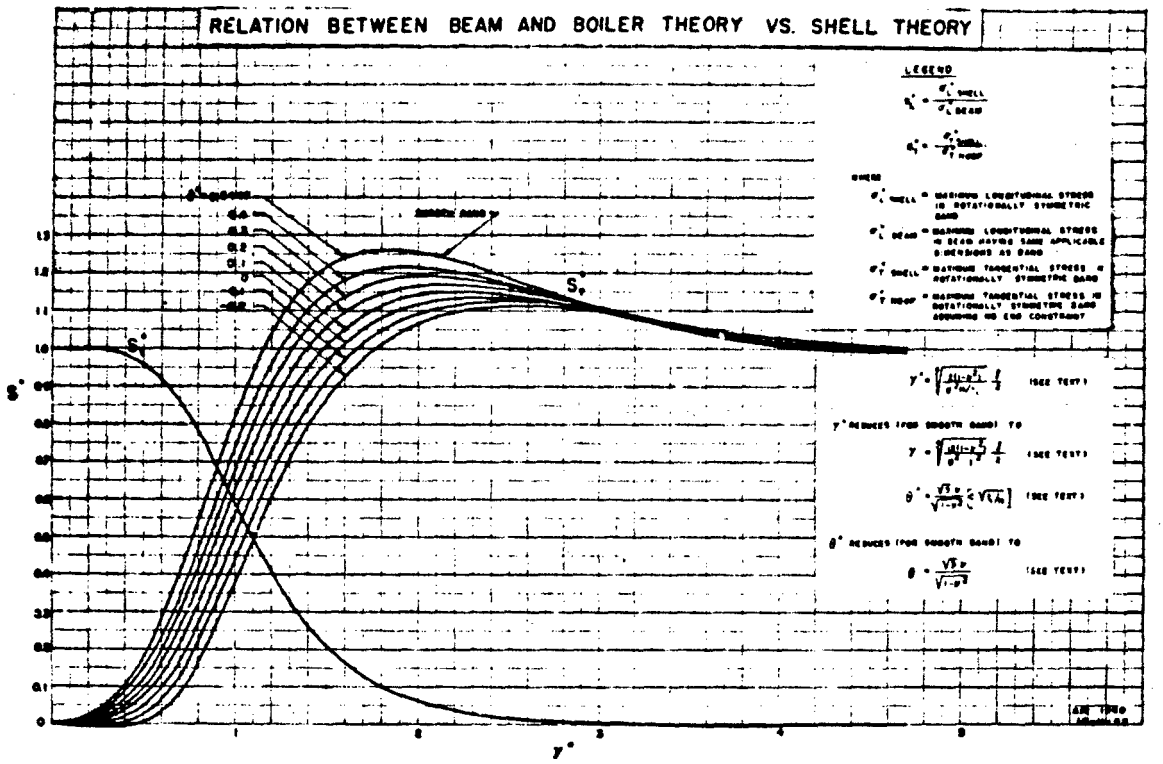

Figure 4-48. Relation between beam and boiler theory versus shell theory

For the case where k = 1 and setting

$$T = \frac{t_2}{t_1}$$

$$\tau = t_1 \left[\frac{1 + 4T - 6T^2 + 4T^3 + T^4}{T + 3T^2 + T^3 - 1} \right]$$

This analysis will give the solution for initial yielding of the band. The graph (figure 4-50) may be used to solve this equation in terms of the following parameters.

G = geometry characteristic

$$= \frac{D\tau}{t^2} \left(\frac{\text{in.}}{\text{in.}} \right)^2$$

S = velocity characteristic

$$= \left(\frac{V}{n} \right)_1 \left(\frac{\text{ft}}{\text{sec}} \right)$$

Q_L = material or stress characteristic

$$= \frac{\sigma_L g}{\rho} \left(\frac{\text{in.}}{\text{sec}} \right)^2$$

4-138. Boiler Analysis. Using the boiler analysis, the maximum permissible velocity or minimum permissible yield stress may be solved for. The following equation is used.

$$144\pi^2 \left(\frac{V}{n} \right)^2 = \frac{\sigma_T g}{\rho}$$

where

V = velocity, fps
n = twist of rifling, calibers per turn
σ_T = tangential stress in material, lb per in.^{2}
g = acceleration of gravity, in. per sec^2
ρ = density of band material, lb per in.^{3}

Figure 4-51 may be used to solve this equation graphically.

4-139. Thin-Walled Theory — Constrained Ends. The constrained shell analysis assumes that failure may occur at any one of three areas. All of these must be checked. They are:

1. The band land surface
2. The band land-groove fillet

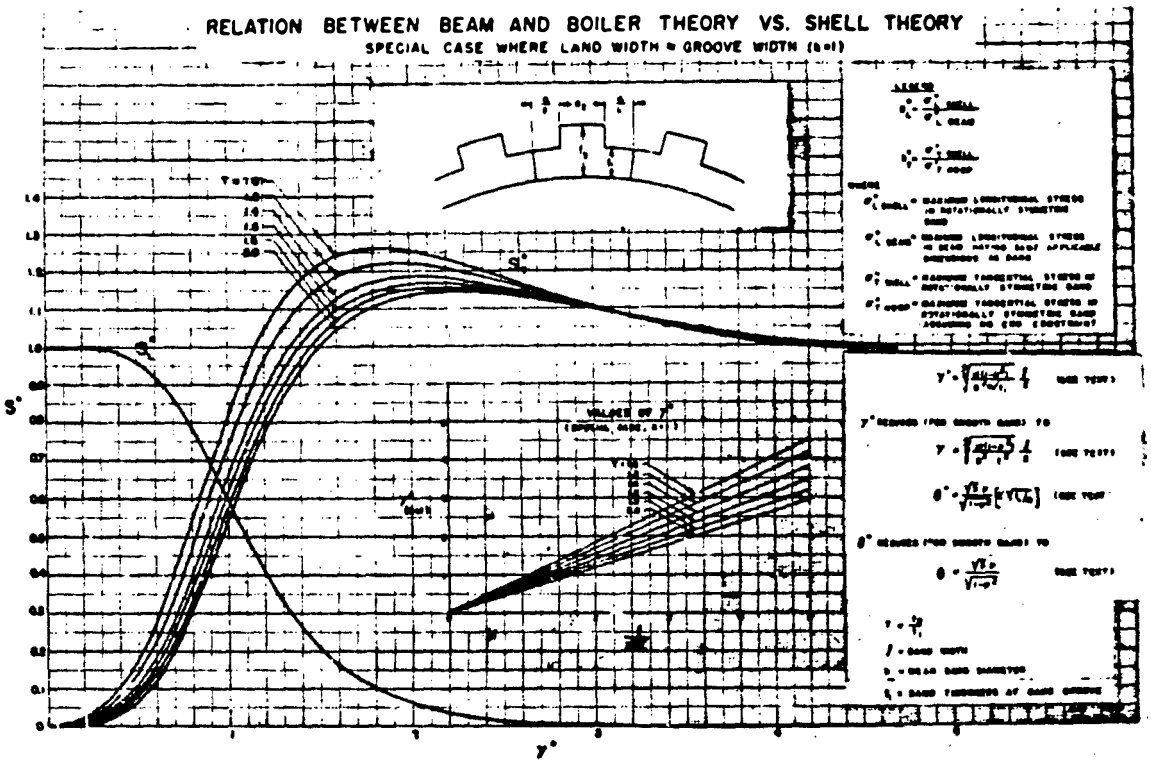

Figure 4-49. Relation between beam and boiler theory versus shell theory: special case of figure 4-50

3. The inner surface of the band.

The following equations are used.

1. Band land surface

$$\sigma_{YP} = 144\pi^2\frac{\rho}{g}S^2\left(\frac{3}{2}\frac{\ell^2}{D\tau_1}\right)S_L$$

2. Band land-groove fillet

$$\sigma_{YP} = \text{S.C.F.}\left[144\pi^2\frac{\rho}{g}S^2S_T\left(\frac{t}{t_1}\right)\right]$$

3. The inner surface of the band

$$\sigma_{YP} = 144\pi^2\frac{\rho}{g}S^2\left[S_T\left(\frac{t}{t_1}\right)-S_L\left(\frac{3}{2}\frac{\ell^2}{D\tau_1}\right)\right]$$

where

σ_{YP} = yield stress of band material, lb per in.^{2}

ρ = density of band material, lb per in.^{3}

g = acceleration of gravity, in. per sec^2

S = velocity characteristic $= \frac{V}{n}$

V = velocity, fps

n = rifling twist, calibers per turn

ℓ = band width, in.

D = mean band diameter, in. = 1/2 (seat diameter + band-groove diameter) $\approx$ shell diameter

τ = thickness of original band (not the equivalent) from inside diameter of equivalent band to outside diameter of original band, in.

t_1 = thickness of equivalent band from seat to band groove, in.

t_2 = thickness of equivalent band from seat to band land, in.

S.C.F. = band land-groove fillet stress concentration factor

$S_T = \frac{\sigma_T \text{ shell}}{\sigma_T \text{ hoop}}$

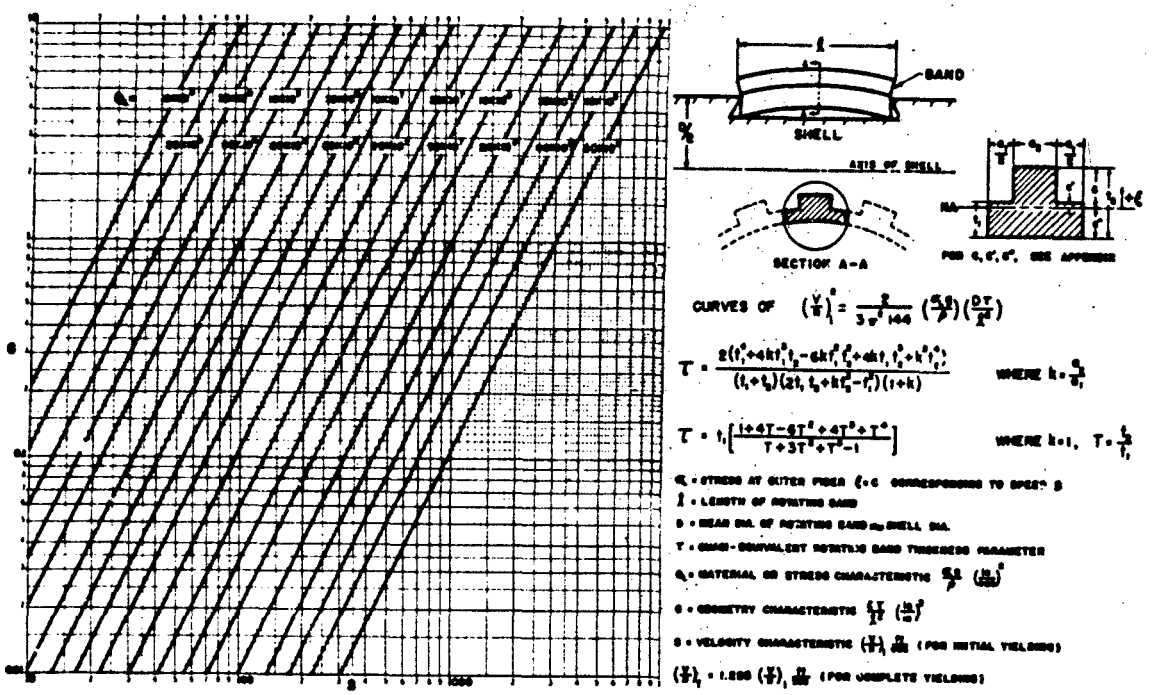

Figure 4-50. Beam analysis

$$S_L = \frac{\sigma_L \text{ shell}}{\sigma_L \text{ beam}}$$

σ beam = maximum longitudinal stress in beam having same applicable dimensions as band

σ shell = maximum longitudinal stress in rotationally symmetric band

σ_T hoop = maximum tangential stress in rotationally symmetric band, assuming no end constraint

σ_T shell = maximum tangerial stress in rotationally symmetric band

Given the value of γ (paragraph 4-136), the values of S_T and S_L may be obtained graphically from figures 4-48 and 4-49.

$$\tau_1 = t_1 \left[\frac{1 + 4kT - 6kT^2 + 4kT^3 + k^2T^4}{(1 + kT)(2T + kT^2 - 1)} \right]$$

$$\tau_2 = -t_1 \left[\frac{1 + 4kT - 6kT^2 + 4kT^3 + k^2T^4}{(1 + kT)(1 + kT^2)} \right]$$

$$k = \frac{a_2}{a_1}$$

a_2 = band land width, in.

a_1 = band groove width, in.

$$T = \frac{t_2}{t_1}$$

$$\theta = \frac{\sqrt{3}\,\nu}{\sqrt{1 - \nu^2}}$$

4-140. Position of Band Seat. Position of the rotating band, and hence the band seat, affects the chamber capacity. The location is, therefore, usually stated with reference to the base of the projectile. From the standpoint of obtaining minimum stress in the shell wall, the rotating band should be located as close to the base of the shell as possible. The position of the rotating band also has an effect upon the initial yaw of the shell, as well as upon the drag in flight. All of these factors must be considered when determining the position of the rotating band. Location is different for (1) flat-base and (2) boat-tail artillery projectiles and, in both instances, depends on whether the ammunition is (1) fixed, (2) semifixed, or (3) separate loading.

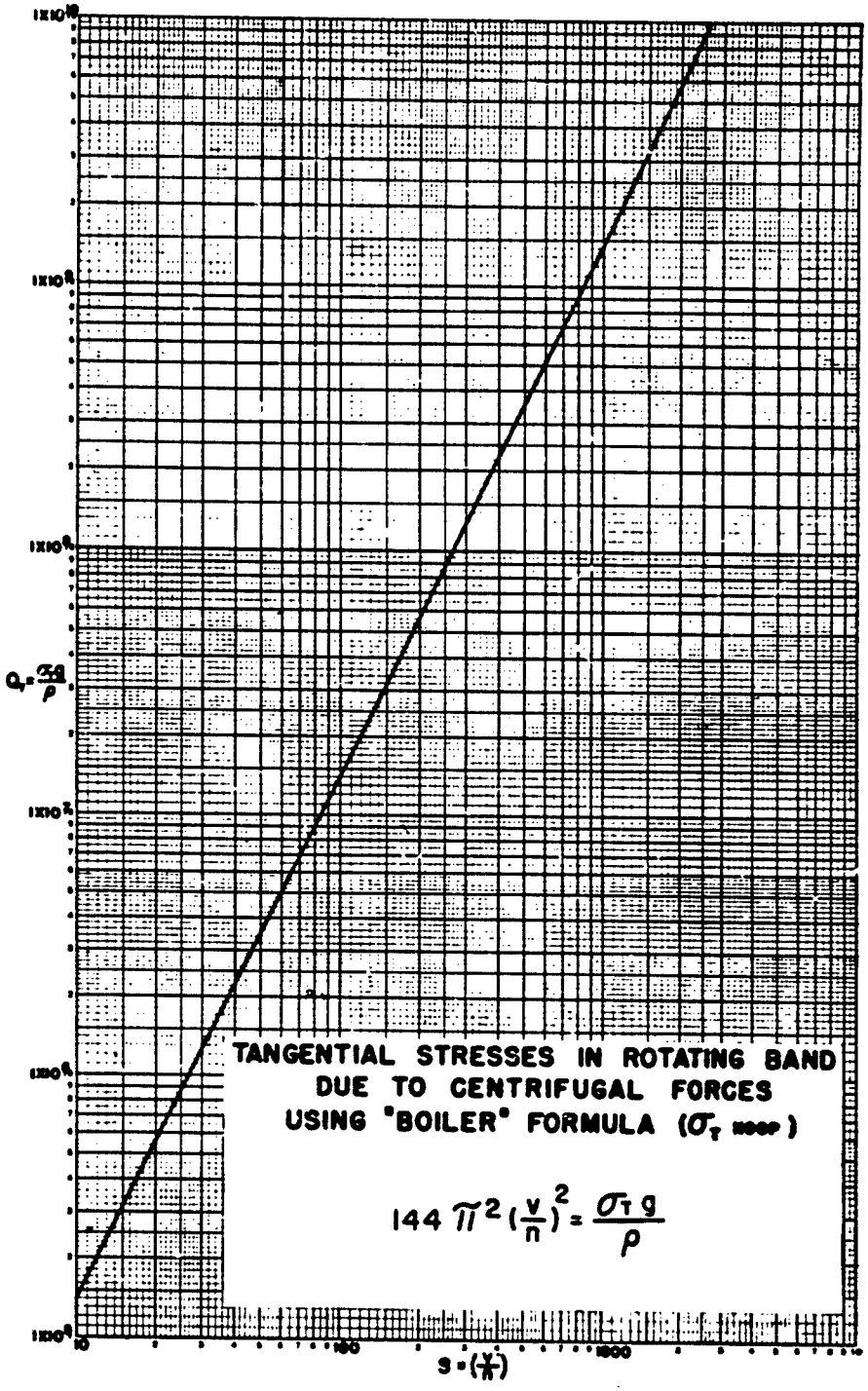

Figure 4-51. Boiler formula

4-141. Flat-Base Projectiles.

a. Fixed Ammunition. The rotating band acts as the stop for the projectile when it is inserted into the cartridge case. The length of the body behind the rotating band should be sufficient to provide ample bearing surface along the wall of the cartridge case. The location of the band seat usually is from 1/4 to 1/3 of a caliber from the base.

b. Semifixed and Separate-Loading Ammunition. In these cases the projectile is not pressed into the case, and the provision of adequate bearing surface is obviated. The location of the band seat usually is from 0.1 to 0.2 of a caliber from the base.

4-142. Boat-Tail Projectiles.

a. Fixed Ammunition. As in the case of the flat-base projectile, sufficient cylindrical surface must be available in front of the boat-tail to provide a good bearing on the walls of the cartridge case. The location of the band seat usually allows about 1/4 of a caliber of cylindrical surface between the band seat and the beginning of the boat-tail.

b. Semifixed and Separate-Loading Ammunition. Location of the band seat is usually such as to provide from 0.2 to 0.25 of a caliber of cylindrical surface between the band seat and the beginning of the boat-tail. Table 4-30, in the column headed "Distance to base," shows the location of the band seat with reference to the base for certain representative projectiles.

4-143. Properties of Rotating Band Materials.

a. Gilding Metal:

1. Composition.

Copper	89 to 91 percent
Zinc	9 to 11 percent
Lead	0.05 percent max.
Iron	0.05 percent max.
Other impurities	0.13 percent max.

2. Mechanical Properties.

	Tensile strength (psi)	Yield strength (psi)	Elongation in 2 in. (percent)	Rockwell hardness	Shear strength (psi)
1/2 hard	52,000	45,000	15	B58	35,000
As hot rolled	37,000	10,000	45	F53	28,000

b. Copper and Alpha Brasses. Tests performed at Frankford Arsenal[1] yielded the true stress-natural strain curves shown in figures 4-52 and 4-53.

Compositions of the materials used are given in table 4-31.

Table 4-31

Element	Material			
	OFHC copper	Commercial bronze	Low brass	Cartridge brass
Cu	99.92	89.39	80.16	70.04
Pb	< 0.003 (ND)	ND	ND	0.01
Fe	< 0.003	0.01	0.01	0.01
Zn	...	10.60	19.83	29.93
Ni	< 0.005	...	...	...
Mn	< 0.003 (ND)	...	...	< 0.001
Ag	< 0.002	...	...	< 0.02 (ND)
Sn	< 0.002 (ND)	...	...	< 0.01
Bi	< 0.0005	...	...	< 0.0005 (ND)
Al	< 0.005 (ND)	...	...	< 0.01
P	< 0.005	...	...	...
Sb	...	...	...	< 0.005 (ND)
Si	...	...	...	< 0.01

ND = none detected
OFHC = oxygen-free high-conductivity

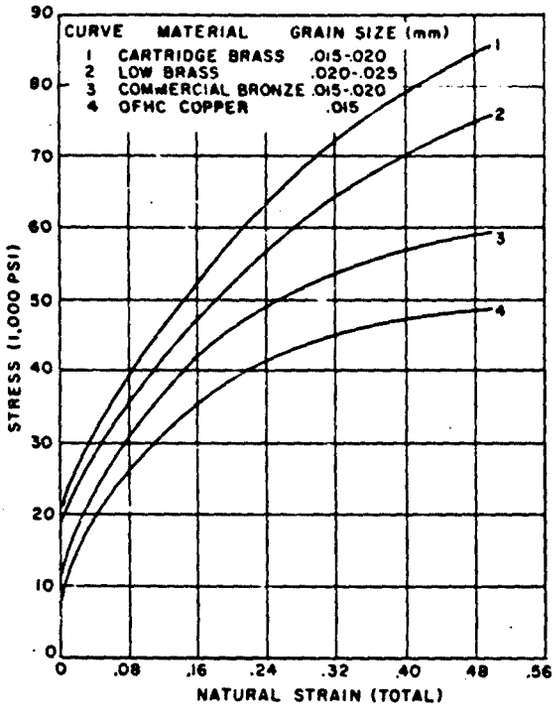

Figure 4-52. Compression test data for OFHC copper and three alpha brasses, grain size range 0.015 to 0.025 mm

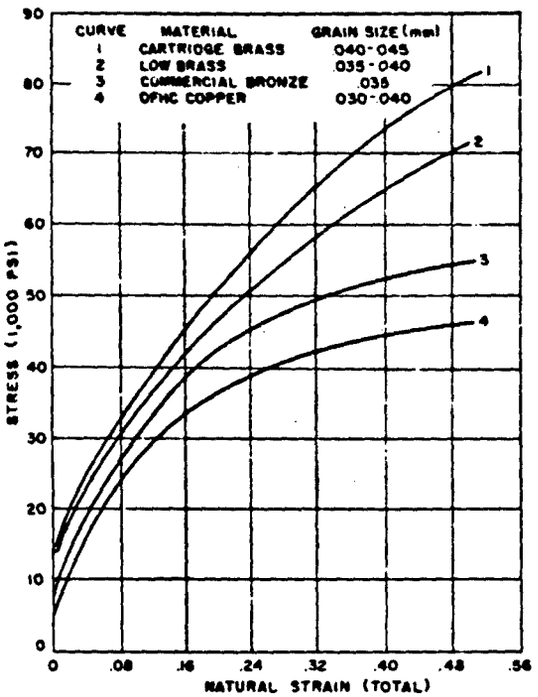

Figure 4-53. Compression test data for OFHC copper and three alpha brasses, grain size range 0.030 to 0.045 mm

c. Sintered Iron. Tests performed by Purdue University to determine the properties of sintered iron yielded the curves shown in figures 4-54 through 4-65. The curves in the figures include:

Figure No.	Title
4-54 through 4-59	True stress-true strain curves in compression
4-60	Variation of modulus of elasticity with density
4-61	Variation of ultimate tensile strength with density
4-62	Variation of yield point with density
4-63	Variation of yield strength with density
4-64	Variation of elongation with density
4-65	Variation of density with final stress in compression

The iron powder was compacted in a double-acting die (free-floating), the faces of which were lubricated with oleic acid and moly-sulfide powder. The compacts of densities 4.4 and 5.5 grams per cc were sintered at 1,100°C for one hour, while the compacts of density 6.4 grams per cc were sintered at 1,150°C for one hour. The compacts were unimpregnated.

The sintered-iron compacts that were tested were pressed from a hydrogen-reduced mill scale powder produced by the Pyron Corporation. The characteristics of this iron powder were as follows.

Apparent Density	Specific Density
2.33 grams per cc	0.416 cc per gram

Compacting Pressures

Nominal density (grams per cc)		
4.4	5.5	6.4
Compacting pressure (10,000 psi)		
16-17	37-38	67-71

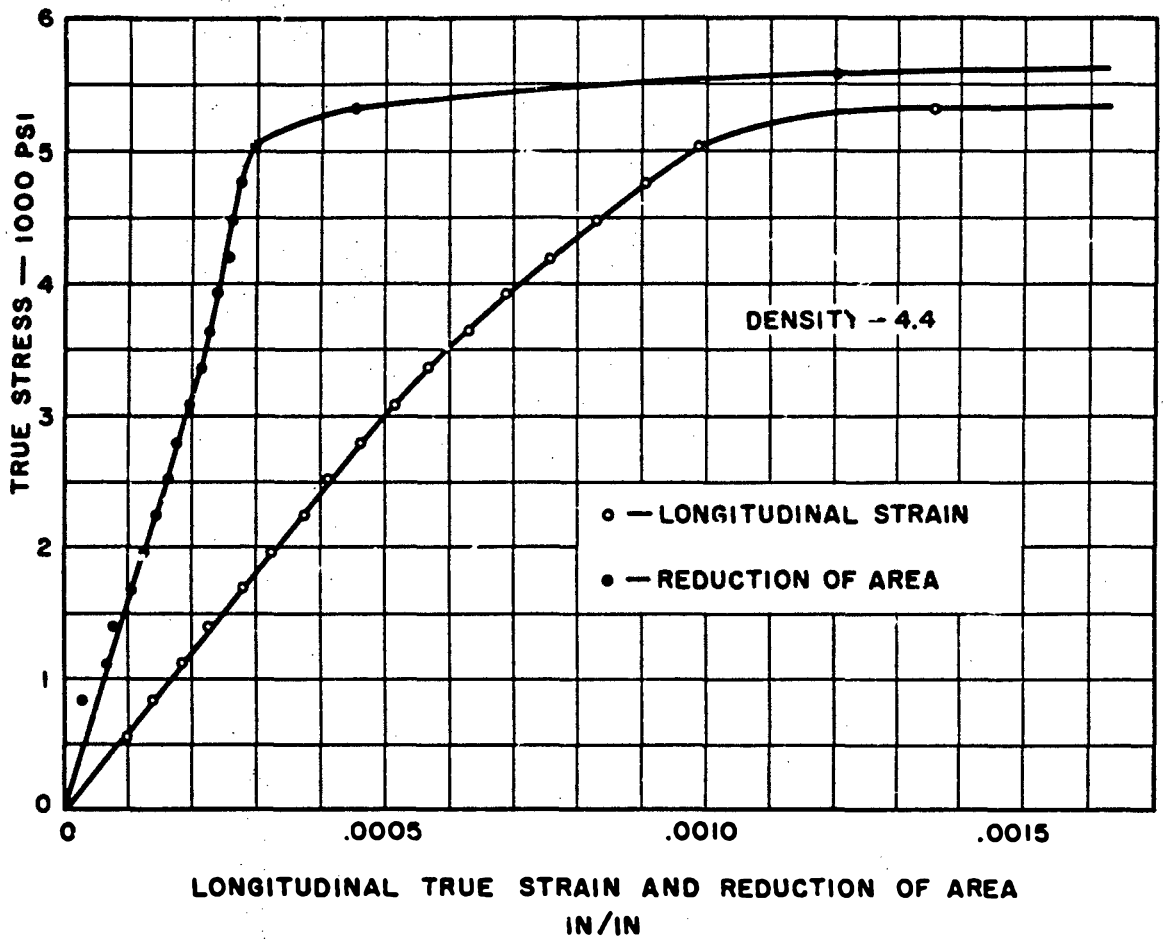

Figure 4-54. True stress-true strain curves in compression, density - 4.4

Chemical Analysis	
Element	Percent by weight
C	0.018
Mn	0.39
Si	0.22
S	0.014
P	0.012
Ni	0.07
Cr	0.05
Mo	0.02
Cu	0.06
V	nil
Fe	remainder

Screen Analysis	
Mesh	Percent by weight
on 100	0.34
pass 100	6.0
on 140	
pass 140	23.7
on 200	
pass 200	14.7
on 270	
pass 270	18.4
on 325	
pass 325	36.5

EROSION OF RIFLING

4-144. Failure of the Gun Tube. Failure of the gun tube may take two forms. The tube may either fail completely or wear to a point at which satisfactory accuracy and muzzle velocity can no longer be obtained. The complete failure may be caused by excessive pressures developed inside the tube as a result of the preence of foreign material, the development of progressive stress cracks, or premature functioning of the fuze of the projectile. Premature functioning may be caused by sudden changes in rotation of the projectile that result from worn rifling. Failure by loss of accuracy or velocity, which is by far the more common mode, usually is caused by erosion of the rifling.

4-145. Erosion. Erosion may be defined as the gradual wearing away of the material of the bore as a result of the firing of the weapon. Erosion takes place throughout the length of the tube, but is most severe in the region of the forcing cone (nomenclature of rifling and cartridge

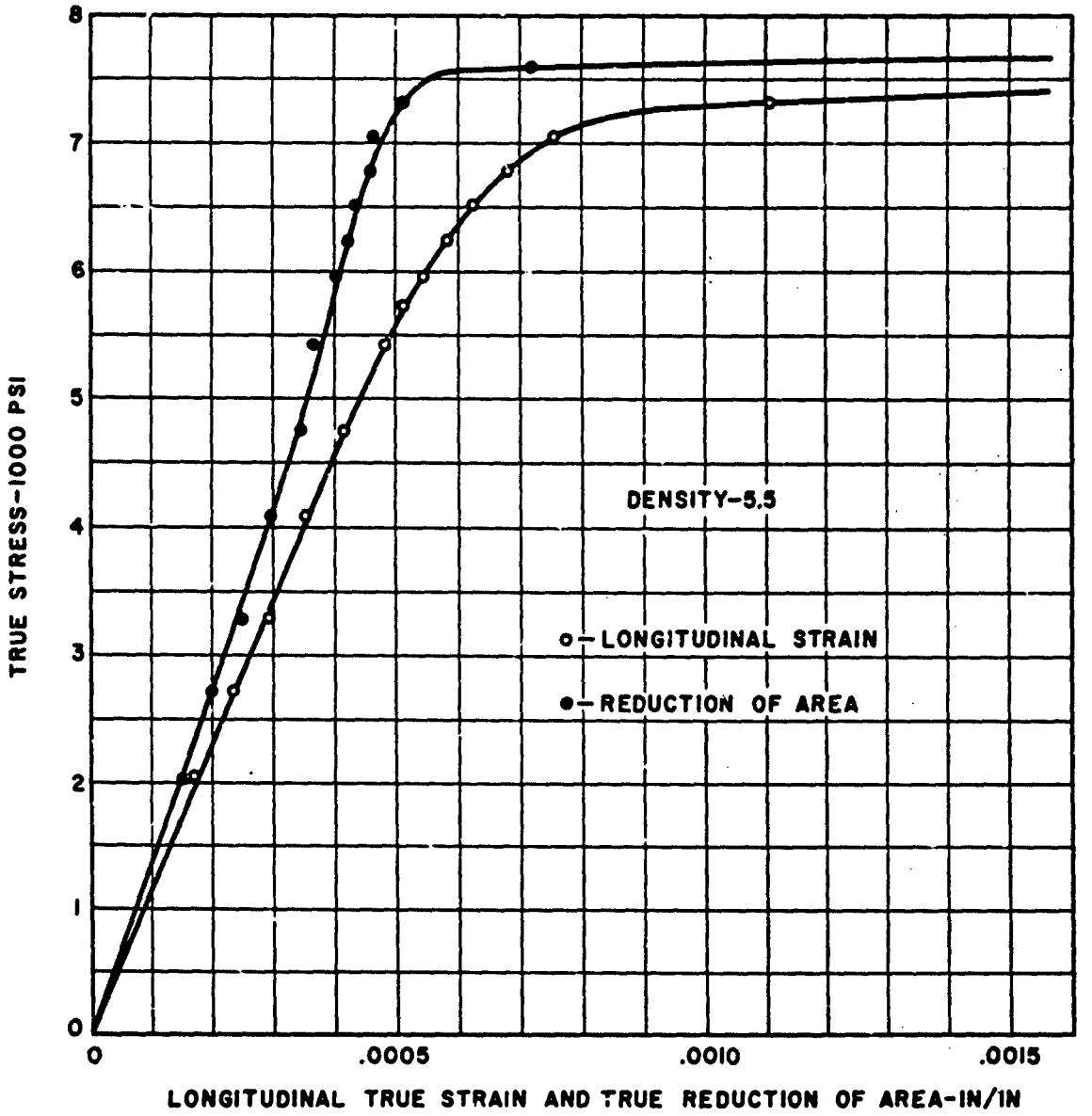

Figure 4-55. True stress-true strain curves in compression, density - 5.5

cases is given in figure 4-66). Figures 4-67 and 4-68 illustrate the effect of erosion and progressive stress cracking on the 105-mm howitzer, muzzle velocity 1,550 feet per second, and on the 76-mm gun M1, muzzle velocity 3,400 feet per second. Note that erosion is much more rapid at the higher muzzle velocity. Erosion usually is specified in terms of the advance of the forcing cone, which is measured by means of a pull-over gage.

4-146. Effects of Erosion. Erosion of the rifling (wear of the lands and advancing of the forcing cone) may have the following effects.

1. Loss in obturation, resulting in drop in muzzle velocity.

2. Loss in shot-start pressure, resulting in slower burning of the propellant and erratic internal ballistics.

3. In separate-loading ammunition, which is rammed into place against the forcing cone, ad-

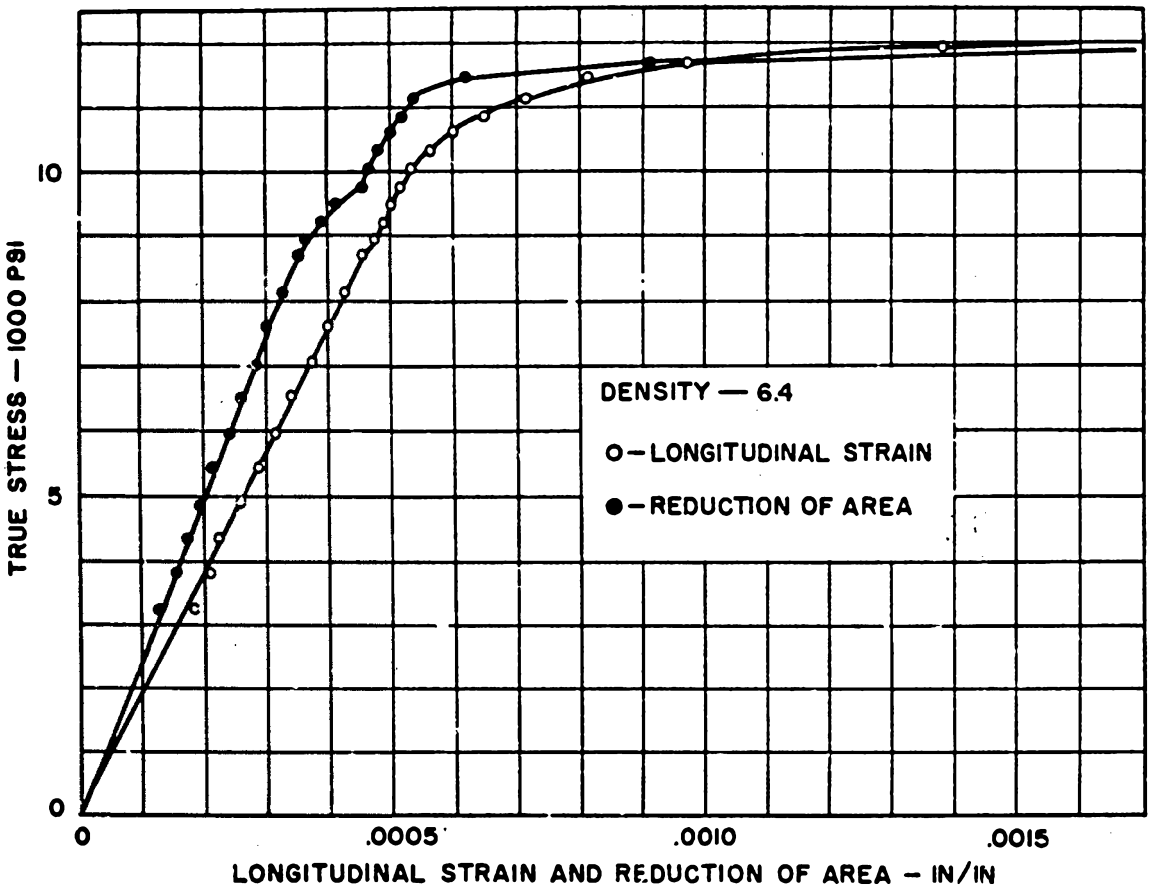

Figure 4-56. True stress-true strain curves in compression, density - 6.4

vance of the forcing cone causes an increase in the chamber volume and a corresponding decrease in the loading density of the propellant. This affects interior ballistics.

4. Wear of the lands may permit a considerable amount of projectile free run. That is, the projectile may travel for some distance in the tube before there is obtained a sufficient depth of engraving of the rotating band to impart spin. This may result in wiping off of the band lands, with attendant failure to attain full spin. In extreme cases, sudden erratic imparting of spin may cause premature functioning of the fuze.

5. Excessive wear permits too much clearance between bourrelet and rifling. This may result in balloting of the projectile and in excessive initial yaw, which in extreme cases can result in tumbling of the projectile.

4-147. Causes of Erosion. The causes of erosion are (1) the scouring action of the hot powder gases, and (2) the interaction between the gun tube and the rotating band. Factors affecting the rate of erosion are:

1. The type of metal used in the bore of the gun
2. The quantity of propellant used
3. The type of propellant used (combustion temperature, products of combustion)
4. The material of the rotating band
5. The radial band pressure
6. Rate of wear of the rotating band. (Excessive "wiping off" of the band lands may permit escape of combustion gases, with attendant scouring of the rifling. This band wear is a function of the band width.)
7. Muzzle velocity

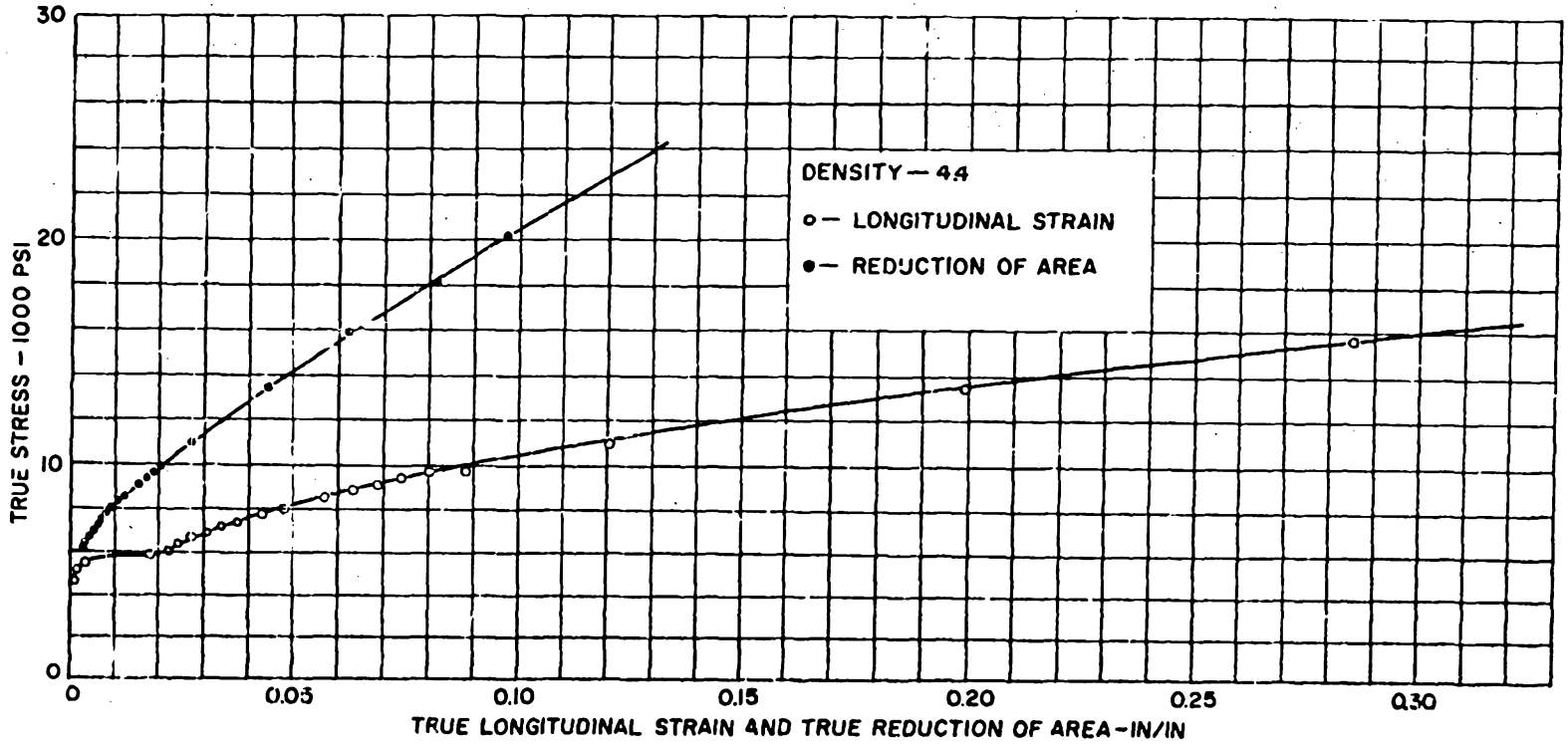

Figure 4-57. True stress-true strain curves in compression, density — 4.4

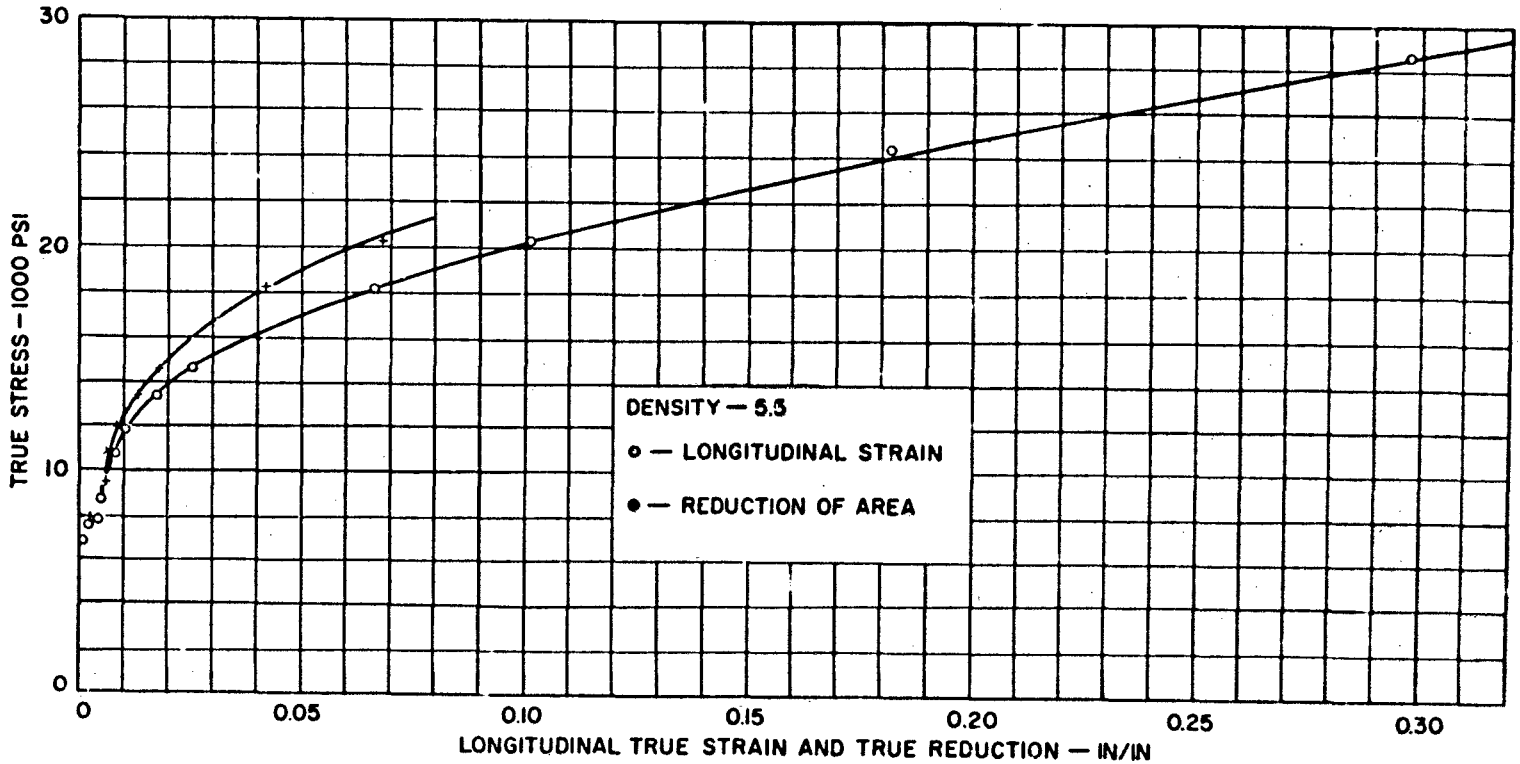

Figure 4-58. True stress-true strain curves in compression, density — 5.5

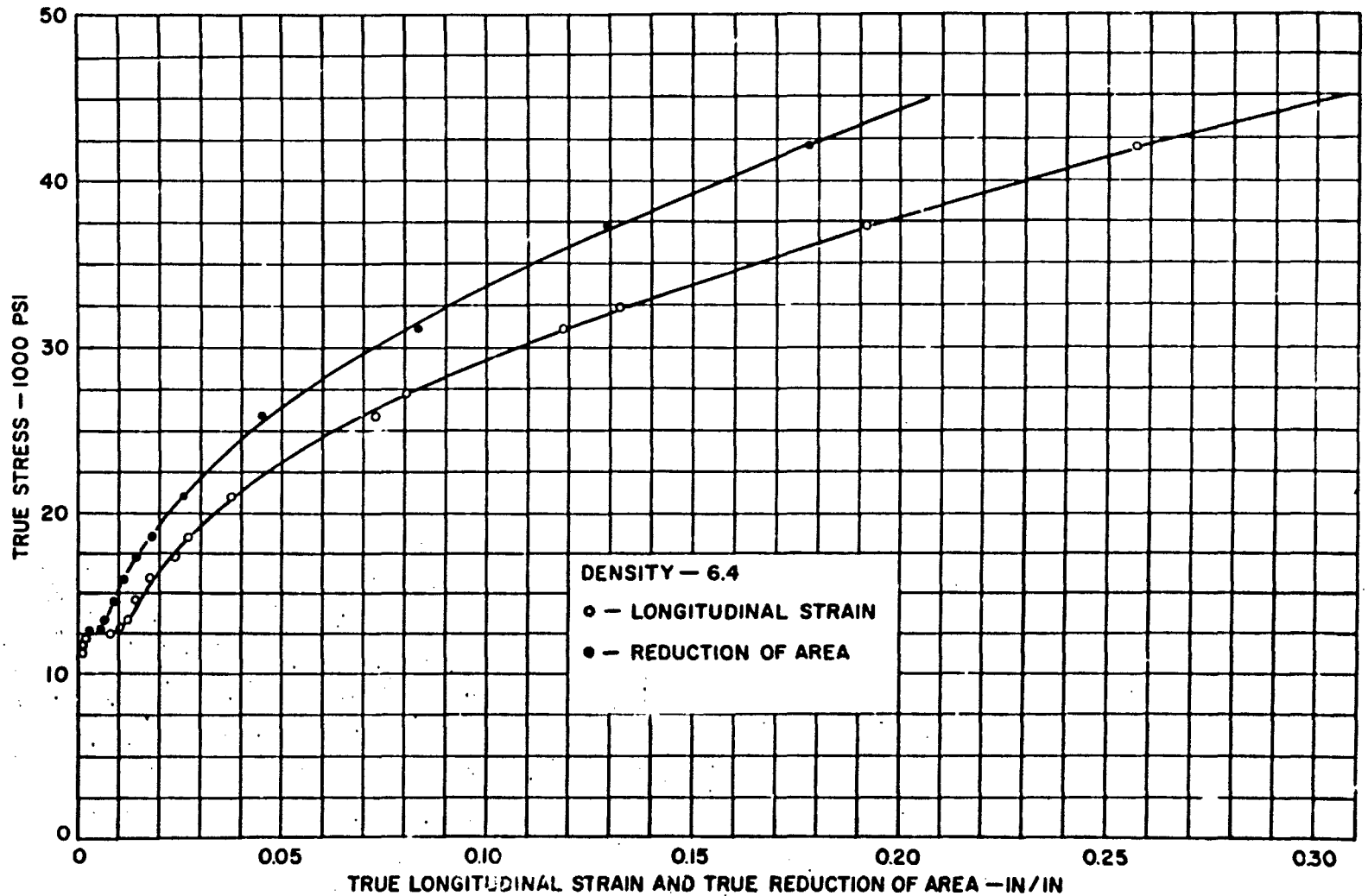

Figure 4-59. True stress-true strain curves in compression, density — 6.4

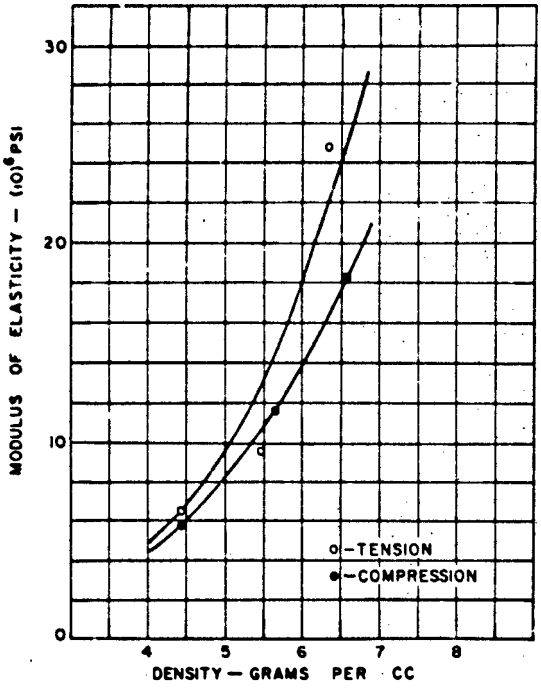

Figure 4-60. Variation of modulus of elasticity with density

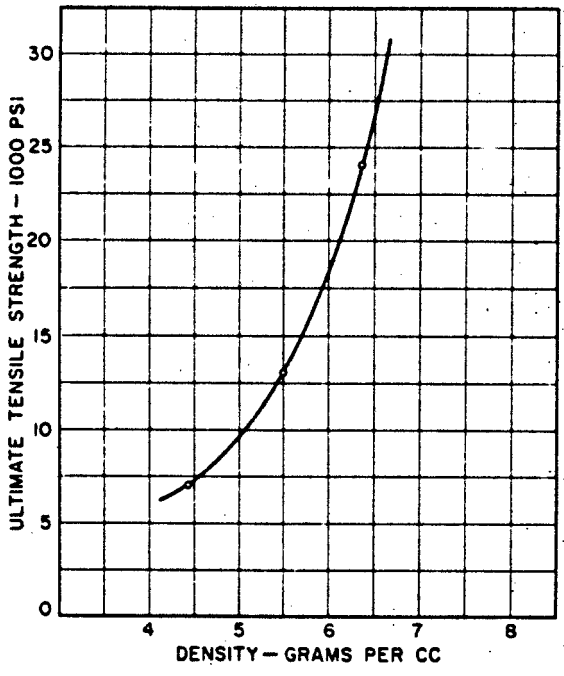

Figure 4-61. Variation of ultimate tensile strength with density

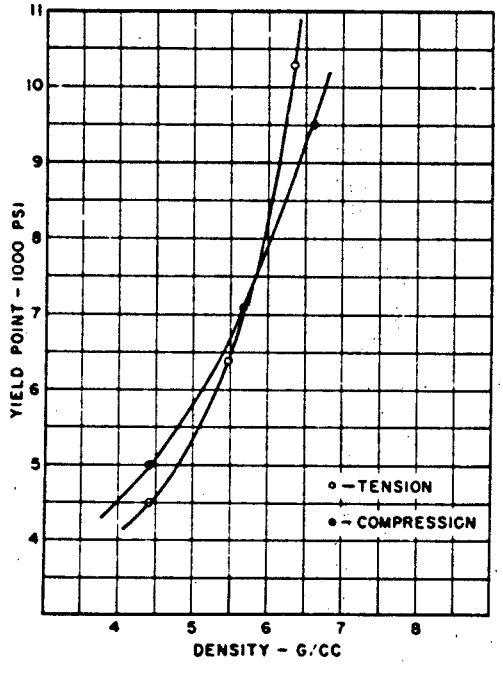

Figure 4-62. Variation of yield point with density

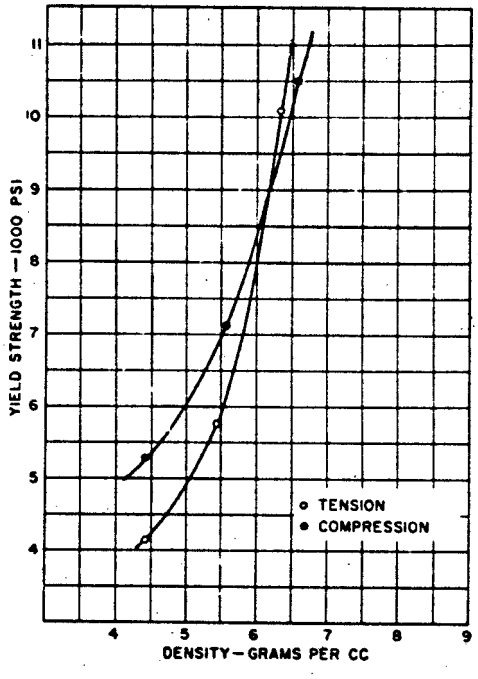

Figure 4-63. Variation of yield strength with density

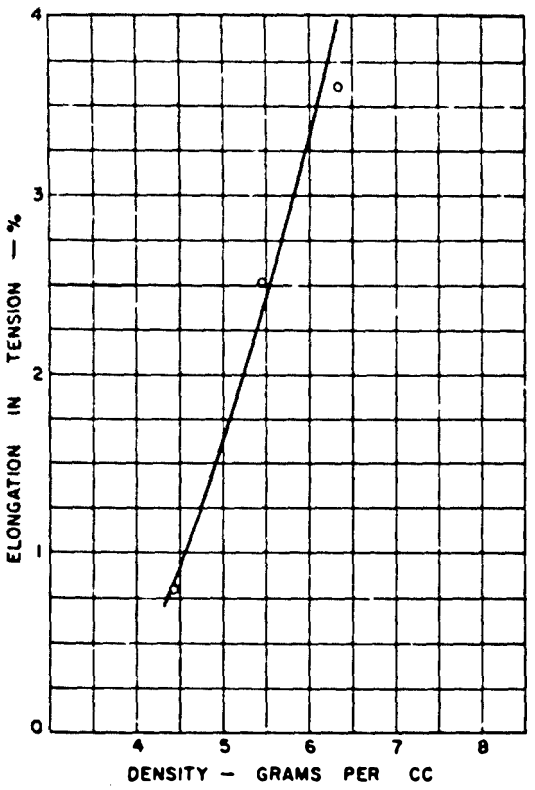

Figure 4-64. Variation of elongation with density

8. Size and number of unburned propellant particles.

4-148. Methods Used to Control Erosion. The most common method used to combat erosion is to use a liner or plating in the tube of the gun. Chromium, or some other material more resistant to erosion by the propellant gases than steel, is used. Another area that is being investigated is the development of cool propellants, which have less erosive effect than those in use at present.

From the standpoint of the rotating band designer, the most important method is the reduction of the radial band pressure and the supplying of sufficient band width to withstand the driving-edge load without wearing excessively. This may be accomplished by designing for minimum or zero interference between band diameter and rifling groove diameter and by the use of caneluring. It is also known that the type of material used for the band affects the rate of erosion. However, the precise nature of this effect is not yet known.

RIFLING DESIGN

In the design of a new gun and its ammunition, two important determinations must be made: (1) profile of rifling, and (2) twist of rifling.

4-149. Profile of Rifling. Design of the profile of rifling involves determination of

1. Number of grooves
2. Depth of groove
3. Width of land
4. Width of groove
5. Radii, slopes, and chamfers.

4-150. Dimensioning of Rifling. Figure 4-69 shows the method used to dimension rifling. The four reference circles (bore circle, groove circle, land base circle, and groove base circle) are drawn in first. In this figure

a = bore diameter (land diameter)
b = groove diameter
c = groove chord
d = land chord
e = slope of side of land
f = angle of chamfer of land
g = width of chamfer of land
h = radius at root of land
i = central angle of land
j = central angle of groove.

The arc intercepted by the groove chord on the bore circle is the length of groove. The arc intercepted by the land chord on the bore circle is the length of land. The depth of rifling is the groove diameter minus the bore diameter.

4-151. Rifling Standard Forms. The rifling standard forms of drawings 15 OKD 2 and 15 OKD 2A (figures 4-70 and 4-71) have been used by the Ordnance Department since shortly after World War I. The trend in modification of these forms is toward a deepening of the grooves on some newer guns. This is being done by Frankford Arsenal, in an effort to reduce excessive erosion caused by the high radial band pressures resulting from "overfill" of the grooves. Frankford reports it to have been successful.

The design of rifling of semielliptical and of pseudo-elliptical forms in order to reduce stress concentrations at the land root fillets

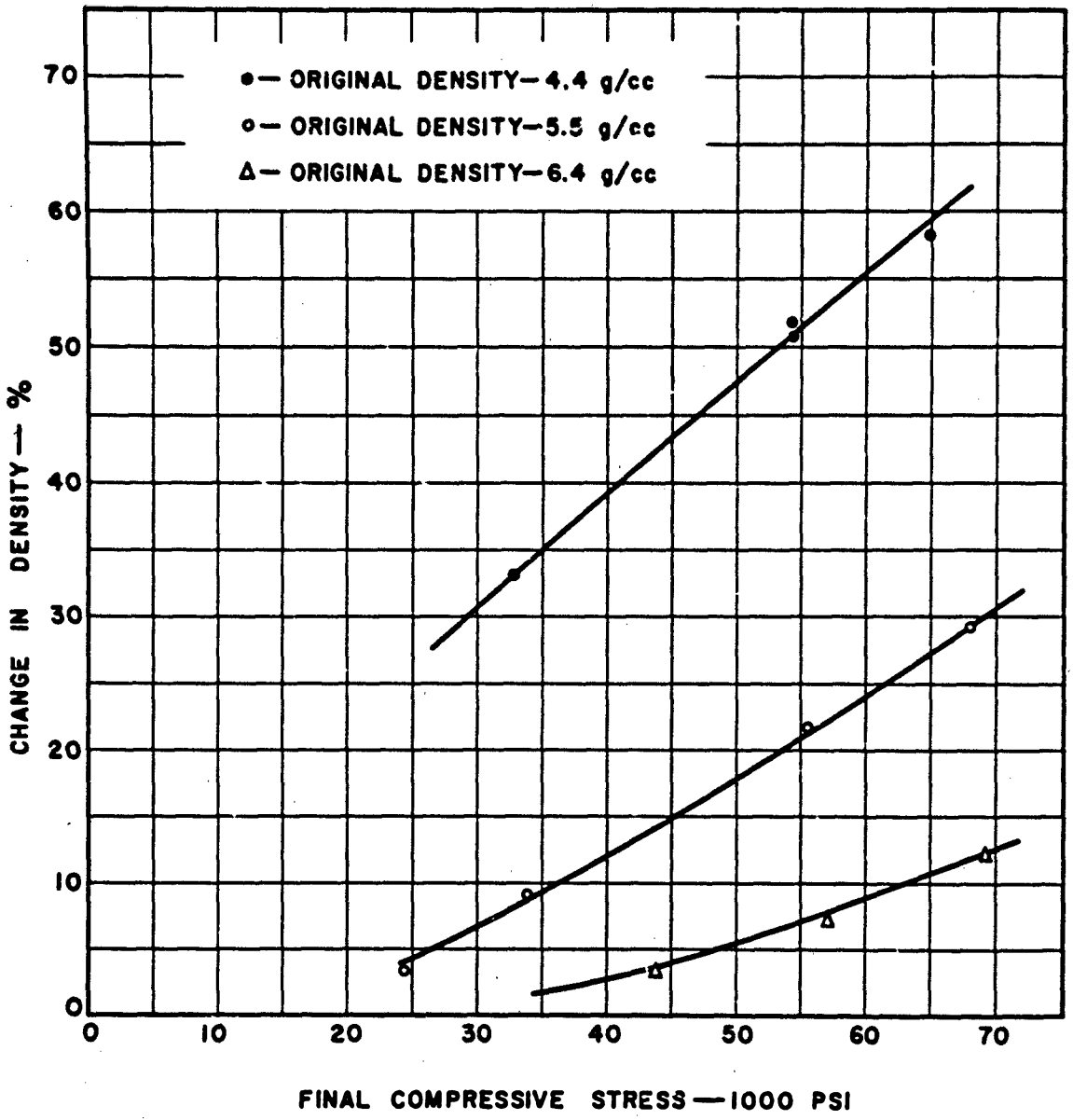

Figure 4-65. Variation of density with final stress in compression

has been contemplated, but no guns with this form of rifling have been made as yet.

4-152. Twist of Rifling. Two types of rifling have been used: (1) uniform twist, and (2) increasing twist (gain twist). Twist usually is specified as n, the number of calibers for one complete turn of the rifling, and is determined by the requirements for the stability in flight of the projectile. Most guns and howitzers in army service have uniform twist.

Both advantages and disadvantages have been claimed for increasing twist.

a. Advantages.

1. Torques on the driving side of the lands and on the driving side of the band engraving are supplied more uniformly throughout the travel of the projectile.

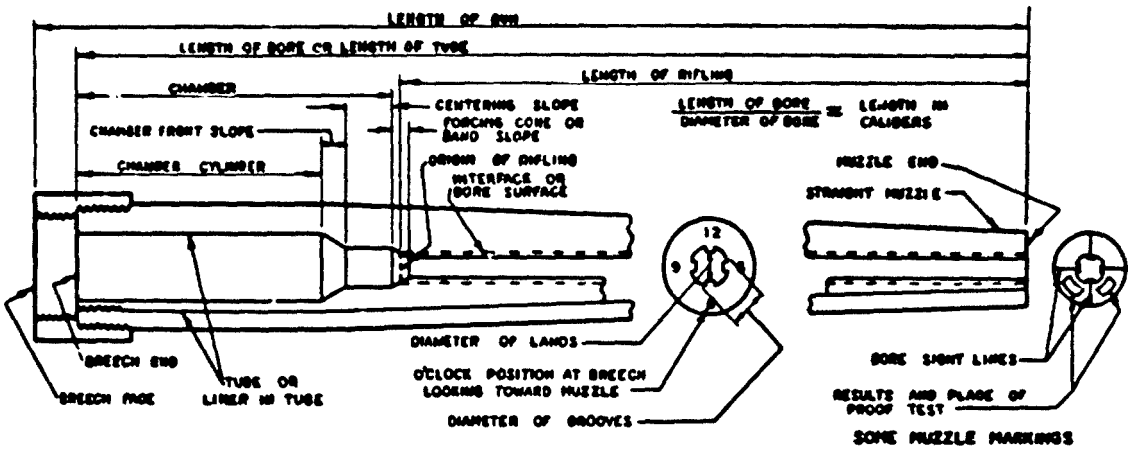

FIGURE A AVERAGE GUN

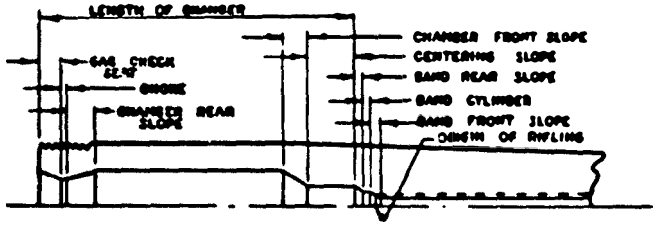

FIGURE B SOME LARGE CALIBER GUNS

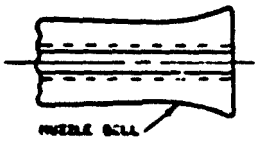

FIGURE A-1

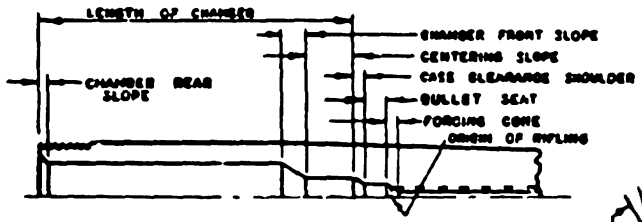

FIGURE C SOME SMALL ARMS

FIGURE F RIFLING IN SMALL GUNS

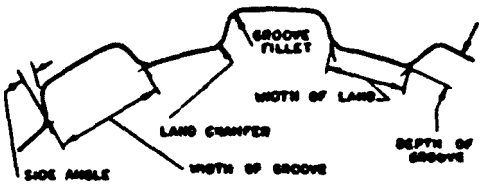

FIGURE G RIFLING IN LARGE GUNS

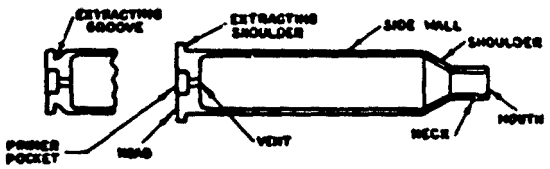

FIGURE D CARTRIDGE CASE

FIGURE H SMALL ARMS BULLET

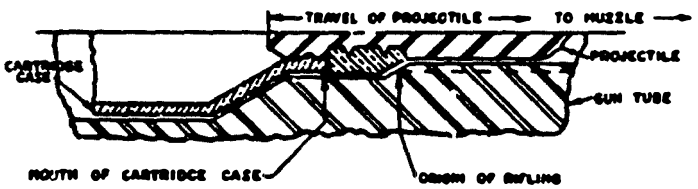

FIGURE E RELATIVE POSITION OF MOUTH OF CARTRIDGE CASE AND ORIGIN OF RIFLING IN GUNS USING FIXED AMMUNITION

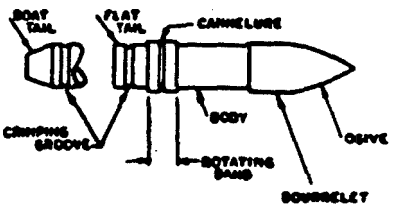

FIGURE I ARTILLERY TYPE PROJECTILE

Figure 4-66. Nomenclature of rifling and cartridge cases

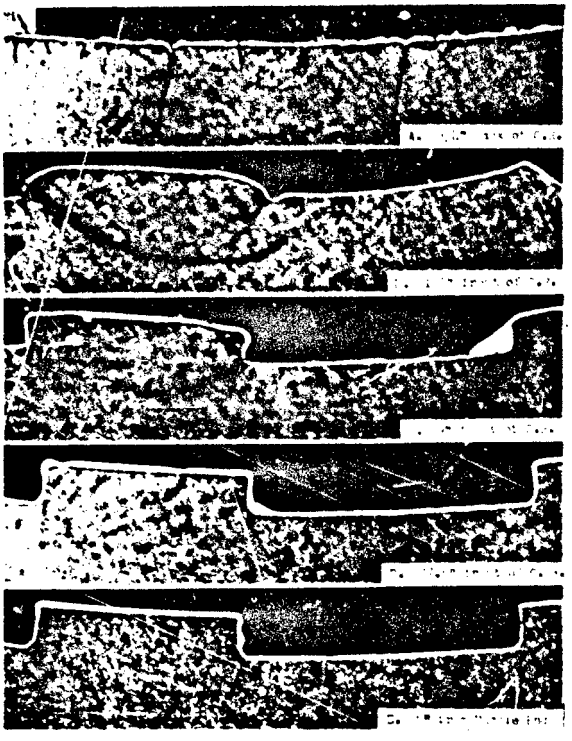

Figure 4-67. Erosion-stress damage, 105-mm howitzer M2A1

Figure 4-68. Erosion-stress damage, 76-mm gun tube M1

2. Since the torque is applied more uniformly, the maximum shearing stress, acting to rupture the engraving, is lower.

3. Some work has been done on the design of guns with zero twist for the first five inches or so of the rifling, and increasing twist for the remainder. It is thought that this type of design will help eliminate the shearing of rotating bands by worn tubes in guns using fixed ammunition. In these guns, the projectile is not rammed, and erosion at the origin of the rifling leaves an unrifled gap, across which the projectile jumps when the gun is fired. The projectile, when it encounters the rifling in present designs, is subjected to very high rotational acceleration, and shearing of the band often results.

b. The Major Disadvantage is that the contour of the engraving changes as the projectile moves forward. This results in shearing of the metal of the band in the grooves of the rifling. The wider the band, the greater the changes of contour of the engraved band.

4-153. Typical Values of Twist. These are shown in table 4-32 for representative guns and howitzers (marked H).

Table 4-32

Values of twist

Caliber	Twist calibers (uniform)
75-mm M1	1 to 20
76-mm M1A1	1 to 40
90-mm M2	1 to 20
105-mm H M3	1 to 20
120-mm M1	1 to 30
155-mm M1	1 to 25
155-mm H M1	1 to 25
8-in. M1	1 to 25
240-mm H M1	1 to 25

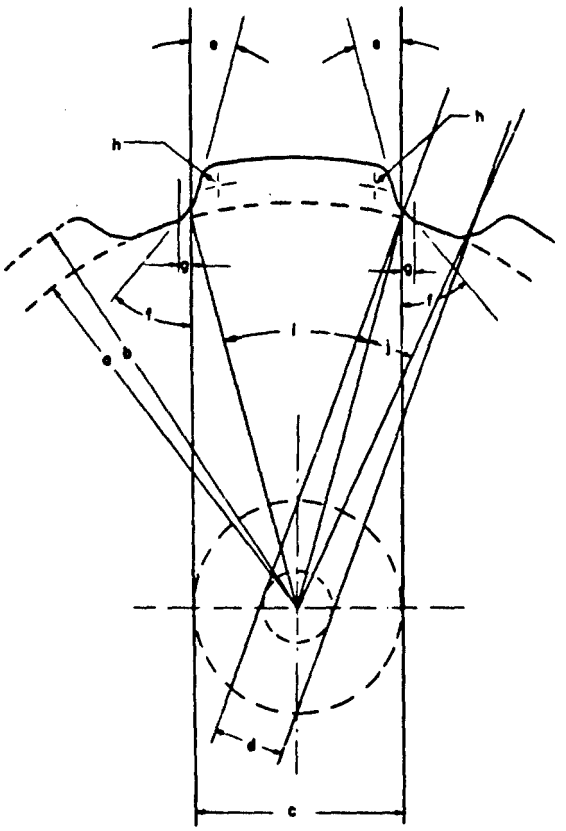

Figure 4-69. Dimensioning of rifling

4-154. Determination of Rifling Twist. Muzzle velocity and twist determine the spin, the sole purpose of which is to stabilize the projectile in flight. If spin rate is too low, the projectile is unstable; if too great, the projectile may be overstable when fired at high angles of quadrant elevation. For a discussion of the twist necessary to assure the stability of a given projectile, refer to paragraphs 3-1 through 3-22.

For uniform twist rifling, the slope of the rifling is constant and is expressed by

$$\tan \theta = \frac{\pi}{n}$$

The developed curve of gain twist rifling usually takes the form of the semicubical parabola

$$x^{3/2} = 2py$$

where x represents the travel through the bore, y represents the distance through which a point on the outside of the projectile has rotated, and p is a constant. This equation assumes zero twist at the origin of the rifling.

The slope of the rifling at any point may be obtained by differentiating:

$$\frac{dy}{dx} = \tan \theta = \frac{3x^{1/2}}{4p} = \frac{\pi}{n}$$

where n varies with the distance along the tube.

The rotational velocity of the projectile ω at any point in its travel is

$$\omega = \frac{2v \tan \theta}{d}$$

where

- v = velocity of translation of the projectile at any point in the bore, fps
- θ = angle of twist of the rifling at the same point
- ω = angular velocity of the projectile, radians per second
- d = bore diameter, ft.

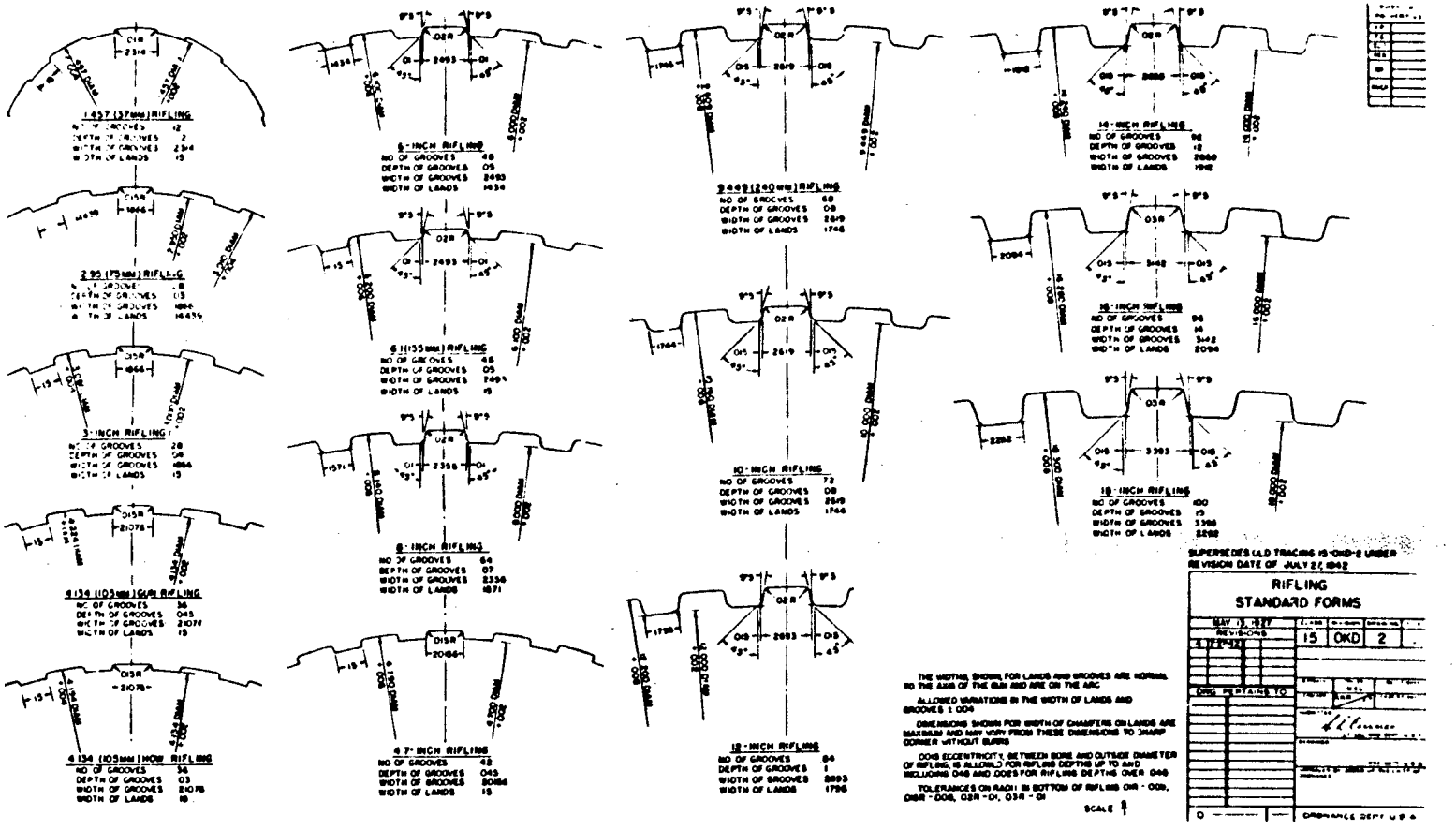

Figure 4-70. Standard rifling forms

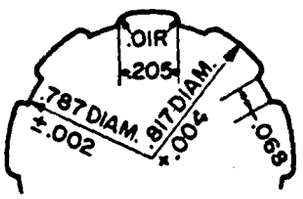

.787 (20MM) RIFLING

NO. OF GROOVES	9
DEPTH OF GROOVES	.015
WIDTH OF GROOVES	.205
WIDTH OF LANDS	.068

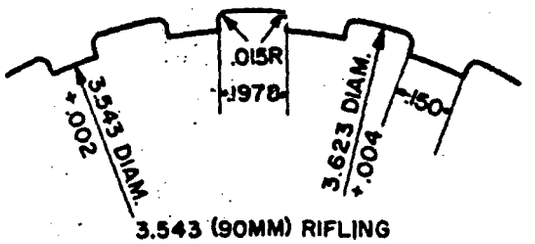

3.543 (90MM) RIFLING

NO. OF GROOVES	32
DEPTH OF GROOVES	.04
WIDTH OF GROOVES	.1978
WIDTH OF LANDS	.150

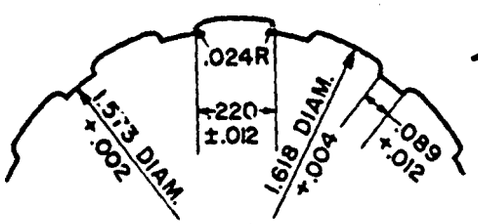

1.573 (40MM) RIFLING

NO. OF GROOVES	16
DEPTH OF GROOVES	.0225
WIDTH OF GROOVES	.220
WIDTH OF LANDS	.089

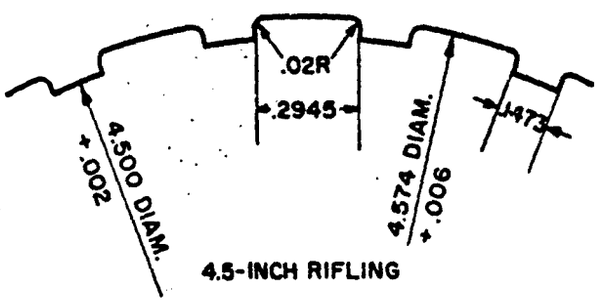

4.5-INCH RIFLING

NO. OF GROOVES	32
DEPTH OF GROOVES	.037
WIDTH OF GROOVES	.2945
WIDTH OF LANDS	.1473

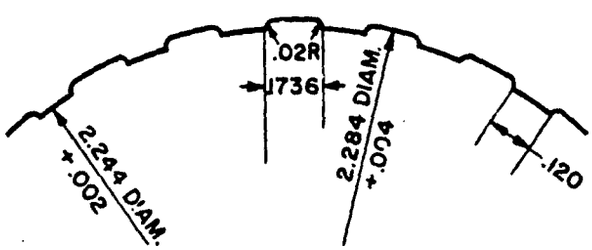

2.244 (57MM) RIFLING

NO. OF GROOVES	24
DEPTH OF GROOVES	.02
WIDTH OF GROOVES	.1736
WIDTH OF LANDS	.120

THE WIDTHS, SHOWN, FOR LANDS AND GROOVES ARE NORMAL TO THE AXIS OF THE GUN AND ARE ON THE ARC.

ALLOWED VARIATIONS IN THE WIDTH OF LANDS AND GROOVES ±.004. UNLESS OTHERWISE SPECIFIED.

DIMENSIONS SHOWN FOR WIDTH OF CHAMFERS ON LANDS ARE MAXIMUM AND MAY VARY FROM THESE DIMENSIONS TO SHARP CORNER WITHOUT BURRS.

.0015 ECCENTRICITY, BETWEEN BORE AND OUTSIDE DIAMETER OF RIFLING, IS ALLOWED FOR RIFLING DEPTHS UP TO AND INCLUDING .045 AND .0025 FOR RIFLING DEPTHS OVER .045

TOLERANCES ON RADII IN BOTTOM OF RIFLING .01R-.005, .015R-008, .02R-.01, .024R-.01.

Figure 4-71. Standard rifling forms

REFERENCES AND BIBLIOGRAPHY

1. Rifling and Rotating Band Design, Report No. WAL 760/410, Watertown Arsenal, Watertown, Mass.

2. Lee, E. H., and B. W. Schaffer, Some Problems of Plastic Flow Arising in the Operation of Engraving Bands on Projectiles, Report No. WAL 893/81-84.

3. Nadai, A., "Plasticity," McGraw-Hill, 1931, pp. 221-225.

4. Ross, E. W., Jr., Theoretical Investigation of Identation Pressures on Rotating Bands, Report No. WAL 760/525, Watertown Arsenal, Watertown, Mass.

5. Bluhm, J. I., On the Influence of End Friction of Undercut Angle on the Failure of a Rotating Band Under Centrifugal Forces, Report No. WAL 760/520, Watertown Arsenal, Watertown, Mass.

6. Deformation Characteristics of Copper and Alpha Brasses, Frankford Arsenal Report No. R-1021.

7. Salmassey, O. K., An Investigation of Properties of Sintered Iron. Purdue University, June 1953.

STRESS IN SHELL

LIST OF SYMBOLS

Symbol	Definition	Unit
A	Area of bore of gun	sq in.
a	Linear acceleration	ft per sec^2
d	Diameter of bore of gun (across lands)	in.
d_1	Inside diameter of projectile	in.
d_2	Outside diameter of projectile	in.
d'_o	Diameter of assumed shear circle in base of shell	in.
F	Maximum force on base of projectile and rotating band	lb
F_T	Maximum tangential force on projectile wall	lb
F_W	Hoop tension (force) in wall of projectile resulting from rotation of shell	lb
F'_T	Tangential force at section of shell	lb
f'	Setback force	lb
g	Acceleration due to gravity	ft per sec^2
h_1	Total depth of filler from nose (head)	in.
h_2	Depth of filler from nose end of cavity to section under consideration	in.
I	Polar moment of inertia	lb-in.^{2}
I'	Polar moment of inertia of metal parts forward of section when section is at front of rotating band, or rearward of section when section is behind rotating band	lb-in.^{2}
n	Twist of rifling	calibers per turn
P	Maximum propellant pressure (usually taken as 1.2 times max. allowable pressure for gun)	lb per sq in.
$P_o{}^h$	Filler pressure due to setback	lb per sq in.
$P_o{}^r$	Filler pressure due to rotation	lb per sq in.
R_o	Inside radius of projectile	in.
R_1	Outside radius of projectile	in.
r	Bourrelet radius	in.
S	Compressive strength of band	lb per sq in.
S_{T_1}, S_{T_2}, etc.	Tangential stresses	lb per sq in.
S_{L_1}, S_{L_2}, etc.	Longitudinal stresses	lb per sq in.
S_{R_1}, S_{R_2}, etc.	Radial stresses	lb per sq in.
S_{S_1}, S_{S_2}, etc.	Shear stresses	lb per sq in.
S_o	Static yield stress in tension	lb per sq in.
S_R	Combined or resultant stress	lb per sq in.
T	Torque applied to projectile	lb-in.
t_b	Base thickness	in.
V	Muzzle velocity	ft per sec
W	Total projectile weight	lb
W'	Weight of metal parts forward of section considered	lb
W_f	Weight of filler forward of section considered	lb
α	Angular acceleration	radians per sec^2
Δ	Density of metal in walls of projectile	lb per cu in.
δ	Density of filler charge	lb per cu in.
ω	Angular velocity	radians per sec

INTRODUCTION

4-155. Failure of the Shell Under Stress may be said to occur when stresses are sufficient to cause enough deformation of the shell components to prevent proper functioning of the shell or cause damage to the gun. A certain amount of deformation can and will take place when the shell is fired. However, if the deformation is not great enough to cause premature detonation of the explosive filler, the shell is considered to be successful, stresswise at least. This criterion is much less stringent than that used for machine parts, which allows only elastic deformation. However, it is based on the fact that a shell is designed to be used only once, and hence this limited amount of permanent deformation may be permitted.

4-156. The Problem of Stress Analysis in the shell resolves itself into the following three phases.

a. The determination of the maximum forces acting on the shell during firing, that is, of the loading conditions on the shell, in the gun.

b. The determination, for critical points in the body of the shell, of the principal stresses resulting from each of these forces.

c. The utilization of yield criteria to determine if the stress state at critical points of the shell body is in an elastic or plastic state of deformation.

FORCES ACTING ON SHELL

4-157. Forces During Loading for Firing. During loading, the following forces must be considered.

a. Forces caused by eccentric loading of the shell can cause bending stresses in the nose of the shell, which might tend to loosen the bond between the armor-piercing cap and the body of the APC shell, or between the windshield and body of the projectile.

b. Excessively hard or eccentric ramming of the separate-loading shell can cause flattening of the lands near the origin of the rifling.

c. Eccentric ramming may cause cocking of the projectile in the chamber. If the projectile is cocked, a transverse moment will be produced by the gas pressure when the gun is fired. This moment, together with the forces induced by the spinning of the projectile, can cause the projectile to ballot (move from side to side) in the bore. If excessive clearance between bourrelet and bore exists, the balloting forces developed may be sufficient to flatten the lands of the rifling. A secondary effect of excessive bourrelet clearance is to induce large values of initial yaw when the projectile leaves the gun (see, in paragraphs 3-23 to 3-48, the discussion of initial yaw). Balloting may be minimized by designing the shell for minimum bourrelet clearance. Present practice defines minimum bourrelet clearance as 0.002 in. plus 0.001 times the caliber in inches, with a minimum of 0.004 in. for 37-mm and smaller projectiles. A tolerance of plus zero minus 0.005 in. is specified for all projectiles. Thus, projectiles may be designed for a maximum clearance of 0.007 in. plus 0.001 times the caliber in inches or, for 37-mm and smaller, 0.009 in.

d. In loading mortar shell there is some possibility of damage to the fins as a result of dropping the projectile into the bore. However, the magnitude of these forces is so small compared to those applied by the pressure of the propellant gases that it can be discounted. A greater possibility of damage to mortar shell is that from rough handling and the uneven pressures resulting from turbulence of the propellant gases. The effect of both of these can be minimized by enclosing the fins in a shroud.

4-158. Forces During Firing. When the gun is fired the following forces are normally considered in deriving shell stress formulas.

a. The force from the pressure of the propellant gases against the base of the projectile, the rear of the rotating band, and the projectile wall to the rear of the rotating band.

b. The inertial or setback forces induced in the shell filler and the shell wall by the forward acceleration of the projectile.

c. The tangential inertia forces in the wall of the shell arising from the angular acceleration imparted to the shell by the rifling.

d. The centrifugal forces induced in the wall of the shell and in the filler by the rotation imparted by the rifling.

e. A radially compressive force applied at the seat of the rotating band when the band is engraved by the rifling in the forcing cone of the gun. A considerable amount of experimental work must be done before this force can be precisely evaluated. Although it is known to be

of relatively large magnitude, in computations of total stress on shell it has been disregarded without apparent bad effect on the design problem. For further information, see paragraphs 4-117 through 4-154.

4-159. Force Resulting from Propellant Gas Pressure. The maximum force (F) on the base of the projectile, the rear of the rotating band, and the shell wall behind the rotating band, is equal to the maximum pressure of the propellant (P) multiplied by the area of the bore (A). For design purposes, the maximum pressure is usually taken as the maximum rated copper pressure for the projectile.

$$F = PA \tag{213}$$

4-160. Setback Forces.

a. Setback Forces are caused by the acceleration (a) of the projectile.

$$a = \frac{F}{W/g} \tag{214}$$

where W is the total weight of the projectile in pounds, and g is the acceleration of gravity in ft per sec^2. Combining equations (213) and (214).

$$a = \frac{PAg}{W} \tag{215}$$

b. Setback of Shell Walls. At any transverse section of the projectile the inertia of the mass of the metal parts of the projectile ahead of that section will exert a compressive force (f') in the projectile wall.

$$f' = \frac{W'}{g} a \tag{216}$$

where W' is the weight of metal forward of the section and a is the common acceleration of all parts of the projectile, assuming the projectile acts as a rigid body. Combining equations (215) and (216)

$$f' = \frac{W'}{W} PA \tag{217}$$

c. Setback of Filler. The filler charge of a projectile is considered to act as a liquid (see subparagraph 4-177d). For the purpose of stress analysis it is convenient to compute the pressures in the charge, rather than the forces. This pressure, acting normal to the walls of the shell, produces both a longitudinal tensile stress and a tangential, or hoop, stress in the shell walls. The pressure p_o^h at any section of the shell is

$$p_o^h = \delta h_2 \frac{a}{g} \tag{218}$$

Combining equations (218) and (215).

$$p_o^h = \frac{\delta h_2 PA}{W} \tag{219}$$

4-161. Tangential Force. The tangential force, induced in the rotating band and transmitted to the wall of the shell, is caused by the angular acceleration. This angular acceleration (α) may be computed from the linear acceleration, the twist of the rifling, and the diameter of the projectile.

$$\alpha = \frac{2\pi a}{n(d/12)} = \frac{24\pi a}{nd} \tag{220}$$

where n is the rifling twist in calibers per turn, and d is the caliber of the projectile in inches.

The torque (T), in lb-in., applied to the projectile to give the angular acceleration (α) is

$$T = \frac{I}{g}\alpha \tag{221}$$

where I is the polar moment of inertia of the projectile in $lb\text{-}in.^2$, and T is in lb-in. The tangential force is

$$F_T = \frac{T}{d/2} \tag{222}$$

Combining equations (222), (221), (220), and (215).

$$F_T = \frac{48\pi IPA}{nd^2W} \tag{223}$$

As a simplification, assume

$$A = \frac{\pi d^2}{4}$$

$$F_T = \frac{12\pi^2 IP}{nW} \qquad (224)$$

since F_T is directly proportional to propellant pressure, maximum F_T will occur when propellant pressure is a maximum. This force is of interest primarily in the design of rotating bands. For shell design the average force acting at a given cross section of the shell is pertinent. If in equation (223) $(d_1^2 + d_2^2)/2$ is substituted for d^2, we obtain

$$F'_T = \frac{96\pi I' PA}{nW(d_1^2 + d_2^2)} \qquad (225)$$

where I' is the polar moment of inertia of the metal parts forward of the section if it is to the front of the rotating band, or rearward of the section if it is behind the rotating band.

4-162. Pressure on Shell Wall Resulting from Rotation of Filler. When the filler is regarded as a liquid, the maximum pressure (p_o^r) resulting from the rotation of the projectile will occur at the periphery of the cylindrical charge. This pressure will act directly on the inner wall of the shell.

$$p_o^r = \frac{\delta d_1^2 \omega^2}{144g} \qquad (226)$$

where δ is the density of the filler in lb per $in.^3$, d_1 is the inside diameter of the shell in inches, ω is the angular velocity of the shell in radians per second, and g is the acceleration of gravity in ft per sec^2. The factor of 12 is introduced in the denominator in order to convert g into units of in. per sec^2.

The angular velocity (ω) may be expressed in terms of the linear velocity (V) and the twist of the rifling (n) and the diameter of the projectile (d).

$$\omega = \frac{24\pi V}{nd} \qquad (227)$$

Combining equations (226) and (227)

$$p_o^r = 1.23\delta \left(\frac{V}{n}\right)^2 \left(\frac{d_1}{d}\right)^2 \qquad (228)$$

4-163. Tension in Wall Resulting from Rotation. The stress in the shell wall, resulting from the rotation of the projectile, is small compared to the stress caused by the setback of the filler. Therefore, in order to avoid the complex calculation required to find stress distribution by a thick-cylinder formula, it is permissible to approximate the stress by considering the shell to be a thin cylinder. See figure 4-72.

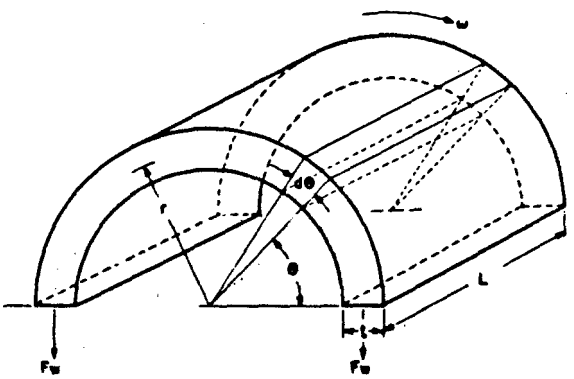

Figure 4-72. Hoop tension force diagram

Assuming a thin shell, r may be taken as the mean radius. The elemental mass is then defined as

$$dm = \frac{r d\theta Lt\Delta}{g} \qquad (229)$$

where Δ is the density of the metal. Considering the semicylinder as a free body and equating the forces

$$2F_W = \frac{\Delta Lt}{g} \int_0^{\pi} r^2\omega^2 \sin\theta \, d\theta$$

$$= \frac{\Delta Lt}{g} 2r^2\omega^2$$

but since r, average radius, equals $\left(\frac{R_1 + R_o}{2}\right)\frac{1}{12}$

where R_1 and R_o are the inner and outer radii (in inches)

$$F_W = \frac{\Delta Lt}{g}(R_1 + R_o)^2\left(\frac{1}{24}\right)^2\omega^2$$

substituting the value of ω in equation (227).

$$F_W = \frac{\Delta Lt}{g}(R_1 + R_o)^2\left(\frac{1}{24}\right)^2\left(\frac{24\pi V}{nd}\right)^2$$

$$= \frac{\Delta Lt}{g}(R_1 + R_o)^2\pi^2\left(\frac{V}{n}\right)^2\left(\frac{1}{d}\right)^2$$

As expressed originally, g is in in. per sec^2. Expressing g in ft per sec^2

$$F_W = \frac{12\Delta Lt\pi^2}{d^2 g}(R_1 + R_o)^2\left(\frac{V}{n}\right)^2 \quad (230)$$

For steel, $\Delta = 0.283$ lb per in.^{3}. We get

$$F_W = 1.04\left(\frac{R_1 + R_o}{d}\right)^2\left(\frac{V}{n}\right)^2 (Lt) \quad (231)$$

4-164. Summary of Forces and Pressures Acting on Projectile During Firing.

a. Force Resulting from Propellant Gas Pressure.

$$F = PA \quad (213)$$

b. Setback of Metal Parts.

$$f' = \frac{W'}{W}PA \quad (217)$$

c. Setback of Filler.

$$p_o{}^h = \frac{\delta h_2 PA}{W} \quad (219)$$

d. Tangential Force on Rotating Band.

$$F_T = \frac{48\pi IPA}{nd^2 W} \quad (223)$$

$$= \frac{12\pi^2 IP}{nW} \quad (224)$$

e. Tangential Force at Given Section of Shell.

$$F'_T = \frac{96\pi I'PA}{nW(d_1^2 + d_2^2)} \quad (225)$$

f. Pressure on Shell Wall Resulting from Rotation of Filler.

$$p_o{}^r = 1.23\left(\frac{V}{n}\right)^2\left(\frac{d_1}{d}\right)^2 \quad (228)$$

g. Tension Force in Wall Resulting from Rotation.

$$F_W = \frac{12\Delta Lt\pi^2}{d^2 g}(R_1 + R_o)^2\left(\frac{V}{n}\right)^2 \quad (230)$$

STRESSES RESULTING FROM FORCES

4-165. Signs of Stresses. It is important to note that the algebraic sign of a stress indicates whether the stress is compressive or tensile. It is arbitrary but standard practice to assign a plus sign to indicate a tensile stress and a minus sign to denote compressive stress. Thus, for example, in equation (232) the plus sign indicates tension and in equation (233) the minus sign indicates compression. The matter of stress signs becomes especially important when the various yield criteria (see paragraphs 4-172 to 4-177) are employed.

Signs are normally attached only to normal stresses acting on an elemental volume of material; the signs of the shear stresses usually are not considered in practice. It should be noted that the tangential, radial, and longitudinal (axial) stresses herein calculated are all normal stresses acting perpendicular to the faces of an elemental volume of shell material

at the section under consideration. These stresses, called principal stresses, are the maximum normal stresses possible under the given loading conditions in the gun — that is, such would be the case if the formulas herein were exact. (See paragraph 4-177.)

4-166. Tangential Stresses. The present practice of Picatinny Arsenal is to base the determination of stress (resulting from internal or external pressure) in the shell walls upon the equations developed by Lamé for open-ended cylinders.

a. Internal Pressure. Maximum tangential stress (S_T) for this case is

$$S_{T_1} = +(p_o^h + p_o^r)\left(\frac{R_1^2 + R_o^2}{R_1^2 - R_o^2}\right) \quad (232)$$

b. External Pressure. Maximum tangential stress for this case is

$$S_{T_2} = -P\left(\frac{2R_1^2}{R_1^2 - R_o^2}\right) \quad (233)$$

c. Stress Resulting from Rotation of Wall. The tension in the shell wall (F_W) resulting from its rotation is

$$F_W = 1.04\left(\frac{R_1 + R_o}{d}\right)^2\left(\frac{V}{n}\right)^2 Lt \quad (231)$$

The resultant stress (S_{T_3}) is

$$S_{T_3} = \frac{F_W}{Lt}$$

$$S_{T_3} = +1.04\left(\frac{R_1 + R_o}{d}\right)^2\left(\frac{V}{n}\right)^2 \quad (234)$$

4-167. Radial Stresses.

a. The radial stress in the inner fiber of the wall of the shell results from the internal pressure acting on that section.

b. The stress in the walls resulting from filler setback S_R is

$$S_R = -p_o^h$$

c. The stress in the walls resulting from filler rotation S_R is

$$S_R = -p_o^r$$

d. The total radial stress is

$$-p_o^h - p_o^r$$

$$S_{R_1} = -(p_o^h + p_o^r) \quad (235)$$

e. The radial stress at the inner fiber of the base results from the moment applied by the wall, in the case of a flat base, or from the moments applied to the base and the wall, in the case of a round base. The pressures producing these moments are:

1. Pressure resulting from setback of the filler, p_o^h, where $h = h_1$;
2. Chamber pressure, P;
3. Pressure resulting from rotation of the filler, p_o^r. Since p_o^r is low compared to the other pressures (in fact, it is zero at the center of rotation), and since the stress formulas used are conservative, p_o^r usually is disregarded.

For a Flat Base, the stress S_{R_2} is

$$S_{R_2} = +\frac{R_o^2}{t_b^2}(P - p_o^h) \quad (236)$$

where t_b is the minimum base thickness.

For a Round Base (internally), separate equations are used to compute stress resulting from chamber pressure and from filler setback.

Stress resulting from chamber pressure (S_{R_3}) is

$$S_{R_3} = -P\left[\frac{3R_1^3}{2(R_1^3 - R_o^3)}\right] \quad (237)$$

Stress resulting from setback pressure (S_{R_4}) is

$$S_{R_4} = +p_o^h\left[\frac{R_1^3 + 2R_o^3}{2(R_1^3 - R_o^3)}\right] \quad (238)$$

The total stress on the base is the sum of the two.

4-168. Longitudinal Stresses. Longitudinal stress in the shell wall is produced by the difference between the setback of the metal parts forward of the section under consideration, and the filler setback and rotational pressure acting on the base and wall of the shell to the rear of the section.

Longitudinal stress in the base results from the filler setback and rotational pressure.

a. Stress in Shell Wall Resulting from Setback of Filler.

$$S_{L_1} \quad \frac{p_o{}^h}{\pi h_2(R_1{}^2 - R_o{}^2)} \pi h_2 R_o{}^2$$

- (vol. filler forward of section)

This may be written

$$\frac{p_o{}^h R_o{}^2}{(R_1{}^2 - R_o{}^2)} - \frac{h_2 \delta PA/W}{\pi h_2(R_1{}^2 - R_o{}^2)}$$

(vol. filler forward of section) (239)

$$= \frac{p_o{}^h R_o{}^2}{R_1{}^2 - R_o{}^2} - \frac{PAW_f}{\pi(R_1{}^2 - R_o{}^2)W}$$

b. Stress in Shell Wall Resulting from Rotation of Filler. This stress results from the average rotational pressure acting on the base. The average pressure may be shown to be equal to $\frac{1}{2} p_o{}^r$.

$$S_{L_2} = +\frac{1}{2} p_o{}^r \left[\frac{R_o{}^2}{R_1{}^2 - R_o{}^2}\right] \qquad (240)$$

Since maximum rotation does not occur until near the gun muzzle, the stress S_{L_2} is small in comparison with S_{L_1} calculated at peak pressure. It is therefore expedient to neglect S_{L_2} in stress calculations.

c. Stress in Wall Resulting from Setback of Metal Parts.

$$S_{L_3} = - \frac{W'/WPA}{\pi(R_1{}^2 - R_o{}^2)} \qquad (241)$$

A simplification can be arrived at by adding $S_{L_1} + S_{L_3}$.

$$S_{L_4} = - \frac{PA(W' + W_f)}{\pi(R_1{}^2 - R_o{}^2)W} + p_o{}^h \frac{R_o{}^2}{(R_1{}^2 - R_o{}^2)} \qquad (242)$$

d. Stress in Base Resulting from Setback of Filler. This stress is numerically equal to $p_o{}^h$

$$S_{L_5} = -p_o{}^h \qquad (243)$$

e. Stress in Base Resulting from Rotation of Filler. This stress varies from zero, at the center of rotation, to $p_o{}^r$ at R_o in accordance with the equation

$$S_{L_6} = - p_o{}^r \left(\frac{R'}{R_o}\right)^2 \qquad (244)$$

where R' is the radius of the element under consideration. Since $p_o{}^r$ is small compared to $p_o{}^h$, and since the element usually considered is at the rotational center, this stress may be disregarded.

4-169. Shear Stresses.

a. In Base. For a flat-bottomed shell with small radius fillets, the shear stress on the area $\pi d_o t_b$ should be computed. The pressure producing this shear is the algebraic sum of the chamber pressure (p), the filler setback pressure ($p_o{}^h$), and the average filler rotational pressure $\frac{1}{2} p_o{}^r$. Because it is extremely small compared with the other pressures, the filler rotational pressure usually is omitted from calculations.

$$S_{S_1} = (P - p_o{}^h) \frac{\pi d_o{}^2}{4\pi d_o t_b}$$

$$S_{S_1} = (P - p_o{}^h) \frac{d_o}{4t_b} \qquad (245)$$

b. At Any Section of Shell Wall. The tangential force resulting from the angular acceleration of the metal parts forward of the section if it is in front of the rotating band, or rearward of the section if it is behind the rotating band, is

$$F'_T = \frac{96\pi I' PA}{nW(d_1{}^2 + d_2{}^2)} \qquad (225)$$

The annular area of the shell wall is

$$\frac{\pi(d_2{}^2 - d_1{}^2)}{4}$$

The stress produced is

$$S_{S_2} = \left[\frac{96\pi l' PA}{nW(d_1^2 + d_2^2)}\right]\left[\frac{4}{\pi(d_2^2 - d_1^2)}\right]$$

$$S_{S_2} = \frac{384 l' PA}{nW(d_2^4 - d_1^4)} \qquad (246)$$

4-170. Summary of Stress in Shell. Table 4-33 summarizes the results obtained in paragraphs 4-166 through 4-169.

4-171. Stresses in Shell. On a new design, several critical elements and sections are chosen for stress analysis. If the design checks for these, it is considered good. The elements and sections ordinarily used are:

a. The inside fiber at the center of the base
b. The inside fiber just under the rear of the rotating band
c. The inside fiber just under the front of the rotating band
d. The inside fiber just to the rear of the bourrelet
e. Shear in the base
f. Shear at the section just to the rear of the rotating band
g. Shear at the section just to the front of the rotating band
h. Shear at the section just to the rear of the bourrelet. These elements and sections are shown in table 4-34, along with a tabulation of the appropriate stresses to be considered at each point.

Table 4-33

*Summary of stress formulas**

Stress	Equation number	Symbol	Formula
Tangential stresses			
Internal pressure	(232)	S_{T_1}	$+(p_o^h + p_o^r)\left(\frac{R_1^2 + R_o^2}{R_1^2 - R_o^2}\right)$
External pressure	(233)	S_{T_2}	$-P\left(\frac{2R_1^2}{R_1^2 - R_o^2}\right)$
Rotation of wall	(234)	S_{T_3}	$+\frac{1.04\,(R_1 + R_o)^2}{d^2}\left(\frac{V}{n}\right)^2$
Radial stresses			
Filler pressure on sidewall	(235)	S_{R_1}	$-\left(p_o^h + p_o^r\right)$
Flat base	(236)	S_{R_2}	$+\frac{R_o^2}{t_b^2}(P - p_o^h)$
Round base — chamber pressure	(237)	S_{R_3}	$-P\left[\frac{3R_1^3}{2(R_1^3 - R_o)^3}\right]$
Round base — filler pressure	(238)	S_{R_4}	$+p_o^h\,\frac{R_1^3 + 2R_o^3}{2(R_1^3 - R_o^3)}$

Table 4-33

Summary of stress formulas (cont)*

Stress	Equation number	Symbol	Formula
Longitudinal stresses			
Filler setback pressure — in wall	(239)	S_{L_1}	$+\left(p_o^{\,h}\right)\left(\frac{R_o^{\,2}}{R_1^{\,2}-R_o^{\,2}}\right)$
Filler rotational pressure — in wall†	(240)	S_{L_2}	$\frac{1}{2}p_o^{\,r}\left(\frac{R_o^{\,2}}{R_1^{\,2}-R_o^{\,2}}\right)$
Setback of metal parts forward of element — in wall	(242)	S_{L_4}	$-\frac{W'/W\,PA}{\pi(R_1^{\,2}-R_o^{\,2})}$
Filler setback pressure — on base	(243)	S_{L_5}	$-p_o^{\,h}$
Shear stresses			
Shear in base	(245)	S_{S_1}	$(P-p_o^{\,h})\frac{d_o}{4t_b}$
Acceleration of metal parts — in wall‡	(246)	S_{S_2}	$\frac{384I'PA}{nW(d_2^{\,4}-d_1^{\,4})}$

* Tensile stresses are defined as positive; compressive stresses are defined as negative.
† Considered expedient to ignore this stress, as it is relatively small.
‡ If section is in front of rotating band, use moment of inertia of metal parts forward of section; if section is in back of rotating band, use moment of inertia of metal parts rearward of section.

YIELD CRITERIA

4-172. Yield Criteria Theories. The maximum or principal stresses in three mutually orthogonal directions on each element having been obtained, it is necessary to determine whether they produce elastic or plastic deformation at the points in question. Several theories to permit this have been advanced. Three widely used theories are:

1. Maximum shear (Tresca's rule of flow)
2. Maximum energy
3. Constant distortion (Hencky-Von Mises).

4-173. Maximum Shear Theory. This theory states that in a complex system of stresses permanent deformation begins when the greatest of the principal shearing stresses reaches the value of shear stress at yielding in a simple tension test. According to this theory, a material should fail in transverse planes that are inclined 45° to the direction of largest and smallest principal stresses. If algebraically S_1 is the greatest and S_3 is the least of the principal stresses, then the maximum shear stress is $\frac{1}{2}\left|S_1 - S_3\right|$, and permanent deformation occurs when $\left|S_1 - S_3\right| > S_o$, where S_o is equal to static yield stress in tension. Ductile materials, including most metals, do fail in this manner, but brittle materials behave otherwise. The critical value for yielding for a given state of stress given by this theory differs from that given by the Von Mises

Table 4-34

Stresses in shell

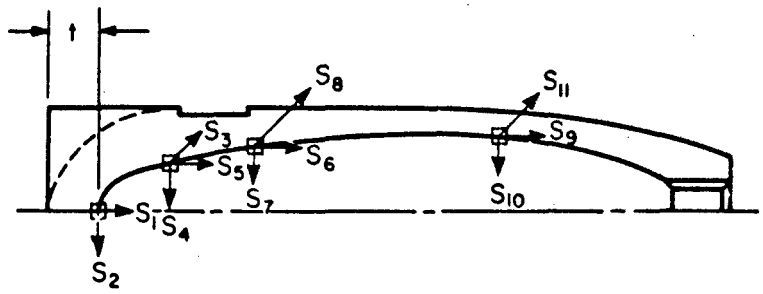

Stress	Type	Equation
S_1	Setback	S_{L_5}
S_2 (flat bottom)	Setback (flexural)	S_{R_2}
S_2 (round bottom)	Setback (flexural	$S_{R_3} + S_{R_4}$
S_3	Hoop of tangential	$S_{T_1} + S_{T_2} + S_{T_3}$
S_4 S_7 S_{10}	Radial	S_{R_1}
S_5 S_6 S_9	Setback	S_{L_4}
S_8 S_{11}	Hoop or tangential	$S_{T_1} + S_{T_3}$
S_{h_1}	Shear at base — thickness t	S_{S_1}
S_{h_2}	Shear at any cross section	S_{S_2}

theory below by 15 percent at most, and is in general smaller. Empirical data plots somewhere between the values predicted by both theories.

4-174. Maximum Energy Theory. According to this theory, failure begins to take place when the energy per unit volume reaches some definite amount equal to the energy per unit volume at which a bar of the material will fail in tension. Results of computations using this theory, however, are frequently difficult to correlate with experimental observations.

4-175. The Constant Distortion or Hencky-Von Mises Theory essays to bring the maximum energy theory into agreement with the fact that materials can sustain large hydrostatic pressure without plastic deformation. The strain energy associated with volume changes does not produce plastic flow. Therefore, this theory states in one form (due to Hencky) that incipient plastic flow occurs when the strain energy per unit volume, which changes the shape of a small cube of the material, reaches a critical value, namely, J/2G (where G is the modulus of rigidity of the material). J is the Von Mises yield function defined below.

Experiments indicate that in general the yield point of pure shear is about 0.6 of the yield point in pure tension for thin specimens, but a limiting value of 0.5 is obtained as the thickness of the test specimen is increased. This is in close agreement with values derived from the Hencky-Von Mises theory, which gives a value of $1/\sqrt{3}$. (The maximum shear theory above predicts a value of 0.5.) It is common practice to use this theory to predict when plastic flow begins, but there is no objection to using the maximum shear yield criterion if desired. The Hencky-Von Mises criterion is a more expedient one in the mathematical development of plasticity theory.

4-176. Mathematical Statement of Von Mises Yield Condition. If the principal stresses S_1, S_2, S_3 at the point of the material are given, where tensile stresses have positive signs and compressive stresses negative signs, then plastic flow or yielding begins when (form due to Von Mises)

$$J = S_1^2 + S_2^2 + S_3^2 - (S_1S_2 + S_2S_3 + S_3S_1) = S_o^2 \qquad (247)$$

where S_o is equal to static yield stress in tension.

If the value of the expression J on the left, called the "Von Mises yield function," obtained by substituting values for S_1, S_2, S_3, has a value less then S_o^2, then the material is still in an elastic state of stress and no yielding occurs. This is the state of stress generally desired in ordnance projectiles.

In the case of two-dimensional stress, one of the three principal stresses is zero, and those terms in the Von Mises yield function containing this principal stress drop out. Thus, if $S_3 = O$ for initial plastic flow, S_1 and S_2 must be such that

$$S_1^2 + S_2^2 - S_1 S_2 = S_o^2 \qquad (248)$$

The simplicity of the mathematical expression stating the Hencky-Von Mises yield criteria makes it unnecessary to use charts and nomograms, which are often found in the literature on the subject: these graphical methods are more of academic interest than practical aids to computation.

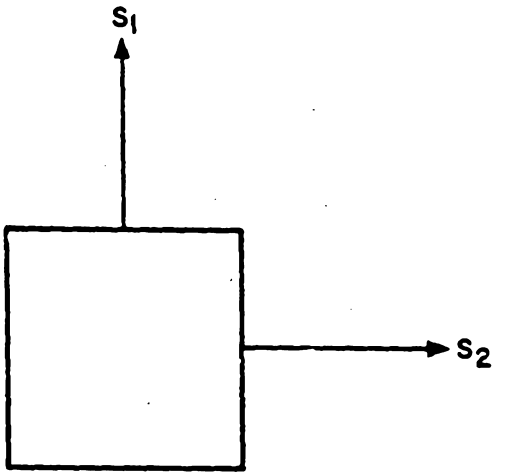

Example 1

Given: $S_1 = -40{,}000$ psi

$S_2 = 80{,}000$ psi

$S_3 = 50{,}000$ psi

$S_o = 100{,}000$ psi

$S_o^2 = 100 \times 10^8$ psi

Von Mises Yield Function.

$$= S_1^2 + S_2^2 + S_3^2 - (S_1 S_2 + S_2 S_3 + S_3 S_1)$$

$$= 16 \times 10^8 + 64 \times 10^8 + 25 \times 10^8 - (-32 \times 10^8 + 40 \times 10^8 - 20 \times 10^8)$$

$$= 105 \times 10^8 + 12 \times 10^8$$

$$= 117 \times 10^8 \text{ psi}$$

$117 \times 10^8 > S_o^2$; therefore, material is in plastic stress state.

Maximum Shear Criterion Solution.

$$S_2 > S_3 > S_1$$

$$|S_2 - S_3| = |80{,}000 - (-40{,}000)| = 120{,}000 > S_o$$

Therefore, material is in plastic state.

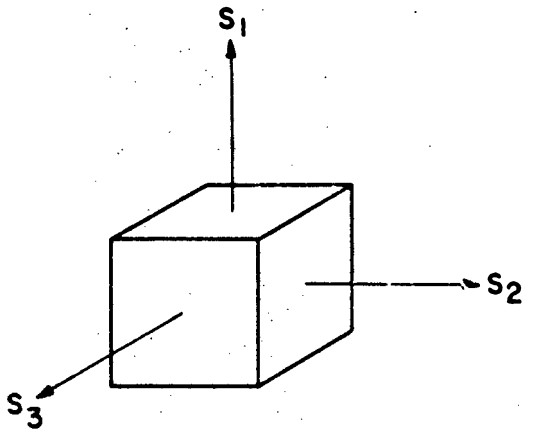

Example 2

$S_1 = -40{,}000$ psi

$S_2 = 60{,}000$ psi

$S_o = 100{,}000$ psi

$S_o^2 = 100 \times 10^8$ psi

Von Mises Yield Function.

$= S_1^2 + S_2^2 - S_1 S_2$

$= 16 \times 10^8 + 36 \times 10^8 + 24 \times 10^8$

$= 76 \times 10^8$ psi

$76 \times 10^8 < S_o^2$; therefore, material is indicated to be in elastic stress state.

Maximum Shear Criterion Solution.

$|S_2 - S_1| = |60{,}000 - (-40{,}000)| = 100{,}000 = S_o$

Therefore, an incipient plastic stress state is indicated.

Since empirical data on yielding plots between the Von Mises and maximum shear values, we can be reasonably assured that the stress state is an elastic one.

4-177. Discussion of Formulas and Methods.

a. Effect of Free-Body Analysis. It is to be noted that the stress formulas used herein are calculated by isolating the shell sections and treating them as free bodies. It is therefore evident that the restraints imposed by joining contiguous sections, that is, considering the shell body as an integral unit, will set up shear stress and bending moments at these junctions. These shear stresses and bending moments, which are caused by the effects of one section of shell on another, are ignored — and assumed (without justification) to be negligible. On the other hand, the mathematical treatment of these additional stresses — or in fact the exact analysis of shell stresses — is a formidable task, analytically and numerically; research on this subject is still in a state of flux.

b. Effect of Base. Presence of the base of the projectile materially increases the strength of the walls to the rear of the rotating band through beam action. The shorter the distance from the base to the band, the more important this reinforcement factor becomes.

c. Maximum Stresses. The forces that produce the linear acceleration are greatest at the point of maximum propellant pressure. (See figure 4-73.) This point is well behind the muzzle. The resultant stresses of these forces are greatest at this point. On the other hand, the forces that result from rotational velocity are greatest at the muzzle. Consequently, at this point, the stresses in the projectile resulting from these forces are greatest.

In the foregoing formulas the propellant pressure (P) usually is taken as 1.12 times the maximum allowable pressure for the projectile.

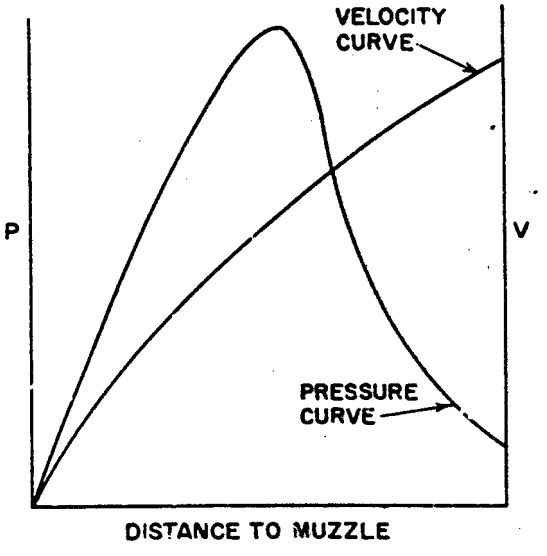

Figure 4-73. Pressure and velocity versus travel

The linear and angular accelerations are maximum when P is maximum. The value for ω (the angular velocity) is derived from the twist of rifling and the muzzle velocity. Using the value of P at maximum pressure and the values dependent upon V at muzzle velocity will give maximum calculated stresses in excess of those which would result from using the values dependent upon V at the point of maximum pressure. The difference is small and usually is on the side of safety. Therefore, it is not ordinarily objectionable.

d. Behavior of Filler. The analysis of stress in shell assumes that the filler acts as a liquid, that is, the setback pressure is assumed to act hydrostatically. This assumption, while it has proved a usable one, has not been substantiated. It is thought, therefore, that the filler may behave as an anisotropic plastic substance, the rheological properties of which have yet to be determined.

e. Weight Distribution. Distribution of metal in the projectile has a substantial effect on its stability. Any change made in weight distribution in order to attain greater strength must be checked to determine the corresponding effect on stability in flight.

f. Fin-Stabilized Projectiles. When a fin-stabilized projectile is fired there is little or no rotation. The stresses therefore are merely those attributable to the propellant pressure and the setback. Formulas, for these two effects, given in preceding paragraphs, are applicable to the fin-stabilized projectile. It is customary to check the stresses in the walls of the projectile just forward of the fin assembly. At that point the stresses are attributable to (1) propellant pressure, (2) setback of filler charge, and (3) setback of the walls ahead of the section and its attached parts.

g. Projectiles with Tapered Backs. Many mortar shells are made with tapered backs and they use no gas check or rotating band. The chamber pressure acts, therefore, on all sections to the rear of the bourrelet. This produces a longitudinal stress on the tapered section which must be considered in design. Consider the portion of such a shell forward of a section through the base. At the section, the outer radius is R_1 and the inner radius is R_o. The bourrelet radius is r, and the propellant pressure is P. The pressure acts on the projected area, $\pi (r^2 - R_1^2)$, forward of the section, and is distributed over the area of the shell wall, $\pi (R_1^2 - R_o^2)$. The stress produced, S_{L_6}, is:

$$S_{L_6} = P \left[\frac{\pi(r^2 - R_1^2)}{\pi(R_1^2 - R_o^2)} \right]$$

$$S_{L_6} = P \left(\frac{r^2 - R_1^2}{R_1^2 - R_o^2} \right) \qquad (249)$$

The total longitudinal stress at the element under consideration is therefore:

$$S_{L_3} + S_{L_4} + S_{L_6}$$

(See equations (241) and (242) for S_{L_3} and S_{L_4}.)

REFERENCES AND BIBLIOGRAPHY

1. Ordnance Engineering Notebook, Ammunition Section, Ordnance School.

2. Memorandum Report MR 51, Picatinny Arsenal Technical Division, 7 January 1954.

3. Schwartz, Picatinny Arsenal Notes.

4. Tschappat, W. H., "Textbook of Ordnance and Gunnery," John Wiley & Sons, New York, 1917.

5. Symposium on Shell Stresses, Picatinny Arsenal, September 1951.

6. Geldmacher, Little, and Roach, Review of Shell Stress Relationships, Physical Research Section Memorandum No. 9, Picatinny Arsenal, April 1955.

☆ U. S. GOVERNMENT PRINTING OFFICE : 1966 O - 211-205 (3687)

ENGINEERING DESIGN HANDBOOK SERIES

Listed below are the Handbooks which have been published or submitted for publication. Handbooks with publication dates prior to 1 August 1962 were published as 20-series Ordnance Corps pamphlets. AMC Circular 310-38, 19 July 1963, redesignated those publications as 706-series AMC pamphlets (i.e., ORDP 20-138 was redesignated AMCP 706-138). All new, reprinted, or revised Handbooks are being published as 706-series AMC pamphlets.

General and Miscellaneous Subjects

No.	Title
106	Elements of Armament Engineering, Part One, Sources of Energy
107	Elements of Armament Engineering, Part Two, Ballistics
108	Elements of Armament Engineering, Part Three, Weapon Systems and Components
110	Experimental Statistics, Section 1, Basic Concepts and Analysis of Measurement Data
111	Experimental Statistics, Section 2, Analysis of Enumerative and Classificatory Data
112	Experimental Statistics, Section 3, Planning and Analysis of Comparative Experiments
113	Experimental Statistics, Section 4, Special Topics
114	Experimental Statistics, Section 5, Tables
121	Packaging and Pack Engineering
134	Maintenance Engineering Guide for Ordnance Design
135	Inventions, Patents, and Related Matters (Revised)
136	Servomechanisms, Section 1, Theory
137	Servomechanisms, Section 2, Measurement and Signal Converters
138	Servomechanisms, Section 3, Amplification
139	Servomechanisms, Section 4, Power Elements and System Design
170(C)	Armor and Its Application to Vehicles (U)
250	Guns--General (Guns Series)
252	Gun Tubes (Guns Series)
270	Propellant Actuated Devices
290(C)	Warheads--General (U)
331	Compensating Elements (Fire Control Series)
355	The Automotive Assembly (Automotive Series), (Revised)

Ammunition and Explosives Series

175	Solid Propellants, Part One
176(C)	Solid Propellants, Part Two (U)
177	Properties of Explosives of Military Interest, Section 1
178(C)	Properties of Explosives of Military Interest, Section 2 (U)
179	Explosive Trains
210	Fuzes, General and Mechanical
211(C)	Fuzes, Proximity, Electrical, Part One (U)
212(S)	Fuzes, Proximity, Electrical, Part Two (U)
213(S)	Fuzes, Proximity, Electrical, Part Three (U)
214(S)	Fuzes, Proximity, Electrical, Part Four (U)
215(C)	Fuzes, Proximity, Electrical, Part Five (U)
244	Section 1, Artillery Ammunition--General, with Table of Contents, Glossary and Index for Series
245(C)	Section 2, Design for Terminal Effects (U)
246	Section 3, Design for Control of Flight Characteristics
247	Section 4, Design for Projection
248	Section 5, Inspection Aspects of Artillery Ammunition Design
249	Section 6, Manufacture of Metallic Components of Artillery Ammunition

Ballistic Missile Series

No.	Title
281(S-RD)	Weapon System Effectiveness (U)
282	Propulsion and Propellants
283	Aerodynamics
284(C)	Trajectories (U)
286	Structures

Ballistics Series

140	Trajectories, Differential Effects, and Data for Projectiles
150	Interior Ballistics of Guns
160(S)	Elements of Terminal Ballistics, Part One, Introduction, Kill Mechanisms, and Vulnerability (U)
161(S)	Elements of Terminal Ballistics, Part Two, Collection and Analysis of Data Concerning Targets (U)
162(S-RD)	Elements of Terminal Ballistics, Part Three, Application to Missile and Space Targets (U)

Carriages and Mounts Series

340	Carriages and Mounts--General
341	Cradles
342	Recoil Systems
343	Top Carriages
344	Bottom Carriages
345	Equilibrators
346	Elevating Mechanisms
347	Traversing Mechanisms

Military Pyrotechnics Series

186	Part Two, Safety, Procedures and Glossary
187	Part Three, Properties of Materials Used in Pyrotechnic Compositions

Surface-to-Air Missile Series

291	Part One, System Integration
292	Part Two, Weapon Control
293	Part Three, Computers
294(S)	Part Four, Missile Armament (U)
295(S)	Part Five, Countermeasures (U)
296	Part Six, Structures and Power Sources
297(S)	Part Seven, Sample Problem (U)

Materials Series*

149	Rubber and Rubber-Like Materials
212	Gasket Materials (Nonmetallic)
691	Adhesives
692	Guide to Selection of Rubber O-Rings
693	Magnesium and Magnesium Alloys
694	Aluminum and Aluminum Alloys
697	Titanium and Titanium Alloys
698	Copper and Copper Alloys
699	Guide to Specifications for Flexible Rubber Products
700	Plastics
721	Corrosion and Corrosion Protection of Metals
722	Glass

*The Materials Series is being published as Military Handbooks (MIL-HDBK-) which are available to Department of Defense Agencies from the Naval Supply Depot, 5801 Tabor Avenue, Philadelphia, Pennsylvania 19120.